The Dissertation Committee for Matthew Blaine West certifies that this is the approved version of the following dissertation:

Nmd3p, the nuclear export adapter for the 60S ribosomal subunit: characterization of its recycling mechanism and novel interaction with the nuclear pore complex in yeast.

Committee:

Arlen Johnson, Supervisor

Dean Appling

Ellen Gottlieb

Jon Huibregtse

Scott Stevens

Nmd3p, the nuclear export adapter for the 60S ribosomal subunit: characterization of its recycling mechanism and novel interaction with the nuclear pore complex in yeast.

by

Matthew Blaine West, B.S.

Dissertation

Presented to the Faculty of the Graduate School of

The University of Texas at Austin

in Partial Fulfillment

of the Requirements

for the Degree of

Doctor of Philosophy

The University of Texas at Austin

December 2005

Dedication

This dissertation is dedicated to my wife, Rachel, for her love and encouragement throughout my graduate career, my pal, Riley, and to my family for their steadfast belief that I could achieve the goals that I set for myself.

Acknowledgements

I wish to extend my utmost gratitude to Arlen W. Johnson for affording me the opportunity to work in his laboratory under his patient and insightful tutelage. I offer my sincerest thanks to my committee members, Jon Huibregtse, Dean Appling, Scott Stevens, and Ellen Gottlieb, for their support and expertise during the course of my dissertation work. I would also like to acknowledge John Hedges for rewarding collaborations, helpful discussions, and his friendship throughout. I wish to thank my former laboratory colleague, George Kallstrom, for providing me with guidance and his unique perspectives during the course of my early graduate work. My gratitude also extends to Alice Wang, Ivy Hung, Ann Hofer, and members of the Stevens lab for their support and suggestions over the years. I am indebted to Anthony Chen, Grace Chen, and Toland Johnson for the isolation of *NMD3* loss-of-function and suppressor mutants. I would also like to extend best wishes to the new members of the Johnson lab, Cyril Bussiere and Kai-Yin Lo. Lastly, I would like to thank my beautiful and gracious wife, Rachel Elizabeth West, for all of her love and support and my family for always believing in me.

Nmd3p, the nuclear export adapter for the 60S ribosomal subunit: characterization of its recycling mechanism and novel interaction with the nuclear pore complex in yeast.

Publication No._____

Matthew Blaine West, Ph.D.

The University of Texas at Austin, 2005

Supervisor: Arlen W. Johnson

Ribosomes are the macromolecular machines dedicated to the fundamental task of converting genetic information encoded within messenger RNAs into the vast complement of proteins that sustain cellular structure and metabolism in all organisms. Eukaryotic ribosomes are composed of two ribonucleoprotein particles, the large (60S) and small (40S) subunits. Although they function in the cytoplasm, the two subunits are initially synthesized and matured in the nucleus and, therefore, require accessory factors to mediate their nuclear export. Our lab and others have shown that export of the 60S subunit requires an adapter protein, Nmd3p, which provides the nuclear export signal (NES) for the subunit *in trans*. The manner in which Nmd3p is recycled to the nucleus to sustain 60S export, however, is largely unknown. We have recently shown that, in yeast, the ribosomal protein Rpl10p is required for Nmd3p's release from exported subunits. Through mutational analysis of the cytoplasmic GTPase, Lsg1p, I have discovered that it also participates in this process, as *lsg1* mutants exhibit a marked defect in 60S biogenesis and export due to the entrapment of Nmd3p on cytoplasmic subunits. Consistent with their common roles in Nmd3p recycling, *lsg1* and *rpl10* mutants are suppressed by dominant mutations in *NMD3* that weaken its affinity for the subunit and

restore nuclear recycling. I also show that *lsg1* mutants accumulate a late cytoplasmic 60S biogenesis intermediate in which Rpl10p is not fully accommodated into the subunit. From these findings, I propose that Lsg1p is required for loading Rpl10p into Nmd3p-bound 60S subunits prior to translation initiation in a process that assesses the structural fidelity of the subunit and triggers the release of the export adapter for future rounds of export.

This work also includes an expanded examination of the manner in which Nmd3p engages the export machinery and is translocated across the nuclear envelope through nuclear pore complexes (NPCs). This analysis was facilitated through the use of Nmd3p mutants that are deficient for 60S binding and arrest within NPCs at an intermediate stage of export complex disassembly. From this analysis, I propose that Nmd3p possesses a particularly potent NES whose interaction with the export machinery is modulated via its association with 60S subunits.

Table of Contents

List of Tables

List of Figures

List of Illustrations

Chapter 1: General Introduction

1.1 Overview

In eukaryotic cells, ribosomes are comprised of two ribonucleoprotein particles, the 40S and 60S subunits, and manufacturing these particles is a highly dynamic and regulated process. Eukaryotic ribosomes are largely pre-assembled in the nuclear subcompartment the nucleolus, where the primary 35S and 5S rRNA transcripts are synthesized via the combined activities of RNA polymerases I and III, respectively. More than 170 different trans-acting factors are required for the complex series of endo- and exoribonucleolytic cleavages, rRNA base modifications, and RNA folding and assembly events that resolve the primary rRNA transcripts into 40S and 60S subunits. Most of the trans-acting factors are shed as the pre-60S and pre-40S subunits enter the nucleoplasm and are exported to the cytoplasm to be activated for translation. Hence, the protein compositions of the subunits that are exported to the cytoplasm are greatly simplified relative to their nucleolar counterparts. Unlike pre-40S particles that are rapidly exported to the cytoplasm following release from the nucleolus, nascent 60S subunits undergo a complex series of nucleoplasmic maturation events that further simplify the composition of the subunit prior to nuclear export. Although many of the key players in this process have been identified through the biochemical purification of distinct pre-ribosomal intermediates, very little is known about their specific substrates and the manner in which they function. I began my dissertation work to identify the 60S biogenesis factor(s) that fails to recycle to the nucleus when the function of the cytoplasmic GTPase, Lsg1p, is disrupted. During the course of my research, I have contributed to a more refined understanding of both the assembly of the 60S export

complex and the late cytoplasmic maturation events that culminate in the release of the nuclear export adapter, Nmd3p, from the 60S subunit prior to translation initiation.

1.2 Maturation of Ribosomal Subunits

Ribosomes are the macromolecular complexes that are dedicated to the fundamental process of protein synthesis in all forms of life. Each ribosome is comprised of two large ribonucleoprotein particles (RNPs) of disproportionate size, the "large" and "small" subunits. The relative sizes of ribosomes and their subunit constituents have been historically described by their sedimentation coefficients in linear sucrose gradients. The bacterial and archaeal 70S ribosome is comprised of a 30S small subunit and a 50S large subunit. The 30S subunit, in turn, is composed of the 16S ribosomal RNA (rRNA) species and 21 core ribosomal proteins (r-proteins), while the 50S subunit contains the 5S and 23S rRNAs and 34 r-proteins. Despite their functional and structural conservation, the eukaryotic 80S ribosome is larger (~30%) and more complex than its prokaryotic counterpart (Doudna and Rath, 2002). In eukaryotes, the small (40S) subunit is composed of the 18S rRNA and 32 core ribosomal proteins (33 in higher eukaryotes), while the large (60S) subunit contains three hydrogen-bonded rRNA species, the 5S, 5.8S, and 25S (28S in higher eukaryotes) rRNAs, and 46 r-proteins.

The early observation that functional bacterial ribosomes could self-assemble *in vitro* from their purified rRNA and r-protein components in the presence of mild heating suggested that ribosome assembly is dictated by its constituent parts and does not require trans-acting factors (Nomura and Erdmann, 1970; Traub and Nomura, 1968). In contrast to bacterial ribosomes, however, the only reported case of *in vitro* reconstitution for eukaryotic ribosomes required the infusion of nuclear extract, suggesting that this process is more complex in nucleated cells (Mangiarotti and Chiaberge, 1997). Indeed, while only a handful of trans-acting assembly factors appear to assist in the formation of

prokaryotic ribosomes *in vivo* (Maki et al., 2002; Woolford, 2002), the culmination of genetic and proteomic analyses from the yeast *Saccharomyces cerevisiae* has revealed that more than 170 non-ribosomal proteins and 100 or more small nucleolar RNAs (snoRNAs) are involved in the formation of eukaryotic ribosomes. As ribosome biogenesis in eukaryotes is largely compartmentalized to the nucleus, this dramatic increase in complexity likely reflects the need to tightly coordinate the spatio-temporal processing, modification, and assembly events that must transpire on nascent ribosomal subunits as they journey from the nucleus to their functional destination in the cytoplasm. Moreover, the increased size and complexity of eukaryotic ribosomes requires that at least 17 different putative ATP-dependent RNA helicases participate in the loading of ribosomal proteins and in the extensive structural rearrangements that transpire within early RNP assemblages ((Fromont-Racine et al., 2003a) and references therein).

In eukaryotic cells, the nucleolus serves as the sub-nuclear "compartment" that is dedicated to both the transcription of ribosomal RNA and the vast majority of the processing and assembly events required to generate the mature 60S and 40S subunits of the ribosome (for recent reviews see (Dundr and Misteli, 2001; Lewis and Tollervey, 2000)). Nucleoli are formed around the spans of chromosomal DNA in which the rRNA genes are tandemly organized, and their size is defined by the extent of ongoing rRNA transcription and the dense network of transacting-factors that engulf the nascent rRNA to aid in assembling the early ribosomal particles (Raue, 2004). In yeast, the rRNA genes are organized as 150-200 identical tandem-repeats situated on a single chromosome (chromosome XII) (Venema and Tollervey, 1999). As a result, this chromosomal region collectively serves as the nucleolar organizing region (NOR) within the yeast nucleus. As its relative size typically reflects the extent of ribosome synthesis occurring in the cell,

the nucleolus in an actively growing yeast cell can occupy as much as one-third to one-half of the nuclear volume (Warner, 1990).

Each repeat of yeast rDNA (~9.1 Kb) is composed of two transcriptional units, the 35S and 5S rRNAs, which are independently transcribed by RNA Polymerases I and III, respectively (Illustration 1.1A) (Venema and Tollervey, 1999). The approximately seven-kilobase, polycistronic 35S transcript contains the precursors of the mature 18S, 5.8S, and 25S rRNAs of the mature 40S and 60S ribosomal subunits (Illustration 1.1B). The 35S pre-rRNA possesses non-coding transcribed spacers at its 5' and 3' ends (external transcribed spacers, ETSs) and between each of the mature rRNA species (internal transcribed spacers, ITS1 and ITS2). Following transcription, the 35S transcript is subsequently processed through a coordinated series of endo- and exonucleolytic cleavages that remove the transcribed spacers and give rise to the mature 18S, 5.8S, and 25S rRNAs. The 18S rRNA gets packaged within the pre-40S ribosomal subunit, while 25S and 5.8S, along with the uniquely processed 5S rRNA, become incorporated within the nascent 60S subunit. By virtue of the fact that rRNA components of the 40S (18S) and 60S (25S and 5.8S) subunits are generated from a common progenitor (35S), the two ribosomal subunits are obligatorily synthesized in equal stoichiometry.

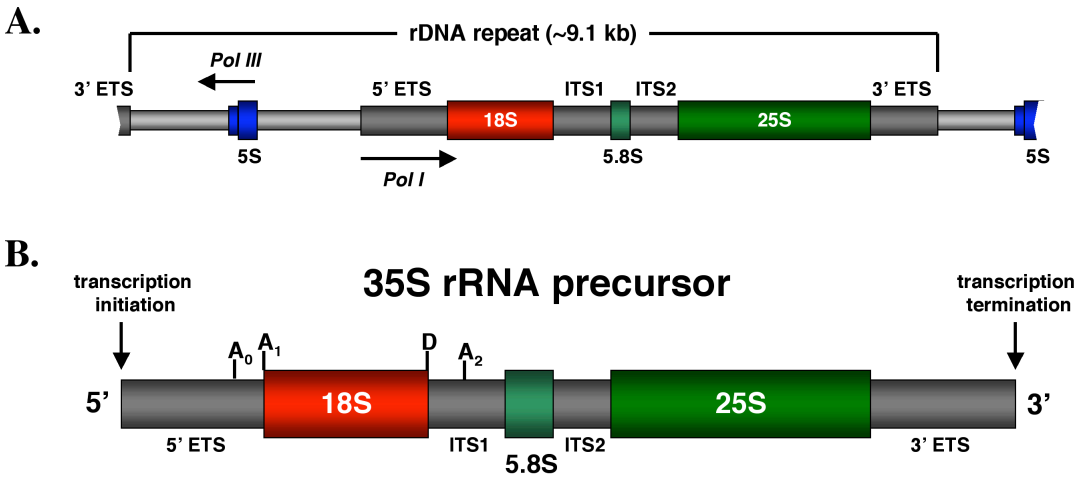

Illustration 1.1 Structural organization of the rDNA unit from *Saccharomyces cerevisae*

(A.) Transcribed regions of the rDNA repeat are indicated. Thick gray bars represent transcribed spacer elements, while the rDNA boundaries of the mature ribosomal RNAs are shown in blue, red, aquamarine, and green. (B.) Simplified representation of the 35S pre-rRNA transcript. Only the cleavage sites described in the text are indicated. [Not shown: A_3, B_0, $B_{1L/S}$, B_2, C_1, C_2 and E]

A conserved feature of rRNAs among eukaryotes and prokaryotes is the covalent modification of nucleotides that cluster around the functional core of each subunit. These nucleotide modifications fall into two classes: isomerization of uridine residues to form pseudouridine (ψ) and 2'-*O*-methylation (Nm) of ribose. In bacteria, the rRNA of the two subunits contains a total of four 2'-*O*-methylations and 11 pseudouridines, which are directly introduced by a few site-specific protein enzymes (Maden, 1998; Ofengand, 2002; Ofengand et al., 2001). In contrast, the site selection of the 55 pseudouridylations and 44 methylations in yeast is dictated by complementary base pairing between rRNA and a battalion of unique snoRNAs that assemble onto the 35S transcript as it is being synthesized and direct core snoRNP proteins to introduce the appropriate modification

(Bachellerie et al., 2002; Kiss, 2001). In yeast, pseudouridylation is performed by members of the box H/ACA family of snoRNPs, while 2'-*O*-methylation is conducted by box C/D snoRNPs (Bertrand, 2004). It is generally accepted that Cbf5p and Nop1p (Fibrillarin) are the core snoRNP constituents that catalyze the methylation and uridine isomerization reactions, respectively (Venema and Tollervey, 1999). Despite their almost universal conservation, comprehensively blocking pseudouridylation or methylation on rRNA in *NOP1* or *CBF5* mutants still yields functional subunits, although growth is severely inhibited in these cells (Tollervey et al., 1993; Zebarjadian et al., 1999). Although the precise functions of these rRNA modifications are not well understood, it is believed that they may facilitate and stabilize the tight packing of nucleotides near the catalytic cores of the two subunits, thus optimizing translation efficiency or subunit assembly (Bertrand, 2004).

The first detectable ribosomal precursor is a ribonucleoprotein particle with a sedimentation coefficient of 90S in velocity gradients. This pre-ribosomal intermediate was first identified among radiolabeled RNA species resolved from HeLa cell extracts more than thirty years ago (Trapman et al., 1975; Udem and Warner, 1972). In addition to the 90S RNP, two additional pre-ribosomal species, a 43S particle and a 66S particle, were identified in this system (Trapman et al., 1975; Udem and Warner, 1972). The principal rRNAs isolated from these three particles were the 35S primary transcript (in the 90S RNP) and two unique species, a 20S rRNA in the 43S particle and a 27S species in the 66S particle (Trapman et al., 1975). A prodigious collection of genetic and molecular approaches have since demonstrated that the 90S particle is the precursor of the 43S and 66S RNPs, which, in turn, are the progenitors of the mature 40S and 60S subunits, respectively ((Venema and Tollervey, 1999) and references therein). The endonucleolytic cleavage at site A_2 in the 35S transcript (see Illustration 1.1B and text

below) results in the severance of the 90S particle to form the 20S- and 27S rRNA-containing intermediates, thus disconnecting the fates of the two nascent ribosomal subunits. While the 43S particle is essentially "export competent," the 27S rRNA of the 66S pre-ribosomal particle must undergo additional processing in the nucleolus and nucleoplasm to yield the 5.8S and 25S rRNA species of the mature 60S subunit (Venema and Tollervey, 1999).

The demonstration that the 90S particle is the precursor of the mature 40S and 60S subunits (Trapman et al., 1975) suggested that the processing components of the individual subunits might assemble onto the 35S primary transcript to form one large complex prior to subsequent maturation. This concept was supported by the general recognition that mutations in 60S biogenesis factors often inexplicably result in delayed 40S-specific processing at sites A_0-A_2 ((Tollervey, 1996; Venema and Tollervey, 1995; Venema and Tollervey, 1999) and Illustration 1.1B). These observations led to the plausible "processosome" model which posited that 40S and 60S production is detained until virtually all of the r-proteins and trans-acting factors for the two subunits are present within the 90S complex. This kind of regulation would exist to ensure that the two subunits were manufactured in an efficient and coordinated fashion.

Recent proteomic analyses from two independent laboratories, however, have led to a marked reinterpretation of the nature of the 90S precursor species. Work from the labs of Susan Baserga and Eduard Hurt have demonstrated that the 90S particle assembles co-transcriptionally onto the 5' end of the nascent 35S primary transcript and is dedicated almost entirely to 40S processing, as 60S biogenesis factors and core r-proteins of the large subunit are virtually absent from this species (Dragon et al., 2002; Grandi et al., 2002). This work has lead to the recognition that ribosome biogenesis is largely biphasic.

Formation of the 90S complex is initiated when the large U3 snoRNP base pairs to a complementary region at the 5' end of the 35S transcript (in ETS1) as it is being synthesized (Dragon et al., 2002). Binding of the U3 snoRNP stimulates the recruitment of the 40S r-proteins and assembly factors in a globular assembly network surrounding the region of the immature 35S transcript that is to become the rRNA of the small subunit (Dragon et al., 2002; Grandi et al., 2002). Strikingly, these 40S-dedicated assembly particles, or "small subunit (SSU) processosomes," represent the terminal knobs that have long been observed by electron microscopy at the 5' ends of nascent 35S transcripts in the unique Christmas tree-like arrays ("Miller spreads") of transcriptionally-active rDNA (Dragon et al., 2002; Miller and Beatty, 1969; Mougey et al., 1993). Following U3 snoRNP-dependent cleavage at site A_2 in ITS1 (see Illustration 1.1B), the SSU processosome is disassembled as the 43S precursor is released from the primary transcript and is rapidly exported to the cytoplasm for further maturation (Trapman et al., 1976; Udem and Warner, 1973). At this time, the trans-acting factors dedicated to 60S processing and assembly associate with the remaining 27S rRNA intermediate to form the 66S ribosomal precursor particle, thus initiating the second phase of ribosome biogenesis (Grandi et al., 2002).

Once in the cytoplasm, the 43S particle undergoes two additional processing steps prior to incorporation into the translational pool. First, in a modification conserved from prokaryotic 16S rRNA, two adenine residues at the 3' end of 20S rRNA become dimethylated ($m^6{}_2Am^6{}_2A$). In yeast, the pre-40S-associated factor, Dim1p, is the enzyme responsible for these cytoplasmic modifications (Lafontaine et al., 1994; Lafontaine et al., 1995). Also at this time, the yeast 20S rRNA species is cleaved at site D in ITS1 (Illustration 1.1B) to yield the mature 18S rRNA species (Moy and Silver, 1999; Udem and Warner, 1973; Vanrobays et al., 2001). Although the mechanism of this cleavage

reaction remains nebulous, it appears to require a subset of factors associated with cytoplasmic pre-40S particles, including Tsr1p, Rio1p/Rrp10p, Rio2p, and Nob1p (Fatica et al., 2003; Gelperin et al., 2001; Vanrobays et al., 2003; Vanrobays et al., 2001). Among these, Nob1p is believed to function as the endonuclease responsible for cleavage at site D, as it possesses an N-terminal PIN domain predicted to have RNase function (Clissold and Ponting, 2000; Makarova and Grishin, 1999). While it was widely believed that the processing of 18S rRNA in mammalian cells is restricted to the nucleus, a recent analysis by Rouquette *et al.* (2005) has demonstrated that pre-40S particles in HeLa cells also undergo a cytoplasmic trimming of 20-30 nucleotides at the 3' end of 18S in a reaction that requires the human homologue of Rio2p (Rouquette et al., 2005).

While 40S precursor particles are rapidly exported to the cytoplasm following cleavage at site A_2 of 35S by the U3 snoRNP, it has long been appreciated that 60S biogenesis involves an extended nucleoplasmic maturation ((Trapman et al., 1976; Udem and Warner, 1973) and Illustration 1.2). This suggests that the large subunit is subjected to additional points of quality control or structural modifications prior to achieving "export competence." While the manner and order of rRNA processing steps are well established, the factors needed for directing the progression of nascent 60S particles from the nucleolus to the cytoplasm generally remain unclear. An extensive inventory of independent genetic and molecular analyses have, thus far, provided only a patchwork-view of the spatial and temporal maturation of 60S subunits. Moreover, the inherently dynamic and coordinated nature of 60S biogenesis has complicated precise functional assignments for the majority of the trans-acting factors involved in this process.

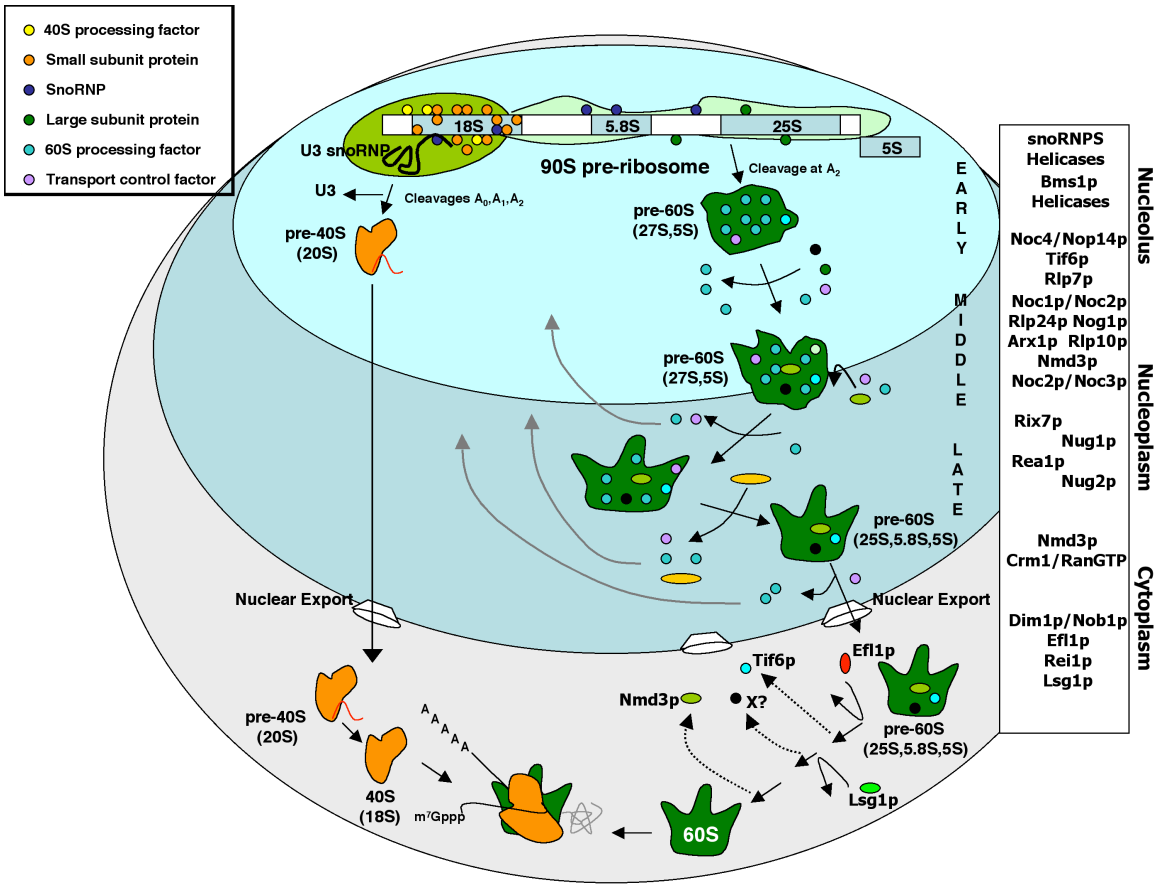

Illustration 1.2 Simplified overview of ribosome biogenesis in yeast

Nucleolar processing and assembly events highlight the biphasic nature of the pre-40S and pre-60S processing machinery, including the greater representation of 40S-associated factors and the U3 snoRNP in the 90S pre-ribosomal particle. Following cleavage at site A_2, pre-40S subunits are rapidly exported to the cytoplasm. The subsequent nuclear maturation of 60S subunits is conceptually divided into early, middle, and late stages based on rRNA processing events and proteomic analyses. Cytoplasmic maturation of the 40S and 60S subunits includes the trimming of 20S rRNA and the release of transacting factors by cytoplasmic GTPases, respectively. A subset of factors known to control the synthesis and intracellular migration of the two ribosomal subunits are listed on the right margin.

The recent advent of large-scale proteomic approaches incorporating TAP (tandem affinity purification)-tagged factors that act throughout 60S biogenesis has allowed for the mass-spectrometric characterization of pre-60S particles at distinct stages during their maturation (Bassler et al., 2001; Dragon et al., 2002; Fatica et al., 2002; Gavin et al., 2002; Grandi et al., 2002; Harnpicharnchai et al., 2001; Nissan et al., 2002; Saveanu et al., 2001). This method has provided a loose framework for correlating our understanding of how specific trans-acting factors elicit their effects during 60S biogenesis with the specific maturation intermediates on which they perform their function. From these analyses, it has become apparent that pre-60S particles become progressively less complex as they migrate from the nucleolus to the cytoplasm (Grandi et al., 2002; Nissan et al., 2002). This has led to the proposal that 60S maturation is governed by sequential structural rearrangements that recycle trans-acting factors back to the nucleolus while priming the subunit for function. As a result, it is not surprising that energy-consuming proteins, such as ATPases and GTPases, have been identified in pre-60S particles throughout their maturation (de la Cruz, 2004; Fromont-Racine et al., 2003b). Furthermore, the acquisition and/or exchange of key trans-acting factors from one 60S intermediate to the next provide a suggestion of how some of these species may be transported between cellular compartments.

1.3 Transport of Nascent Subunits from the Nucleolus to the Cytoplasm

The event(s) that trigger the release of nascent 60S particles from the nucleolus are ill-defined. A series of protein exchanges appears to coincide with this transition, however. One intriguing subset of factors that are required for nucleolar release of both the pre-40S and pre-60S particles are the essential and highly conserved Noc (nucleolar complex associated) proteins. Noc1p and Noc2p form a heterodimer in the nucleolus that associates with both 90S and 66S particles and is distinct from a nucleoplasmic 66S-

associated Noc2p/Noc3p duplex (Milkereit et al., 2001). Temperature sensitive (*ts*) *noc1* mutants trap the 60S visual reporter protein, Rpl25-eGFP, in the nucleolus at restrictive temperature, whereas Rpl25-eGFP accumulates throughout the nucleoplasm in *noc3 ts* mutants (Milkereit et al., 2001). The distinct sub-nuclear accumulation of Rpl25-eGFP between *noc1* and *noc3* mutants suggests that these two factors are critical for the sequential intra-nuclear migration of pre-60S particles. In light of their common association with Noc2p and their distinct compartmentalization, it is possible that the exchange of Noc1p for Noc3p on Noc2p-bound pre-60S particles is a requisite step for the release of 60S from the nucleolus.

The Noc4 protein possesses the ~45 amino acid "Noc box" motif found in both Noc1p and Noc3p and forms a heterodimeric complex with the 40S biogenesis factor Nop14p (Milkereit et al., 2001; Milkereit et al., 2003). *noc4 ts* mutants trap the 40S visual reporter protein, Rps2-eGFP, in the nucleolus yet have no negative effect on 60S export (Milkereit et al., 2003). This has led to the proposal that, like its pre-60S-associated counterparts, the Noc4p/Nop14p complex may be involved in the nucleolar release and subsequent export of 43S particles to the cytoplasm (Milkereit et al., 2003). In this way, Noc proteins may play a conserved role in influencing the release of nascent 40S and 60S particles from the nucleolus in response to independent maturational cues.

A second class of trans-acting factors that influence the release of pre-60S particles from the nucleolus exhibit high sequence homology throughout their primary sequence with core ribosomal proteins. Two such r-protein-like factors, Rlp7p and Rlp24p, are associated with 66S pre-ribosomal particles during their early maturation in the nucleolus. Rlp7p and Rlp24p show strong sequence homology with the mature 60S proteins Rpl7p and Rpl24p, respectively (Dunbar et al., 2000; Lalo et al., 1993; Saveanu et al., 2003). Thus, it has been proposed that Rlp7p and Rlp24p occupy the same sites on

nascent pre-60S particles that will later be occupied by Rpl7p and Rpl24p in the mature subunits. Consistent with this rationale, Rlp7p is a nucleolar protein that, in contrast to its r-protein counterpart, is absent from mature 60S subunits (Nissan et al., 2002). Moreover, Rpl25-eGFP accumulates in the nucleolus in *rlp7* (*rix9-1*) mutants, leading to the hypothesis that the exchange of Rlp7p for Rpl7p is a requisite step for governing the release of nascent 60S particles into the nucleoplasm (Gadal et al., 2002). Like Rlp7p. Rlp24p associates with 66S particles in the nucleolus and is absent from mature subunits (Saveanu et al., 2003). Rlp24p has been shown to recruit the trans-acting GTPase, Nog1p, to nucleolar particles through a direct protein-protein interaction (Saveanu et al., 2003). As Nog1p is required for nucleolar release of pre-60S subunits (see below), Rlp24p may also play a critical role in modulating the nature or timing of this event (Kallstrom et al., 2003).

Several lines of evidence suggest that the Crm1(Xpo1p)-dependent 60S nuclear export adapter, Nmd3p (see section 1.3), also loads onto pre-60S particles in the nucleolus and is required for their subsequent intra-nuclear migration. First, *nmd3*^{ts} mutants accumulate the 60S visual reporter protein, Rpl25-eGFP, in the nucleolus, indicating that Nmd3p function is required for the release of subunits into the nucleoplasm (Kallstrom et al., 2003). In contrast, treating sensitized yeast cells with the Crm1-specific inhibitor, leptomycin B (LMB), or introducing mutations in Nmd3p that specifically disrupt its interaction with Crm1, results in the accumulation of 60S subunits throughout the nucleoplasm (Gadal et al., 2001b; Hedges et al., 2005; Ho et al., 2000b). This disparity suggests that Nmd3p affects the transition of nascent 60S particles at two distinct stages: nucleolar release and nuclear export, only the latter of which requires Crm1 interaction. Consistent with a transient population of Nmd3p in the nucleolus, a subset of nucleolar proteins are enriched on subunits that co-purify with a mutant Nmd3p

allele deleted for its nuclear export signal (Nmd3Δ100p) (Kallstrom and Johnson, unpublished). Furthermore, human Nmd3 accumulates in the nucleolus when rRNA synthesis is inhibited by actinomycin D (Trotta et al., 2003), demonstrating that, in the absence of export cargo (i.e. nascent 60S subunits), functional Nmd3 remains at the site at which it is recruited to 60S. As additional ill-defined nucleoplasmic events are required for 60S "export competence," it is likely that, following nucleolar release, pre-60S subunits must undergo further processing or structural rearrangements before Nmd3p is capable of engaging the export machinery (see section 1.3).

Consistent with this notion, two members of the AAA-ATPase (ATPases associated with various cellular activities) family of ATP-binding proteins have been shown to play an important role in 60S maturation prior to subunit export. Members of this family of ATPases form hexameric ring-like structures upon binding ATP and undergo conformational changes as ATP is hydrolyzed that enable them to disassemble protein complexes or behave as ATP-dependent motors (Vale, 2000). Rix7p is a member of this class of proteins that has been implicated in 60S export. *rix7-1*^{ts} mutants trap Rpl25-eGFP in the nucleolus at non-permissive temperature, yet do not dramatically accumulate 60S-specific rRNA intermediates (Gadal et al., 2001a). During active growth, Rix7p localizes throughout the nucleoplasm. Strikingly, as ribosome biogenesis is quiescent during stationary phase, Rix7p redistributes to the nucleolus, and temporarily relocalizes to the nuclear boundary when active growth is resumed (Gadal et al., 2001a). The intra-nuclear migration of Rix7p upon initiation of ribosome biogenesis coupled with its requirement for nucleolar release of pre-60S particles suggests that it may chaperone subunits through the nucleoplasm and induce a late structural rearrangement on the subunit that recycles nucleolar biogenesis factors prior to nuclear export.

A second AAA-ATPase, Rea1p/Mdn1p, associates with late pre-60S intermediates in the nucleoplasm (Bassler et al., 2001; Nissan et al., 2002). At 560 kDa in size, Rea1p is the largest protein in yeast and, intriguingly, exhibits significant sequence homology to the molecular motor, dynein (Garbarino, 2002). Rea1p co-purifies with a late pre-60S particle that is enriched in the nucleoplasmic protein, Rix1p (Galani et al., 2004; Nissan et al., 2004). Mutations in either *RIX1* or *REA1* result in the accumulation of Rpl25-eGFP-bound 60S intermediates in the nucleoplasm, with *rea1* mutants exhibiting a slight bias in 60S localization at the nuclear periphery (Galani et al., 2004). Remarkably, when Rea1p-bound subunits are incubated with exogenous ATP, both Rea1p and the nuclear GTPase, Nug2p (see below), are efficiently released from late nuclear pre-60S particles (Nissan et al., 2004). In light of its effects on 60S export and its putative ability to dissociate trans-acting factors from a late 60S intermediate, it is possible that Rea1p (perhaps in cooperation with Rix1p and/or Nug2p) remodels subunits in the nucleoplasm, releasing biogenesis factors and priming them for export. In this way, the AAA-ATPases, Rix7p and Rea1p, may act sequentially or in concert to govern the proper assembly of subunits prior to nuclear release.

In addition to ATPases, GTP-hydrolyzing proteins have been shown to play key roles throughout ribosome biogenesis. GTPases are generally thought to behave as energy-transducing "molecular switches" that differentially regulate key cellular processes through their cycles of GTP hydrolysis (Bourne, 1995; Saraste et al., 1990). These enzymes typically bind to their target substrates in their GTP-bound form, or "on' state (Bourne et al., 1991). In response to some regulatory or structural cue, their intrinsically weak GTPase activity is stimulated to induce intra- or intermolecular conformational changes that alter the functional properties of protein complexes. As ribosome biogenesis is a highly dynamic and coordinated process, it is likely that

GTPases act at distinct stages in the biogenesis pathway to alter protein-protein or protein-RNA interactions within pre-ribosomal particles through GTP-hydrolysis-dependent conformational changes.

To date, only one GTPase has been implicated in the biogenesis of the small ribosomal subunit. This protein, Bms1p, is an essential nucleolar protein that associates with U3 snoRNP complexes on 35S transcripts and is required for the endonucleolytic cleavages at sites A_0-A_2 (Gelperin et al., 2001; Wegierski et al., 2001). In light of its broad effects on 40S-specific processing, it has been suggested that Bms1p "senses" the proper assembly of the processing complex and gives the "green light" to initiate the early cleavage reactions by way of GTP-hydrolysis (Wegierski et al., 2001).

The nuclear maturation of the 60S subunit has been shown to require three independent GTPases, Nog1p, Nug1p, and Nug2p/Nog2p. All three proteins are present on the same late pre-60S particle, yet they do not have redundant functions, as each is essential for viability (Bassler et al., 2001; Kallstrom et al., 2003; Nissan et al., 2002; Park et al., 2001; Saveanu et al., 2001). Consistent with their distinct intra-nuclear localization patterns, *nog1* mutants trap pre-60S particles in the nucleolus, while *nug1* and *nug2* mutants accumulate Rpl25-eGFP throughout the nucleus (Bassler et al., 2001; Kallstrom et al., 2003; Saveanu et al., 2001). This suggests that Nog1p may function upstream of Nug1p and Nug2p, a hypothesis that is supported by the observation that Nog1p's association with early 60S intermediates is a prerequisite for Nug2p/Nog2p loading (Saveanu et al., 2003). Perturbation of Nog1p function results in early rRNA processing defects that lead to pre-60S subunit instability. Although *nug1* and *nug2* mutants do not exhibit significant rRNA processing defects, the nuclear subunits that accumulate in these mutants are also unstable (Bassler et al., 2001; Saveanu et al., 2001). These observations suggest that Nog1p likely participates in a late nucleolar structural

rearrangement that is required for proper rRNA processing and nucleolar release, whereas Nug1p and Nug2p load onto Nog1p-bound subunits in the nucleolus but do not function until later in the nuclear maturation pathway. Prior to export, Nug1p and Nug2p may proofread the proper assembly of late pre-60S particles and, perhaps in conjunction with Rix7p and Rea1p, perform coordinated remodeling events to facilitate subunit export. In their absence, a key checkpoint in 60S maturation may not be achieved, thus targeting these late pre-60S intermediates for destruction

The series of putative structural rearrangements and coordinated release of trans-acting biogenesis factors that highlight the late nuclear maturation of 60S subunits culminate in the formation of an export complex on 60S via Nmd3p (see section 1.3). Following translocation to the cytoplasm, however, the nascent 60S subunits are further matured before they can engage the translational machinery. Again, GTP-binding proteins appear to play key roles in moderating these events.

The functional context of the cytoplasmic GTPase Ria1p/Efl1p is one of the best understood among 60S biogenesis factors. Immature 60S subunits emerge from the nucleus bound by the essential nucleolar protein, Tif6p (Senger et al., 2001). Tif6p appears to play a critical, yet ill-defined, role in facilitating the nucleolar processing of 25S and 5.8S rRNAs (Basu et al., 2001). As a result, Tif6p must be recycled from newly-exported 60S subunits to sustain 60S biogenesis in the nucleolus. Remarkably, Tif6p (eIF6) was initially isolated from wheat germ by virtue of its ability to block 60S/40S joining *in vitro* ((Russell and Spremulli, 1979), a characteristic that is conserved in yeast (Si and Maitra, 1999). This has led to the speculation that Tif6p remains associated with pre-60S particles to prevent precocious interaction between the two ribosomal subunits prior to nuclear export and/or before 60S acquires translational competency. The

efficient release of Tif6p from nascent cytoplasmic subunits prior to translation initiation has recently been shown to require Ria1p/Efl1p (Senger et al., 2001).

efl1Δ mutants exhibit a severe slow-growth phenotype that coincides with a marked steady-state redistribution of Tif6p from the nucleolus to the cytoplasm (Senger et al., 2001). The negative growth phenotype of an *efl1Δ* mutant is suppressed by dominant mutations in *TIF6* that are believed to weaken Tif6p's interaction with 60S, thus bypassing the requirement for Efl1p in mediating its release (Senger et al., 2001). Intriguingly, Ria1p/Efl1p shows sequence similarity to translation elongation factor 2 (EF-2) and inhibits EF-2's 60S-dependent GTPase activity in a concentration-dependent manner *in vitro*, suggesting that these two proteins may have overlapping 60S binding sites (Graindorge et al., 2005a). Therefore, it has been proposed that Efl1p proofreads the fidelity of the nascent EF-2 binding site on immature 60S subunits and, upon a positive assessment, releases Tif6p to facilitate subunit joining. As a result, Efl1p may participate in coupling 60S biogenesis with translation initiation.

Our lab recently performed an initial characterization on a second cytoplasmic GTPase known to participate in 60S biogenesis, Lsg1p (Kallstrom et al., 2003). Lsg1p is an essential, non-shuttling protein that stably associates with late, Nmd3p-bound pre-60S particles in the cytoplasm (Kallstrom et al., 2003; Nissan et al., 2002). Lsg1p likely binds nascent subunits as they emerge from the nucleus and performs its role in 60S maturation prior to translation initiation, as it only co-sediments with free 60S subunits (i.e non-translating ribosomes) in sucrose gradients (Kallstrom et al., 2003; Nissan et al., 2002). An *lsg1-1* conditional mutant shows a deficit in 60S levels and accumulates Rpl25-eGFP in the nucleolus at non-permissive temperature (Kallstrom et al., 2003), indicating that Lsg1p is needed for the release of subunits from the nucleolus. In light of the fact that Lsg1p is restricted to the cytoplasm, it likely mediates its affect on nuclear maturation

events in an indirect manner. This led us to propose that, like Ria1p/Efl1p, Lsg1p may be necessary for recycling a 60S biogenesis factor back to the nucle(ol)us that is exported on nascent 60S subunits. In light of its sustained interaction with cytoplasmic subunits prior to translation initiation, GTP hydrolysis on Lsg1p may serve as a molecular switch that coordinates the release of a critical nuclear biogenesis factor with the onset of translation.

1.4 Export of ribosomal subunits to the cytoplasm

While compartmentalization of ribosome synthesis prevents the untimely incorporation of immature subunits into the translational pool, it also poses a unique challenge to eukaryotic cells. In an actively growing yeast cell, for instance, the population of free ribosomal subunits is relatively small, requiring continuous ribosome assembly to meet the metabolic needs of the cell. Thus, as an average yeast cell maintains approximately 200,000 ribosomes, it must generate about 4,000 ribosomal subunits each minute during its 100-minute generation time (Warner, 1999). In light of the fact that yeast nuclei are punctuated by only 150-180 nuclear pores (Rout and Blobel, 1993; Winey et al., 1997), a single pore must accommodate the export of an estimated 20-25 subunits per minute. This substantial flux requires that a mechanism be in place to efficiently negotiate the considerable mass of each subunit across the nuclear envelope.

Initial attempts to dissect this export pathway in *Xenopus* oocytes were successful in demonstrating that ribosomal subunit export is energy-dependent, saturable, and unidirectional through nuclear pore complexes (NPCs) (Bataille et al., 1990). The saturable nature of subunit export suggested that ribosomal subunit translocation is receptor-mediated. Indeed, work from our lab and others have shown that, in yeast, the export of both the large (60S) and small (40S) subunits requires the importin-β family export receptor, Crm1 (Xpo1p in yeast) (Gadal et al., 2001b; Ho et al., 2000b; Moy and Silver, 1999). Subsequent work in higher eukaryotes has revealed that the Crm1-

dependence for ribosome export is a conserved pathway (Thomas and Kutay, 2003; Trotta et al., 2003). Crm1 recognizes cargo that possess nuclear export signals (NESs) composed of short, leucine-rich stretches of amino acids (canonical sequence: $\underline{\phi}$-X_{2-3}-$\underline{\phi}$-X_{2-3}-$\underline{\phi}$-X-$\underline{\phi}$; where ϕ = L/F/V/I/M) (Fornerod and Ohno, 2002; Kutay and Guttinger, 2005; la Cour et al., 2004). Typically, these NESs reside within the cargo molecule itself, although in a few prominent cases, an NES-containing adapter protein may serve to bridge the interaction between Crm1 and its substrate. A classical example of this kind of facilitated interaction is the viral RNA-binding protein, HIV-1 Rev, which commandeers Crm1 function to mediate the nuclear export of unspliced viral transcripts within host cells (reviewed in Pollard and Malim, 1998).

Crm1 binds to its export cargo in the nucleus cooperatively with the triphosphate nucleotide-bound form of the Ras-like GTPase, Ran (Gsp1p in yeast) (reviewed in (Gorlich and Kutay, 1999)). The formation of this "ternary complex" (RanGTP/Crm1/NES[cargo]) is required to stabilize Crm1's inherently weak association with its substrate during export (Fornerod et al., 1997a). Following translocation of the export complex into the cytoplasm, Ran's intrinsically slow GTPase activity is strongly induced (10^5-fold stimulation) upon the recruitment of Ran's cytoplasmic GTP-activating protein, RanGAP (Rna1p), and RanGTP-binding proteins, RanBP1 (Yrb1p) or RanBP2 (specific to higher eukaryotes) to the export complex (Bischoff, 1994; Bischoff 1995; Becker 1995; Richards 1995). As the GDP-bound form of Ran has low affinity for Crm1, the ternary complex rapidly dissociates in the cytoplasm following GTP hydrolysis, allowing for release of the export cargo and recycling of Ran-GDP and Crm1 back to the nucleus (Bischoff and Gorlich, 1997; Floer et al., 1997; Lounsbury and Macara, 1997). Upon nuclear reentry, the GTP-bound form of Ran is regenerated in the presence of its chromatin-bound nucleotide exchange factor, RanGEF/RCC1 (Prp20p), to

reset the export cycle. The faithful partitioning of Ran's effector molecules between the nucleus (chromatin-bound RanGEF) and cytoplasm (RanGAP, RanBP1/RanBP2) generates a steep RanGTP gradient across the nuclear envelope, which, in turn, allows for the facilitated diffusion of Crm1-bound export complexes across the nuclear envelope into the cytoplasm.

Consistent with its critical roles in maintaining the integrity of Crm1-bound export complexes and in imparting directionality to the export process, RanGTP was also identified as a necessary component for ribosome export among eukaryotes (Hurt et al., 1999; Moy and Silver, 1999). Mutations in either *GSP1* (Ran homologue in yeast) or its effector molecules, *RNA1* (RanGAP), *PRP20* (RanGEF), and *YRB1* (RanBP1), result in the nuclear accumulation of both the large and small ribosomal subunits in visual reporter assays conducted in live cells (Hurt et al., 1999; Moy and Silver, 1999; Stage-Zimmermann et al., 2000). The contribution of RanGTP to the ribosome export pathway accounts for the initial observation that ribosome export is an energy-consuming process (Bataille et al., 1990). However, this energy consumption is required to sustain subunit export through regenerating RanGTP and not for the export event itself, as export assays in *Xenopus* oocytes have demonstrated that the actual translocation event is energy-independent (Englmeier et al., 1999; Ribbeck et al., 1999; Schwoebel et al., 1998).

More recently, experimentation has been focused on identifying the factors that provide the nuclear export signals for the two ribosomal subunits and on the timing and nature of their recruitment to 40S and 60S to signal "export competence." Although the factor that provides the leucine-rich NES for 40S subunits is unknown, our lab and others have shown that the shuttling protein, Nmd3p, is the Crm1-dependent export adapter for the large subunit in yeast ((Gadal et al., 2001b; Ho et al., 2000b) and section 1.2). As Nmd3p is not a core component of mature ribosomes (Ho and Johnson, 1999), it provides

the leucine-rich export signal for 60S subunits *in trans*, thus bridging the interaction between 60S and Crm1/RanGTP in a manner analogous to that described for HIV-1 Rev in the export of viral RNA (Illustration 1.3). Deletion of the canonical NES in yeast Nmd3p (LLDELDEMTL) results in nuclear entrapment of both Nmd3p and nascent 60S subunits coupled with a marked growth arrest (Ho et al., 2000b). Remarkably, fusing the Crm1-specific NES from cAMP-dependent protein kinase inhibitor (PKI) to this mutant Nmd3p allele restores both viability and the export of Nmd3p and 60S from nuclei (Ho et al., 2000b), thus demonstrating that the presence of a Crm1-dependent NES on Nmd3p is both necessary and sufficient for subunit export. Equivalent lines of experimentation in *Xenopus* oocytes (Trotta et al., 2003) and human (HeLa) cells (Thomas and Kutay, 2003) have demonstrated that Nmd3's role as the 60S export adapter is conserved across species boundaries.

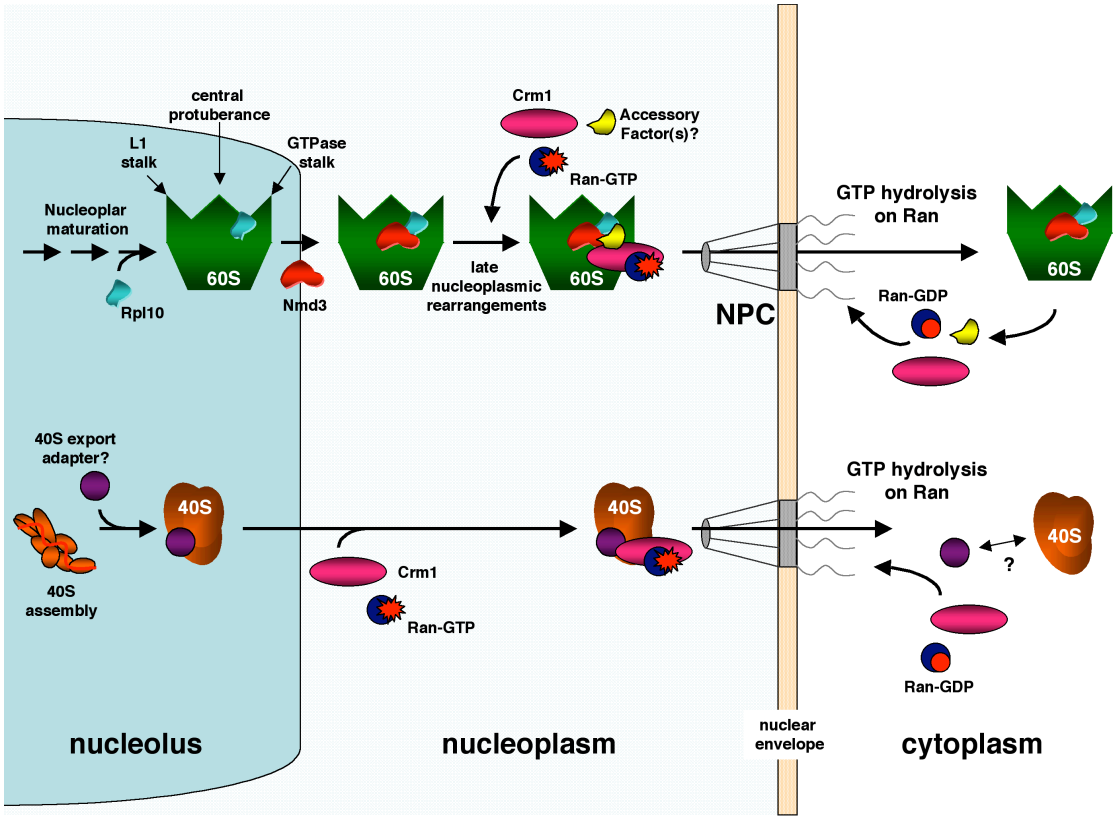

Illustration 1.3 Nuclear export of ribosomal subunits

The 40S and 60S ribosomal subunits are independently assembled and exported from the nucleus. The export of both subunits, however, likely requires the assembly of an export complex with Crm1 and Ran-GTP for recruitment and translocation through nuclear pore complexes (NPCs). The Crm1-dependent nuclear export signal for 60S subunits is provided *in trans* by the shuttling protein Nmd3p. The 40S export adapter is still unknown. Following translocation through the NPC, GTP hydrolysis on Ran results in the disassembly of the export complex. At this time, RanGDP and Crm1 are recycled back to the nucleus for additional rounds of export. Nmd3p remains associated with 60S subunits until late in their cytoplasmic maturation, at which time it is recycled back to the nucleus prior to subunit joining.

The specific timing and manner in which Nmd3p is recruited to 60S subunits is currently unclear. As described in the previous section, several lines of evidence suggest that Nmd3p loads onto nascent subunits at the point of their release from the nucleolus. It has been proposed that incorporation of the ribosomal protein, Rpl10p, into pre-60S particles at this time is required for Nmd3p loading (Gadal et al., 2001b; Nissan et al., 2002). In this model, Rpl10p is predicted to load onto 60S subunits late during nuclear 60S maturation and, in turn, physically recruits Nmd3p to 60S by serving as part of its binding site on the subunit (Illustration 1.3). In support of this model, initial experiments that monitored the endogenous rate at which ribosomal proteins assemble onto 60S subunits demonstrated that Rpl10p loads significantly later than other core subunit proteins (Kruiswijk et al., 1978). Consistent with its proposed role in 60S export, *rpl10* conditional mutants (*rix5-1* and *rpl10[G161D]*) trap the 60S reporter protein, Rpl25-eGFP, in the nucleus at restrictive temperatures (Gadal et al., 2001b; Hedges et al., 2005). Furthermore, independent reports of genetic and physical interactions between *NMD3* and *RPL10* (Gadal et al., 2001b; Karl et al., 1999; Zuk et al., 1999), including the observation that over-expression of Nmd3p suppresses an *rpl10* conditional allele (*rpl10[F85S]*) (Zuk et al., 1999), lend credence to a functional link between these two proteins.

Recent work from our lab, however, has shown that the nuclear accumulation of Rpl25-eGFP in *rpl10* mutants results from in a block in recycling Nmd3p off of cytoplasmic 60S subunits rather than a failure to load Nmd3p in the nucleus (Hedges et al., 2005; West et al., 2005). Moreover, over-expression of Nmd3p is sufficient to restore subunit export under conditions in which *RPL10* transcription is repressed, suggesting that Rpl10p loading is dispensable for the Nmd3p-mediated export event (Hedges et al.,

2005). In light of these new findings, the manner in which Nmd3p is recruited to 60S subunits in the nucleus warrants closer inspection.

Consistent with Nmd3's role as the Crm1-dependent 60S export adapter, ternary complexes containing Crm1, RanGTP, and either human or yeast Nmd3 have been reconstituted *in vitro* ((Thomas and Kutay, 2003) and Kallstrom and Johnson, unpublished). Surprisingly, export complex formation has not been recapitulated for Nmd3 bound to purified 60S subunits. This discrepancy could reflect differences in the structure or protein composition of the mature, cytoplasmic subunits used in the reconstitution assays relative to Nmd3p's endogenous substrate (i.e. nuclear pre-60S molecules). The absence of a protein factor from the *in vitro* system that typically modulates the presentation of Nmd3's NES or is needed to stabilize the export complex in the nucleus could preclude reconstitution and may hint at an additional point of control in 60S export. It is intriguing that a conditional allele of the mRNA export factor, *MTR2*, was isolated from yeast that disrupted 60S, but not mRNA export (*mtr2-33*)(Bassler et al., 2001). Combining specific *mtr2* and *nmd3* conditional mutants (*mtr2-33 nmd3-2*) results in synthetic lethality, perhaps alluding to a functional link between these two proteins (Bassler et al., 2001). Additionally, Mtr2p has been shown to co-purify with nuclear pre-60S particles that contain Nmd3p (Nissan et al., 2002). In its most notorious export function, Mtr2p cooperates with Mex67p (p15/NXT and TAP, respectively, in humans) to recruit nascent mRNAs to nuclear pore complexes to facilitate their export via a Crm1-independent pathway (reviewed in (Rodriguez et al., 2004)). Therefore, its influence on 60S export and functional interaction with Nmd3p may be direct, perhaps by helping to engage Nmd3p with the export machinery, or indirect, by influencing the flux of competing cargoes through nuclear pores.

Irrespective of the requirement for putative "accessory factors," once formed, the Nmd3p-bound export complex must be recruited to nuclear pore complexes (NPCs) for translocation to the cytoplasm. In yeast, NPCs are comprised of multiple copies of approximately 30 unique nuclear pore proteins, or nucleoporins (Nups)(Rout et al., 2000). These nucleoporins are organized into the hierarchical structure of the NPC, which is comprised of three prominent features, a nuclear basket, a central core encased within the nuclear envelope, and cytoplasmic fibrils (Illustration 1.3). The nucleoporins that comprise the nuclear basket and cytoplasmic fibrils possess phenylalanine-glycine (FG) repeats that facilitate the "docking" of cargo-bound transport receptors. As a member of the importin-β family of nuclear transport receptors, Crm1 is capable of engaging these FG repeats to facilitate the export of ribosomal subunits. Although it remains unclear whether Crm1 binds and escorts ribosomal subunits along a specific pathway through the NPC, mutations in a subset of Nups have been shown to inhibit 60S export, suggesting a degree of specificity for this process (Gleizes et al., 2001; Hurt et al., 1999; Stage-Zimmermann et al., 2000).

The maximal functional diameter of a nuclear pore is ~40 nanometers (Pante and Kann, 2002). Only relatively small molecules are capable of passing through the channel by simple diffusion, however, as the actual passable diameter (~10 nm) is significantly reduced by the meshwork of hydrophobic Nups that extends into the aqueous center of the NPC (Fried and Kutay, 2003). As a result, nuclear pores behave as semi-permeable hydrophobic barriers.

According to the "selective phase" model of translocation, the weak hydrophobic interactions that arise between nucleoporins and Crm1 during docking of the export complex may be sufficient to partition the ribosomal subunits into the hydrophobic environment of the central core of the NPC (Ribbeck and Gorlich, 2002). However, as

the large and small subunits are highly anionic in nature (due to rRNA), the insertion of these macromolecules into the hydrophobic phase of the NPC would seem to be a daunting task. Recently, it was demonstrated that the heat shock protein, Hsp90 (Hsp82p in yeast), is required for the efficient export of 60S subunits in transport assays using resealed rat liver nuclei or in microinjection experiments in *Xenopus* oocytes (Schlatter et al., 2002). The authors proposed that Hsp90 acts to remodel the 60S subunit by altering the presentation of hydrophobic regions on its surface to aid in its passage through the non-aqueous environment of the nuclear channel. Although the functional relevance of these results remain to be elucidated, it is possible that the partitioning of subunits into the meshwork of the channel may involve factors that "shield" the hydrophilic nature of the ribosomal particles during translocation.

Although the diameter of an average ribosomal subunit (~25-30nm) approaches the effective size limitations of the central channel (~39nm), subunits are nonetheless exported at a considerable rate. In the context of the large subunit, this may rely on the persistence of a subset of biogenesis factors, which prevent precocious interactions that would pose a steric barrier to export (Illustration 1.3B). Nascent 60S subunits enter the cytoplasm bound by the trans-acting factors Tif6p, Arx1p, and Nmd3p (Nissan et al., 2002). As introduced in section 1.3, the nucleolar 60S biogenesis factor, Tif6p, was initially isolated as a 60S-associated protein that prevented subunit joining (i.e. 80S formation) (Russell and Spremulli, 1979). Its sustained association with pre-60S particles prior to and during translocation would inhibit premature 80S formation in the nucleus, thus averting a potential steric hindrance to subunit export. Likewise, the presence of Tif6p on pre-60S particles throughout their residency in the nucleus has been used as an argument against nuclear translation.

Arx1p is a methionyl-aminopeptidase(MetAP)-related 60S binding protein that loads onto subunits late in the nucleus (Hung and Johnson, 2005; Nissan et al., 2002). Although its function in 60S biogenesis is currently unclear, molecular and genetic analyses suggest that it binds to 60S subunits at the polypeptide exit tunnel, likely interacting with the ribosomal proteins Rpl25p and Rpl35p (Hung and Johnson, 2005). This putative binding site for Arx1p on 60S overlaps with that of the signal recognition particle (SRP), an RNP that is assembled in the nucleus and functions in the cytoplasm to direct ribosomes translating secretory polypeptides to the endoplasmic reticulum (ER). Therefore, Arx1p may serve as a "packaging factor" that aids in the export efficiency of 60S subunits by blocking the untimely association of SRP prior to export.

Lastly, Nmd3p, and perhaps the export complex itself, may further contribute to export efficiency by acting as an additional block to 60S/40S coupling in the nucleus. Structural modeling of the large subunit has shown that Rpl10p (L16 in bacteria) occupies a position on the joining face of the large subunit between the central protuberance and the GTPase stalk (Ban et al., 2000; Spahn et al., 2001). Therefore, if Nmd3p does indeed physically interact with Rpl10p on 60S (see above), it would likely bind to the joining surface of the subunit and sterically oppose 80S formation.

Following translocation to the cytoplasm, GTP hydrolysis on Ran allows for dissociation of the 60S export complex. At this time, Crm1 and RanGDP are independently imported for subsequent rounds of export. Tif6p, Arx1p, and Nmd3p must also be released from subunits following translocation to sustain 60S biogenesis and export. As none of these factors remain associated with translating subunits in polysomes, their release must precede or coincide with translation initiation. Indeed, the persistence of Tif6p would, in fact, inhibit translation by blocking subunit joining. As desribed in section 1.3, the cytoplasmic GTPase Ria1p\Efl1p has been implicated in the

release of Tif6p from 60S during a putative structural rearrangement that occurs shortly after subunit export (Senger et al., 2001).

The release of Arx1p from nascent subunits appears to require the cytoplasmic 60S-binding protein, Rei1p (Hung and Johnson, 2005). Although Rei1p's precise function during 60S maturation is not well understood, our lab has shown that deletion of *REI1* results in a cold-sensitivity phenotype that coincides with a failure to release Arx1p from free 60S subunits in the cytoplasm. The inability to recycle Arx1p to the nucleus, in turn, leads to a disruption in 60S biogenesis and export (Hung and Johnson, 2005).

While Efl1p and Rei1p appear to play critical roles in Tif6p and Arx1p recycling, respectively, little is known about the nature in which the export adapter, Nmd3p, is released from 60S subunits prior to translation. As stated previously, our lab has shown that disruption of Rpl10p function leads to cytoplasmic entrapment of Nmd3p on free 60S subunits (Hedges et al., 2005; West et al., 2005). This observation could reflect a requirement for Rpl10p in recruiting an additional trans-acting factor(s) that facilitates Nmd3p's release. Alternatively, as loading of Rpl10p into 60S subunits has previously been implicated as a requisite step for subunit joining (Eisinger et al., 1997b), Nmd3p's release may coincide with the initiation event itself. In this scenario, a block in initiation resulting from a disruption in Rpl10p structure or function would preclude the release of Nmd3p from cytoplasmic subunits, simultaneously arresting translation initiation and 60S export.

1.5 Translation initiation

Following late maturation events in the cytoplasm, the two ribosomal subunits become incorporated into the pool of translating ribosomes. During translation, the small subunit interacts with both mRNA and the anticodon portion of aminoacylated-tRNA and governs the fidelity of the peptidyl-transferase reaction by ensuring proper (cognate)

codon-anticodon base-pairing. The large ribosomal subunit, on the other hand, interacts with the acceptor ends of tRNAs and catalyzes the peptidyl-transferase reactions between the incoming tRNA-bound amino acids and the growing polypeptide chain.

Translation is conceptually divided into four dynamic stages that are conserved in all organisms: initiation, elongation, termination, and recycling ((Kapp and Lorsch, 2004) and references therein). Initiation entails the assembly of the ribosome at the initiation codon of an mRNA with a unique methionyl "initiator" tRNA positioned in its peptidyl (P) site (see below). During elongation, or peptide synthesis, an aminoacylated-tRNA in a complex with the GTPase EF-Tu (EF1A in eukaryotes) is delivered to the acceptor/aminoacyl (A) site of the large subunit, and a proper codon-anticodon interaction stimulates EF-Tu's GTPase activity, releasing it from the ribosome. The rRNA (23S in bacteria and 25/28S in eukaryotes) of the large subunit then catalyzes the formation of a peptide bond between the incoming amino acid and the nascent polypeptide chain, while the GTPase EF-G (EF2 in eukaryotes) binds to the large subunit at the A-site. The tRNAs and mRNA are then "translocated" by GTP-hydrolysis on EF-G such that the next codon on mRNA is moved into the A-site, and the P- and A-site tRNAs are transferred to the E (exit) and P sites of the ribosome, respectively. This process occurs in an iterative fashion until a stop codon is encountered, at which time the full-length nascent polypeptide is released from the ribosome in a peptidyl-tRNA hydrolysis reaction mediated by peptide release factors (RF1/RF2 and RF3 in bacteria; eRF1 and eRF3 in eukaryotes). Recycling subunits for subsequent rounds of translation requires the dissociation of the two subunits in conjunction with release of the mRNA and de-acylated tRNA. This phase of translation is mediated by a dedicated ribosome-recycling factor (RRF) in prokaryotes that cooperates with EF-G and IF3 to destabilize the interaction between the two subunits, while releasing mRNA and tRNA. Although no

analogous mechanism has been characterized in eukaryotes, the circularization of eukaryotic mRNA during translation (see below) may promote the efficient recycling of ribosomes upon a particular transcript.

In eukaryotes, translation initiation requires no less than twelve initiation factors (composed of 23 different polypeptides) to assemble the translation-competent 80S ribosome (Kapp and Lorsch, 2004). Assembly of the initiation complex begins with the selection of the initiator tRNA (Met-$tRNA_i^{MET}$) among the pool of elongator tRNAs. In eukaryotes, this is accomplished by eukaryotic initiation factor 2 (eIF2) in autonomy from the small ribosomal subunit. The eIF2/GTP/Met-$tRNA_i^{MET}$ ternary complex is then recruited along with eIF3, eIF1, and eIF1A to the 40S (small) subunit to generate the 43S pre-initiation complex (Benne and Hershey, 1978). The 43S pre-initiation complex, in turn, is recruited to the 5' m^7G cap of an mRNA via an interaction between eIF3 and eIF4G of the cap-binding complex. Eukaryotic mRNAs lack Shine-Dalgarno sequences in their 5' sequences. Therefore, the cap-binding complex, anchored to the 5' end of the transcript by eIF4E, functionally replaces the rRNA:mRNA prokaryotic binding strategy by physically bridging the interaction between the 43S pre-initiation complex and the mRNA. Upon delivery to an mRNA, the 43S complex "scans" along the 5' untranslated region (5' UTR) of the transcript until it encounters the initiation codon (AUG), where it pauses due to codon-anticodon base-pairing between the mRNA and the initiator tRNA. The fidelity of initiation codon recognition is thought to be governed by eIF1, the eukaryotic homologue of IF3 (Pestova and Kolupaeva, 2002; Yoon and Donahue, 1992). Once formed, this 48S initiation complex is primed for engaging the 60S (large) subunit to begin elongation.

The recruitment of the 60S subunit to the initiation complex is coordinated with the displacement of initiation factors that would sterically block 80S formation or inhibit

elongation. Base-pairing between the initiation codon and the anticodon of MET-$tRNA_i^{MET}$ triggers GTP hydrolysis on eIF2, which deposits the initiator tRNA in the P site of 40S and releases eIF2-GDP from the initiation complex. eIF2's inherently weak GTPase activity is induced by the GTPase-activating protein (GAP), eIF5, which recognizes the appropriate conformation adopted by the codon-anticodon interaction on AUG (Raychaudhuri, 1985). Historically, eIF1, eIF1A, and eIF3 were also thought to dissociate from the 48S complex at this time. It has recently been shown, however, that these factors remain associated with the initiation complex after eIF2-GDP release and are not displaced until subunit joining (Unbehaun et al., 2004). 80S formation is triggered by a second GTPase, eIF5B, the eukaryotic homologue of bacterial IF2 (Pestova et al., 2000). While it is believed that eIF5B binds to the 48S initiation complex just before or after GTP hydrolysis on eIF2, the manner in which it stimulates 60S joining is poorly understood. Nevertheless, the eIF5B-mediated recruitment of the 60S subunit is the step at which eIF1, eIF1A, and eIF3 are released from the initiation complex (Unbehaun et al., 2004). Therefore, like its prokaryotic counterpart (IF2), eIF5B coordinates the release of initiation factors in conjunction with subunit joining.

In contrast to early models, the GTPase activity of eIF5B has been shown to be dispensable for subunit joining (Lee et al., 2002; Pestova et al., 2000; Shin et al., 2002). Instead, GTP hydrolysis acts to release eIF5B from the initiation complex only after 60S joins in a late regulatory step that is required for protein synthesis (Shin et al., 2002). This has led to the formulation of a model in which it is predicted that eIF5B's GTPase activity is not induced until it "senses" that the 80S ribosome is competent for elongation (Kapp and Lorsch, 2004). It is intriguing that IF2 (bacterial eIF5B) makes extensive contacts with the ribosomal protein L16 in recent cryo-EM reconstructions of translation initiation complexes from *Escherichia coli* (Allen et al., 2005). It has separately been

reported that L16 forms part of the tRNA acceptor site (A site) in the crystal structure of the bacterial 50S subunit (Bashan et al., 2003; Nishimura et al., 2004; Yusupov et al., 2001). In both prokaryotes and eukaryotes, L16 (Rpl0p in yeast) loads onto the large subunit late in the assembly pathway (Dohme and Nierhaus, 1976; Kruiswijk et al., 1978), and in yeast, this event has been described as a requisite step for subunit joining (Eisinger et al., 1997b). In light of its putative interaction with L16 (Rpl10p) and its delayed release from 70S subunits, IF2, and eIF5B by analogy, may proofread the structural integrity of the A site on the large ribosomal subunit before conferring translation competence through GTPase-dependent release from the initiation complex. In this way, eIF5B may serve as the last control point in assessing the fidelity of the ribosome prior to translation.

While the 5' ends of mRNAs recruit the 43S ternary complex via a direct interaction between eIF3 and eIF4G (of the 5' m^7G cap-binding complex), the 3' end of an mRNA is thought to play a key role in initiation as well. Early work in yeast translation extracts demonstrated that the 3' poly(A) tail was capable of enhancing the delivery of 43S pre-initiation complexes to mRNAs (Tarun and Sachs, 1995). Biochemical and genetic analyses have since demonstrated that the poly(A) tail likely mediates its influence on translation initiation through the activity of the poly(A) binding protein, PABP (Pab1p in yeast)((Mangus et al., 2003) and references therein). The observation that PABP is capable of binding to eIF4G *in vitro* led to the proposal that efficient recycling of ribosomes to the initiation site may result from the circularization of mRNAs in response to a direct interaction between PABP and the cap-binding complex (Jacobson and Peltz, 1996). In this scenario, the association between factors at the 3' and 5' ends of mRNA could allow 40S to ferry over the poly(A) tail back to the 5' end of the transcript. This model gained considerable momentum when PABP along with eIF4G

and eIF4E were shown to circularize capped and polyadenlyated mRNAs *in vitro* (Wells et al., 1998). It has also been suggested that the persistence of PABP at the 3' ends of viable mRNAs aids initiation complex formation by enhancing the rate at which the cap-binding complex is recruited to the 5' end of transcripts, which, in turn would enhance 43S binding via the eIF3-eIF4G interaction (Le et al., 1997; Sachs and Varani, 2000; Wei et al., 1998).

Several lines of evidence indicate that PABP may also stimulate translation initiation in a poly(A)-independent manner, most likely at the point of subunit joining. First, the addition of exogenous Pab1p to yeast extracts enhances the translation of capped mRNAs lacking poly(A) tails, indicating that Pab1p is capable of eliciting its effects independent of its association with the 3' ends of transcripts ((Otero et al., 1999). Furthermore, mutations in eIF4G in yeast that disrupt its interaction with Pab1p, and likely block circularization of mRNA, elicit no observable growth defects *in vivo* (Tarun et al., 1997). An early study by Sachs and Davis, in which it was it observed that inhibition of *PAB1* expression in yeast resulted in a block in subunit joining (Sachs and Davis, 1989), indicated that Pab1p might also play a role in late stages of initiation. In support of this observation, *pab1* temperature-sensitive mutants accumulate free 60S subunits at non-permissive temperature, consistent with a block in the 60S joining step of initiation (Sachs and Davis, 1989). Recent work in a mammalian cell-free system revealed that depletion of PABP from extract inhibited the formation of *both* 48S and 80S initiation complexes on mRNAs, while also impairing the recruitment of the cap-binding complex to the 5' ends of mRNAs (Kahvejian et al., 2005). The unexpected observation that PABP-depletion led to a preferential block in 80S formation relative to 48S (~ two-fold greater inhibition) in this system, however, points toward a unique role for PABP in the 60S joining step of initiation (Kahvejian et al., 2005). Therefore, while its precise

role(s) in translation initiation is currently unclear, it is not inappropriate to consider PABP (Pab1p) as a *bona fide*, multi-functional translation initiation factor that likely facilitates the formation of both the 48S and 80S initiation complexes.

As outlined above, established models for translation initiation in eukaryotes largely center on the binding and release of factors on the small ribosomal subunit. In general, the joining of the large subunit to the initiation complex is viewed as a default state that is predominately governed by the need to release factors on the surface of 40S that sterically-oppose 80S formation. In reality, subunit joining in eukaryotes is likely regulated by events that occur on both subunits. The obligatory release of the anti-association factor, Tif6p, from nascent 60S subunits in the cytoplasm, for instance, could be viewed as a translation initiation step for immature subunits that may be coordinated with a positive structural assessment of the large subunit by Efl1p (Senger et al., 2001).

While the Efl1p-mediated release of Tif6p is specific to newly-exported subunits, pulse chase analyses conducted with radiolabeled ribosomes have demonstrated that Nmd3p, Lsg1p, and the ribosomal protein Rpl10p exchange on mature subunits in the free 60S pool (Kallstrom et al., 2003). As Nmd3p has orthologues in Archaea, which lack nuclei, its association with mature subunits may reflect a more fundamental role in ribosome maintenance than nuclear export. It is also worth noting that Rpl10p is sub-stoichiometric to other core ribosomal proteins in the free 60S population (~1:10) (Eisinger et al., 1997b), residing on non-translating subunits at a ratio that is more closely in line with trans-acting factors such as Nmd3p or Lsg1p (~1:9)((Ho et al., 2000a) and West and Johnson, unpublished). This may be indicative of a regulatory function for Rpl10p within the free 60S population. Intriguingly, dominant mutations in *NMD3* are capable of suppressing mutant alleles of *RPL10* (Karl et al., 1999). In light of the fact that Rpl10p is reputedly required for 80S formation (Eisinger et al., 1997b), Nmd3p and

Rpl10p may cooperate either directly or indirectly in the subunit-joining phase of translation initiation. As the GTPase Lsg1p shows a similar pattern of exchange, it may also participate in the regulation or timing of this event through its cycles of GTP hydrolysis. Alternatively, Nmd3p, Rpl10p, and/or Lsg1p may aid in the recycling (i.e. dissociation) of mature 60S subunits from post-translational ribosomes, a conserved process that remains poorly understood in eukaryotes. As initiation and recycling are most likely intimately connected events, these possibilities are not mutually exclusive. These speculations will hold more weight in the context of the data presented in the body of this dissertation.

1.6 Dissertation Objectives

I began my dissertation work with the intention of identifying the nucle(ol)ar 60S biogenesis factor(s) that failed to recycle to the nucleus in the absence of proper Lsg1p function. This objective was based predominately on the published observation that, while restricted to the cytoplasm, the putative GTPase Lsg1p paradoxically influences nucleolar rRNA processing and subsequent nuclear export of the large ribosomal subunit (Kallstrom et al., 2003). Through the course of my research, I have demonstrated that the essential 60S nuclear export adapter, Nmd3p, fails to recycle off of cytoplasmic 60S subunits to the nucleus when Lsg1p function is perturbed, accounting for the block in 60S export observed in *lsg1* mutants. I also provide evidence that Lsg1p and the ribosomal protein, Rpl10p, function cooperatively to release Nmd3p prior to translation initiation. Moreover, in a departure from previously-published models (Gadal et al., 2001b), my findings support a role for Lsg1p in facilitating the loading of Rpl10p into a late cytoplasmic 60S biogenesis intermediate in the context of Rpl10p's molecular chaperone, Sqt1p. These observations have led me to propose that GTP-hydrolysis on Lsg1p results in a late structural rearrangement on cytoplasmic 60S subunits that loads Rpl10p and

releases Nmd3p, priming the subunits for translation and sustaining 60S export. This proposal is supported by the results presented in the first two results chapters of this dissertation. The last results chapter is a synthesis of my most recent work aimed at further characterizing the manner in which Nmd3p interacts with components of the nuclear transport apparatus, including the identification of *NMD3* mutants that exhibit a "supraphysiological" interaction with the nuclear export receptor, Crm1 (Xpo1p).

In the past few years, our appreciation of the breadth and intricacy of ribosome biogenesis has undergone a renaissance with the advent of affinity purification techniques that have allowed for the characterization of pre-ribosomal intermediates at different stages of their maturation. This new approach has bolstered our understanding of when trans-acting biogenesis factors might perform their functions in subunit maturation, yet in most cases, has provided little insight into the specificity or consequences of these activities. Therefore, much work is still needed to dissect the specific functions of proteins that participate in this complex pathway in order to gain a true appreciation of how this process is both orchestrated and regulated. My research has provided a significant contribution to this understanding, as it includes one of the few direct functional contexts for a ribosome biogenesis factor (Lsg1p).

This dissertation is comprised of five separate chapters. Chapter 1 has already provided a broad overview of our current understanding of ribosome biogenesis with a particular emphasis on factors and events that influence the transport of ribosomal subunits from the nucleus and the manner in which they initially engage the translational machinery. Chapter 2 contains a description of the materials and methods that I incorporated in the research described within the body of Chapters 3 through 5. The third chapter will provide evidence that proper Lsg1p function is necessary for recycling the 60S export adapter, Nmd3p, back to the nucleus. Chapter 4 extends upon the themes

presented in Chapter 3 to include evidence that Lsg1p and the ribosomal protein, Rpl10p, function synergistically to mediate the release of Nmd3p from cytoplasmic 60S subunits prior to translation initiation. Moreover, results presented in this chapter stand in opposition to previously published models for the spatio-temporal loading of Rpl10p onto 60S subunits, leading to a paradigm shift in our interpretation of late 60S maturation. Lastly, Chapter 5 includes a preliminary characterization of a class of *nmd3* mutants that provides insight into the manner in which Nmd3p engages the nuclear export machinery. As a whole, this body of work considerably enhances our understanding of the cytoplamic events that transpire on nascent 60S ribosomal subunits prior to and at the point at which they are incorporated into the cellular pool of translating ribosomes.

Chapter 2: Description of Materials and Methods

The experimental materials and methods used in the results chapters (3-5) of this dissertation are described in detail within this chapter. The first time that a particular plasmid, strain, or method is introduced it will be described in full. The standard yeast genetics methods and media that are incorporated throughout this chapter have been described previously in (Kaiser et al., 1994). All yeast strains were cultured at 30°C in drop-out (synthetic complete) or rich (yeast extract-peptone) media containing either 2% glucose, 1% raffinose or 1% galactose as the carbon source unless stated otherwise in figure legends or text.

2.1 Materials and Methods for Chapter 3

2.1.1 Strains, plasmids, and culture media

The strains used in Chapter 3 are listed in Table 2.1. Yeast transformations, sporulations, and tetrad dissections were conducted according to standard protocols (Gietz et al., 1992). The *NMD3-GFP* genomic fusion strain was generated by homologous recombination according to established techniques (Longtine et al., 1998). Briefly, the oligonucleotide primers 5'-AGAAGATGGAGTCGAGAACACACCCGTTGAATCTCAGCAGCGGATCCCCG GGTTAATTAA and 3'-ACTGAAATGCTAGTGTTTGTTAAGAGTATATACTACTCTCGAATTCGAGC TCGTTTAAAC were used to PCR-amplify the GFP moiety from plasmid pFA6a-KanMX6-GFP(S65T). The PCR product was transformed into the wild-type haploid strain CH1305 (Kranz and Holm, 1990). Geneticin-resistant transformants were selected, and integration was confirmed by PCR and fluorescence microscopy to yield the strain AJY1708. AJY1539 and AJY1548, haploid strains containing a point mutation in genomic *CRM1* that renders it sensitive to the drug leptomycin B (LMB), were produced

as follows. A *crm1Δ::KanMX4/CRM1* heterozygous diploid strain (Research Genetics) was transformed with a derivative of pDC-CRM1 (Neville and Rosbash, 1999) in which *LEU2* was replaced with *URA3*. Cells were sporulated, and a *crm1::KanMX* containing spore clone was transformed with the *Bgl*II-*Sca*I *CRM1(T539C)*-containing fragment from pDC-CRM1(T539C) (Neville and Rosbash, 1999) for *in vivo* homologous recombination into the genomic locus. Recombinants were incubated on YPD plates overnight and then replicated twice to 5-FOA-containing plates. 5-FOA-resistant clones were scored for G418 sensitivity and integration was confirmed by PCR analysis utilizing the HA-tag within *CRM1(T539C)* to give strains AJY1539 and AJY1548 (A. Johnson). AJY1708 was crossed with AJY1548, and the resulting heterozygous diploid was sporulated and dissected to generate the spore clone AJY1705 (*NMD3-GFP crm1[T539C]*). *nmd3-3 lsg1-2* and *nmd3-4 lsg1-3* strains were produced in the following manner. AJY729 and AJY736, haploid strains containing genomically-integrated *nmd3-3* and *nmd3-4* mutant alleles (alternate spore clones of those described previously) (Ho and Johnson, 1999), respectively, were mated with AJY1171 (*lsg1Δ::KanMX4*), possessing a wild-type copy of *LSG1* on a pRS316 vector (pAJ626) (Kallstrom et al., 2003). The resulting heterozygous diploids were sporulated to yield spore clones AJY1511 (*lsg1Δ::KanMX4* [pAJ626]), AJY1512 **(***lsg1Δ::KanMX4 nmd3-3::HIS3* [pAJ626]), AJY1513 (*nmd3-3::HIS3*), and AJY1518 **(***nmd3-4::HIS3***)** and AJY1521 **(***lsg1Δ::KanMX4 nmd3-4::HIS3* [pAJ626]). AJY1511, AJY1512, and AJY1521 were then transformed with either pAJ741 (*lsg1-2*) or pAJ742 (*lsg1-3*) (Kallstrom et al., 2003), and pAJ626 was replaced by the appropriate mutant *lsg1* allele by streaking transformants onto 5-FOA plates.

TABLE 2.1 Strains used in Chapter 3.

Strain	Genotype and notes	Source or Reference
CH1305 (wt)	*MAT*a *ade2 ade3 leu2 lys2-801 ura3-52*	(Kranz and Holm, 1990)
W303 (wt)	*MAT*a *leu2-3,112 his3-11 ura3-1 trp1-1 ade2-1 can1-100 SSD1-d*	J. Warner
AJY729	*MAT*a *ade2 ade3 leu2 lys2-801 ura3-52 trp1 nmd3-3*	(Ho and Johnson, 1999)
AJY1171	*MAT*a *his3Δ1 leu2Δ0 met15Δ0 ura3-52 lsg1Δ::KanMX4*	(Kallstrom et al., 2003)
AJY1511	*MAT*α *leu2 ura3 lsg1Δ::KanMX4*	This study
AJY1512	*MAT*a *leu2 ura3 lsg1::KanMX4 nmd3-3*	This study
AJY1513	*MAT*a *leu2 ura3 nmd3-3*	This study
AJY1518	*MAT*a *leu2 ura3 nmd3-4*	This study
AJY1521	*MAT*α *leu2 ura3 lsg1::KanMX4 nmd3-4*	This study
AJY1539	*MAT*a *leu2Δ0 ura3Δ0 his3Δ1 met15Δ0 CRM1(T539C)-HA*	This study
AJY1548	*MAT*α *leu2Δ0 ura3Δ0 his3Δ1 met15Δ0 CRM1(T539C)-HA*	This study
AJY1705	*MAT*a *leu2 ura3 NMD3-GFP::KanMX6 CRM1(T539C)-HA*	This study
AJY1708	*MAT*a *ade2 ade3 leu2 lys2-801 ura3-52 NMD3-GFP::KanMX6*	This study

Plasmids used in Chapter 3 are listed in Table 2.2. pAJ879 (*GAL10*::*cmyc-LSG1*) was generated by restriction digestion of pAJ289 (*cmyc-LSG1* in pRS315)(Kallstrom et al., 2003) with *Nco*I and *Nhe*I followed by ligation into the same sites of pAJ368 (pRS315 with the *GAL10* promoter). The *lsg1-2* and *lsg1-3* conditional mutants (pAJ741 and pAJ742) were generated by random PCR mutagenesis of pAJ289 with the oligonucleotides AJO285 and AJO286 (see section 2.1.2) and isolated in the previously-described screen for *lsg1* conditional mutants (Kallstrom et al., 2003). pAJ409 (*NMD3* on *CEN* plasmid) was constructed by removing the open reading frame of *NMD3* from pAJ123 (Ho and Johnson, 1999) by digestion with *Sma*I and *Hind*III and ligation into the same sites of pRS416. pAJ903 (*LSG1-13xcmyc*) was made by amplifying *LSG1* from its genomic locus using 5' oligo AJO428

(GCGGCGGCCGCCCATGGGACGTCTGGCCAGCATGCGGTACTTTATACGTGTG CATTATTC) and 3' oligo AJO415 (CGCGCTAGCATTATTTTCAATGCTAAAAAC), digesting with NotI and NheI, and ligating into pRS315 along with *13xcmyc* sequence from XbaI-and HindIII-digested pAJ910 (*13xcmyc* in pRS416). pAJ908 (*RPL25-eGFP*) was constructed by introducing the *RPL25-eGFP* open reading frame from pASZ11-RPL25-eGFP (Gadal et al., 2001a) into pRS416. pAJ363 (*NMD3* on *2μ* plasmid) was constructed by transferring the open reading frame of *NMD3* as a *SnaB*I-*Sal*I digested fragment from pAJ78 (Ho and Johnson, 1999) into the same sites of a derivative of pRS426 that also contained *ADE3* (G. Schlenstedt). The original plasmids harboring the dominant negative *LSG1* mutants identified in the screen described in section 2.1.2 (pAJ1109, pAJ1117, pAJ1119, pAJ1131, pAJ1132, pAJ1310, pAJ1610, pAJ1613, pAJ1614, and pAJ1615) were derived by random PCR mutagensis of pAJ879 (see below). pAJ1143 (*GAL1::NMD3)* was obtained as a high-copy suppressor of *LSG1(N173Y,L176S)* (see section 2.1.10) in a screen using a *GAL1* yeast cDNA library (Liu et al., 1992). pAJ1312 (*GAL10::cmyc-LSG1*) and pAJ1278 (*GAL10::cmyc-LSG1[K349T]*) were made by introducing the BamHI-SalI restriction fragment from pAJ879 or pAJ1109, respectively, into the same sites of pRS316.

TABLE 2.2 Plasmids used in Chapter 3.

Plasmid	Relevant markers and notes	Source or Reference
pASZ11-Rpl25eGFP	*ADE2 CEN* (*RPL25-eGFP*)	(Gadal et al., 2001a)
pDC-CRM1(T539C)	*LEU2 CEN* (*CRM1(T539C)-HA*)	(Neville and Rosbash, 1999)
pAJ60	*ADE2 URA3 2μ* [pPS719]	(Silberstein et al., 1998)
pAJ78	*LEU2 2μ (NMD3)*	(Ho and Johnson, 1999)
pAJ289	*LEU2 CEN (cmyc-LSG1)*	(Kallstrom et al., 2003)
pAJ363	*URA ADE3 2μ (NMD3)*	This section
pAJ368	*LEU2 CEN (GAL10::NMD3Δ100-13xcmyc)*	(Kallstrom et al., 2003)
pAJ379	*URA3 2μ (GAL10::GSP1)* [pPS832]	(Schlenstedt et al., 1995a)
pAJ380	*URA3 2μ* (*GAL10::GSP1(G21V)* [pPS833]	(Schlenstedt et al., 1995a)
pAJ409	*URA3 CEN (NMD3)*	(Kallstrom et al., 2003)
pAJ538	*LEU2 CEN (NMD3-13xcmyc)*	(Ho et al., 2000a)
pAJ741	*LEU2 CEN (lsg1-2)*	(Kallstrom et al., 2003)
pAJ742	*LEU2 CEN (lsg1-3)*	(Kallstrom et al., 2003)
pAJ754	*LEU2 CEN (NMD3AAA-GFP)*	(Hedges et al., 2005)
pAJ755	*URA3 CEN (NMD3-GFP)*	(Hedges et al., 2005)
pAJ879	*LEU2 CEN (GAL10::myc-LSG1)*	This section
pAJ903	*LEU2 CEN (LSG1-13xcmyc)*	This section
pAJ908	*URA3 CEN (RPL25-eGFP)*	This section
pAJ910	*URA3 2μ (13xcmyc)*	This section
pAJ1109	*LEU2 CEN (GAL10::cmyc-LSG1[K349T])*	This section
pAJ1117	*LEU2 CEN (GAL10::cmyc-LSG1[T179A,L591F])*	This section
pAJ1119	*LEU2 CEN (GAL10::cmyc-LSG1[S107T,S351F,N406S])*	This section
pAJ1131	*LEU2 CEN (GAL10::cmyc-LSG1[N173Y,L176S])*	This section
pAJ1132	*LEU2 CEN (GAL10::cmyc-LSG1[I204T])*	This section
pAJ1143	*URA3 CEN (GAL1::NMD3)*	This section
pAJ1278	*URA3 CEN (GAL10::cmyc-LSG1[K349])*	This section
pAJ1310	*LEU2 CEN (GAL10::cmyc-LSG1[S350P])*	This section
pAJ1312	*URA3 CEN (GAL10::cmyc-LSG1)*	This section
pAJ1610	*LEU2 CEN (GAL10::cmyc-LSG1[Q536R])*	This section
pAJ1613	*LEU2 CEN (GAL10::cmyc-LSG1[K349N])*	This section
pAJ1614	*LEU2 CEN (GAL10::cmyc-LSG1[R267G])*	This section

2.1.2 Isolation of *LSG1* dominant negative mutants

Random PCR mutagenesis of *LSG1* was conducted using *Taq* polymerase (GeneChoice) with pAJ879 as template and the primers AJO285 (5'-CATGCCATGGAACAAAAGTTGATTTCTGAAGAAGACTTGAGCTCTATGCCAC CAAAAGAAGCT) and AJO286 (3'-CGTGACGTCTAATTATTTTCAATGCT). 20 independent reactions were performed in parallel, using 12 rounds of amplification in order to increase the number of independent mutagenic events. PCR products were gel-purified, pooled, and co-transformed with *Bcl*I- and *Bgl*II-linearized pAJ879 into wild-type CH1305 cells for *in vivo* homologous recombination of PCR products behind the control of the galactose-inducible *GAL10* promoter. Recombinants were plated onto SC-leu ura drop-out medium supplemented with 2% glucose. Colonies were then replica-plated onto drop-out media containing either glucose or galactose (1%) to identify colonies from glucose plates that failed to grow or grew slowly on galactose plates. Plasmids were recovered from selected mutants and transformed into *Escherichia coli* (DH5α) to amplify plasmid DNA. Out of approximately 35,000 colonies screened, 10 well-behaved dominant negative mutants were identified. Table 2.3 contains a listing of the *LSG1* dominant negative mutants derived from this screen. Sequencing of mutant *LSG1* alleles was conducted by the DNA Sequencing Facility at the ICMB Core (UT Austin).

TABLE 2.3 Dominant negative *LSG1* mutants.

Original isolate designation	Amino Acid Substitutions	Designation in publications	Plasmid Name
LSG1 DN- #1	K349T	*LSG1-10*	pAJ1109
LSG1 DN- #2	Q536R	*LSG1-20*	PAJ1610
LSG1 DN- #3	I204T	*LSG1-30*	pAJ1132
LSG1 DN- #5	T179A, L591F	*LSG1-5*	pAJ1117
LSG1 DN- #7	S107T,S351F,N406S	*LSG1-7*	pAJ1119
LSG1 DN- #14	S350P	*LSG1-14*	pAJ1310
LSG1 DN- #41	K349N	*LSG1-41*	pAJ1613
LSG1 DN- #51	R267G	*LSG1-51*	pAJ1614
LSG1 DN- #52	N173Y,L176S	*LSG1-52*	pAJ1131
LSG1 DN- #53	K349R	*LSG1-53*	pAJ1615

2.1.3 Isolation of *lsg1* loss-of-function mutants

Random PCR mutagenesis of *LSG1* was conducted using *Taq* polymerase (GeneChoice) with pAJ903 as template and the primers AJO285 (5'-CATGCCATGGAACAAAAGTTGATTTCTGAAGAAGACTTGAGCTCTATGCCAC CAAAAGAAGCT) and AJO286 (3'-CGTGACGTCTAATTATTTTCAATGCT). 20 independent reactions were performed in parallel, using 12 rounds of amplification in order to increase the number of independent mutagenic events. PCR products were gel-purified, pooled, and co-transformed with *Bcl*I- and *Bgl*II-linearized pAJ903 for *in vivo* homologous recombination into strain AJY1171 (*lsg1Δ::KanMX4* [pAJ626]), which maintained growth by harboring wild-type *LSG1* on a low-copy (*CEN*) *URA3* plasmid. Recombinants were selected on SC-leu glucose plates and replica plated onto 5-fluoroorotic acid (5-FOA)-containing media to identify constitutive slow growth mutants or cells incapable of supporting growth after eliminating the wild-type *LSG1* plasmid. Plasmids were recovered from selected mutants and transformed into *Escherichia coli* (DH5α) to amplify plasmid DNA. Comparative western analysis against the C-terminal

oligomeric c-myc tag was incorporated to eliminate truncation mutants. Out of approximately 12,000 colonies screened, 18 full-length, loss-of-function mutant alleles were identified. Appendix B contains a listing of the *lsg1* loss-of-function mutants derived from this screen. Sequencing of mutant *LSG1* alleles was conducted by the DNA Sequencing Facility at the ICMB Core (UT Austin).

2.1.4 Polysome analysis

For the sucrose linear density gradients in Figures 3.2, 3.7, and 3.12, dense overnight cultures of the wild-type yeast strain (CH1305) harboring relevant plasmids were diluted to OD_{600} ~0.1 into 150 ml of fresh raffinose-containing drop-out medium and incubated at 30°C. When cultures reached OD_{600} ~0.25, they were supplemented with galactose for induction of the *LSG1* alleles and cultured for an additional 3-6 hrs. Cycloheximide (150μg/mL final concentration) was then mixed with each culture followed by a 20-minute incubation on ice. Cells were harvested, and pellets were frozen at –80°C until use. Subsequent steps were carried out on ice or at 4˚C. Cell pellets were washed once with one ml of "polysome lysis buffer" (10mM Tris-HCl pH 7.5, 100mM KCl, 10mM $MgCl_2$, 6mM BME, 150μg/ml cycloheximide, and protease inhibitors [1μg/ml each of leupeptin and pepstatin A and 1mM phenylmethylsulfonylfluoride [PMSF]). Cells were pelleted and resuspended in ~ one volume of the same buffer and lysed via glass bead abrasion (4x30 second intervals on vortexer separated by one minute periods of cooling on ice). Extracts were clarified by pelleting-out insoluble material via centrifugation at 15,000Xg for 10 minutes. 9 OD_{260} units of supernatant were loaded onto linear 7-47% sucrose gradients prepared in polysome lysis buffer. After a 2.5-hour spin at 40,000 rpm (4˚C) in a Beckman SW40 rotor, gradients were fractionated while monitoring absorbance at 254 nm on an ISCO density gradient fractionator. Automated collection of ~900μl fractions was conducted by the fractionator. Where appropriate,

proteins were precipitated from gradient fractions by the addition of 10% trichloroacetic acid followed by a 30-minute incubation on ice prior to centrifugation at 15,000Xg for 10 minutes (4˚C). Pellets were air-dried and resuspended in 50µl of 1X Laemmli buffer at 99˚C, and proteins from fractions were resolved on 12% SDS-PAGE gels. Western analysis was performed as described in section 2.1.5, using either α-Nmd3p or α-L1a (F. Lacroute) antibodies.

2.1.5 Western blotting

Proteins were resolved on SDS-PAGE gels and subsequently transferred to nitrocellulose membranes in a semi-dry transfer cell (BIORAD) by eletrophoresis with Towbin's buffer (192mM Glycine, 25mM Tris-Base, 20% methanol, and 0.01% SDS). Following transfer, membranes were blocked for 30 min. in TBS (10mM Tris-HCl pH 8.0, 150mM NaCl) plus 3% dry milk solution. Membranes were then washed with TBST (TBS + 0.1% Tween 20) and incubated for 3 hours with primary antibody (as denoted in figure legends) diluted in TBST. After washing membranes extensively with TBST, they were incubated with appropriate secondary antibodies (alkaline phosphatase or horseradish peroxidase conjugates) in TBST for 30 min. followed by extensive washing in TBST then TBS. Western blots were developed for colorimetric (alkaline phosphatase) or chemiluminscent (horseradish peroxidase) analysis where appropriate.

2.1.6 GFP fluorescence microscopy

Visualization of fluorescence emitted upon excitation of GFP was adapted from a protocol established by the laboratory of Pamela Silver (Stage-Zimmermann et al., 2000). Specific strains and their growth conditions are described in each figure legend. After culturing cells, 37% formaldehyde was added to each culture to a volumetric ratio of 1:9 to fix the cells. Fixation was carried-out for 40 minutes, and cells were washed two times with PBS (0.1M potassium phosphate pH 6.6) and resuspended in KSorb buffer (0.1M

potassium phosphate pH 6.6, 1.2M sorbitol). Cells were permeabilized for 4 minutes in the presence of 0.05% TritionX-100, and nuclei were stained with DAPI (1μg/ml) for 2 minutes. Cells were washed twice with PBS and mounted on glass slides. Fluorescence was visualized on a Zeiss Axiophot microscope fitted with a X100 objective lens and a Princeton Electronics Micro-MAX charge-coupled device camera controlled by IPLab Spectrum P software from Signal Analytics Corp. or on a Nikon E800 microscope fitted with a X100 objective and a Diagnostic Instruments SPOT II camera controlled by SPOT software. Cell images were prepared using Adobe Photoshop 5.0.

2.1.7 Indirect immunofluorescence microscopy

Immunofluorescence microscopy was performed using a previously-described protocol (Ho and Johnson, 1999). Specific strains and their growth conditions are described in Figure 4.3. Cell fixation was conducted as described in section 2.1.6. Cells were then washed two times in KSorb buffer (0.1M potassium phosphate pH 6.6, 1.2M sorbitol). Cells were resuspended in 100μl of KSorb containing 10mM dithiothreitol (DTT). "Yeast lytic enzyme" (Zymolyase T100) was added to the suspensions at a concentration of 0.1mg/ml to spheroplast the cells. Cells were incubated at 30°C followed by two washes with KSorb plus 1mM PMSF. 10μl from each cell suspension was aliquoted into an individual poly-lysine-coated well on a multi-well slide. Residual liquid was aspirated off after 1 minute. Bound cells were then permeabilized in ice cold methanol for six minutes at –20˚C followed by treatment with ice cold acetone for 30 seconds. After completely air-drying the slides, cells were blocked in PBS plus 1% BSA solution for 30 minutes. Primary antibody (α-myc, Covance [9e10]) was added to cells at a 1:500 dilution in PBS plus 1% BSA and incubated for two hours in a damp chamber at ambient temperature. Cells were washed three times in PBS plus 1% BSA followed by incubation with Cy2-conjugated goat anti-mouse secondary antibody (Jackson IRL) at a

1:500 dilution in PBS plus 0.1% BSA solution for one hour in a damp chamber at ambient temperature. After washing cells in PBS plus 0.1% BSA, a 1μg/ml solution of DAPI (in PBS plus 0.1% BSA) was added to each well for staining nuclei (DNA). Cells were washed three additional times (5 min./wash) and were mounted in AquaPolymount (Poly Biosciences) beneath a coverslip. Fluorescence was visualized as described in section 2.1.6.

2.1.8 LMB treatment

For the experiment depicted in Figure 3.5, dense overnight cultures of cells grown in raffinose-containing drop-out media were diluted to an OD_{600} reading of ~0.1 in fresh drop-out media with 1% raffinose as non-inducing carbon source. Cells were cultured at 30˚C until an OD_{600} reading of ~0.2 was reached. Cultures were then supplemented with galactose to 1% and cultured an additional 3 hrs. Cells were concentrated ten-fold, and leptomycin B (LMB) (M. Yoshida) was added to each culture at a final concentration of 0.1μg/ml. After 20 minutes, cells were fixed and prepared for visualization as described in section 2.1.6.

2.1.9 Growth assay for *nmd3* and *lsg1* synthetic lethality

AJY1511 (*lsg1Δ::KanMX4/*pAJ626[*LSG1/URA3*]), AJY1512 (*lsg1Δ::KanMX4/*pAJ626[*LSG1/URA3*] *nmd3-3*), and AJY1521 (*lsg1Δ::KanMX4/*pAJ626[*LSG1/URA3*] *nmd3-4*) were transformed with either *lsg1-2* or *lsg1-3* mutant alleles on *LEU2* plasmids, pAJ741 and pAJ742, respectively. Transformants were re-streaked onto 5-FOA plates to replace wild-type *LSG1::URA3* plasmids with the appropriate mutant allele of *lsg1*. AJY1513 (*nmd3-3*), AJY1518 (*nmd3-4*), and wild-type strains were streaked alongside the mutant *lsg1*-containing strains for growth comparisons. Plates were incubated at room temperature (~25°C) for 10 days.

2.1.10 High-copy suppressor screen for *LSG1(N173Y,L176S)*

To screen for high-copy suppressors of *LSG1[N173Y,L176S]*, yeast strain CH1305 (wild-type) harboring pAJ1131 (*GAL10::LSG1[N173Y,L176S]/LEU2*) was transformed with a *URA3 GAL1*-inducible cDNA library (Liu et al., 1992). Transformants were selected on SC-ura leu/glucose plates at 30°C. Cells were washed off plates and resuspended in 15% glycerol to generate a library of transformants. The transformant library was aliquoted and stored at –80˚C. Library stock was diluted to yield ~1000 CFUs per plate for incubation on SC-ura leu/galactose plates. From ~26,000 transformants, 56 colonies exhibited enhanced growth on galactose-containing media relative to cells transformed with empty vector. Putative suppressors were isolated and re-tested for growth suppression on SC-ura leu/galactose plates. Growth suppression was then shown to be plasmid-dependent for 14 of the suppressors. Six strong suppressors were chosen for further analysis. Diagnostic restriction digests eliminated two of these candidates, as they were determined to correspond to *LSG1*. Sequence analysis of the remaining cDNAs revealed that *PAB1* (3 isolates) or *NMD3* (1 isolate) were responsible for the observed strong suppression.

2.1.11 Comparative growth assays

Saturated overnight cultures were either streaked onto appropriate growth media to resolve single colonies or aliquoted onto media from ten-fold serial dilutions after standardizing the starting concentrations according to cell density readings at OD_{600}. Growth conditions were maintained as described in section 2.1 with specific modifications listed in figure legends.

2.2 Materials and Methods for Chapter 4

2.2.1 Strains, plasmids, and culture media

The strains used in Chapter 4 are listed in Table 2.4. The *rpl10(F85S)* genomic integrant was generated by PCR-amplifying the mutant locus from strain AJY1320 (*grc5ts942*) (Zuk et al., 1999) using 5' oligo AJO264 (CGCGGATCCGAAACTAGTTAGCAC) and 3' oligo AJO265 (CGCCCATGGCTACCCAACATGCTGAAC). The PCR product was transformed into AJY1435 (*rpl10::KanMX4*/pAJ730 [*RPL10/URA3*]) for *in vivo* homologous recombination into the *RPL10* genomic locus. Cells were plated on YPD at 25°C, and after two days, were replica-plated onto a 5-FOA-containing medium to select for loss of the *URA3* plasmid containing the wild-type gene. 5-FOA-resistant colonies were streaked onto G418 plates to score for geneticin sensitivity. Among geneticin-sensitive recombinants, integration of the *rpl10(F85S)* allele was confirmed by sequencing to yield AJY1440 (J. Hedges). AJY1896 (*nmd3::TRP1 CRM1[T539C]-HA*) was generated by mating AJY531 (*nmd3::TRP1/*pAJ112 [*NMD3/URA3*]) (a spore clone derived from the mating previously described in (Ho and Johnson, 1999) with AJY1548 (section 2.1.1). The resultant diploid strain was sporulated and dissected to isolate spore clones possessing both of the altered loci (*nmd3::TRP1 CRM1[T539C]-HA*). Genomic DNA was isolated from 5-FOA-sensitive spore clones, and PCR verification was carried-out using primers specific to the mutant *CRM1[T539C]-HA* allele. AJY1961 was made by PCR amplifying *3xHA*::*KanMX6* from pFA6a-3HA-KanMX6 (Longtine et al., 1998) using the 5' oligonucleotide AJO718 (GAAAACAACATCAGAGAATTCCCAGAATACTTTGCTGCTCAAGCTCGGATCC CCGGGTTAATTAA) and the 3' oligonucleotide AJO719 (TAATAAACTAGAATTTAAATCAAAAAAATTTCTCTTTTAAGTTAGGAATTCG

AGCTCGTTTAAAC). The resultant PCR product was transformed into wild-type strain W303 for *in vivo* homologous recombination. Recombinants were selected on G418 plates, and a clone containing hemagglutinin (HA)-tagged *RPL10* was verified by PCR analysis.

TABLE 2.4 Strains used in Chapter 4.

Strain	Genotype and notes	Source or Reference
CH1305 (wt)	*MAT*a *ade2 ade3 leu2 lys2-801 ura3-52*	(Kranz and Holm, 1990)
W303 (wt)	*MAT*a *leu2-3,112 his3-11 ura3-1 trp1-1 ade2-1 can1-100 SSD1-d*	J. Warner
AJY531	*MAT*a *ade2 his3Δ1 leu2 ura3 trp1 (nmd3::TRP1)* (pAJ112)	(Ho and Johnson, 1999)
AJY1134	*MAT*α *ura3-52 leu2-3 pep4-3 prb1-1122 reg1-501 gal1*	(Hovland et al., 1989)
AJY1320	*MAT*a *ade2-101 his3-200 tyr1 ura3-52 grc5ts942*	(Zuk et al., 1999)
AJY1435	*MAT*a *lys2Δ0 met15Δ0 his3Δ1 leu2Δ0 ura3Δ0 rpl10::KanMX4 (pDEGQ2)*	Hedges and Johnson, unpublished
AJY1440	*MAT*a *lys2Δ0 met15Δ0 his3Δ1 leu2Δ0 ura3Δ0 rpl10[F85S]*	This section
AJY1548	*MAT*α *leu2 ura3 his3Δ1 met15Δ0 CRM1(T539C)-HA*	Section 2.1.1
AJY1657	*MAT*a *ura3 leu2 rpl10(G161D)*	(Hedges et al., 2005)
AJY1896	*MAT*a *ura3 his3Δ1 leu2 trp1 nmd3:TRP1 CRM1[T539C]-HA*	This section
AJY1961	*MAT*a *leu2-3,112 ura3-1 trp1-1 ade2-1 his3-11 can1-100 SSD1-d RPL10-3xHA::KanMX6*	This section

Plasmids used in Chapter 4 are listed in Table 2.5. pAJ415 (*NMD3[L291F]*) was constructed in the following manner. First, inverse PCR using the 5' oligo AJO303 (GCGGATCTGTCACCATCT) and the mutagenic 3' oligo AJO304 (GGTTTGGAAAGTAGTCGGGTCCATAAACTG) was conducted. [The first underlined nucleotide substitution is responsible for the amino acid change, while the second introduces a silent mutation that eliminates a BamHI restriction site.] The PCR

product was then digested with BglII and MscI, and the resultant fragment was ligated into the same sites of pAJ123 (*NMD3* in YEp351**;** (Ho and Johnson, 1999)). To produce pAJ582 (*NMD3-GFP*), the *GFP* moiety was amplified from pFA6a-GFP(S65T)-KanMX6 (Longtine et al., 1998) using the primers AJO230 (5'-AGAAGATGGAGTCGAGAACACACCCGTTGAATCTCAGCAGCAGCGGATCCC GGGTTAATTAA) and AJO307 (3'-GCGAAGCTTGGCCTCGAAACGTGAGTC). PCR product was digested with PacI and HindIII and subsequently ligated into the same sites of pAJ538 (*NMD3-13xcmyc*; (Ho et al., 2000a)). pAJ1108 (*GAL10::LSG1[K349T]-13xcmyc]*) was made by digesting pAJ903 (*LSG1-13xcmyc*) with BsaBI and SalI and ligating the resultant restriction fragment into the same sites of pAJ1109. pAJ1107 (*GAL10::LSG1-myc*) was constructed by ligating the NcoI-BsaBI fragment from pAJ879 (*GAL10::cmyc-LSG1*) into the same sites of pAJ1108. pAJ1105 (*GAL10::LSG1[N173Y,L176S]-13xcmyc*) was made by ligating the NcoI-BsaBI fragment from pAJ1131 into the same sites of pAJ1108. pAJ1313 was generated by ligating the BsaBI-SalI restriction fragment from pAJ1105 into the same site of pAJ1310. The isolation of *NMD3* loss-of-function mutants *nmd3(H108P)* (pAJ1295), *nmd3(L82P)* (pAJ1296), *nmd3(H108R)* (pAJ1297), *nmd3(V340D)* (pAJ1299), and others not specifically shown in Figure 4.1 were isolated from the previously-described, PCR-based random mutagenesis screen (pAJ538 [*NMD3-13xcmyc*] as template DNA) designed to identify mutations in *NMD3* that were unable to support wild-type growth during complementation analysis in an *nmd3* deletion strain (Hedges et al., 2005). The *NMD3* suppressor mutant *NMD3(I112T,I362T)* (pAJ1315) and others not specifically shown in Figure 4.1 were isolated from an independent PCR-based mutagenesis screen (pAJ538 as template DNA) designed to identify mutations in *NMD3* that suppressed the temperature-sensitivity phenotypes of *rpl10(G161D)* (AJY1657) and *rpl10(F85S)* (AJY1440) at

restrictive temperature (35˚C) (Hedges et al., 2005). pAJ1287 (*NMD3[I112T,I362T]-GFP*) was made by introducing the BglII-PacI and PacI-HindIII restriction fragments from pAJ582 into the BglII-HindIII sites of pAJ1315. pAJ1334 was constructed by sub-cloning the I112T mutation from pAJ1315 (*NMD3[I112T,I362T]-13xcmyc*) as a SacII-digested fragment into the same sites of pAJ515 (*NMD3ΔN123-13xcmyc/URA3*) to produce pAJ1327 followed by ligating the MscI-PacI fragment from pAJ1327 into the same sites of pAJ512 (*NMD3Δ100-13xcmyc*). pAJ1326 was made by sub-cloning the I362T mutation from pAJ1315 as a BamHI-digested fragment into the same sites of pAJ512. To produce pAJ1343 (*GAL10::LSG1-3xHA/URA3*) and pAJ1344 (*GAL10::LSG1[K349T]-3xHA/URA3*), the ClaI-digested restriction fragment from pAJ1340 (*GAL10::LSG1-3xHA/LEU2*) or pAJ1341 (*GAL10::LSG1[K349T]-3xHA/LEU2*) was ligated into the ClaI site of pRS416.

TABLE 2.5 Plasmids used in Chapter 4.

Plasmid	Relevant markers and notes	Source or Reference
pAJ123	*LEU2 CEN (NMD3)*	(Ho and Johnson, 1999)
pAJ415	*LEU2 CEN (NMD3[L291F])*	This section
pAJ512	*LEU2 CEN (NMD3ΔC100-13xcmyc)*	This section
pAJ515	*URA3 2μ (NMD3ΔN123-13xcmyc)*	This section
pAJ538	*LEU2 CEN (NMD3-13xcmyc)*	(Ho et al., 2000a)
pAJ582	*LEU2 CEN (NMD3-GFP)*	This study
pAJ690	*URA2 2μ (GAL10::GST-NMD3)*	This study
pAJ903	*LEU2 CEN (LSG1-13xcmyc)*	Section 2.1.2
pAJ1070	*LEU2 CEN* (*NMD3[L291F]-13xcmyc*)	(Hedges et al., 2005)
pAJ1100	*URA3 2μ* (*GAL10::RPL10N187-GFP*)	(West et al., 2005)
pAJ1105	*LEU2 CEN (GAL10::LSG1[N173Y,L176S]-13xcmyc)*	This section
pAJ1107	*LEU2 CEN (GAL10::LSG1-13xcmyc)*	This section
pAJ1108	*LEU2 CEN (GAL10::LSG1[K349T]-13xcmyc)*	This section
pAJ1109	*LEU2 CEN (GAL10::cmyc-LSG1[K349T])*	Section 2.1.2
pAJ1131	*LEU2 CEN (GAL10::cmyc-LSG1[N173Y,L176S])*	Section 2.1.2
pAJ1278	*URA3 CEN (GAL10::cmyc-LSG1[K349])*	Section 2.1.2
pAJ1287	*LEU2 CEN (NMD3[I112T,I362T]-GFP)*	This section
pAJ1291	*URA3 2μ (GAL10::GST-NMD3[L291F])*	(Hedges et al., 2005)
pAJ1292	*URA3 2μ (GAL10::GST-NMD3[I112T,I362T])*	(Hedges et al., 2005)
pAJ1293	*URA3 2μ (GAL10::GST-NMD3[V340D])*	(Hedges et al., 2005)
pAJ1295	*LEU2 CEN (NMD3[H108P]-13xcmyc)*	This section
pAJ1296	*LEU2 CEN (NMD3[L82P]-13xcmyc)*	This section
pAJ1297	*LEU2 CEN* (*NMD3[H108R]-13xcmyc*)	This section
pAJ1299	*LEU2 CEN* (*NMD3[V340D]-13xcmyc*)	This section
pAJ1310	*LEU2 CEN (GAL10::cmyc-LSG1[S350P])*	Section 2.1.2
pAJ1312	*URA3 CEN (GAL10::cmyc-LSG1)*	Section 2.1.2
PAJ1313	*LEU2 CEN (GAL10::LSG1[S350P]-13xcmyc)*	This section
pAJ1315	*LEU2 CEN* (*NMD3[I112T,I362T]-13xcmyc*)	This section
pAJ1316	*LEU2 CEN* (*NMD3[R113G]-13xcmyc*)	This section
pAJ1326	*LEU2 CEN (NMD3[I362T]-13xcmyc)*	This section
pAJ1327	*URA3 2μ (NMD3[I112T]-13xcmyc)*	This section
pAJ1334	*LEU2 CEN (NMD3[I112T]-13xcmyc*	This section
pAJ1340	*LEU2 CEN (GAL10::LSG1-3xHA)*	This section
pAJ1341	*LEU2 CEN (GAL10::LSG1[K349T]-3xHA)*	This section
pAJ1343	*URA3 CEN (GAL10::LSG1-3xHA)*	This section
pAJ1344	*URA3 CEN (GAL10::LSG1[K349T]-3xHA)*	This section

2.2.2 Comparative growth assays

In Figure 4.1, Table 4.1, or Table 4.2, AJY1657 (*rpl10[G161D]*) or a wild-type strain (W303) harboring either *GAL10*-regulated *LSG1(K349T)* (pAJ1278), *LSG1[N173Y,L176S]* (pAJ1131), *LSG1[I204T]* (pAJ1132), *LSG1[S350P]* (pAJ1310), or *LSG1[S351F]* (pAJ1119) was transformed with empty vector (pRS315), wild-type *NMD3* (pAJ538), or *NMD3* mutant alleles. Dense overnight cultures of the transformants were plated onto either SC-leu (glucose)(AJY1657) or SC-ura leu (glucose or galactose)(W303/mutant *LSG1*) as described in section 2.1.11. AJY1657 transformants were grown for five days at either 25˚C (permissive temperature) or 35˚C (restrictive temperature) before assessing suppression phenotypes. W303 transformants were grown for 5 days at 30˚C on either glucose (non-inducing) or galactose (inducing) plates before assessing suppression phenotypes. Three independent platings were performed for each *NMD3* allele in a given *LSG1* mutant strain.

For the growth comparisons shown in Figure 4.2B, pAJ582 (*NMD3-GFP*) or pAJ1287 (*NMD3[I112T,I362T]-GFP*) were transformed into AJY1896 (*CRM1[T539C] nmd3:TRP1/NMD3::URA3*) to replace the plasmid-borne wild-type *NMD3* allele after growth on 5-FOA plates. These cells were transformed with either empty vector (pRS426), pAJ1312 (*GAL10::LSG1*), or pAJ1278 (*GAL10::LSG1[K349T]*), and transformants were grown for 5 days at 30˚C on either glucose- or galactose-containing SC-ura leu medium.

2.2.3 GFP fluorescence microscopy

In Figure 4.2, dense overnight cultures of AJY1896 (*nmd3:TRP1 CRM1[T539C]*) containing pAJ582 (*NMD3-GFP*) or pAJ1287 (*NMD3[I112T, I362T]-GFP*) as the sole copies of *NMD3* along with either empty vector (pRS426), pAJ1312 (*GAL10::LSG1*) or pAJ1278 (*GAL10::LSG1[K349T]*) were diluted to OD_{600}~0.1 into fresh SC- ura leu drop-

out medium containing raffinose as the non-inducing carbon source (two cultures for each strain) and cultured at 30˚C. Upon reaching OD_{600}~0.2, galactose (1% final concentration) was added to one of the cultures for each strain and induced expression of the appropriate *LSG1* allele was carried-out for 3 hours (final OD_{600}~0.3-0.4). Cells were treated with leptomycin B (LMB) and prepared for visualization as described in section 2.1.8.

2.2.4 LMB treatment

The growth conditions and LMB treatment of cells shown in Figure 4.2 were carried-out as described in section 2.1.8.

2.2.5 Polysome analysis

Polysome profiles shown in Figures 4.3 and 4.6 were prepared as described in section 2.1.4 with the exception that, following the addition of cycloheximide, cultures were immediately poured over ice and harvested before storage at –80˚C. Specific growth conditions are listed in the figure legends. Protein constituents of gradient fractions in Figure 4.6 were concentrated by TCA-precipitation as described in section 2.1.4.

2.2.6 Western blotting

Western blotting was performed as described in section 2.1.5 using antibodies against the c-myc epitope on Nmd3p or the core ribosomal protein Rpl12p. Densitometric traces of chemiluminescent α-myc blots in Figure 4.6 were conducted using NIH Image V.1.62.

2.2.7 Purification of 60S ribosomal subunits

60S ribosomal subunits were purified essentially as described in (Ho et al., 2000a). Cultures of W303 (wild-type strain) were cultured to mid-log phase in YPD and harvested by centrifugation. Cell pellets were frozen at -80°C prior to purification.

Pellets were thawed on ice and washed one time with 1X lysis buffer (20mM Tris-HCl pH 7.6, 500mM KCl, 10mM $MgCl_2$, 6mM β-mercaptoethanol (BME) and protease inhibitors). Cells were then resuspended in one volume of ice-cold 1X lysis buffer and were lysed by vortexing in the presence of glass beads (5x30 second intervals on vortexer separated by one-minute periods of cooling on ice). Lysates were clarified two times by centrifugation for 10 minutes each at 15,000 rpm (4°C). Clarified extracts were then incubated at 4°C for two hours to allow for the dissociation of 80S ribosome couples into 40S and 60S subunits. 350 OD_{260} units of extract were layered onto linear 10-40% sucrose gradients prepared in lysis buffer. Gradients were subjected to centrifugation at 20,000 rpm in a Beckman ultracentrifuge (SW-28) rotor for 17 hours at 4°C. Gradients were fractionated while monitoring absorbance at 280 nm on an ISCO density gradient fractionator. Automated collection of ~900µl fractions was conducted by the fractionator. Fractions corresponding with the resolved 60S ribosomal subunit peak were pooled and dialyzed overnight at 4°C against storage buffer (10mM Tris-HCl pH 7.6, 10mM $MgCl_2$, 50mM KCl and 6mM BME).

2.2.8 Purification of GST fusion proteins

GST-fusion proteins were expressed in strain AJY1134 (*reg1-501*) from pAJ690 (*NMD3*), pAJ1291 (*NMD3[L291F]*), pAJ1292 (*NMD3[I112T,I362T]*) or pAJ1293 (*NMD3[V340D]*) (*reg1-501*) and purified as described previously (Ho et al., 2000a). Briefly, dense overnight cultures were diluted to OD_{600}~0.10 in SC-ura (glucose) media (500 mL). Cultures were incubated for 4 hours at 30˚C before galactose was added. Induction of GST-Nmd3p expression was carried-out for 6 hours. Cells were harvested by centrifugation and frozen at -80°C until use. Subsequent steps were carried out on ice or at 4˚C. Cell were thawed and washed once in lysis buffer (20mM Tris pH 7.6, 500mM LiCl, 1mM EDTA, 10% glycerol, 1mM DTT and protease inhibitors). Cells were then

resuspended in one volume of ice-cold lysis buffer and were lysed by vortexing in the presence of glass beads (5x30 second intervals on vortexer separated by one minute periods of cooling on ice). Lysates were transferred to eppendorf tubes on ice and supplemented with an additional 1mM PMSF and 1% Triton X-100 to aid in the solubilization of proteins. After rocking for one hr., extracts were clarified two times by centrifugation for 10 minutes each at 15,000 rpm (4°C). 1/10 bed volume of Glutathione Sepharose 4B (Amersham) was added to clarified extracts, and the suspension was rocked for two hours at 4°C. The suspension was then loaded into a BioRad micro-spin chromatography column, and the extract was eluted by gravity flow. The resin was washed three times with ten volumes of ice-cold high-salt wash buffer (20mM Tris-HCl pH 7.6, 500mM LiCl, 1mM EDTA and protease inhibitors followed by two washes with ten volumes of low-salt wash buffer (20mM Tris-HCl pH 7.6, 100mM NaCl, 1mM EDTA and protease inhibitors). The column was then capped, and one bed volume of glutathione elution buffer (50mM Glutathione and 50mM Tris-HCl pH 8.0) was added. The column was then allowed to equilibrate at room temperature for 20 min. prior to elution. Five total fractions of one bed volume each were collected. Fractions containing GST-Nmd3p were determined by SDS-PAGE analysis before pooling and dialyzing against 100 volumes of storage buffer (10mM Tris-HCl pH 7.6, 50mM KCl and 6mM BME) at 4°C. Final protein concentrations were measured using the Bradford assay. *Performed by J. Hedges.*

2.2.9 Composite gel analysis

For the *in vitro* 60S/GST-Nmd3p reconstitution reactions, increasing amounts of a GST-Nmd3 protein (see Figure 4.4, 1X~30ng) were mixed with 0.018 OD_{260} units (2µl) of purified free 60S subunits (see section 2.2.7) in 10 µl of "low Mg^{2+}" TKM buffer (25mM Tris-OAc pH 7.6, 60mM KOAc and 1mM $MgOAc_2$, plus protease inhibitors).

After a 30 min. incubation at 25˚C, samples were placed on ice and sucrose loading dye (TKM + 5% sucrose + bromophenol blue) was added to each reaction prior to loading onto the composite gel. During the reconstitutions, composite gels were pre-run at 60V for 1 hr. in "low Mg^{2+}" TKM buffer while cooling with continuous circulation of 4°C ddH_2O. Gels were loaded with fresh buffer, and samples were loaded and resolved with cooling for 4 hrs. at 60V with a second buffer change after 2 hrs. The gels were transferred to nitrocellulose, and western blotting using α-GST (Sigma) or α-Rpl12p was performed as described in section 2.1.5. Gels were also stained with ethidium bromide (EtBr) for visualization of the 60S subunit position.

Composite gels were prepared according to published protocols (Dahlberg and Grabowski, 1990). A buffer containing 25mM Tris-OAc pH 7.6, 60mM KOAc, 1mM $MgOAc_2$, 0.4% dimethylpropionitrile and 2.5% (29:1) bis-acrylamide (final concentrations) was prepared with continual mixing. 0.5% agarose (final concentration) was melted in 23.5 ml of ddH_2O and cooled to ~60°C before it was added to the acrylamide mixture to yield a final volume of 30 ml. 80 µl of 10% APS was then added to the mixture, stirred, and injected with a syringe into Hoefer 8 X 10 X 0.0015 cm gel forms containing 10-well combs. *Performed by J. Hedges.*

2.2.10 Immunoprecipitations

For the immunoprecipitations shown in Figure 4.5, dense overnight cultures of strain W303 harboring either empty vector (pRS425), pAJ538 (*NMD3-myc*), pAJ1315 (*NMD3[I112T,I362T]-myc*), pAJ1070 (*NMD3[L291F]-myc*), or pAJ1299 (*nmd3[V340D]-myc*) were diluted to OD_{600}~0.15 in 200mL of fresh drop-out medium (with glucose) and cultured at 30˚C to OD_{600}~0.5. Cells were harvested by centrifugation and stored at –80˚C until use. Co-immunoprecipitations with Nmd3-myc proteins were carried out as follows. Cells were washed once in lysis buffer (20mM Tris-HCl pH7.5,

150mM NaCl, 10% glycerol, 0.1% NP40, 1mM $MgCl_2$ and protease inhibitors) and pelleted. The cells were resuspended in one volume of lysis buffer, and extracts were prepared by glass bead abrasion (5x50 sec. cycles on vortexer with one-minute intervals on ice). Insoluble material was pelleted at 15,000xg for 10 min. at 4°C. 1.5 µl of α-c-myc (9E10; Covance) antibody was added to equal OD_{260} units of sample supernatants, and extracts were rocked for 1 hr. at 4°C. 40µl of BSA-blocked protein A agarose bead slurry (Invitrogen) were added to each extract, and samples were rocked for an additional 1 hr. at 4˚C. Beads were washed 3x with lysis buffer (five min. of rocking at 4˚C per wash) and eluted at 99˚C in 50µl of 1x Laemmli sample buffer without β-mercaptoethanol after removing all residual lysis buffer. Proteins were resolved on a 12% SDS-PAGE gel and either stained directly with Coomassie stain or transferred to nitrocellulose. Western blots were performed as described in section 2.1.5 with α-c-myc or α-Rpl8p as noted in the figure legend.

For immunoprecipitations of Nmd3-myc from the free 60S sucrose gradient fraction in Figure 4.7, cultures of AJY1961 (*RPL10-3xHA*) containing pAJ538 (*NMD3-myc*) were harvested at mid-log phase in the presence of cycloheximide as described in section 2.2.5. Extracts were prepared and resolved on 7-47% sucrose gradients for fraction collection as described in section 2.1.4. Half of the fraction corresponding to the free 60S peak was diluted with an equal volume of IP buffer (10 mM Tris [pH 7.6], 50 mM KCl, 10 mM $MgCl_2$, and protease inhibitors), and subsequent steps were carried out as described above using 1.5µl of α-c-myc. Western blotting was performed as described in section 2.1.5 using α-c-myc (9e10; Covance), α-HA (HA.11; Covance), or α-Rpl12p (J. Ballesta).

The co-immunoprecipitations and subsequent sample analyses of Lsg1-myc and Nmd3-myc-bound complexes shown in Figures 4.8 and 4.9 were carried out essentially

as described for Figure 4.5. Specific culture conditions are listed in the figure legends. Preparation of extracts and immunoprecipitations using α-c-myc (9e10; Covance) or α-HA (HA.11; Covance) were conducted in buffer containing 40mM NaCl in place of 150mM NaCl. Eluates were resolved on SDS-PAGE gels, transferred to nitrocellulose, and subjected to western blotting using α-c-myc, α-HA, α-Sqt1p (B. Trumpower), α-Rpl12p (J. Ballesta), α-GFP (Santa Cruz Biotechnology, Inc.), or α-Rpl8p as described in section 2.1.5.

2.3 Materials and Methods for Chapter 5

2.3.1 Strains, plasmids, and culture media

The strains used in Chapter 5 are listed in Table 2.6. AJY1849 (*NIC96-mRFP::KanMX6 CRM1(T539C)-HA*) was generated by mating AJY1848 (*NIC96-mRFP::KanMX6*) with AJY1539 (*CRM1[T539C]-HA*), and the resulting heterozygous diploid strain was sporulated and dissected to isolate spore clones. Spore clones were tested for G418-resistance, and the co-segregation of the *CRM1[T539C]-HA* allele among G418-resistant spore clones was confirmed by PCR as described in section 2.1.1. To produce AJY2122 (*nup120::ClonNat*^{r}), the 1.2Kb EcoRI fragment from p4339 (Goldstein and Tucker, 1999) was transformed into AJY1608 (*nup120*Δ*::KanMX4*) for *in vivo* homologous recombination, and ClonNat-resistant, G418-sensitive isolates were identified. The strains bearing chromosomally-integrated, GFP-tagged NPC-associated proteins were acquired from the University of California, San Francisco (UCSF) yeast GFP collection (Invitrogen).

TABLE 2.6 Strains used in Chapter 5.

Strain	Genotype and notes	Source or Reference
AJY1134	*MAT*α *ura3-52 leu2-3 pep4-3 prb1-1122 reg1-501 gal1*	(Hovland et al., 1989)
BJ5464	*MAT*α *ura3-52 leu2Δ1 trp1 his3Δ200 pep4::HIS3 prb1Δ1.6R can1 [RKY1293 = BJ5464]*	E. Jones
AJY1539	*MAT*a *leu2 ura3 his3Δ1 met15Δ0 CRM1(T539C)-HA*	Section 2.1.1
AJY1848	*MAT*α *leu2Δ0 ura3Δ0 his3Δ1 lys2Δ0 NIC96-mRFP::KanMX6*	(Huh et al., 2003)
AJY1849	*MAT*a *leu2 ura3 his3Δ1 NIC96-mRFP::KanMX6 crm1(T539C)-HA*	This section
AJY2122	*MAT*a *leu2Δ0 ura3Δ0 his3Δ1 nup120::Clonat^r*	This section
AJY2154	*MAT*a *leu2Δ0 ura3Δ0 his3Δ1met15Δ0 NUP159-GFP::HIS3*	Invitrogen/UCSF coll.
AJY2155	*MAT*a *leu2Δ0 ura3Δ0 his3Δ1 met15Δ0 NIC96-GFP::HIS3*	Invitrogen/UCSF coll.
AJY2156	*MAT*a *leu2Δ0 ura3Δ0 his3Δ1 met15Δ0 NUP100-GFP::HIS3*	Invitrogen/UCSF coll.
AJY2157	*MAT*a *leu2Δ0 ura3Δ0 his3Δ1 met15Δ0 NUP116-GFP::HIS3*	Invitrogen/UCSF coll.
AJY2158	*MAT*a *leu2Δ0 ura3Δ0 his3Δ1 met15Δ0 NUP49-GFP::HIS3*	Invitrogen/UCSF coll.
AJY2159	*MAT*a *leu2Δ0 ura3Δ0 his3Δ1 met15Δ0 PSE1-GFP::HIS3*	Invitrogen/UCSF coll.
AJY2161	*MAT*a *leu2Δ0 ura3Δ0 his3Δ1 met15Δ0 NUP82-GFP::HIS3*	Invitrogen/UCSF coll.
AJY2162	*MAT*a *leu2Δ0 ura3Δ0 his3Δ1 met15Δ0 NUP85-GFP::HIS3*	Invitrogen/UCSF coll.
AJY2163	*MAT*a *leu2Δ0 ura3Δ0 his3Δ1 met15Δ0 NUP53-GFP::HIS3*	Invitrogen/UCSF coll.
AJY2164	*MAT*a *leu2Δ0 ura3Δ0 his3Δ1 met15Δ0 NUP84-GFP::HIS3*	Invitrogen/UCSF coll.
AJY2165	*MAT*a *leu2Δ0 ura3Δ0 his3Δ1 met15Δ0 NUP57-GFP::HIS3*	Invitrogen/UCSF coll.
AJY2166	*MAT*a *leu2Δ0 ura3Δ0 his3Δ1 met15Δ0 NUP59-GFP::HIS3*	Invitrogen/UCSF coll.
AJY2167	*MAT*a *leu2Δ0 ura3Δ0 his3Δ1 met15Δ0 NUP60-GFP::HIS3*	Invitrogen/UCSF coll.
AJY2168	*MAT*a *leu2Δ0 ura3Δ0 his3Δ1 met15Δ0 NUP133-GFP::HIS3*	Invitrogen/UCSF coll.
AJY2169	*MAT*a *leu2Δ0 ura3Δ0 his3Δ1 met15Δ0 NUP145-GFP::HIS3*	Invitrogen/UCSF coll.
AJY2170	*MAT*a *leu2Δ0 ura3Δ0 his3Δ1 met15Δ0 NUP157-GFP::HIS3*	Invitrogen/UCSF coll.
AJY2171	*MAT*a *leu2Δ0 ura3Δ0 his3Δ1 met15Δ0 NUP170-GFP::HIS3*	Invitrogen/UCSF coll.
AJY2172	*MAT*a *leu2Δ0 ura3Δ0 his3Δ1 met15Δ0 NSP1-GFP::HIS3*	Invitrogen/UCSF coll.
AJY2173	*MAT*a *leu2Δ0 ura3Δ0 his3Δ1 met15Δ0 GLE1-GFP::HIS3*	Invitrogen/UCSF coll.
AJY2174	*MAT*a *leu2Δ0 ura3Δ0 his3Δ1 met15Δ0 SEH1-GFP::HIS3*	Invitrogen/UCSF coll.
AJY2175	*MAT*a *leu2Δ0 ura3Δ0 his3Δ1 met15Δ0 SEC13-GFP::HIS3*	Invitrogen/UCSF coll.
AJY2176	*MAT*a *leu2Δ0 ura3Δ0 his3Δ1 nup120:: Clonat^r 4* (pAJ1608)	This section

Plasmids used in Chapter 5 are listed in Table 2.7. pAJ414 (*NMD3-13xcmyc*) was made by excising *NMD3-myc* from pAJ408 (*NMD3-myc*) as a EheI-HindIII fragment and ligating it into SmaI-HindIII-cut pRS416. To produce pAJ516 (*nmd3ΔN167-13xcmyc*), the oligomeric c-myc tag was excised as a BglII-BglII restriction fragment from pAJ401 (*13xmyc-NMD3*) and ligated into the same sites of pAJ522 (*nmd3NΔ167*). pAJ693 (*GAL10::GST-nmd3ΔN167*) was constructed by ligating the EcoRI-HindIII

restriction fragment from pAJ522 (*nmd3ΔN167*) into the same sites of pAJ690 (*GAL10::GST-NMD3*). The *NMD3* loss-of-function mutants *nmd3(I139T,L259S,L296P)* (pAJ1298), *nmd3(V340D)* (pAJ1403), and *nmd3(L263P,F318I)* (pAJ1404) were isolated as described in section 2.2.1. To create plasmids pAJ1406 (*nmd3[I139T,L259S,L296P]-GFP*), pAJ1407 (*nmd3[L263P,F318I]-GFP*), and pAJ1408 (*nmd3[V340D]-GFP*), pAJ1298 (*nmd3[I139T,L259S,L296P]-13xcmyc*), pAJ1403 (*nmd3[V340D]13xcmyc*), and pAJ1404 (*nmd3[L263P,F318I]-13xcmyc*) were cut with PacI and SpeI and transformed into wild-type strain W303 along with BsgI-BspHI-digested pAJ582 (*NMD3-GFP*) for gap-rescuing the GFP tag onto the 3' end of the mutant *NMD3* alleles via *in vivo* homologous recombination. pAJ1409 was constructed by replacing the BglII-HindIII fragment from pAJ1406 (*nmd3[I139T,L259S,L296P]-GFP*) with the BglII-HindIII restriction fragment from pAJ753 (*nmd3[AA]-GFP*). pAJ1412 (*nmd3[I139T,L259S,L296P][AAA]-GFP*), pAJ1413 (*nmd3[L263P,F318I][AAA]-GFP*), and pAJ1414 (*nmd3[V340D][AAA]-GFP*) were generated in the same manner as pAJ1409 with the exception that the BglII-HindIII fragment from pAJ754 was introduced into the BglII-HindIII sites of each of plasmid. To construct pAJ1515 (*nmd3[I139T,L259S,L296P][AAA]-13xcmyc*) and pAJ1516 (*nmd3[L263P,F318I][AAA]-13xcmyc*), the oligomeric c-myc tag from pAJ538 (*NMD3-13xcmyc*) was excised as a PacI-HindIII fragment and ligated into the same sites of pAJ1412 and pAJ1413. pAJ1527 (*nmd3[I139T,L259S,L296P][ΔCC]-13xcmyc*), pAJ1528 (*nmd3[I139T,L259S,L296P][ΔCC][AA]-13xcmyc*), and pAJ1529 (*nmd3[I139T,L259S,L296P][ΔCC][AAA]-13xcmyc*) were constructed by replacing the BglII-PacI restriction fragment from pAJ1298 (*nmd3[I139T,L259S,L296P]-13xcmyc*) with the BglII-PacI fragment from pAJ1416 (*nmd3[ΔCC]-13xcmyc*), pAJ1423 (*nmd3[ΔCC][AAA]-13xcmyc*), and pAJ1424 (*nmd3[ΔCC][AAA]-13xcmyc*), respectively.

To create plasmids pAJ1531 (*nmd3[I139T,L259S,L296P][ΔCC]-GFP*), pAJ1533 (*nmd3[I139T,L259S,L296P][ΔCC][AAA]-GFP*), and pAJ1534 (*nmd3[I139T,L259S,L296P][ΔCC][AA]-GFP*), the PacI-HindIII fragment from pAJ582 (*NMD3-GFP*) was ligated into the same sites of pAJ1527, pAJ1529, and pAJ1528, respectively. pAJ1536 (*nmd3ΔN167-GFP*) was generated by ligating the PacI-EagI fragment from pAJ582 (*NMD3-GFP*) into the same sites of pAJ516 (*nmd3ΔN167-13xcmyc*). pAJ1538 (*GST-[PKI]NES*) was constructed by phosphorylating the complementary oligonucleotides AJO322 (5'-AGCTTTGTCTTGTTGATATCAAGACCTGCAATTTCAAGGCTAATTCATTG) and AJO325 (3'-GATCCAATGAATTAGCCCTTGAAATTAGCAGGTCTTGATATCAACAAGACATAAA), annealing the oligos, and subsequently ligating them into BamHI-cut pAJ893 (pGEX4T-3). To create pAJ1541 (*XPO1-His$_6$*), the PCR product generated by amplifying *XPO1(CRM1)* from its genomic locus using AJO813 (5'-GCGGGATCCATGGAAGGAATTTTGG) and AJO814 (3'-CGCGCGGCCGCATCATCAAGTTCGGAAGG) was digested with BamHI and NotI and ligated into the same sites of pAJ1106 (pET-21[a]+). pAJ1548 (*nmd3ΔN167ΔC100-13xcmyc*), pAJ1549 (*nmd3ΔN193ΔC100-13xcmyc*), pAJ1550 (*nmd3ΔN226ΔC100-13xcmyc*), pAJ1601 (*nmd3ΔN282ΔC100-13xcmyc*), and pAJ1602 (*nmd3ΔN332ΔC100-13xcmyc*) were constructed using an equivalent strategy. The restriction fragment from pAJ516 (*nmd3ΔN167-13xcmyc*), pAJ517 (*nmd3ΔN193-13xcmyc*), pAJ518 (*nmd3ΔN226-13xcmyc*), pAJ519 (*nmd3ΔN282-13xcmyc*), or pAJ520 (*nmd3ΔN332-13xcmyc*) was ligated into the same sites of pAJ535 (*nmd3ΔC100-13xcmyc*) to produce pAJ1548, pAJ1549, pAJ1550, pAJ1601, and pAJ1602, respectively.

TABLE 2.7 Plasmids used in Chapter 5.

Plasmid	Relevant markers and notes	Source or Reference
pAJ414	*URA3 2μ (NMD-13xcmyc)*	(Ho and Johnson, 1999)
pAJ516	*URA3 2μ (nmd3ΔN167-13xcmyc)*	This section
pAJ535	*LEU2 CEN (nmd3ΔC100-13xcmyc)*	(Ho et al., 2000b)
pAJ538	*LEU2 CEN (NMD3-13xcmyc)*	(Ho et al., 2000a)
pAJ582	*LEU2 CEN (NMD3-GFP)*	Section 2.2.1
pAJ693	*URA3 2μ (GAL10::GST-nmd3ΔN167)*	This section
pAJ752	*LEU2 CEN (nmd3[AAA]-13xcmyc)*	J. Hedges, 2004
pAJ754	*LEU2 CEN (nmd3[AAA]-GFP)*	(Hedges et al., 2005)
pAJ1298	*LEU2 CEN* (*nmd3[I139T,L259S,L296P]-13xcmyc*)	This section
pAJ1403	*LEU2 CEN (nmd3[V340D]-13xcmyc)*	This section
pAJ1404	*LEU2 CEN (nmd3[L263P,F318I]-13xcmyc)*	This section
pAJ1406	*LEU2 CEN* (*nmd3[I139T,L259S,L296P]-GFP*)	This section
pAJ1407	*LEU2 CEN (nmd3[L263P,F318I]-GFP)*	This section
pAJ1408	*LEU2 CEN (nmd3[V340D]-GFP)*	This section
pAJ1409	*LEU2 CEN* (*nmd3[I139T,L259S,L296P][AA]-GFP*)	This section
pAJ1412	*LEU2 CEN* (*nmd3[I139T,L259S,L296P][AAA]-GFP*)	This section
pAJ1413	*LEU2 CEN (nmd3[L263P,F318I][AAA]-GFP)*)	This section
pAJ1414	*LEU2 CEN (nmd3[V340D][AAA]-GFP)*	This section
pAJ1515	*LEU2 CEN* (*nmd3[I139T,L259S,L296P][AAA]-13xcmyc*)	This section
pAJ1516	*LEU2 CEN (nmd3[L263P,F318I][AAA}-13xcmyc)*	This section
pAJ1527	*LEU2 CEN (nmd3[I139T,L259S,L296P][ΔCC]-13xcmyc*	This section
pAJ1528	*LEU2 CEN (nmd3[I139T,L259S,L296P][ΔCC][AA]-13xcmyc)*	This section
pAJ1529	*LEU2 CEN (nmd3[I139T,L259S,L296P][ΔCC][AAA]-13xcmyc)*	This section
pAJ1531	*LEU2 CEN (nmd3[I139T,L259S,L296P][ΔCC]-GFP)*	This section
pAJ1533	*LEU2 CEN (nmd3[I139T,L259S,L296P][ΔCC][AAA]-GFP)*	This section
pAJ1534	*LEU2 CEN (nmd3[I139T,L259S,L296P][ΔCC][AA]-GFP)*	This section
pAJ1536	*LEU2 CEN (nmd3ΔN167-GFP)*	This section
pAJ1538	*(GST-[PKI]NES)*	This section
pAJ1541	*(CRM1[XPO1]-His_6)*	This section
pAJ1542	*(His6-RAN[GSP1])* [pKW581]	(Maurer et al., 2001)
pAJ1548	*LEU2 CEN (nmd3ΔN167ΔC100-13xcmyc)*	This section
pAJ1549	*LEU2 CEN (nmd3ΔN193ΔC100-13xcmyc)*	This section
pAJ1550	*LEU2 CEN (nmd3ΔN226ΔC100-13xcmyc)*	This section
pAJ1601	*LEU2 CEN (nmd3ΔN282ΔC100-13xcmyc)*	This section
pAJ1602	*LEU2 CEN (nmd3ΔN332ΔC100-13xcmyc)*	This section
pAJ1608	*URA3 CEN (NUP120-GFP)*	This section

2.3.2 GFP fluorescence microscopy

Dense overnight cultures of AJY1539 (*crm1[T539C]*), AJY1848 (*NIC96-mRFP*), or AJY1849 (*NIC96-mRFP crm1[T539C]*) expressing GFP-tagged Nmd3p alleles were diluted to OD_{600}~0.15 in fresh glucose-containing drop-out media and cultured at 30˚C. When cultures had reached an OD_{600}~0.4-0.5, cells were either visualized directly or treated with leptomycin B (LMB) prior to visualization as described in section 2.1.8.

2.3.3 Immunoprecipitations

Dense overnight cultures of the appropriate strains were diluted to OD_{600}~0.15 in 150ml of fresh drop-out medium (with glucose) and cultured at 30˚C to OD_{600}~0.4. Cells were harvested by centrifugation and stored at –80˚C until use. Immunoprecipitations with Nmd3-myc proteins were carried out as follows. Cells were washed once in lysis buffer (20mM Tris-HCl pH7.5, 40mM NaCl, 10% glycerol, 0.1% NP40, 1mM $MgCl_2$ and protease inhibitors) and pelleted. The cells were resuspended in one volume of lysis buffer, and extracts were prepared by glass bead lysis (5x50 sec. cycles on vortexer with one-minute intervals on ice). Insoluble material was pelleted at 15,000xg for 10 min. at 4°C. 1.5 µl of anti-c-myc (9E10; Covance) antibody was added to equal OD_{260} units of sample supernatants, and extracts were rocked for 1 hr. at 4°C. 40µl of protein A agarose bead slurry (Invitrogen) were added to each extract, and samples were rocked for an additional 1 hr. at 4˚C. Beads were washed 3 times with lysis buffer (five min. of rocking at 4˚C per wash) and eluted at 99˚C in 50µl of 1X Laemmli sample buffer after removing all residual lysis buffer.

2.3.4 Western blotting

Proteins were resolved on 8 or 10% SDS-PAGE gels and transferred to nitrocellulose, using a semi-dry electrophorectic transfer cell (BIORAD). Western blots

were performed as described in section 2.1.5 with the antibodies designated in each figure legend.

2.3.5 Purification of recombinant fusion proteins

The Nmd3p GST-fusion proteins were expressed in strain BJ5464 (*pep4 prb1Δ1.6R*) from pAJ690 (*NMD3*) or pAJ693 (*nmd3ΔN167*) and purified essentially as described in section 2.2.8. Briefly, dense overnight cultures were diluted to OD_{600}~0.15 in SC-ura (raffinose) media (3L). Cultures were incubated for 6 hours at 30˚C before galactose was added. Induction of GST-Nmd3p expression was carried-out for 6 hours. Cells were harvested by centrifugation and frozen at -80°C until use. Subsequent steps were carried out on ice or at 4˚C. Cells were thawed and washed once in lysis buffer (20mM Tris pH 7.5, 500mM KCl, 10% glycerol, 1mM DTT and protease inhibitors). Cells were then resuspended in 5 volumes of ice-cold lysis buffer and were lysed as described in section 2.28. Following centrifugation at 15,000*g* (4˚C), 1/10 bed volume of glutathione-Sepharose 4B (Amersham) was added to clarified extracts, and the suspension was rocked for one hour at 4°C. The suspension was then loaded into a 15ml BioRad chromatography column, and the extract was eluted by gravity flow. The resin was washed three times with ten volumes of ice-cold lysis buffer. Glutathione elution buffer (50mM Glutathione and 50mM Tris-HCl pH 8.0) was added to the column, and eight fractions of one bed volume each were collected. Fractions containing GST-Nmd3p were identified by SDS-PAGE analysis before pooling and dialyzing against 100 volumes of storage buffer (50mM Tris-HCl pH 7.5, 200mM KCl, 10% glycerol, 10mM $MgCl_2$, and 1mM BME) at 4°C. Final protein concentrations were measured using the Bradford assay.

GST-(PKI)NES was purified in the following manner. A dense overnight culture of Stratagene codon+ strain (RIL) containing pAJ1538 was diluted to an OD_{600}~0.1 in

Luria broth containing 75µg/ml ampicillin and 30µg/ml chloramphenicol and cultured at 37˚C to an OD_{600}~0.4. The culture was then supplemented with IPTG (0.5mM) to induce expression of the GST-fusion protein. Induction of GST-(PKI)NES was carried-out for five hours at 30˚C before cells were harvested by centrifugation and frozen at -80°C until use. Subsequent steps were carried out on ice or at 4˚C. Cells were thawed and washed once in lysis buffer (20mM Tris pH 7.5, 300mM KCl, 10% glycerol, 1mM DTT and protease inhibitors). Cells were resuspended in ten volumes of lysis buffer and lysed via sonication using a Branson Sonifier 250. Subsequent purification steps were carried-out as described for the GST-Nmd3p fusion proteins.

Purification of Crm1-His_6 was accomplished as follows. A dense overnight culture of Stratagene codon+ strain (RIL) containing pAJ1541 (*CRM1-His_6*) was diluted back to an OD600~0.1 in Luria broth containing 75µg/ml ampicillin and 150µg/ml chloramphenicol and cultured at 37˚C to an OD_{600}~0.4. The culture was then supplemented with IPTG (0.5mM final concentration) to induce expression of the His_6-tagged protein. Induction was carried-out for five hours at room temperature (~25˚C) before cells were harvested by centrifugation and frozen at -80°C until use. Subsequent steps were carried out on ice or at 4˚C. Cell were thawed and washed once in lysis buffer (50mM Tris pH 8.0, 300mM NaCl, 10% glycerol, 15mM imidazole and protease inhibitors). Cells were resuspended in ten volumes of lysis buffer and lysed via sonication using a Branson Sonifier 250. Following clarification of extracts via centrifugation (10 min. at 15,000g, 4˚C), 1 ml of Ni-NTA resin was added to the extracts and the suspension was rocked at 4˚C for 1 hour. The suspension was then sequentially-loaded onto a 10 ml chromatography column to collect the resin via gravity flow. The column was washed 3 times with ten volumes of lysis buffer. Bound protein was eluted in lysis buffer containing 150mM imidazole in seven fractions of 400µl. Fractions

containing Crm1-His_6 were identified by SDS-PAGE analysis before pooling and dialyzing against 100 volumes of storage buffer (50mM Tris-HCl pH 7.5, 200mM NaCl, 10% glycerol, 10mM $MgCl_2$) at 4°C. Final protein concentrations were measured using the Bradford assay.

His_6-Ran was purified according to the conditions described by Maurer *et al.* (Maurer et al., 2001). Briefly, a dense overnight culture of *E. coli* strain SG13009 containing pAJ1542 (*His_6-RAN*) was diluted to an OD_{600}~0.1 in Luria broth containing 75µg/ml ampicillin and 50µg/ml kanamycin and cultured at 37˚C to an OD_{600}~0.4. After cooling the culture to room temperature, IPTG (0.5mM final concentration) was added to induce expression of the His_6-tagged protein. Induction was carried-out for five hours at room temperature (~25˚C) before cells were harvested by centrifugation and frozen at -80°C until use. Subsequent steps were carried out on ice or at 4˚C. Cells were thawed and washed once in lysis buffer (30mM KPO_4 buffer (pH 8.0), 300mM KOAc, 20mM imidazole, 2mM $MgOAc_2$, 2µM GTP and protease inhibitors). Lysis and affinity purification were conducted as described for Crm1-His_6. Bound protein was eluted in lysis buffer containing 120mM imidazole in seven fractions of 400µl. Fractions containing His_6-Ran were identified by SDS-PAGE analysis before pooling. To load Ran with GTP, pooled fractions were supplemented with EDTA to 6mM and incubated on ice for 40 minutes in the presence of a 50-fold molar excess of GTP. $MgOAc_2$ was then titrated into the protein pool to a final concentration of 25mM and the mixture was incubated an additional 10 minutes on ice. The pooled fractions were dialyzed against 100 volumes of storage buffer (30mM KPO_4 (pH 7.6), 50mM KOAc, 7% glycerol, 2mM $MgOAc_2$, 2mM BME, 2µM GTP) at 4°C. Final protein concentrations were measured using the Bradford assay.

2.3.6 Export complex assays

Purified GST-(PKI)NES, GST-Nmd3p, or GST-Nmd3ΔN167p (~75 pmol) were combined with ~75 pmol of Crm-His_6 in the presence or absence of 125 pmol of RanGTP in a final volume of 200µl in binding buffer containing 40mM NaCl, 50mM KPO_4 (pH 7.4), 10% glycerol, 2mM $MgCl_2$, 0.1mM DTT, 0.005% Triton X-100, and protease inhibitors). Reactions were incubated on ice for 30 minutes before diluting the contents one-fold with fresh binding buffer. At this time, 20µl of glutathione-Sepharose beads were added to each reaction, and the samples were rocked at 4˚C for 1 hour. The beads were recovered by gentle centrifugation (2,000 rpm at 4˚C) and washed three times with 750µl of binding buffer for five minutes per wash. Bound proteins were eluted from the resin with 1X Laemmli buffer at 99˚C for 5 minutes. ~1/4 of the eluate volume from each reaction was loaded onto an 8% SDS-PAGE gel, and proteins were resolved and analyzed as described in the legend for Figure 5.9.

Chapter 3: Recycling Nmd3p from cytoplasmic 60S subunits requires Lsg1p, a cytoplasmic GTPase-family protein

3.1 Introduction

The work in this chapter was initiated in the anticipation of identifying the nucle(ol)ar biogenesis factor(s) that fails to recycle from cytoplasmic 60S ribosomal subunits to the nucleus in the absence of Lsg1p function. Previous work from our lab had demonstrated that nuclear processes, including 60S export, were perturbed in *lsg1* mutants (Kallstrom et al., 2003). As Lsg1p is exclusively localized to the cytoplasm, it was suggested that Lsg1p might indirectly affect nuclear 60S maturation events by mediating the release of a shuttling biogenesis factor from nascent cytoplasmic subunits prior to translation initiation. The results presented in this chapter initially focus on the generation of dominant negative mutants of Lsg1p and their utilization to recapitulate the 60S biogenesis defects previously observed for *lsg1* conditional alleles. I demonstrate that disruption of Lsg1p function leads to the cytoplasmic entrapment of the 60S nuclear export adapter, Nmd3p, on nascent subunits. In support of the suggested functional link between these two factors, I show that *LSG1* and *NMD3* interact genetically and demonstrate that over-expression of Nmd3p suppresses both the growth and biogenesis defects that arise upon expression of dominant negative *LSG1* alleles. I conclude this chapter with a discussion centered on the potential functional implications of these findings in the context of 60S biogenesis with particular emphasis on late maturation events in the cytoplasm.

3.2 Background

More than 170 different trans-acting factors are required for the complex series of endo- and exoribonucleolytic cleavages, rRNA base modifications, and RNA folding and

assembly events, that resolve the primary rRNA transcripts into 40S and 60S subunits (Fromont-Racine et al., 2003a; Kressler et al., 1999; Venema and Tollervey, 1995). Therefore, the need to release biogenesis factors from nascent cytoplasmic 60S subunits reflects a general problem of assembly and disassembly of protein complexes encountered at many steps along the ribosome biogenesis pathway. These events may be coupled with energy-dependent conformational changes in the subunits. Consistent with this rationale, several GTPases have been implicated in the biogenesis of the large subunit. While the nuclear/nucleolar putative GTPases, Nog1p, Nug1p, and Nog2p/Nug2p are each essential, their effects on rRNA processing appear to be indirect (Bassler et al., 2001; Jensen et al., 2003; Kallstrom et al., 2003; Saveanu et al., 2001). Perturbing the functions of these factors leads to blockages in the export of the 60S subunit from the nucleolus (Nog1p) or nucleus (Nug1p, Nog2p/Nug2p), leading to the interpretation that they may act in tandem or sequentially to confer export competence on the subunit through essential structural rearrangements or through the release of specific retention factors.

GTPases have also been implicated in cytoplasmic events on pre-60S subunits prior to translation. Deletion of the cytoplasmic GTPase, Efl1p/Ria1p, leads to accumulation of Tif6p in the cytoplasm, a condition that can be suppressed by mutations in *TIF6* that restore its normal cellular localization (Becam et al., 2001; Senger et al., 2001). These observations have led to the conclusion that Efl1p/Ria1p is needed for Tif6p recycling (Senger et al., 2001). Work in our lab has demonstrated the importance of another essential, cytoplasmic putative GTPase, Lsg1p, in the biogenesis of the large subunit. Lsg1p is associated with free 60S subunits but does not shuttle between the nucleus and cytoplasm (Kallstrom et al., 2003). Surprisingly, disruption of its function leads to defects in nucleolar rRNA processing and entrapment of pre-60S subunits in the

nucleolus. We had proposed that Lsg1p, like Efl1p, may be necessary for the release of a nucle(ol)ar biogenesis factor(s) from cytoplasmic subunits prior to translation initiation, conferring an indirect effect on nuclear events in 60S assembly.

3.3 Results

3.3.1 Dominant negative mutations in *LSG1*

We previously characterized *LSG1* as a cytoplasmic protein of the YawG/YlqF family of GTPases (Leipe et al., 2002) that is essential for the biogenesis of the 60S ribosomal subunit in *Saccharomyces cerevisiae* (Kallstrom et al., 2003). GTPases share a common structural core composed of several conserved sequence motifs. In particular, the universally-conserved Walker A (G1) and Walker B (G3) motifs are required for proper spatial coordination of the bound nucleotide and the catalytic magnesium, respectively, and are typically located upstream of the GTP-specificity (G4) motif (i.e. G1-G3-G4). However, members of the YawG/YlqF family of GTPases, which also include the nucle(ol)ar biogenesis factors Nug1p and Nug2/Nog2p, possess an unusual circular permutation of their catalytic domain, such that the GTP-specificity motif is juxtaposed N-terminal to the Walker A and Walker B motifs (G4-G1-G3; Figure 3.1A). Despite this non-canonical domain architecture, a bacterial member of this family of GTPases, YjeQ, has recently been shown to possess GTPase activity *in vitro* (Daigle et al., 2002), demonstrating that the circular permutation of the G-motif has not disrupted the active site.

lsg1 mutants accumulate pre-60S subunits in the nucleolus, which we suggested was likely due to a failure to recycle an exported biogenesis factor back to the nucleus. In order to gain further insight into the function of *LSG1*, I initiated a screen for dominant negative mutants. The screen was designed to identify dominant negative alleles of *LSG1* that, by definition, retained their ability to bind and sequester their substrate(s), thereby

interfering with the function of the endogenous wild-type protein. Through the use of these mutants, I hoped to trap a specific reaction intermediate(s) in the 60s biogenesis pathway in order to identify the specific nature and timing of Lsg1p's function. The characterization of dominant negative mutants of other GTPases has played a critical role in the identification of their regulatory factors and substrates (Powers et al., 1989; Robinson et al., 1999; Schlenstedt et al., 1995b).

Mutant alleles of *LSG1*, expressed under the control of the galactose-inducible *GAL10* promoter, were generated *in vitro* by random PCR mutagenesis. The mutants were introduced into expression vectors by *in vivo* recombination upon co-transformation of the PCR product with a linearized *GAL10::cmyc-LSG1* vector in which the majority of the *LSG1* open reading frame had been deleted. Out of 35,000 transformants screened, ten dominant negative mutants were identified that exhibited a strong growth arrest on galactose-containing media but grew normally on glucose-containing media (Figure 3.1A). I also observed that over-expression of wild-type *LSG1* resulted in a modest slow growth phenotype.

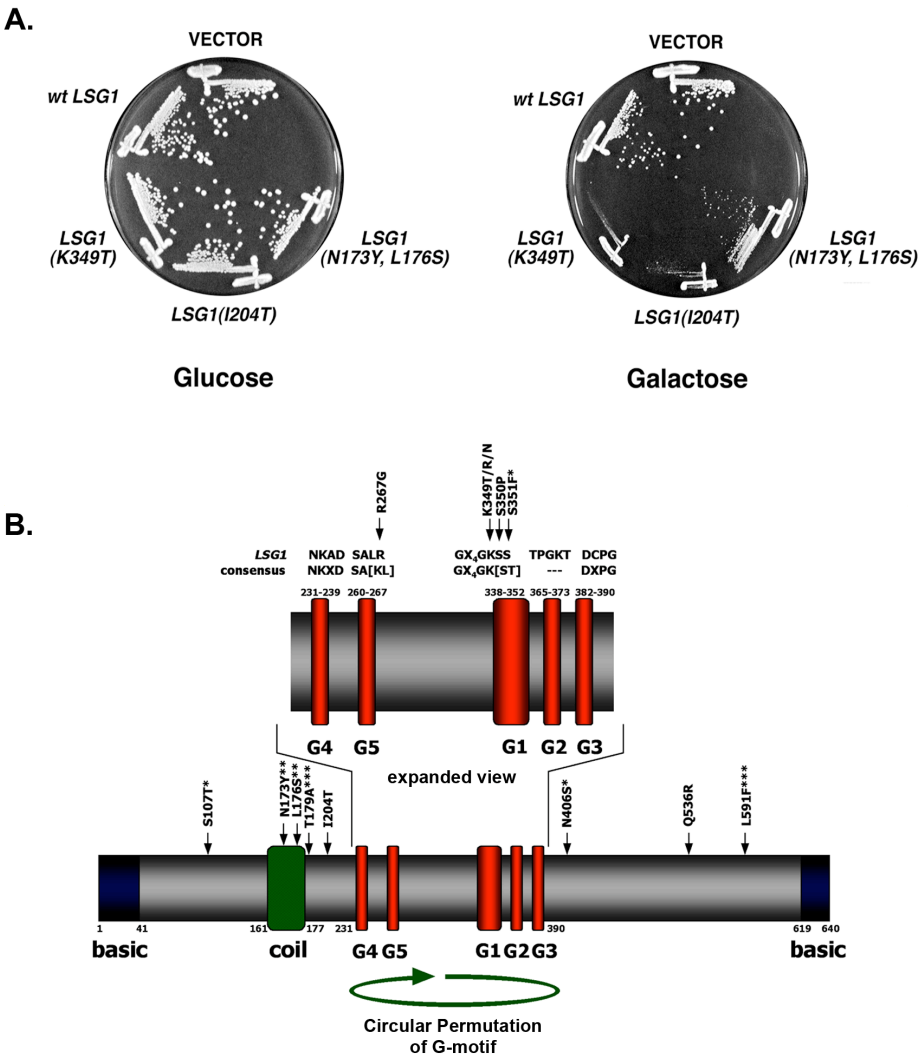

Figure 3.1. *LSG1* dominant negative mutants.

(A.) Growth of *LSG1* dominant negative mutants. CH1305 (wild-type) transformants containing empty vector (pRS425), pAJ879 (*GAL10::LSG1*), or *LSG1* dominant mutants [*LSG1(K349T)* (pAJ1109), *LSG1(I204T)* (pAJ1132), or *LSG1(N173Y, L176S)* (pAJ1131)] under the control of the *GAL10* promoter were streaked onto drop-out plates containing either glucose (non-inducible) or galactose (inducible) as the sole carbon source. Plates were incubated at 30°C for 5 days. (B.) Diagram depicting positions of dominant negative mutations within *LSG1*. Domains with predicted functional significance are demarcated. Designation of the putative G5 motif varies from that previously published (Kallstrom et al., 2003). Arrowheads indicate positions of point mutations in dominant negative mutants. Dominant negative alleles are as follows: *LSG1-2(Q536R), LSG1-5(T179A,L591F), LSG1-7(S107T,S351F,N406S), LSG1-10 (K349T), LSG1-14(S350P), LSG1-30(I204T), LSG1-41(K349N), LSG1-51(R267G), LSG1-52(N173Y,L176S),* and *LSG1-53(K349R).* Asterisks denote multiple point mutations within a single dominant mutant.

The majority of the dominant negative mutations in *LSG1* clustered within the G1 (Walker A) motif ($GX_4GK[S/T]$) and a putative coiled-coil domain (Figure 3.1B). The G1 motif is required for coordinating GTP-binding and catalysis (Saraste et al., 1990), and mutations in the invariant lysine (K349 in Lsg1p) and serine (S350 in Lsg1p) residues of this motif give rise to dominant negative phenotypes in heterologous GTPases (Daigle et al., 2002; Damke et al., 2001; Fujimura et al., 1993; Park et al., 2001). I identified three independent mutants, each containing different substitutions of the invariant lysine (*LSG1-10*: *K349T*, *LSG1-41*: *K349N*, and *LSG1-53*: *K349R*). Dominant negative mutations within this domain may trap the mutant *LSG1* proteins in dead-end conformations or complexes.

Mutations were also found in a putative coiled-coil motif in *LSG1* (Figure 3.1B). Coiled-coils are important in protein-protein interactions (Burkhard et al., 2001), and mutations in this motif may affect intra- or intermolecular interactions within Lsg1p or between Lsg1p and its substrate(s) or cofactor(s). These mutations (*LSG1*-52: *LSG1*(*N173Y,L176S*), *LSG1-5*: *LSG1(T179A,L591F)*; Figure 3.1A and Appendix A) did not inhibit growth as completely as did mutations in the G1 motif. The coiled-coil mutants are likely to be competent for GTP hydrolysis but may not properly receive regulatory information or transduce the intended effects on their interaction partners.

The functional significance of these two motifs was further highlighted during the course of a mutagenic screen designed to identify *LSG1* "loss-of-function" mutants. As summarized in Appendix B, the majority of the non-functional *lsg1* mutants that I identified were also clustered within or directly proximal to these two regions of the protein. Again, the G1 motif of the GTPase core was shown to be particularly critical for Lsg1p function, as a large proportion of the "loss-of-function" mutants possessed point mutations within these residues. Likewise, the dominant negative alleles with mutations

in these motifs were also incapable of supporting growth as the sole copies of *LSG1* in an *lsg1* knock-out strain (data not shown).

Several of the dominant negative mutations mapped to regions of the protein outside the recognized motifs. Mutants within this group exhibited varying degrees of growth inhibition with one mutant, *LSG1(I204T)*, showing particularly strong growth arrest (Figure 3.1A and Appendix A). Using several mutants with alterations in various regions of the protein, I next examined their effects on ribosome biogenesis.

3.3.2 *LSG1* dominant negative mutants exhibit defects in 60S biogenesis

We previously demonstrated that, at non-permissive temperature, strains bearing temperature-sensitive alleles of *LSG1* show a reduction in free 60S levels and the accumulation of half-mer polysomes on sucrose gradients (Kallstrom et al., 2003). Half-mers, representing mRNAs with 48S initiation complexes not joined to 60S, result from either a lack of free 60S subunits available to participate in joining or from a defect in subunit joining. Expression of dominant negative *LSG1* mutants resulted in sucrose gradient profiles similar to those observed for *lsg1* temperature-sensitive mutants. As shown in Figure 3.2, galactose-induction of *LSG1(K349T)* or *LSG1(I204T)* resulted in reduced free 60S levels and the appearance of halfmers in polysomes. Similar results were observed upon induction of other dominant negative *LSG1* mutants (Appendix C).

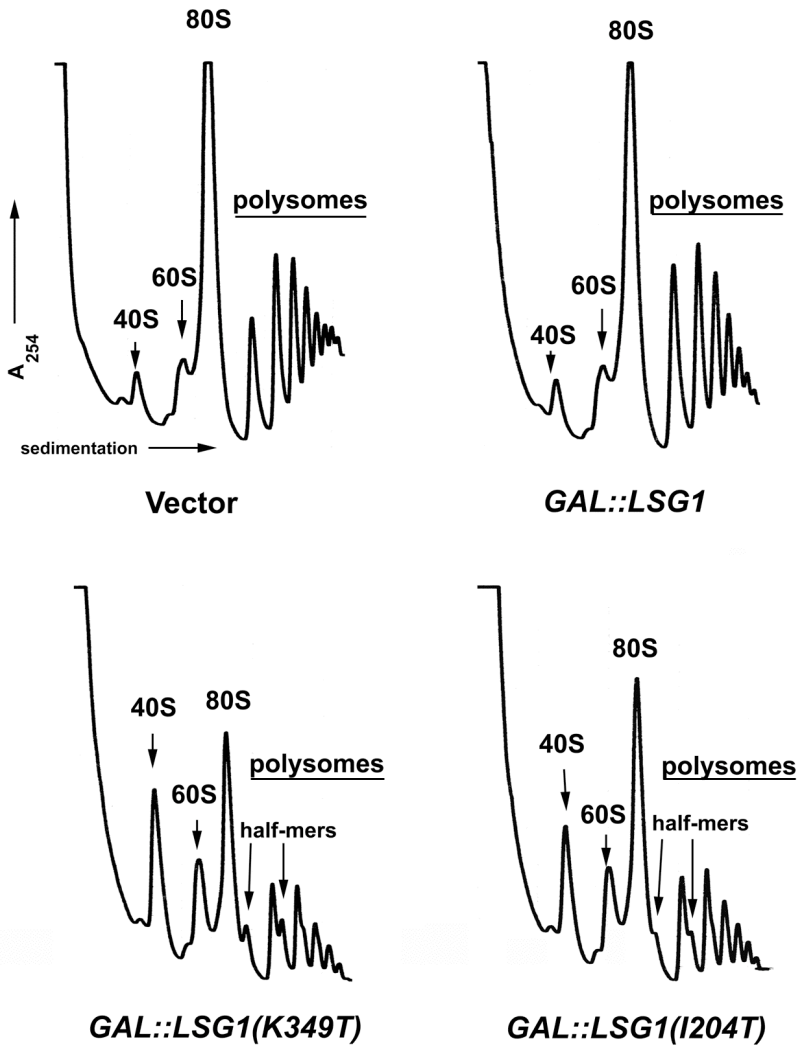

Figure 3.2 Expression of dominant negative *LSG1* mutants reduces 60S subunit levels and leads to defects in polysomes.

CH1305 (wild-type strain) transformed with empty vector (pRS425), pAJ879 (*GAL10::LSG1*), pAJ1109 (*GAL10::LSG1[K349T]*), or pAJ1132 (*GAL10::LSG1[I204T]*) was cultured in drop-out media containing 1% raffinose. Galactose was added to 1%, and the cells were cultured for an additional 6 h. at which time cycloheximide was added and cells harvested. Extracts were prepared in the presence of cycloheximide and sedimented through 7 to 47% sucrose gradients. Gradients were analyzed by monitoring the absorbance at 254 nm. Arrows indicate reduced free 60S peaks and half-mers in polysomes.

In order to assess the effect of the dominant *LSG1* mutants on 60S export, I utilized the ribosomal reporter protein, Rpl25-eGFP (Gadal et al., 2001a), to monitor the localization of 60S subunits following induction of dominant negative *LSG1* alleles. This reporter has been shown to be faithfully incorporated into 60S subunits, and its localization serves as a reliable indication of 60S distribution in cells (Gadal et al., 2001a). After three hours of galactose-induction of the *LSG1(K349T)* and *LSG1(I204T)* alleles, Rpl25-eGFP accumulated dramatically in the nucleus with a noticeable nucleolar enrichment (observe offset in GFP signal with respect to DAPI staining; Figure 3.3), indicating that 60S export is blocked by dominant negative *LSG1* mutants. The extent of nuclear entrapment for Rpl25-eGFP among the dominant *LSG1* mutants correlated with the strength of the dominant negative growth phenotypes (i.e. weaker entrapment upon *LSG1(N173Y,L176S)* induction, Appendix D). This 60S nuclear accumulation is consistent with that seen for strains bearing temperature sensitive alleles of *LSG1* at non-permissive temperature (Kallstrom et al., 2003). Since both wild-type and the dominant negative Lsg1p mutant proteins are cytoplasmic (Kallstrom et al., 2003; Nissan et al., 2002), I concluded that dominant negative alleles of *LSG1* are unable to effectively recycle a biogenesis factor needed for subunit export back to the nucleus, resulting in nucle(ol)ar entrapment of Rpl25-eGFP-containing pre-60S subunits.

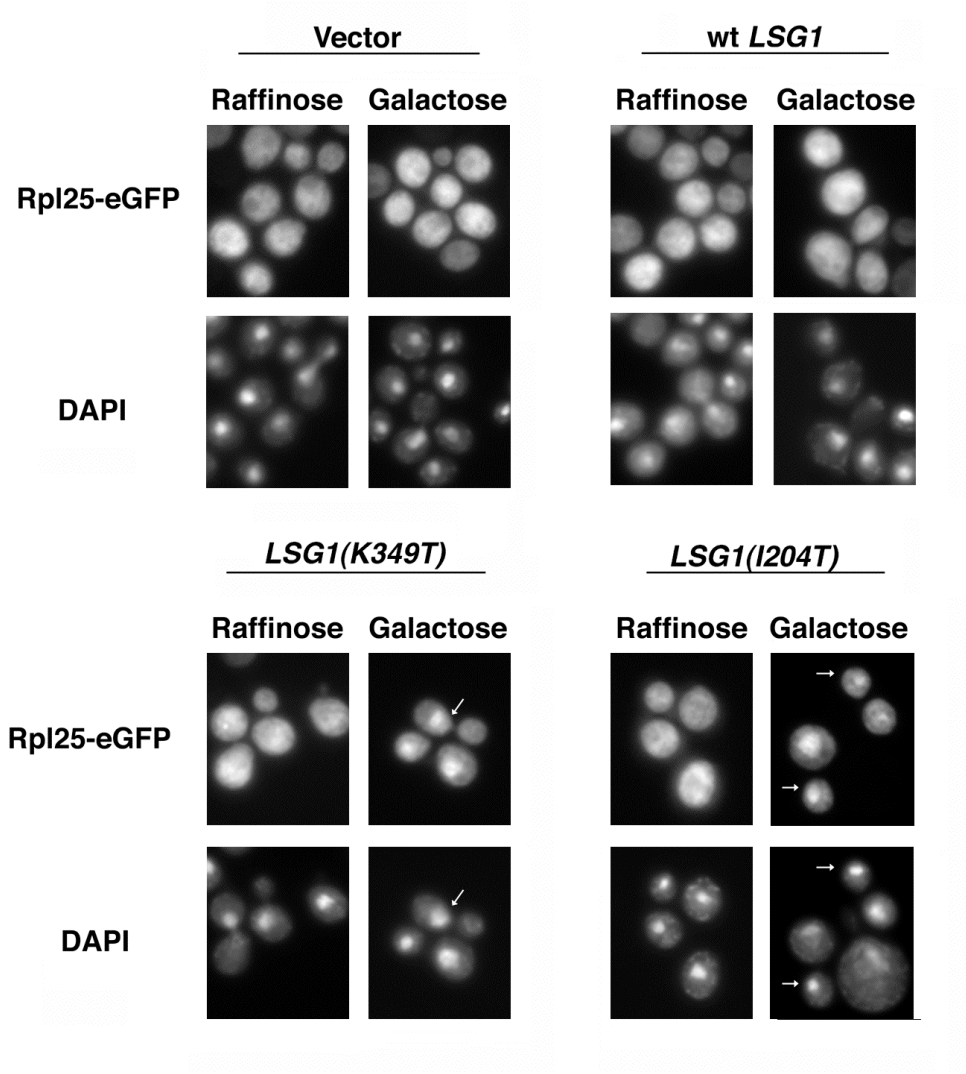

Figure 3.3 Nuclear accumulation of Rpl25-eGFP in dominant negative *LSG1* mutants.

Rpl25-eGFP (pAJ908) was continuously expressed in strain CH1305 (wild-type) carrying empty vector (pRS425), pAJ879 (*GAL10*::*LSG1*), pAJ1109 (*GAL10*::*LSG1[K349T]*), or pAJ1132 (*GAL10*::*LSG1[I204T]*). Overnight cultures were diluted to an OD_{600}~0.1 in fresh medium containing raffinose as a non-inducing carbon source. At OD_{600}~0.2, one half of each culture was induced by the addition of galactose (1% final concentration) for 3 h. Cells were fixed and DAPI stained as described in Chapter 2. Arrows indicate position of nucleoplasm as demarcated by DAPI staining.

To confirm that Lsg1p is not acting in the nucleus to elicit its effects on 60S biogenesis, I monitored its localization in cells co-expressing a dominant negative Ran allele, Gsp1(G21V)p. This Ran mutant is defective for GTP hydrolysis and accumulates in a dead-end complex with its co-regulator, RanBP1(Yrb1p), resulting in the global inhibition of exportin-directed nuclear export (Schlenstedt et al., 1995a). As a control for nucleocytoplasmic shuttling, I independently monitored the localization of c-myc-tagged Nmd3p in the context of the mutant Ran allele by immunoflourescence. Although Nmd3p shuttles between the nucleus and cytoplasm to mediate the nuclear export of 60S subunits, its steady-state distribution is predominately cytoplasmic (Gadal et al., 2001b; Ho et al., 2000b). In cells induced to express wild-type Ran (Gsp1p), Nmd3p exhibited its typical cytoplasmic distribution (Figure 3.4A). In cells expressing the dominant negative Ran allele (Gsp1(G21V)p), however, Nmd3p strongly accumulated in nuclei, indicating an efficient block in its nuclear export. In contrast to Nmd3p, c-myc-tagged Lsg1p remained cytoplasmic in the context of the dominant negative Ran allele (Figure 3.4B). Thus, Lsg1p is indeed confined to the cytoplasm and, therefore, must influence nuclear events in 60S biogenesis indirectly.

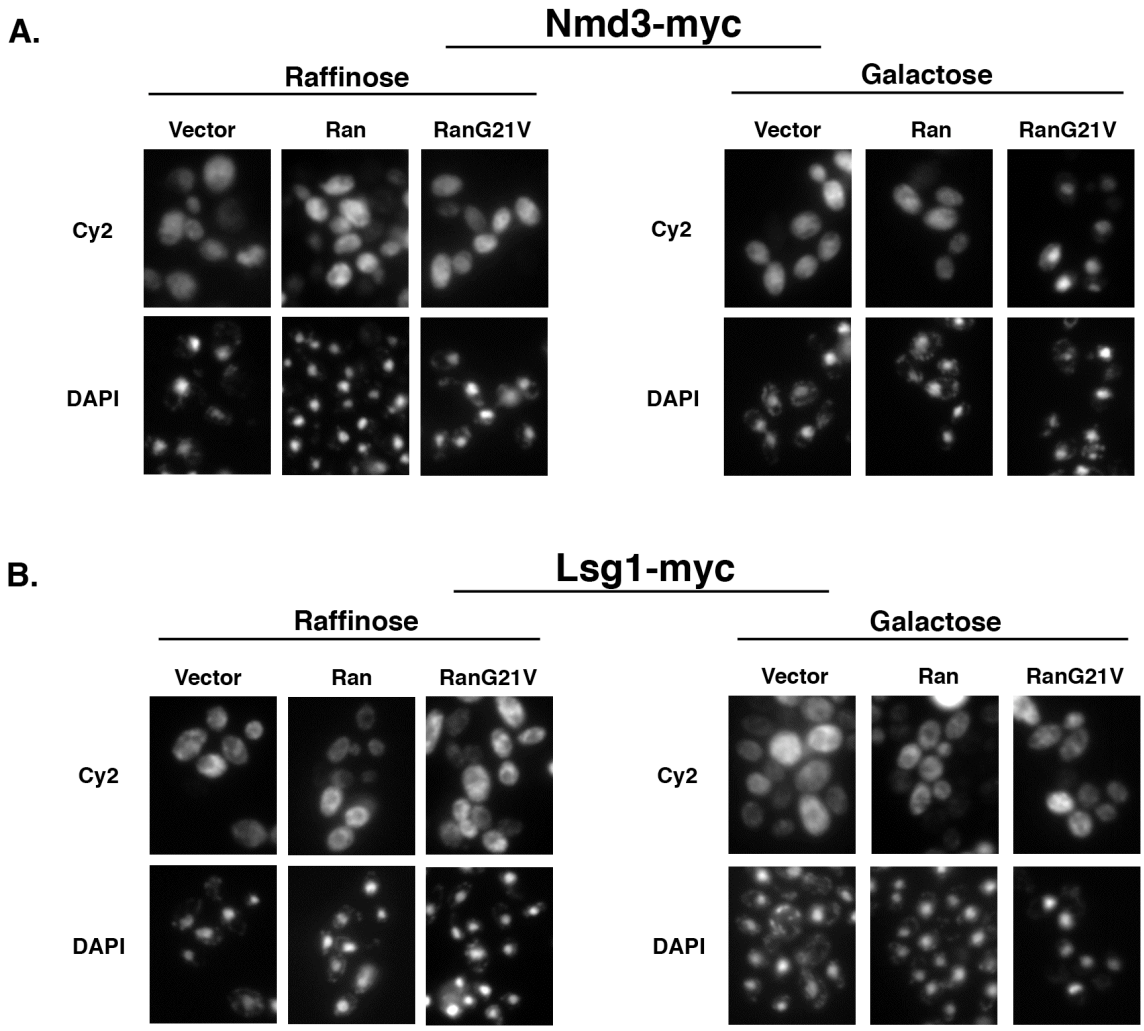

Figure 3.4 Localization of Nmd3p and Lsg1p upon expression of a dominant negative Ran mutant.

Cultures of strain W303 (wild-type) transformed with pRS416 (empty vector), pAJ379 (*GAL10::GSP1*), or pAJ380 (*GAL10::GSP1[G21V]*) along with either (A) pAJ538 (*NMD3-13myc*) or (B) pAJ903 (*LSG1-13myc*) were grown to saturation in SC-ura leu raffinose medium and diluted to an O D_{600}~0.15 in fresh medium. After 5 hrs. at 30˚C, galactose was added and the cultures were grown for an additional 3.5 hrs. Cells were fixed and treated for immunofluorecence microscopy as described in Chapter 2.

3.3.3 Dominant negative Lsg1p mutants trap the 60S export adapter, Nmd3p, in the cytoplasm

To identify the putative factor that fails to shuttle in *lsg1* mutants, I monitored the localization of various candidate 60S biogenesis factors. No obvious re-localization was observed for ectopically-expressed, GFP-labeled Nog1p, Nog2(Nug2p), Nug1p, Arx1p, or Tif6p in the presence of dominant negative *LSG1* mutants (data not shown). I also examined ectopically-expressed Nmd3-GFP. As shown in Figure 3.4A, Nmd3p exhibits a predominantly cytoplasmic localization under steady-state conditions. As Nmd3p's export from nuclei occurs in a Crm1-dependent manner, its export can be blocked by the Crm1 inhibitor, leptomycin B (LMB), in LMB-sensitized yeast cells (Gadal et al., 2001b; Ho et al., 2000b). In order to monitor potential cytoplasmic retention of Nmd3p, cells were treated with LMB following galactose-induction of the dominant negative *LSG1* alleles. Dominant negative *LSG1* mutants did not prevent accumulation of ectopically-expressed Nmd3p in the nucleus in the presence of LMB (Figure 3.5A).

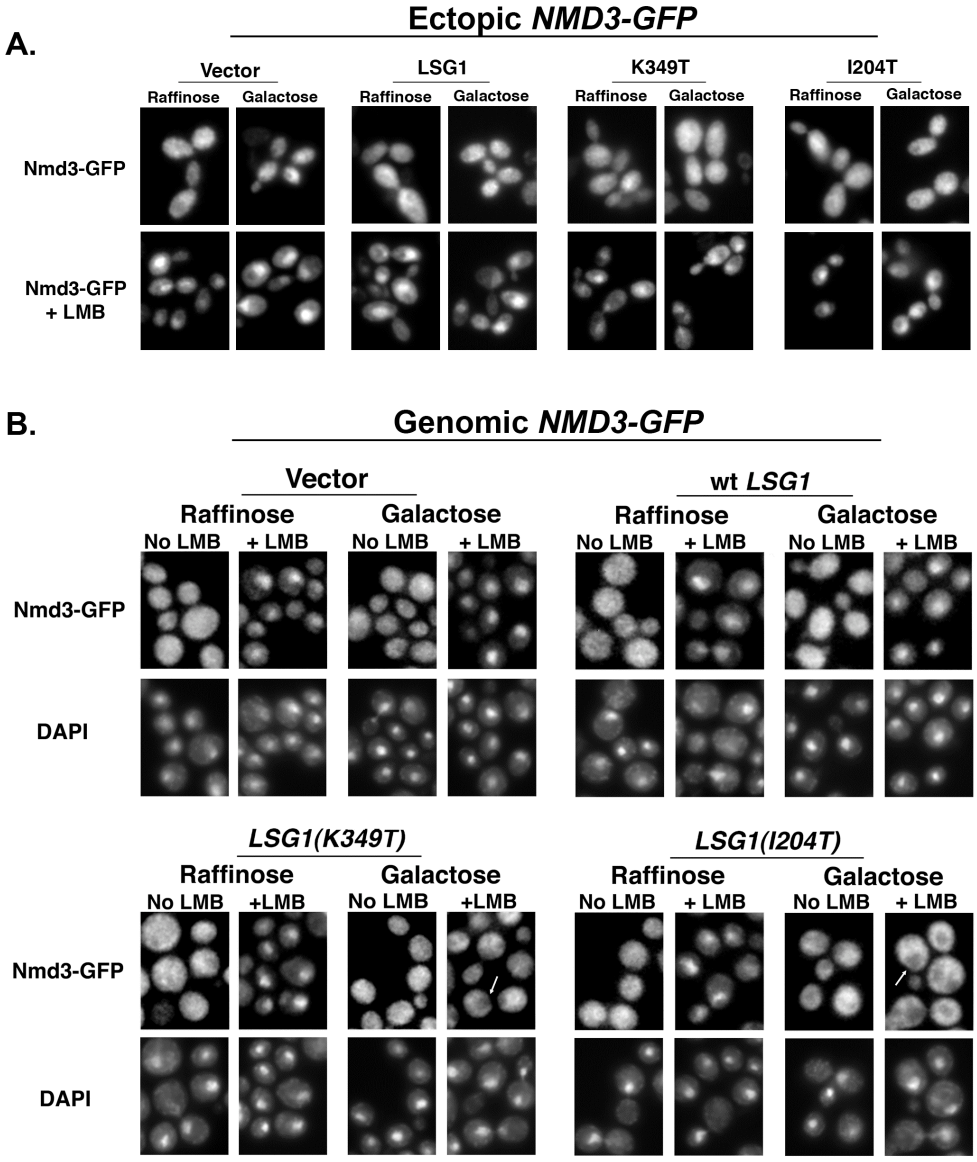

Figure 3.5 Localization of Nmd3-GFP expressed ectopically or from its genomic locus in dominant *LSG1* mutants.

(A.) Localization of ectopically-expressed Nmd3-GFP in the presence of LMB. Nmd3-GFP (pAJ755) was visualized in strain AJY1539 (*crm1[T539C*]) + empty vector (pRS425), pAJ879 (*GAL10::LSG1*), or pAJ1109 (*GAL10::LSG1[K349T]*) after culturing to mid-log phase followed by galactose-induction of *LSG1* expression for 3 hours. Cells were treated with LMB, fixed, and stained with DAPI as described in Chapter 2. (B.) Localization of chromosomally-expressed Nmd3-GFP in the presence of LMB. Nmd3-GFP was visualized in strain AJY1705 (*NMD3-GFP::KanMX6 crm1[T539C]*) carrying empty vector (pRS425), pAJ879, pAJ1109, or pAJ1132 (*GAL10::LSG1[I204T]*) after handling cells as described in (A.). Arrows indicate position of nuclei as demarcated by DAPI staining.

Temperature sensitive *nmd3* mutants show accumulation of Rpl25-eGFP in the nucleolus at restrictive temperature (Kallstrom et al., 2003). In addition, mutant human *NMD3* that is defective for nuclear export accumulates in the nucleolus in human cells (Trotta et al., 2003). These results suggest that Nmd3p is required for release of subunits from the nucleolus. Since *LSG1* mutants also accumulate Rpl25-eGFP in the nucleolus, Nmd3p remained an attractive candidate for the factor that might be trapped on 60S subunits in the cytoplasm in Lsg1p mutants. Because Lsg1(K349T)p did not trap Nmd3-GFP in the cytoplasm when it was expressed from a low-copy centromeric vector, I considered that the proper regulation of Nmd3p shuttling may depend on its stoichiometry with other factors, including free 60S subunits and Lsg1p. To address this concern, I introduced the GFP moiety genomically at the 3'-end of endogenous *NMD3* through homologous recombination. I also integrated the *crm1(T539C)* allele for a more uniform response to LMB.

Nmd3-GFP expressed from its genomic locus showed the expected cytoplasmic bias during active growth and a marked nuclear accumulation when cells were treated with LMB in the absence of dominant negative *LSG1* expression (Figure 3.5B). However, in cells induced for the expression of either Lsg1(K349T)p or Lsg1(I204T)p, genomically-expressed Nmd3-GFP failed to accumulate in the nucleus in the presence of LMB and exhibited a dramatic cytoplasmic retention. Indeed, these cells showed a virtual absence of nuclear signal for Nmd3-GFP (see arrows, Figure 3.5B). This cytoplasmic retention for Nmd3-GFP was common among all of the dominant negative *LSG1* mutants tested (Appendix D). Thus, when Nmd3-GFP is expressed from its genomic locus, and presumably at wild-type stoichiometry with other cellular factors, its ability to shuttle is blocked by dominant negative Lsg1p mutants. The disparity in cytoplasmic entrapment between endogenously- versus ectopically-expressed Nmd3-GFP

underscores the importance of maintaining appropriate stoichiometries for accurate assessment of molecular events in the 60S biogenesis pathway.

As an alternative means of demonstrating the need for proper Lsg1p function in maintaining Nmd3p shuttling and to circumvent pleiotropic effects arising from LMB treatment, I incorporated the use of an Nmd3p mutant for which nuclear export is rate-limiting. This mutant protein, Nmd3(AAA)p, possesses three point mutations (I493A, L497A, L500A) in critical residues within its nuclear export signal, perturbing its ability to interact with Crm1 for efficient export (Hedges et al., 2005). Thus, Nmd3(AAA)p binds to nascent 60S subunits in the nucle(ol)us and subsequently fails to efficiently export them to the cytoplasm, resulting in a strong nuclear bias for the mutant allele in actively growing cells.

Using a GFP-tagged version of this Nmd3p mutant, I assessed its cellular distribution in cells expressing either wild-type or dominant negative Lsg1p alleles by fluorescence microscopy. While induction of wild-type Lsg1p did not detectably alter the nuclear predisposition of Nmd3(AAA)-GFP, the over-expression of Lsg1(K349T)p dramatically redistributed the mutant Nmd3p allele to the cytoplasm (Fig. 3.6). The altered localization for Nmd3(AAA)-GFP in the context of the dominant Lsg1p mutant suggests that import has now become rate-limiting in superposition to the export defect. This result further supports a role for Lsg1p in recycling Nmd3p to the nucleus for additional rounds of subunit export.

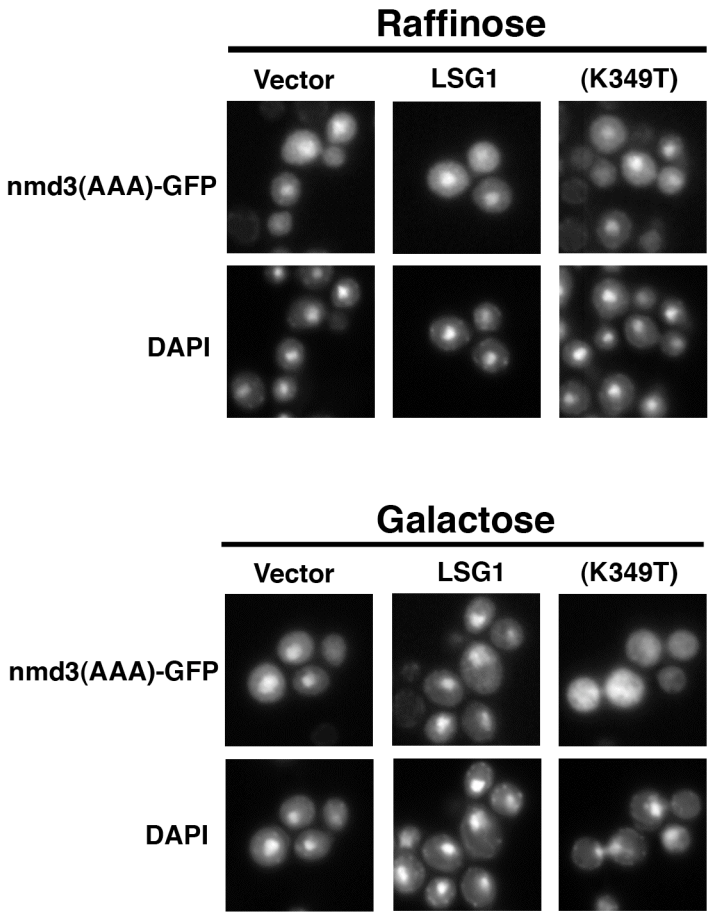

Figure 3.6 Disruption of Lsg1p function leads to cytoplasmic entrapment of Nmd3p

Nmd3(AAA)-GFP (pAJ754) was visualized in strain W303 (wild-type) harboring either pRS426 (empty vector), pAJ1312 (*GAL10::LSG1*), or pAJ1278 (*GAL10::LSG1[K349T]*) after culturing cells to mid-log phase followed by galactose-induction for 3 hours. Cells were fixed and DAPI stained as described in Chapter 2.

A failure to recycle Nmd3p to the nucleus could reflect a block in Nmd3p's release from the subunit or a subsequent failure to import Nmd3p into the nucleus after release from the subunit. Western blotting among sucrose gradient fractions showed that Nmd3p co-sedimented with free 60S subunits in the presence of dominant negative Lsg1p (Figure 3.7). Furthermore, a free pool of Nmd3p was not observed at the top of the gradient, suggesting that the observed cytoplasmic entrapment for Nmd3-GFP was not due to an import failure for unbound Nmd3p upon disruption of Lsg1p's function. Thus, Nmd3p that is unable to recycle to the nucleus remains associated with 60S subunits in the cytoplasm, possibly locked onto the subunits by mutant Lsg1p protein.

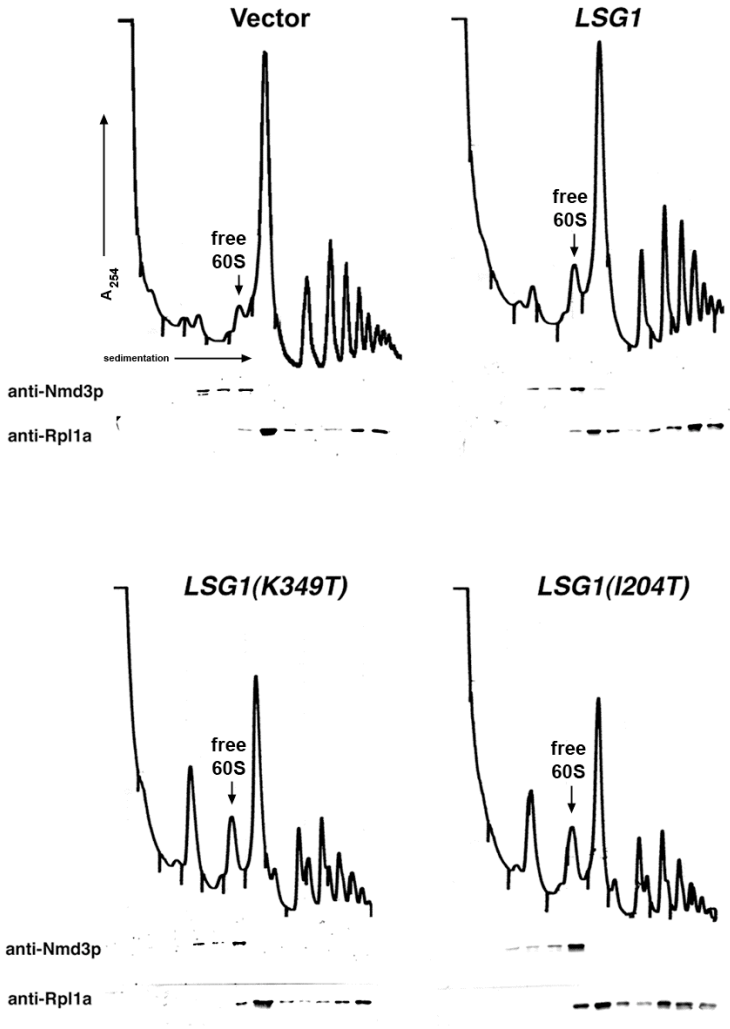

Figure 3.7 Nmd3p co-sediments with free 60S subunits in the presence of dominant negative Lsg1p.

Lysates were prepared in the presence of cycloheximide from strain CH1305 (wild-type) containing empty vector (pRS425), pAJ879 (*GAL10*::*LSG1*), pAJ1109 (*GAL10*::*LSG1[K349T]*), or pAJ1132 (*GAL10*::*LSG1[I204T])* following galactose-induction of the *LSG1* alleles for 3 h. Lysates were fractionated and analyzed as described in Chapter 2. Proteins from each fraction were precipitated with trichloroacetic acid, resolved on SDS-PAGE gels, transferred to nitrocellulose membranes, and immunoblotted for Nmd3p and the ribosomal protein Rpl1Ap as indicated.

3.3.4 *LSG1* and *NMD3* show genetic interaction

To further examine the apparent functional interaction between *LSG1* and *NMD3*, I tested for genetic interaction. Strains bearing temperature-sensitive *nmd3* mutant alleles were crossed to an *lsg1*Δ mutant containing wild-type *LSG1* on a *URA3* plasmid. Single and double mutants were obtained after sporulating the diploid. I then asked if wild-type *LSG1* could be replaced by a conditional allele by selecting against the wild-type allele on 5-FOA-containing media. While strains bearing a single conditional allele of either *NMD3* or *LSG1* grew well at permissive temperature in the presence of 5-FOA, double mutants exhibited either a pronounced growth defect (*nmd3-3 lsg1-2* and *nmd3-4 lsg1-2*, Figure 3.8) or synthetic lethality (*nmd3-3 lsg1-3* and *nmd3-4 lsg1-3,* Figure 3.8). The negative synergy between the *lsg1* and *nmd3* conditional alleles is consistent with a molecular interaction between these factors during 60S biogenesis.

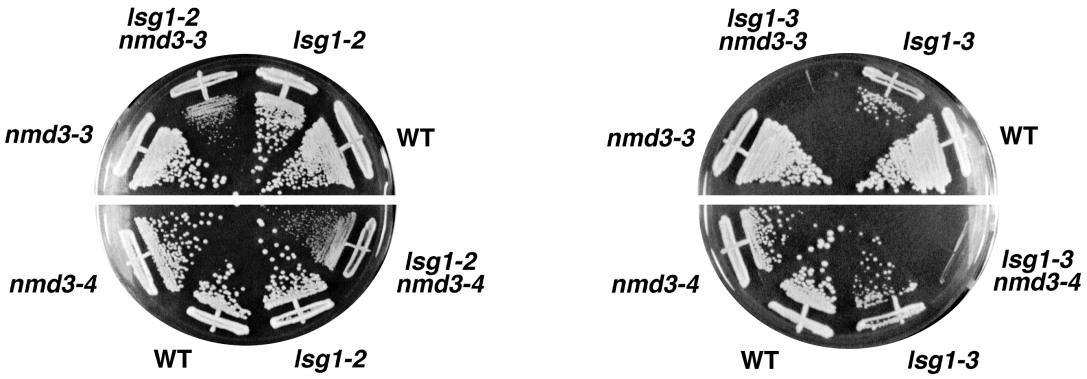

Figure 3.8 *lsg1* and *nmd3* mutants exhibit synthetic lethality.

AJY1511 (*lsg1Δ::KanMX4/*pAJ626[*LSG1 URA3*]), AJY1512 (*lsg1Δ::KanMX4/*pAJ626[*LSG1 URA3*] *nmd3-3*), and AJY1521 (*lsg1Δ::KanMX4/*pAJ626[*LSG1 URA3*] *nmd3-4*) were transformed with *lsg1-2* and *lsg1-3* mutant alleles on a *LEU2* plasmid. Transformants were restreaked onto 5-FOA plates along with AJY1513 (*nmd3-3*), AJY1518 (*nmd3-4*), and wild-type strains to replace wild-type *LSG1::URA3* plasmids with the appropriate mutant allele of *lsg1*. Plates were incubated at room temperature (~25°C) for 10 days.

Independently, I identified *NMD3* in a high-copy suppressor screen for genes that, when over-expressed, could suppress the dominant negative growth phenotype of the *LSG1(N173Y,L176S)* allele, lending further support for a functional interaction between these two biogenesis factors. Surprisingly, the multifunctional mRNA binding protein, *PAB1*, was also isolated as a high-copy suppressor in this screen (data not shown). Pab1p plays key roles in polyA-tail biogenesis, translation efficiency, and in the stability of mRNA (Caponigro and Parker, 1996; Zhao et al., 1999) and has recently been shown to be required for the efficient export of mRNA from the nucleus in yeast (Brune et al., 2005). Over-expression of *PAB1* may enhance the translational efficiency and overall fitness of the cell, partially compensating for the negative growth effects imparted by the

LSG1(N173Y,L176S) allele. Alternatively, *PAB1* over-expression may help to bypass the dominant negative phenotype by playing a more direct role in 60S or related export pathways (see Discussion). Unlike high-copy *NMD3*, however, *PAB1* suppression was specific to the *LSG1(N173Y, L176S)* allele (see below and data not shown).

I then asked if high copy Nmd3p could suppress other dominant negative *LSG1* alleles. Indeed, the growth arrest resulting from expression of *LSG1(K349T)* or *LSG1(I204T)* was markedly alleviated by expression of *NMD3* from a 2 micron plasmid (Figure 3.9A). Suppression by high-copy *NMD3* was observed among all of the dominant negative *LSG1* alleles isolated in the screen, with greater suppression observed for the weaker dominant mutants. The degree of suppression increased with copy number up to a point (compare suppression of *NMD3* on *CEN* versus *2μ* vectors, Figure 3.9A), however. At very high levels of Nmd3p expression (galactose-induction), the degree of suppression was less pronounced, perhaps alluding to a relevant functional consequence of high Nmd3p levels in this genetic background (compare expression levels from Figure 3.9B with degree of suppression from Figure 3.9A and see discussion). Although high-copy *NMD3* suppressed the growth defect of *LSG1* dominant mutants, growth was not restored to wild-type levels (Figure 3.9C).

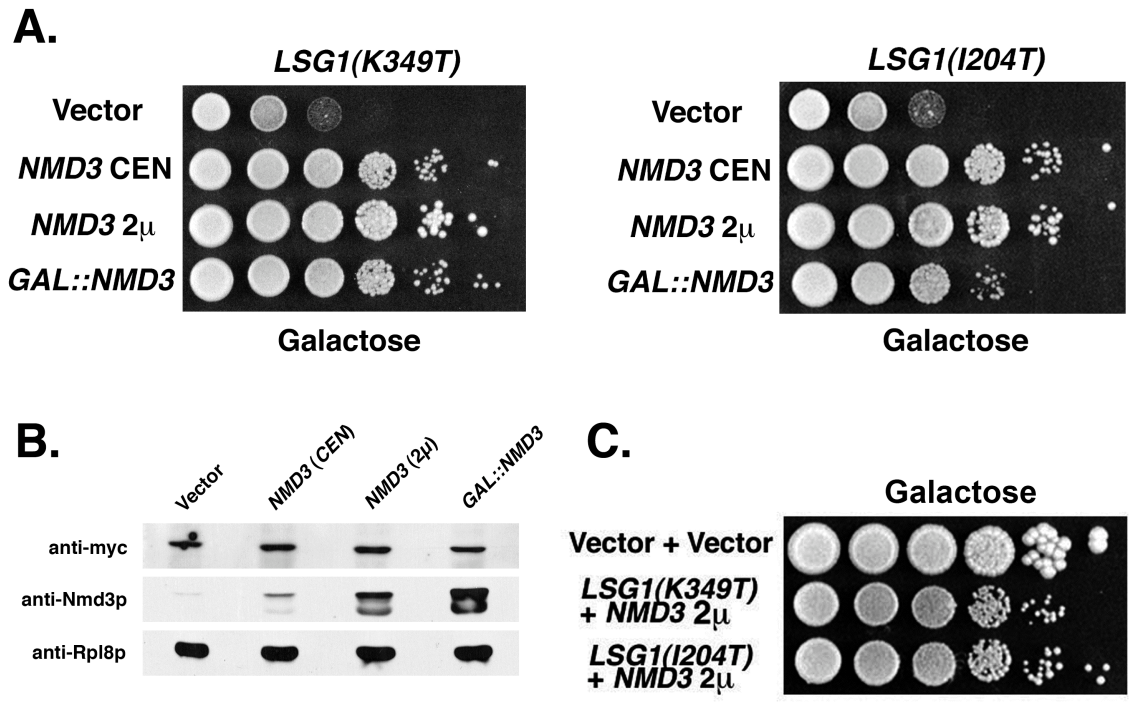

Figure 3.9 Growth suppression of dominant negative *LSG1* alleles by high-copy *NMD3*.

(A.) Tenfold serial dilutions from liquid cultures of strain CH1305 (wild-type) transformed with either pAJ1109 (*GAL10*::*LSG1[K349T]*) or pAJ1132 (*GAL10::LSG1[I204T]*) in combination with empty vector (pRS416), pAJ409 (*NMD3, CEN*), pAJ363 (*NMD3, 2μ*) or pAJ1143 (*GAL1::NMD3,CEN*) were spotted onto drop-out plates containing galactose as the sole carbon source and incubated for 5 days at 30°C. (B.) Western blots against Nmd3p, Rpl8p, and cmyc-Lsg1p(K349T)p among extracts derived from cultures of strain CH1305 harboring pAJ1109 (*GAL10::cmyc-LSG1[K349T]*) and either empty vector (pRS426), pAJ409 (*NMD3 CEN*), pAJ363 (*NMD3* 2μ), or pAJ1143 (*GAL10::NMD3*) following galactose-induction for 5 hours. (C.) Growth comparison between wild-type (empty vectors), *LSG1(K349T),* and *LSG1(I204T)* + high-copy *NMD3* (2μ) on galactose media after 6 days at 30°C.

As a control for the specificity of suppression of *lsg1* mutants by *NMD3*, I tested if high copy Nmd3p also could suppress *nog1* temperature sensitive mutants. *NOG1* encodes an essential nucleolar GTPase required for early processing events in the 60S biogenesis pathway and has been identified on Nmd3p-bound 60S subunits in the nucleus (Kallstrom et al., 2003; Park et al., 2001). We had previously shown that strains bearing either *lsg1* or *nog1* temperature sensitive alleles exhibit nuclear accumulation of Rpl25-eGFP and decreased levels of 60S subunits at non-permissive temperatures (Kallstrom et al., 2003). Only *lsg1* conditional alleles, however, were suppressed by high-copy *NMD3* (data not shown).

3.3.5 Restored shuttling of high-copy Nmd3p

Although genomically-expressed Nmd3-GFP was trapped in the cytoplasm by dominant negative *LSG1* mutants, ectopically-expressed Nmd3-GFP was not efficiently trapped (Figure 3.5A). Apparently, increasing the levels of Nmd3p provides a free pool of Nmd3p for recycling to the nucleus. To test this idea, I examined if shuttling of chromosomally-expressed Nmd3-GFP could be restored by increased levels of untagged Nmd3p in the presence of dominant negative Lsg1p alleles. Untagged *NMD3* on a two-micron vector was co-transformed with empty vector or galactose-inducible wild-type *LSG1*, *LSG1(K349T)*, or *LSG1(I204T)* into an LMB-sensitive strain bearing genomically-integrated *NMD3-GFP*. Nmd3-GFP localization was monitored in these cells following galactose-induction of the *LSG1* alleles and subsequent treatment with LMB.

Whereas chromosomally-expressed Nmd3-GFP was retained in the cytoplasm on 60S subunits in the presence of *LSG1(K349T)* or *LSG1(I204T)* mutant alleles (Figure 3.5B), ectopic expression of untagged Nmd3p partially alleviated this phenotype. As shown in Figure 3.10, induction of *LSG1(K349T)* or *LSG1(I204T)* no longer efficiently blocked redistribution of Nmd3-GFP to the nucleus, following treatment with LMB. I

conclude that high-copy Nmd3p provides sufficient Nmd3p for recycling to the nucleus to escape the dominant negative effect of Lsg1p mutants trapping Nmd3p in the cytoplasm. This explains my initial inability to observe cytoplasmic retention of Nmd3-GFP when it was ectopically expressed (Figure 3.5A). These findings also illustrate the general caution that should be taken when making interpretations based upon the localization of proteins that are ectopically-expressed in yeast or transiently-transfected in cells of higher eukaryotes.

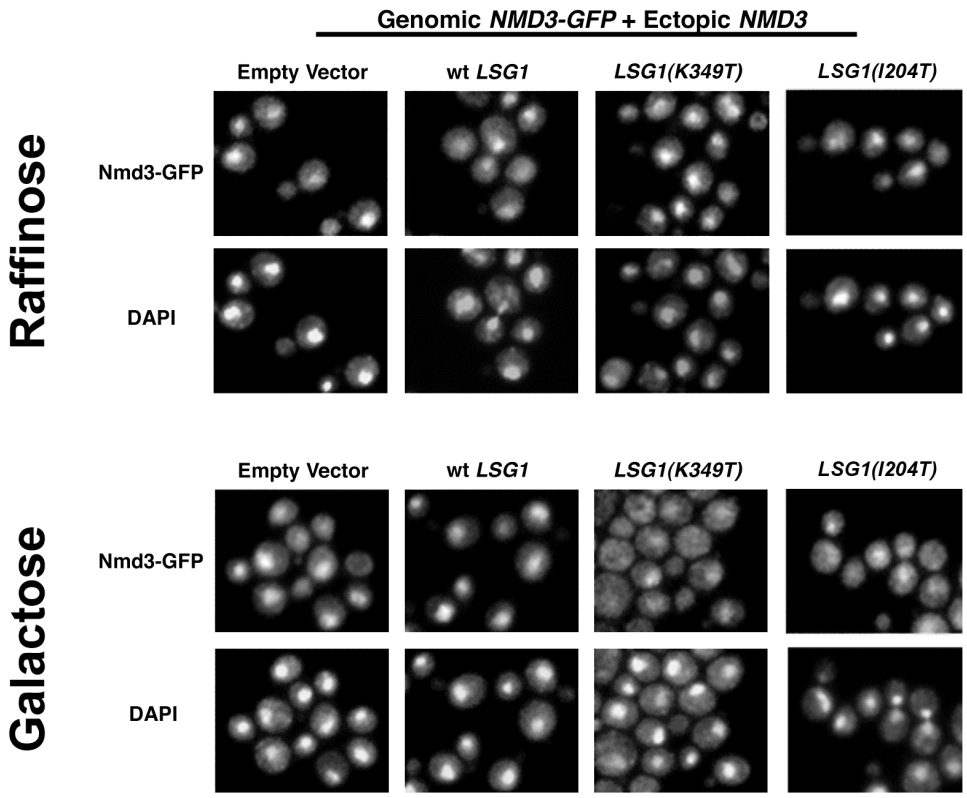

Figure 3.10 Ectopic expression of wild-type *NMD3* allows genomically expressed *NMD3-GFP* to recycle in the presence of dominant negative Lsg1p.

Visualization of Nmd3-GFP in strain AJY1705 (*NMD3-GFP CRM1[T539C]*) containing pAJ363 (*NMD3, 2μ*) and either empty vector (pRS425), pAJ879 (*GAL10::LSG1*), pAJ1109 (*GAL10::LSG1[K349T]*), or pAJ1132 (*GAL10::LSG1[I204T]*) after culturing to mid-log phase followed by galactose-induction for 3 hours. Cells were treated with LMB, fixed, and DAPI stained as described in Chapter 2.

It is unlikely that Nmd3p levels exceeded the level of galactose-induced dominant negative *LSG1* in these experiments. Nevertheless, high copy Nmd3p suppresses dominant negative *LSG1* alleles. This suggests that the stoichiometry of Nmd3p to another factor is critical for determining the availability of Nmd3p for recycling to the nucleus. If Lsg1p acts only on Nmd3p on the 60S subunit, then the ratio of Nmd3p to the free 60S subunit, as well as to Lsg1p, may be critical.

3.3.6 High-copy Nmd3p partially alleviates the 60S biogenesis defects of dominant negative Lsg1p mutants

If high-copy Nmd3p suppresses dominant negative *LSG1* mutants by restoring export of 60S subunits, the steady-state distribution of Rpl25-eGFP should be shifted back to the cytoplasm. Rpl25-eGFP localization was monitored in cells ectopically-expressing *NMD3* from a two-micron vector following induction of either *LSG1(K349T)* or *LSG1(I204T)*. Indeed, the localization of Rpl25-eGFP in these cells showed a pronounced redistribution to the cytoplasm dependent upon the increased copy number of Nmd3p (compare Figure 3.11 to Figure 3.3). The bulk shift of Rpl25-eGFP from the nucle(ol)us to the cytoplasm in cells co-expressing dominant negative Lsg1p alleles and high copy-Nmd3p suggests that Nmd3p was rate-limiting for 60S export.

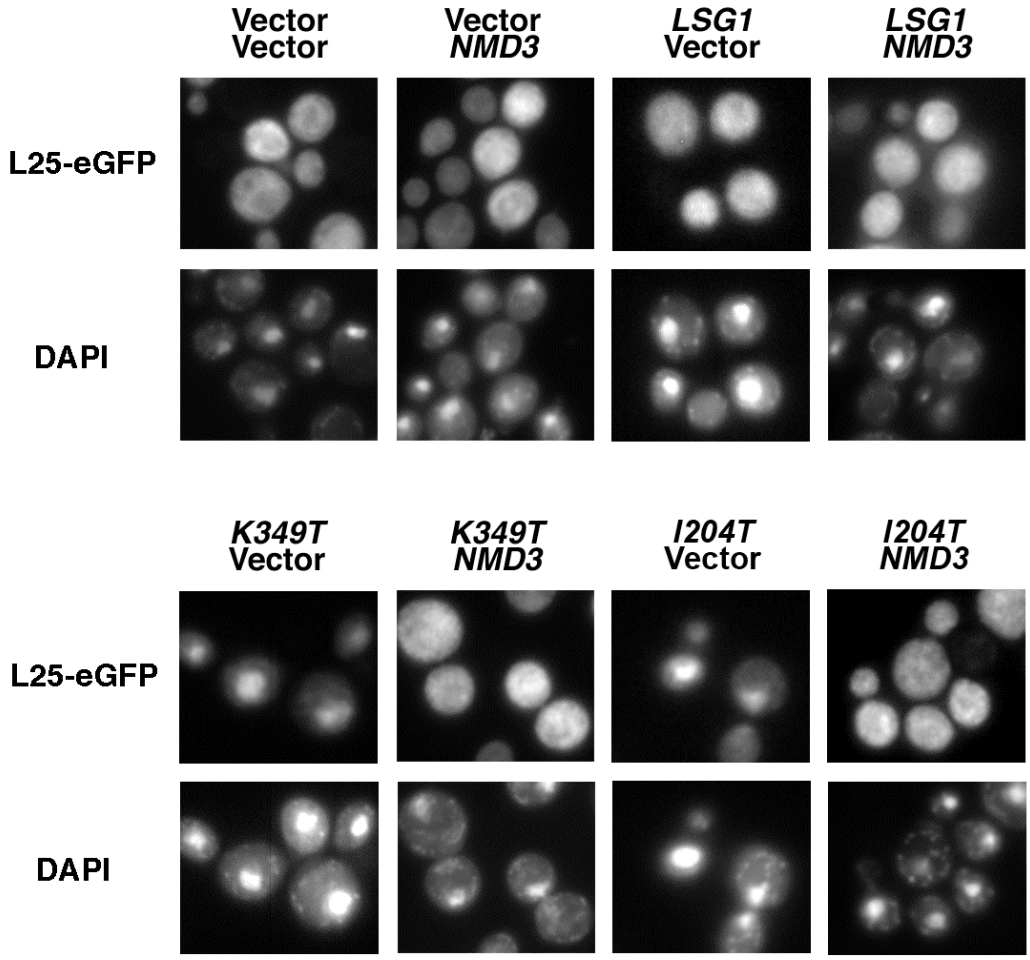

Figure 3.11 High-copy *NMD3* restores 60S export in cells expressing dominant negative *LSG1*.

Rpl25-eGFP (pASZ11-RPL25-eGFP) and Nmd3p (pAJ363) were ectopically expressed in strain CH1305 (wild-type) carrying empty vector (pRS425), pAJ879 (*GAL10*::*LSG1*), pAJ1109 (*GAL10*::*LSG1[K349T]*), or pAJ1132 (*GAL10*::*LSG1[I204T]*). Cells were handled as described in the legend to Figure 3.3.

In order to assess whether suppression by Nmd3p correlated with restored 60S biogenesis, I analyzed polysome profiles in strains bearing exogenous copies of *NMD3* following induction of either *LSG1(K349T)* or *LSG1(I204T)*. Profiles from these cells showed an increase in the free 60S population (Figure 3.12) and a decrease in half-mers with a corresponding increase in polysomes (see arrows, Figure 3.12). These results demonstrate that high-copy Nmd3p enhances the pool of free 60S subunits, likely by increasing their export out of the nucleus (Figure 3.11). Consistent with this line of thinking, a mutant allele of Nmd3p that was previously shown to be blocked for nuclear import (*NMD3Δ120*) (Ho et al., 2000b), and thus subunit export, was unable to suppress the growth inhibition phenotype of Lsg1p dominant negative mutants (data not shown). Hence, suppression of dominant negative Lsg1p requires import of Nmd3p. Although the block in 60S export was alleviated by increasing Nmd3p expression, polysome profiles were not fully restored, and the free subunit pools remained relatively high. Apparently, many of the cytoplasmic subunits fail to enter the translating pool, possibly because of the persistence of Lsg1p and/or Nmd3p on the 60S subunit blocks subunit joining or because another requisite step for joining has been disrupted in the absence of proper Lsg1p function.

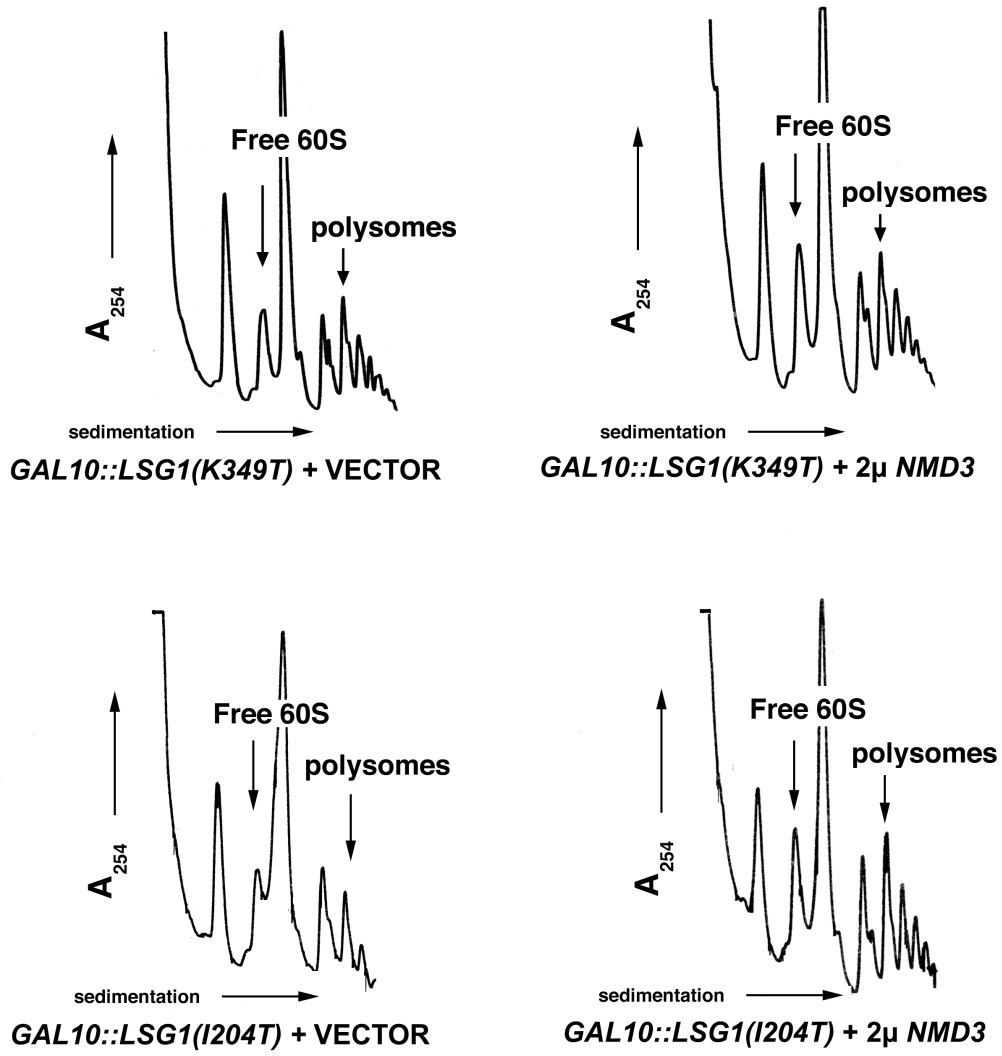

Figure 3.12 High-copy *NMD3* partially suppresses the low 60S levels and polysome defects observed in the presence of mutant Lsg1p.

CH1305 (wild-type strain) constituitively-expressing ectopic Nmd3p (pAJ363) and carrying either empty vector (pRS425), pAJ879 (*GAL10::LSG1*), pAJ1109 (*GAL10::LSG1[K349T]*), or pAJ1132 (*GAL10::LSG1[I204T]*) were cultured in drop-out media containing 1% raffinose as the non-inducible carbon source. Galactose was added to 1%, and the cells were cultured for an additional 4 h. Cells were harvested and extracts were prepared in the presence of cycloheximide and analyzed on sucrose gradients as described in Chapter 2. Arrows indicate increased 60S levels and polysomes in cells co-expressing Lsg1p dominant negative alleles and high-copy Nmd3p.

3.4 Discussion

The assembly of ribosomal subunits requires more than 170 trans-acting factors. However, only a handful of biogenesis factors remain associated with the nascent 60S subunits upon entering the cytoplasm (Fromont-Racine et al., 2003a; Tschochner and Hurt, 2003). These late factors include the nuclear export adapter, Nmd3p (Gadal et al., 2001b; Ho et al., 2000b); the subunit anti-association factor, Tif6p (Senger et al., 2001); and Arx1p (Nissan et al., 2002), a protein that binds at the exit tunnel and may block premature association of other exit tunnel-binding proteins (Hung and Johnson, 2005). While Nmd3p, Tif6p, and Arx1p accompany the subunit from the nucleoplasm, Lsg1p binds subunits only after they have been exported to the cytoplasm (Nissan et al., 2002). Prior to the initial round of translation, Nmd3p, Tif6p, Lsg1p, and possibly Arx1p must be released from 60S subunits, as they are not observed to sediment at the position of polysomes in sucrose gradients (Ho and Johnson, 1999; Hung and Johnson, 2005; Kallstrom et al., 2003; Nissan et al., 2002; Si and Maitra, 1999).

Here, I have identified dominant mutations in the essential, cytoplasmic ribosomal biogenesis factor *LSG1*. Although Lsg1p has not yet been shown to have GTPase activity, the catalytic GTPase motifs are highly conserved, and mutations altering residues known to be essential for GTPase activity in other proteins yielded dominant negative phenotypes for Lsg1p. Furthermore, a closely related protein, YjeQ, from *Escherichia coli* has recently been shown to have GTPase activity (Daigle et al., 2002). The mutant Lsg1p proteins retain the ability to bind 60S, as demonstrated by their co-sedimentation with free 60S subunits in sucrose gradients and by their ability to co-immunoprecipitate 60S subunits from cell extracts (data not shown). Consequently, the dominant negative effects of these mutant proteins most likely arise from the inhibition of events that ordinarily occur on nascent subunits in the cytoplasm.

Expression of dominant negative Lsg1p mutants prevented Nmd3p recycling to the nucleus, resulting in its cytoplasmic retention and apparent nuclear exclusion. The non-shuttling pool of Nmd3-GFP remained associated with free 60S subunits, suggesting that Nmd3-GFP was not released from cytoplasmic 60S under these conditions. Induction of dominant negative *LSG1* alleles also resulted in the marked nucle(ol)ar accumulation of the 60S reporter protein Rpl25-eGFP. In light of the fact that Nmd3p is the export adapter for 60S subunits and that *nmd3* mutants also accumulate Rpl25-eGFP in the nucleolus, it is expected that a failure to recycle Nmd3p would lead to such nucle(ol)ar entrapment of 60S subunits. This result also supports the idea that Nmd3p loads onto the pre-60S subunit in the nucleolus.

We had previously speculated that temperature-sensitive alleles of *LSG1* failed to recycle a biogenesis factor at non-permissive temperature (Kallstrom et al., 2003). Due to the cytoplasmic localization of Lsg1p, we had concluded that the defects in rRNA processing and the accumulation of 60S subunits in nucleoli observed upon disrupting Lsg1p function were most likely indirect, resulting instead from a failure in recycling a nucle(ol)ar biogenesis factor. Although Nmd3p was an attractive candidate for this factor, we were not able to show a recycling failure for ectopically-expressed Nmd3-GFP in these mutants at restrictive temperature. Here, I have demonstrated that this was due to the fact that ectopic expression of Nmd3p suppresses mutations in *LSG1*, including the restoration of Nmd3p's nucleocytoplasmic shuttling (Figure 3.10). This result suggests that Nmd3p shuttling is highly dependent on the stoichiometry of Nmd3p to other factors.

Ectopic expression of Nmd3p led to release of 60S subunits from the nucle(ol)us and significantly improved cell growth. This restoration of 60S export most likely relies on the larger pool of free Nmd3p that is able to bypass Lsg1p and enter the nucleus to perpetuate export. Once in the cytoplasm, Nmd3p will be trapped on subunits that also

contain mutant Lsg1p, leading to cytoplasmic accumulation of nascent subunits. However, the support of continued export by high copy Nmd3p will increase the chance that wild-type Lsg1p acts on subunits, allowing a fraction of them to progress into the translational pool.

On the other hand, the increase in polysomes in the presence of high-copy Nmd3p is relatively modest. This raises the question of whether or not improved cell growth is due in part to relieving other defects as well. It is possible that the nuclear accumulation of pre-60S particles itself is detrimental. Blockage in 60S export that arises from a failure to recycle Nmd3p may also impinge upon other export pathways by blocking access to export machinery or by titrating-out a necessary export factor. Consistent with this hypothesis, our lab has identified Pab1p, a key factor required for translation (Caponigro and Parker, 1995) and mRNA stability (Tarun and Sachs, 1995), as a high-copy suppressor of both *LSG1(N173Y,L176S)* and *nmd3-1* mutants (Ho et al., 2000a). Pab1p has recently been shown to be required for the efficient export of mRNAs from the nucleus in yeast (Brune et al., 2005), and its over-expression can compensate for the mRNA export defects associated with mutations in the shuttling hnRNP protein, Nab2p (Hector et al., 2002). Additionally, the mRNA transport factor, Mex67p, was shown to be a high-copy suppressor of *nmd3-1*, while combination of the *mex67-5* and *nmd3-1* alleles results in synthetic lethality (Ho et al., 2000b). The Mex67p cofactor Mtr2p is required for both mRNA and rRNA export, and *MTR2* and *NMD3* also show allele-specific synthetic lethality (Bassler et al., 2001). Taken together, it is possible that a defect in 60S export indirectly impinges upon the export pathway for mRNA and that this indirect effect is relieved by restoring 60S export.

Although high-copy Nmd3p prevents accumulation of pre-60S subunits in the nucleus caused by dominant negative *LSG1*, its release from 60S subunits would still be

expected to require *LSG1* function. Under these conditions, a large pool of free cytoplasmic 60S subunits accumulates. As Nmd3p and Lsg1p are not associated with translating 60S subunits by sucrose gradient analyses, their release may be a requisite step prior to subunit joining. Genetic and biochemical evidence have established an interaction between *NMD3* and the ribosomal protein *RPL10* (Gadal et al., 2001b; Hedges et al., 2005; Karl et al., 1999; Zuk et al., 1999). The binding site for Rpl10p (archaeal L10E, L16 in *Escherichia coli*) on eukaryotic 60S subunits is situated on the joining face in close proximity to the peptidyl-transferase center and the GTPase stalk (Spahn et al., 2001; Yusupov et al., 2001). By extrapolation, the binding site for Nmd3p and Lsg1p may also be located on the joining face of the 60S subunit (Gadal et al., 2001b), and the persistence of these proteins on 60S subunits could pose a direct steric hindrance to subunit joining. Consistent with this hypothesis, a preliminary cryo-EM reconstruction of purified Nmd3p bound to a free 60S subunit has revealed that Nmd3p occupies a position on the joining face of the subunit just below Rpl10p and adjacent to the GTPase stalk (West, Johnson, Gupta, and Frank, unpublished).

High-copy *NMD3* suppresses not only *LSG1* dominant negative mutants but also mutations in *RPL10* (Hedges et al., 2005; Zuk et al., 1999). Furthermore, depletion of Rpl10p or its cytoplasmic chaperone, Sqt1p, leads to nuclear accumulation of Rpl25-eGFP and a marked cytoplasmic retention of Nmd3p, and as I have shown for Lsg1p dominant mutants, increasing the copy number of Nmd3p is able to bypass the nuclear accumulation of 60S subunits in these cells (Hedges et al., 2005; West et al., 2005). The similar behavior of *LSG1* dominant mutants and depletion of Rpl10p could underlie a common role for these two factors in mediating the release of Nmd3p from 60S subunits. Lsg1p may monitor the correct assembly of Nmd3p and Rpl10p on the subunit, thereby

providing structural proofreading of subunit structure prior to release of Nmd3p. These possibilities will addressed further in Chapter 4.

Illustration 3.1 depicts our model for the function of Lsg1p in 60S biogenesis. Nmd3p loads onto pre-60S particles in the nucleolus and provides the nuclear export signal to direct their export to the cytoplasm. Lsg1p, most likely in its GTP-bound form, binds nascent subunits as they emerge from the nucleus, potentially through a direct interaction with Nmd3p. In response to some molecular cue, the GTPase activity of Lsg1p is triggered, leading to a structural rearrangement of the subunit and the dissociation of Lsg1p, Nmd3p and, perhaps, other factors from the 60S subunit prior to translation initiation (Illustration 3.1A). Alternatively, the catalytic activity of Lsg1p could be triggered in response to the subunit acquiring an additional factor(s) or adopting a late conformation that primes it for functionality. In this way, Lsg1p could serve a proofreading function, allowing only properly assembled subunits to enter the translational pool.

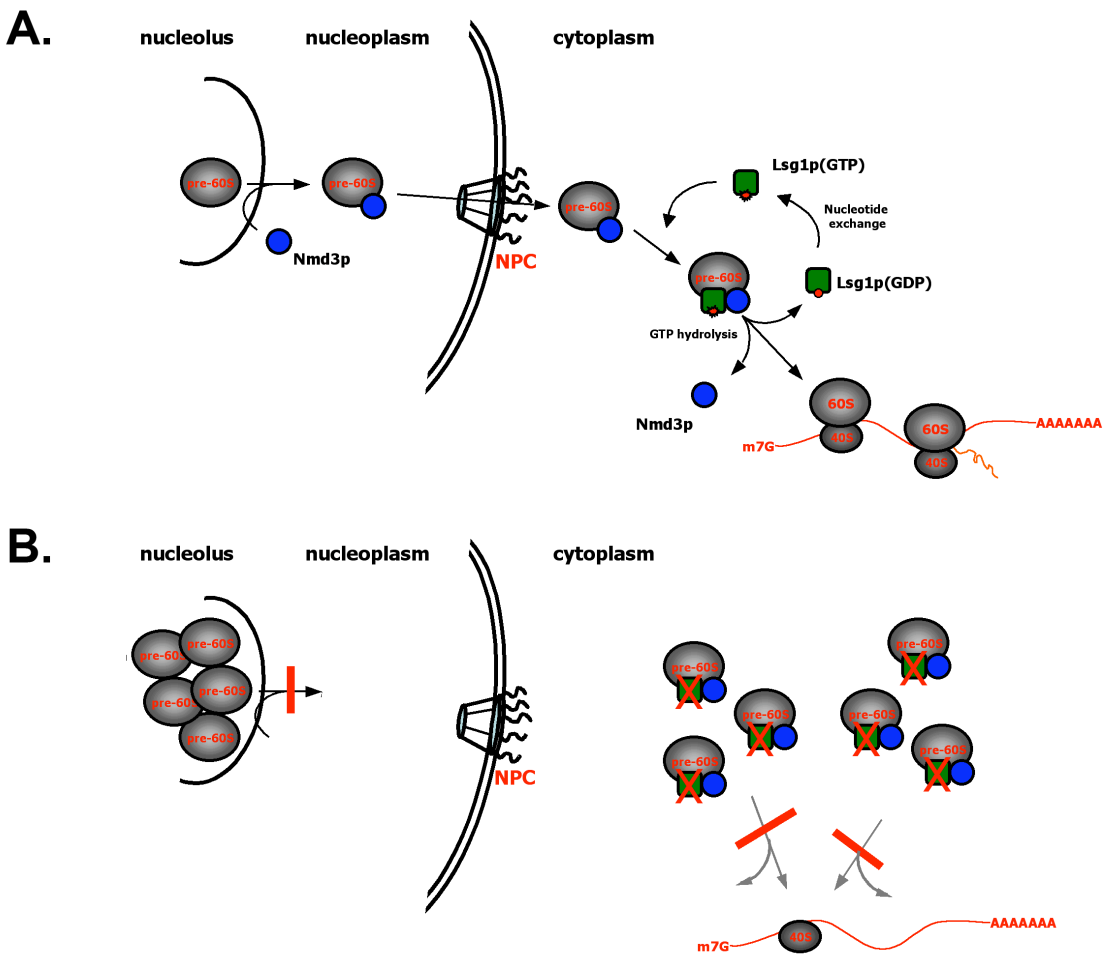

Illustration 3.1 Model for Lsg1p-mediated release of Nmd3p from cytoplasmic 60S subunits.

See text for a detailed discussion of the model. (A.) Lsg1p binds to the newly-exported 60S subunit and is required for recycling Nmd3p to the nucleus for additional rounds of subunit export. (B.) Dominant negative Lsg1p binds to newly-exported free 60S subunits but is incapable of mediating the release of Nmd3p, resulting in the accumulation of nascent 60S subunits in the nucleolus and a block in subunit joining.

Disruption of Lsg1p function, as in the case of dominant negative mutants, would lead to a block in Nmd3p release from subunits and a potential barrier to subunit joining (Illustration 3.1B). The free pool of Nmd3p would rapidly become depleted due to its retention on cytoplasmic subunits containing mutant Lsg1p, leading to accumulation of nascent subunits in the nucle(ol)us. In this way, both 60S subunit export and activation of cytoplasmic subunits would be affected simultaneously.

Like Lsg1p, another cytoplasmic GTPase, Efl1p/Ria1p, was shown to be required for a late step in 60S biogenesis. Disruption of Efl1p activity leads to a 60S biogenesis defect (Becam et al., 2001; Senger et al., 2001), coinciding with the cytoplasmic accumulation of the nucle(ol)ar biogenesis factor, Tif6p (Senger et al., 2001), and a blockage in subunit joining (Spremulli et al., 1979). The authors proposed that Efl1p induces a conformational change in nascent 60S subunits in the cytoplasm, thereby releasing Tif6p and contributing to translational-competence (Senger et al., 2001). Subsequent work has suggested that Efl1p may interact with 60S at a position that overlaps with the EF-2 binding site on the GTPase stalk, perhaps structurally assessing or inducing an appropriate conformational state prior to release of Tif6p (Brune et al., 2005). As Lsg1p appears to play a similar role in facilitating the release of Nmd3p, it is possible that Lsg1p and Efl1p act on subunits in a concerted manner. The two factors may act in tandem or sequentially at discrete positions on 60S to induce structural rearrangements that result in the release of persistent biogenesis factors, priming subunits for translation.

In conclusion, results from this chapter support a role for Lsg1p in mediating the release of the 60S export adapter, Nmd3p, from nascent cytoplasmic subunits prior to translation initiation. As little is currently known about the cytoplasmic events associated with the late maturation of the 60S ribosomal subunit, the elucidation of Lsg1p's role in

this pathway may prove critical to our understanding of how cells have evolved to assess the functional or structural competence of nascent subunits prior to their incorporation into the translational pool. Further characterization of the role of Lsg1p and timing of Nmd3p release during late subunit maturation is the focus of Chapter 4.

Chapter 4: Coordinated release of Nmd3p and loading of Rpl10p by Lsg1p

4.1 Introduction

Results presented in the previous chapter provide evidence that Lsg1p plays a critical role in recycling Nmd3p, the 60S nuclear export adapter, back to the nucleus for sustained subunit export. In this chapter, I investigate the broader functional context for the release of Nmd3p during the late maturation of 60S ribosomal subunits. Consistent with their common effects on Nmd3p shuttling, I show that mutations in *NMD3* that suppress *rpl10* mutants also suppress dominant negative *LSG1* mutants. Upon examination of the functional basis for the observed growth suppression, I demonstrate that, unlike wild-type Nmd3p, a suppressor allele is capable of recycling to the nucleus in the presence of a dominant negative Lsg1p mutant. I then show that the Nmd3p suppressor alleles exhibit a decreased affinity for 60S subunits, accounting for their ability to support growth and avoid cytoplasmic entrapment in the presence of mutant Lsg1p. In contrast to published predictions, I demonstrate that wild-type Nmd3p binds tightly to mutant Rpl10p-bound subunits, while suppressor mutations weaken this interaction rather than enhance it. Furthermore, in a departure from a published model in which Rpl10p is predicted to form the binding site for Nmd3p on 60S, I provide evidence that Nmd3p is capable of binding to 60S subunits independently of Rpl10p. Lastly, experimental data is presented that supports a model in which the release of Nmd3p from 60S in the cytoplasm is coordinated with the accommodation of Rpl10p into subunits in the context of Lsg1p activity. A discussion of the broader functional implications of the spatio-temporal relationship between Rpl10p loading and Nmd3p release prior to translation initiation is also provided.

4.2 Background

As described in Chapter 1, the shuttling protein, Nmd3p, mediates the Crm1-dependent nuclear export of nascent 60S ribosomal subunits in a pathway that is conserved from yeast to humans (Johnson et al., 2002). A widely-accepted model for Nmd3p recruitment to pre-60S particles predicts that the loading of the ribosomal protein, Rpl10p, onto the subunit late in the nucleus is required to provide a binding surface for Nmd3p (Gadal et al., 2001b; Nissan et al., 2002). This model was conceived in support of an accumulating body of evidence that pointed toward a functional interaction between *RPL10* and *NMD3*. In an initial report, three spontaneous extragenic revertants of the temperature sensitive mutant *rpl10[G161D]* all mapped to Nmd3p (Karl et al., 1999). In an independent analysis, over-expression of Nmd3p was shown to suppress the negative growth phenotype associated with a second conditional mutant of *RPL10* (*rpl10[F85S]*) (Zuk et al., 1999). In support of the genetic interactions observed between *NMD3* and *RPL10*, Gadal *et al.* (2001) demonstrated that Nmd3p exhibits a modest affinity for purified Rpl10p in a directed *in vitro* binding assay. They also provided evidence that an *rpl10* (*rix5-1*) mutant accumulates the ribosomal reporter protein, Rpl25-eGFP, in the nucleus, an observation that is consistent with the block in 60S export that would arise from disrupting Nmd3p recruitment to nuclear subunits (Gadal et al., 2001b). Taking into account the delayed rate of Rpl10p incorporation into subunits relative to other ribosomal proteins (Kruiswijk et al., 1978) and the apparent functional interaction between Rpl10p and Nmd3p, it was postulated that the late loading of Rpl10p onto 60S in the nucleus would provide a structural cue to signal the acquisition of "export competence," allowing for the recruitment of Nmd3p to mediate nuclear export (Gadal et al., 2001b).

In light of Lsg1p's role in releasing Nmd3p from subunits in the cytoplasm, Rpl10p and Lsg1p would seem to play opposing roles in modulating Nmd3p's binding affinity for the subunit (Illustration 4.1). Several significant observations, however, are more closely in line with the two factors acting in a cooperative fashion with respect to Nmd3p's shuttling behavior. Work from our lab has shown that disrupting the function of either Rpl10p or its essential chaperone, Sqt1p (Eisinger et al., 1997a), results in the cytoplasmic entrapment of Nmd3p on 60S subunits, leading to an accumulation of nascent 60S subunits in the nucleus (Hedges et al., 2005; West et al., 2005). Furthermore, like cells harboring Lsg1p dominant negative mutants, increasing the copy number of Nmd3p restores Nmd3p shuttling and 60S export in cells depleted for Rpl10p, suggesting that Rpl10p is not required for the Nmd3p-dependent export event (Hedges et al., 2005; West et al., 2005). The cytoplasmic entrapment of Nmd3p on 60S subunits upon depletion of Rpl10p, rather than the accumulation of a large free pool of Nmd3p, is surprising if Rpl10p does, indeed, serve as the binding site for Nmd3p on nuclear subunits. Contrary to expectations, our lab has shown that Rpl10p and Sqt1p are, in fact, restricted to the cytoplasm under conditions that trap Nmd3p and 60S subunits in the nucleus, perhaps indicating that Rpl10p loads onto subunits after their export to the cytoplasm ((West et al., 2005) and Hedges and Johnson, unpublished). Consistent with this observation, the loading of the human homologue of Rpl10p (QM) into subunits is thought to be a cytoplasmic event (Nguyen et al., 1998).

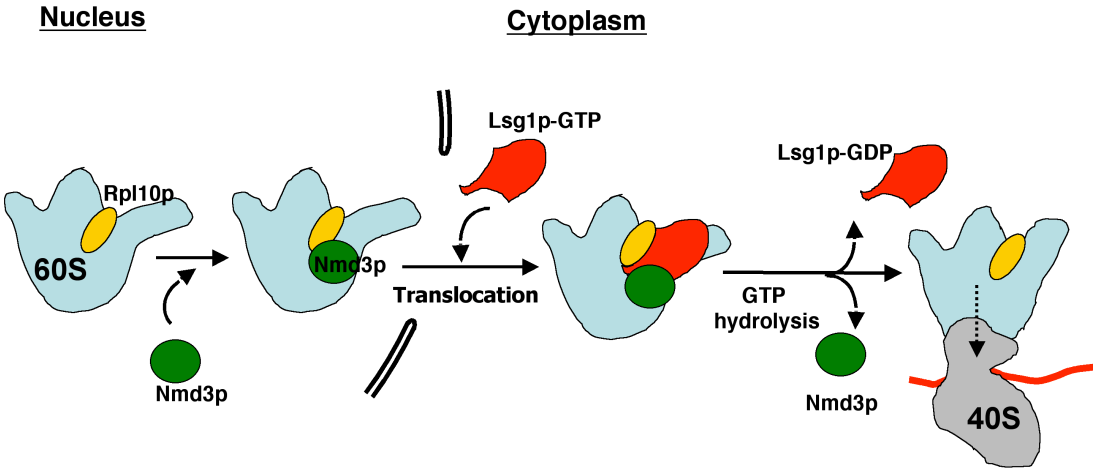

Illustration 4.1 Cartoon depicting the pre-existing model for Rpl10p-dependent recruitment of Nmd3p to nuclear subunits and the Lsg1p-dependent release of Nmd3p in the cytoplasm

Nmd3p binds to an "export-competent" 60S subunit loaded with Rpl10p in the nucleus. Following translocation to the cytoplasm, Lsg1p (presumably in its GTP-bound form) is recruited to 60S and, upon some maturational cue, hydrolyzes GTP to release Nmd3p for subsequent rounds of 60S export.

4.3 Results

4.3.1 *NMD3* suppressors of *rpl10* mutants also suppress dominant negative *LSG1* mutants

Disruption of Rpl10p function, like expression of dominant negative Lsg1p mutants, blocks Nmd3p's ability to shuttle by trapping it on cytoplasmic 60S subunits (Hedges et al., 2005; West et al., 2005). Furthermore, the inhibition of Nmd3p shuttling in *rpl10* and *lsg1* mutants leads to a nuclear export defect for newly-synthesized pre-60S particles as well as a subunit joining defect, phenotypes which can be suppressed by increasing the copy number of free Nmd3p ((Hedges et al., 2005; West et al., 2005), and see Chapter 3). In light of the common phenotypes observed for *rpl10* and *lsg1* mutants, I sought to determine if there existed a functional interaction between these two 60S-associated factors.

Previous analysis of a strong *RPL10* conditional allele (*rpl10[G161D]*) resulted in the isolation of three spontaneous revertant mutants that all traced to amino acid substitutions in Nmd3p (I279F, L291F, and A336P) and mapped to a region just upstream of Nmd3p's nuclear localization signal (NLS)(Figure 4.1A)(Karl et al., 1999). The ability of these mutants to suppress the *rpl10[G161D]* allele led to the interpretation that they behaved as gain-of-function mutants that restored Nmd3p's interaction with 60S subunits for nuclear export (Gadal et al., 2001b). This rationale was offered in support of the model in which Rpl10p loads late in the nucleus and serves as the binding site for Nmd3p on 60S prior to subunit export (Illustraton 4.1) (Gadal et al., 2001b; Nissan et al., 2002). In light of our observations that depletion of Rpl10p leads to cytoplasmic entrapment rather than nuclear accumulation of Nmd3p (Hedges et al., 2005; West et al., 2005), this interpretation seemed insufficient to account for the functional interaction between Nmd3p and Rpl10p.

In an attempt to achieve a more precise understanding of the functional dynamics between Nmd3p and Rpl10p, we had previously conducted PCR-based mutagenic screens to identify additional mutations in Nmd3p that could suppress the negative growth phenotypes of the *rpl10[G161D]* and *rpl10[F85S]* temperature-sensitive mutants (Hedges et al., 2005). Suppressor mutations in *NMD3* that were identified in these screens most typically mapped to two distinct regions in Nmd3p (suppressor domain I: amino acids 100-115 and suppressor domain II: 290-380; Figure 4.1A and Table 4.1). In general, substitutions in the carboxy-terminal "suppressor domain" (aa 290-380), which encompasses the residues (I279, L291, and A336) that had been altered in the original *rpl10[G161D]* spontaneous suppressor mutants, conferred the most robust suppression for both *rpl10* mutants (Figure 4.1B and Table 4.1). The consistency of suppressor

mutations mapping within these two discrete regions of Nmd3p suggests that they are either directly or indirectly important for facilitating Rpl10p's function in 60S biogenesis.

To assess the possibility that Rpl10p and Lsg1p might act in concert to mediate Nmd3p's release from cytoplasmic 60S subunits, I examined whether the *rpl10*-specific *NMD3* suppressor alleles were also able to overcome the negative growth phenotypes of dominant negative *LSG1* mutant*s*. To this end, I introduced plasmids bearing either wild-type or suppressor *NMD3* alleles into strains harboring the galactose-inducible dominant negative *LSG1* mutants to monitor the degree of suppression under inducing conditions. After four days of growth on galactose-containing media, virtually all of the suppressor alleles showed significantly greater suppression of the *LSG1* mutants in comparison to wild-type *NMD3* (Figure 4.1B and Table 4.1). Furthermore, a strong correlation was observed between the *rpl10* and *LSG1* mutants with respect to the degree of suppression conferred by specific suppressor alleles (compare suppression profiles for the representative mutants *rpl10[G161D]* and *LSG1(K349T)* in Figure 4.1 and Table 4.1). Consistent with the results obtained from characterization of the *rpl10* mutants, point mutations within the carboxy-terminal suppressor region in *NMD3* appeared to provide the most robust suppression of the dominant *LSG1* mutants. The relative extent of suppression imparted by the various *NMD3* suppressor alleles in the *LSG1(K349T)* strain background (shown here) were common among all of the dominant negative *LSG1* mutants that I tested (*LSG1[N173Y,L176S], LSG1[I204T], LSG1[S350P], LSG1[S351F];* data not shown).

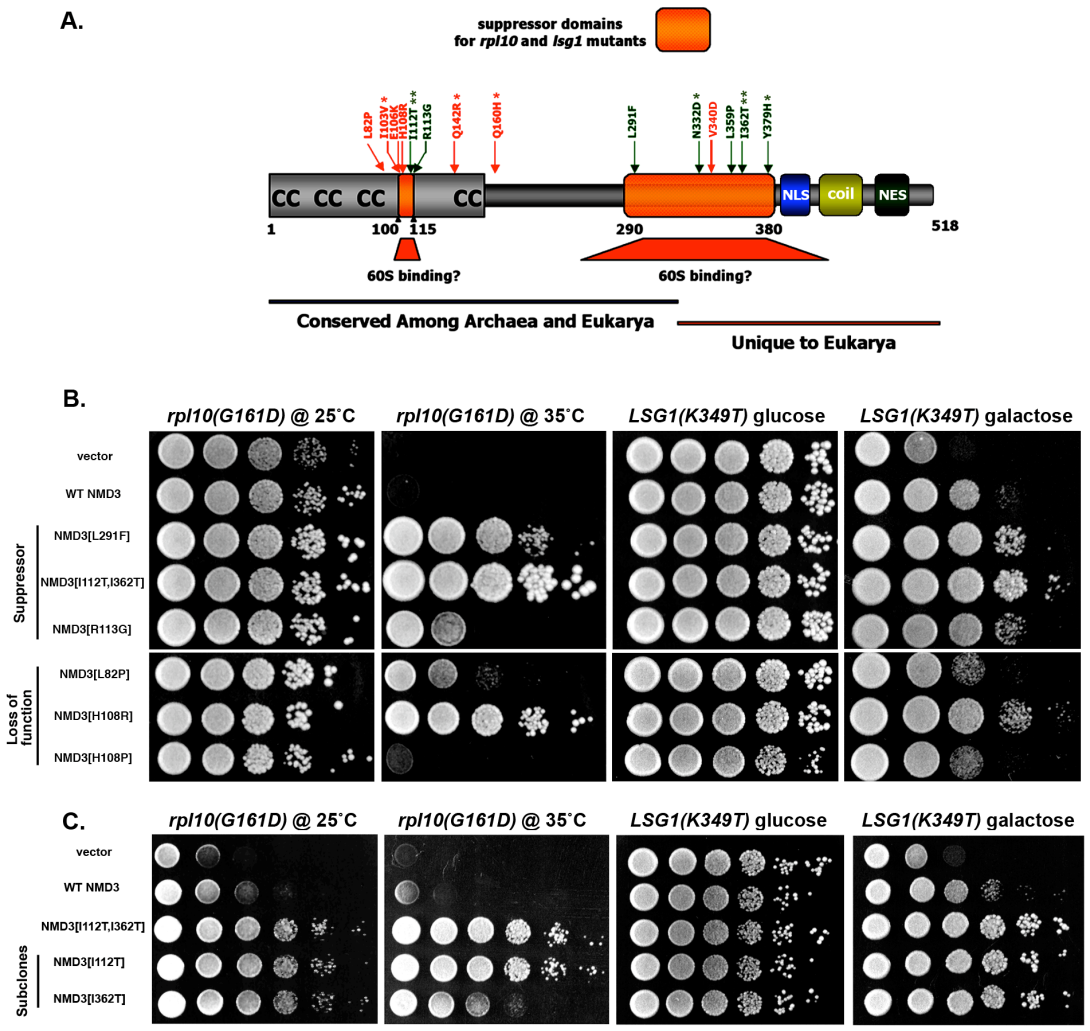

Figure 4.1 Comparison of the effects of *NMD3* suppressor and loss-of-function mutants on the growth phenotypes of *rpl10(G161D)* and *LSG1(K349T)*

(A.) Schematic diagram of Nmd3p showing positions of relevant suppressor mutations (green) and loss-of-function mutations (red). (*) denotes multiple mutations within a single mutant allele. Also shown are the putative zinc-binding Cys-X_2-Cys motifs (CC), nuclear localization signal (NLS), putative coiled-coil (coil), and nuclear export signal (NES). Orange boxes indicate regions in which suppressor mutations were most commonly identified. C-terminal region of Nmd3p containing the majority of the second suppressor domain and the nuclear shuttling sequences is unique to eukaryotes. (B.) AJY1657 (*rpl10[G161D]*) or a wild-type strain (W303) harboring *GAL10*-regulated *LSG1(K349T)* (pAJ1278) were transformed with pRS315 (empty vector), pAJ538 (*NMD3*), pAJ415 (*NMD3[L291F]*), pAJ1315 (*NMD3[I112T,I362T]*), pAJ1316 (*NMD3[R113G]*), pAJ1296 (*NMD3[L82P]*), pAJ1297 (*NMD3[H108R]*), or pAJ1295 (*NMD3[H108P]*). Rpl10p data contributed by John Hedges. Cells were spotted onto plates and grown under the conditions indicated and as described in Chapter 2. (C.) As in (B.) with inclusion of pAJ1334 (*NMD3[I112T]*) and pAJ1326 (*NMD3[I362T]*).

Suppressor allele	*rpl10* mutant used in screen	Δ*nmd3* complementation	*rpl10[G161D]* suppression	*LSG1(K349T)* Suppression
empty	**-**	**-**	**-**	**-**
WT	**-**	+++	**-**	+
T105I	***rpl10[F85S]***	+++	+	+
I112T,I362T	***rpl10[G161D]***	+++	+++	+++
R113G	***rpl10[F85S]***	+++	+	++
L291F	***rpl10[G161D]***	+++	++	++
L359P	***rpl10[G161D]***	+++	+++	+++
N332D,Y379H	***rpl10[F85S]***	+++	+++	+++
V349H,G360D, E476D	***rpl10[F85S]***	+++	++	ND

Table 4.1 *NMD3* suppressor alleles

Relative extent of growth suppression for *LSG1* mutants was compiled from triplicate platings for each *NMD3* allele as described in Chapter 2. *LSG1(K349T)* is included as a representative for the effects observed among dominant negative *LSG1* mutants. *rpl10(G161D)* data provided by John Hedges.

Not surprisingly, an *NMD3* suppressor allele, *NMD3(I112T,I362T)*, possessing point mutations in both of the "suppressor domains" provided the greatest growth restoration among the dominant negative *LSG1* mutants (Figure 4.1 and Table 4.1). Subsequent sub-cloning of these two mutations demonstrated that both were independently capable of suppressing the dominant growth phenotypes, yet neither single mutant could recapitulate the extent of suppression observed for the double mutant (Figure 4.1C). This suggests that these two regions may synergistically contribute to Nmd3p's behavior in the context of Lsg1p activity during cytoplasmic 60S maturation. Although the *NMD3(I112T,I362T)* double mutant also acted as the most robust suppressor of *rpl10* mutants (Figure 4.1B and Table 4.1), the I112T mutation appeared to

account for the bulk of the suppression in the context of the *rpl10[G161D]* mutant (Figure 4.1C).

To achieve a deeper understanding of the functional significance of specific residues and motifs in *NMD3*, we had previously carried-out a PCR-based mutagenic screen for *NMD3* loss-of-function (LOF) mutants (Hedges et al., 2005). Among the mutants identified in the LOF screen, several amino acid substitutions fell adjacent to or within the "suppressor domains" (Figure 4.1A). Remarkably, despite their slow growth phenotype when expressed as the sole copy of *NMD3*, three of these mutants, *nmd3(L82P)*, *nmd3(H108R)*, and *nmd3(I103V,Q142R,Q160H)*, were shown to suppress the *rpl10[G161D]* mutant allele, with the H108R substitution imparting a level of suppression comparable to that observed for the suppressor alleles (Figure 4.1B). To test whether LOF mutants could also suppress *LSG1* dominant mutants, I introduced plasmids bearing either wild-type or LOF *NMD3* alleles into strains harboring the galactose-inducible dominant negative *LSG1* mutants to monitor the degree of suppression under inducing conditions. Under these conditions, only the *nmd3(L82P)*, *nmd3(H108R)*, and *nmd3(I103V,Q142R,Q160H)* mutants were capable of suppressing dominant negative *LSG1* mutants (Figure 4.1B and Table 4.2). Furthermore, the H108R LOF mutant suppressed the dominant *LSG1* alleles better than did wild-type *NMD3*, again closely mirroring the results obtained for *rpl10* mutants (Figure 4.1B and Table 4.2). Surprisingly, a LOF mutant introducing a proline in place of the suppressor arginine substitution at position 108 was incapable of restoring growth and, instead, acted in a dominant negative fashion in wild-type strains (Figure 4.1B).

Loss-of-function allele	Δ*nmd3* complementation	60S Binding	*rpl10[G161D]* suppression	*LSG1(K349T)* suppression
WT	+++	+++	-	+
C35R	+	+++	-	-
C58R,Y,S	-	+	-	-
L82P	+	++	+	+
E106K	+	+++	-	+
H108P	-	+++	-	-
H108R	++	+++	++	++
S109F	-	+	-	-
C145R	+	+	-	-
S230P	-	++	-	-
V340D	-	-	-	-
I103V,Q142R, Q160H	+	+++	+	+
I139T,L259S, L296P	-	-	-	-
L263P,F318I	+	-	-	-

Table 4.2 *nmd3* loss-of-function mutants

Relative extent of growth suppression for *LSG1* mutants was compiled from triplicate platings for each *NMD3* allele as described in Chapter 2. *LSG1(K349T)* is included as a representative for effects observed among dominant negative *LSG1* mutants. Extent of 60S binding determined by immunoprecipitation analysis using c-myc-tagged versions of indicated Nmd3p alleles under low salt conditions (50mM NaCl). *rpl10(G161D)* data provided by John Hedges. 60S binding analysis provided by A.W. Johnson.

The observation that loss-of-function alleles were capable of suppressing both *RPLl10* and *LSG1* mutants suggests that an attenuation of Nmd3p's function rather than a gain-of-function is important for suppression. Indeed, among the loss-of-function *NMD3* alleles that mapped adjacent to or within the "suppressor domains," several mutations resulted in weakened binding to 60S subunits *in vivo* (Table 4.2). While the LOF mutants that were capable of acting as suppressors did not exhibit loss of 60S binding

when analyzed under low salt conditions (50mM NaCl; A.W. Johnson, unpublished), a mutation in the carboxy-terminal suppressor region, V340D, which completely blocked 60S interaction, was incapable of either supporting growth as the sole copy of *NMD3* or suppressing *LSG1* or *rpl10* mutants (Figure 4.1B and Table 4.2). Likewise, other LOF mutants with substitutions in the suppressor domains that severely disrupted 60S binding were also incapable of acting as suppressors (Table 4.2).

As mutations in the "suppressor domains" often gave rise to weakened 60S binding, it is possible that a weakened 60S interaction, rather than an enhancement of interaction, may account for their ability to suppress mutations in *RPL10* or *LSG1*. This would stand in opposition to the previously-published model in which mutations mapping to the carboxy-terminal suppressor region of Nmd3p (*NMD3[I279F]*, *NMD3[L291F]*, and *NMD3[A336P]*; Figure 4.1A) were interpreted to restore growth by compensating for a failure to recruit Nmd3p to 60S in the context of the *rpl10(G161D)* allele through a gain-of-function interaction between the two proteins (Gadal et al., 2001b). This divergence in interpretation will be further addressed in subsequent sections.

4.3.2 Suppressor mutations restore Nmd3p shuttling in the presence of dominant negative *LSG1*

As shown in Chapter 3, a disruption in Lsg1p function results in the cytoplasmic entrapment of Nmd3p on 60S subunits when Nmd3-GFP is expressed at wild-type levels from its genomic locus. In these cells, high-copy Nmd3p was shown to bypass this cytoplasmic entrapment by restoring Nmd3p shuttling, which, in turn, allowed for sustained 60S export. Therefore, in light of the similar levels of growth suppression conferred by high-copy *NMD3* (i.e. from 2μ plasmid) and the low-copy suppressor alleles (i.e. from *CEN* plasmid), it was possible that the suppressor mutants were capable of

partially bypassing Lsg1p function by escaping cytoplasmic entrapment in the presence of dominant negative Lsg1p mutants.

To test this possibility, I introduced GFP-tagged versions of either wild-type *NMD3* or the strongest suppressor allele, *NMD3(I112T,I362T)* on *CEN* vectors into an LMB-sensitive, *nmd3* deletion strain sustained by untagged wild-type *NMD3* on a *URA3* plasmid. After eliminating the plasmids bearing untagged wild-type *NMD3* following growth on 5-FOA-containing media, these strains were transformed with either empty vector or plasmids harboring galactose-inducible wild-type or dominant negative *LSG1*. The localization of wild-type and mutant Nmd3-GFP was then monitored in these strains after culturing cells in the presence of galactose for 3.5 hours followed by treatment with LMB.

Following either mock induction (empty vector) or induction of wild-type *LSG1*, both Nmd3-GFP and Nmd3(I112T,I362T)-GFP readily accumulated in the nuclei of cells after LMB treatment (Figure 4.2A). However, similar to results obtained for genomically-expressed Nmd3-GFP, expression of Lsg1(K349T)p resulted in the dramatic redistribution of wild-type Nmd3-GFP to the cytoplasm in the presence of LMB (Figure 4.2A: + GALACTOSE). In contrast to wild-type Nmd3-GFP, the Nmd3(I112T,I362T)-GFP was not efficiently retained in the cytoplasm upon expression Lsg1(K349T)p, instead showing a significant nuclear enrichment following treatment with LMB. As the mutant protein is not expressed at detectably higher levels than the wild-type allele (data not shown), this observation suggests that the suppressor allele is not tightly retained on 60S subunits in the cytoplasm in the presence of Lsg1(K349T)p. A similar restoration of shuttling was observed for the Nmd3(I112T,I362T)p mutant in the context of the *rpl10[G161D] ts* mutant, perhaps pointing toward a common underlying mechanism for

bypassing cytoplasmic entrapment in the context of either *rpl10* or *lsg1* mutants (Hedges et al., 2005).

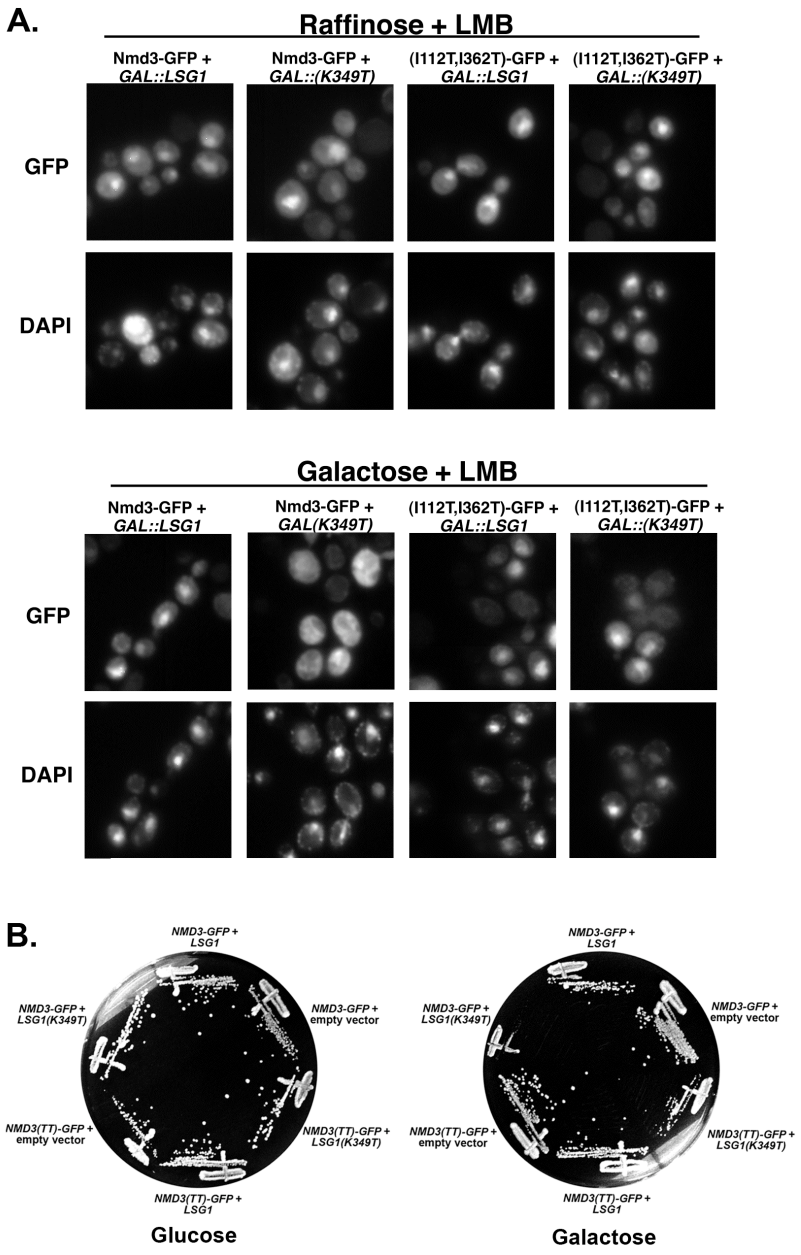

Figure 4.2 Suppressor mutations in *NMD3* restore shuttling and growth in the presence of dominant negative *LSG1*.

(A.) Overnight cultures of strain AJY1896 (*nmd3:TRP1 CRM1[T539C]*) containing pAJ582 (*NMD3-GFP*) or pAJ1287 (*NMD3[I112T, I362T]-GFP*) as the sole copies of *NMD3* and either empty vector (pRS426), pAJ1312 (*GAL10::LSG1*) or pAJ1278 (*GAL10::LSG1[K349T]*) were diluted into fresh medium containing raffinose and cultured to mid-log phase followed by galactose-induction for 3 hours. After 3 hrs., cells were treated with LMB and prepared for visualization as described in Chapter 2. (B.) Strains from (A.) were grown for 5 days at 30˚C on glucose- or galactose-containing SC-ura leu medium. *NMD3(I112T,I362T)-GFP* is denoted here as *NMD3(TT)-GFP*.

In the strain in which *NMD3-GFP* existed as the only copy of the gene, cytoplasmic entrapment of Nmd3p was accompanied by a strong growth arrest upon expression of the Lsg1(K349T)p mutant allele (Figure 4.2B). Remarkably, in cells harboring the *NMD3(I112T,I362T)-GFP* mutant as the sole copy of Nmd3p, the growth arrest was incomplete, allowing for sustained viability in the presence of the dominant negative Lsg1p mutant (Figure 4.2B). The inability of this Nmd3p allele to support viability in the complete absence of *LSG1* (i.e. in an *lsg1* knock-out mutant), however, demonstrated that the presence of the suppressor allele does not make Lsg1p function dispensable (data not shown). Therefore, some Lsg1p function must be retained (perhaps by endogenous wild-type Lsg1p) in the context of the Nmd3(I112T,I362T)p suppressor allele to bypass the growth arrest elicited by the dominant negative Lsg1(K349T)p mutant.

4.3.3 *NMD3* suppressors of *rpl10* and *lsg1* mutants partially restore the imbalance of free ribosomal subunits and polysome defects

The restoration of shuttling and growth observed for Nmd3(I112T,I362T)-GFP in the presence of mutant Lsg1p or Rpl10p suggests that 60S biogenesis and export is also improved. To test this possibility, I analyzed polysome profiles in an *rpl10(G161D)* mutant suppressed by *NMD3(I112T,I362T)* or in a strain co-expressing *LSG1(K349T)* and the suppressor mutant. In the context of the *rpl10(G161D)* allele, ectopic expression of wild-type Nmd3p significantly improved the subunit ratio, as indicated by the increase in free 60S subunits relative to free 40S subunits (compare *rpl10[G161D]* + vector versus *NMD3* in Figure 4.3A). We had previously shown that subunits blocked for export in an *nmd3* mutant are rapidly degraded, exhibiting a half-life of only about 4 minutes (Ho and Johnson, 1999). Therefore, this increase in free 60S levels is likely attributable to an increase in 60S stability imparted by high-copy Nmd3p's ability to sustain 60S export in the absence of Rpl10p function.

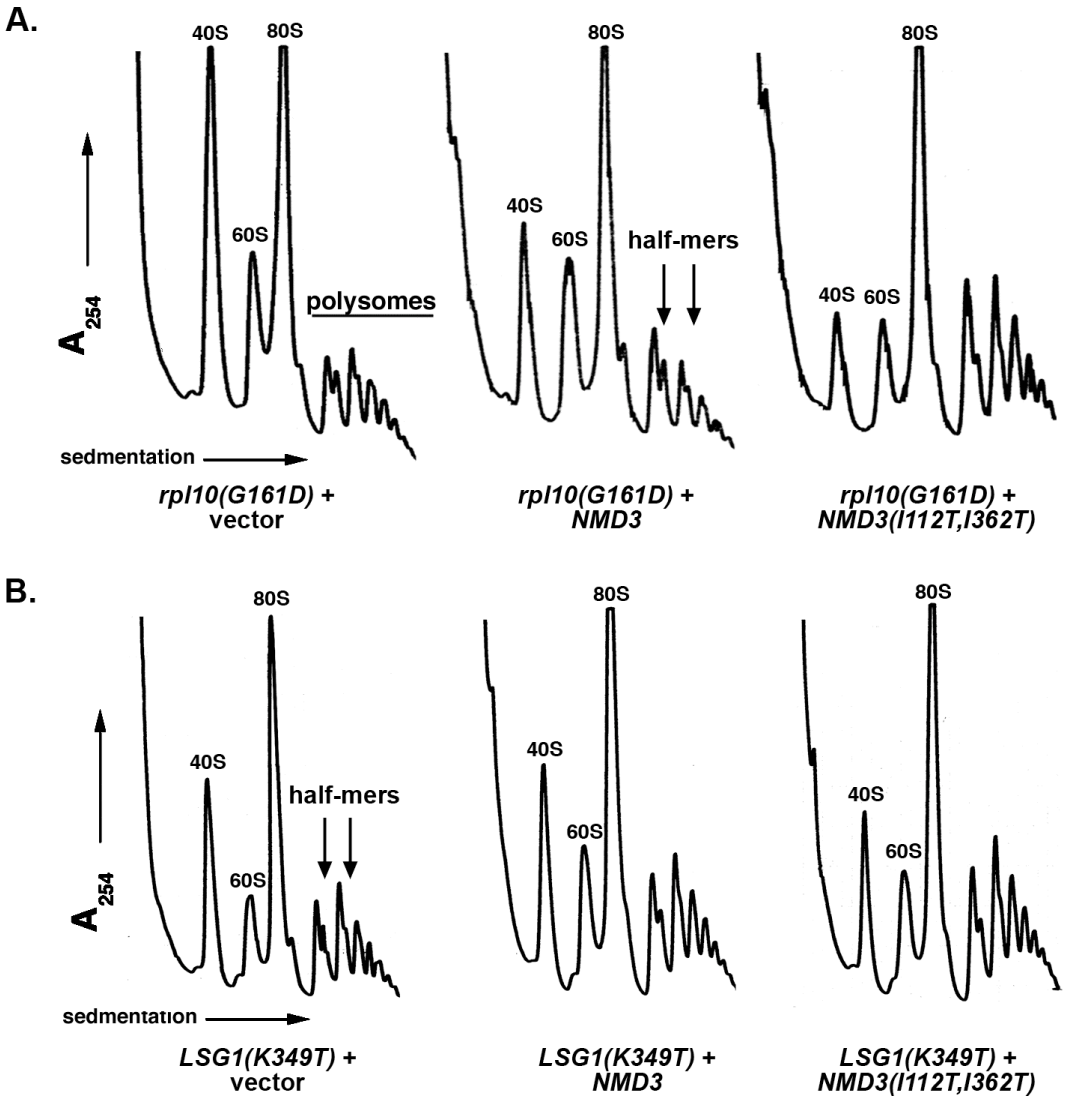

Figure 4.3 *NMD3* suppressor mutations partially restore subunit imbalance and suppress polysome defects in the presence of mutant *rpl10* or *lsg1*

(A.) AJY1657 (*rpl10[G161D]*) harboring empty vector (pRS425), pAJ538 (*NMD3-myc*) or pAJ1315 (*NMD3[I112T, I362T]-myc*) were cultured to mid-log phase at room temperature before being shifted to 37°C for 3 hrs. before harvesting. Extracts were prepared in the presence of cycloheximide followed by analysis on sucrose gradients as described in Chapter 2. (B.) A wild-type strain (CH1305) harboring pAJ1278 (*GAL10::LSG1[K349T]*) with either empty vector (pRS425), pAJ538 (*NMD3-myc*), or pAJ1315 (*NMD3[K349T]-myc*) were cultured in raffinose media to mid-log phase followed by induction with galactose for 4.5 hours before harvesting. Extracts were prepared and gradients run as in (A.).

Polysomes in these cells were only modestly enhanced, as polysomal peaks remained low and exhibited a persistence of half-mers, indicative of un-joined 48S initiation complexes on transcripts (see arrows Figure 4.3A). Upon ectopic expression of the *NMD3(I112T,I362T)* allele, however, not only was the free subunit imbalance further improved, but the polysome profiles reflected a marked restoration of translation efficiency, as evidenced by increased polysomal peaks and a decrease in half-mer formation (Figure 4.3A). Thus, in comparison to wild-type Nmd3p, the Nmd3p(I112T,I362T)p suppressor mutant is capable of strongly suppressing the defects in 60S stability (improved subunit imbalance) and translation (enhanced polysome profiles) that are typically observed for the *rpl10(G1161D)* mutant.

Ectopic-expression of wild-type Nmd3p from a low-copy (*CEN*) plasmid also moderately improved the free subunit imbalance and polysome defects observed upon expression of dominant negative Lsg1(K39T)p (Figure 4.3B). Expression of the Nmd3(I112T,I362T)p suppressor allele from a low-copy plasmid, however, significantly reduced the subunit imbalance in the context of the mutant Lsg1(K349T)p, while the half-mer defect in polysomes was further suppressed (Figure 4.3B). Thus, the Nmd3(I112T,I362T)p suppressor allele strongly suppresses the translational defects associated with both *rpl10* and *lsg1* mutants, correlating with its ability to enhance growth and Nmd3p shuttling in the absence of proper *LSG1* and *RPL10* function. In light of their sustained shuttling in the absence of proper Lsg1p or Rpl10p function, it is reasonable to conclude that the suppressor alleles are more efficiently released from these defective subunits, allowing for uninterrupted 60S export. Furthermore, the ability of the Nmd3(I112T,I362T)p allele to escape entrapment on free 60S subunits may, in turn, alleviate a physical or functional barrier to subunit joining (see subsequent sections and Discussion).

4.3.4 *NMD3* suppressors of *lsg1* and *rpl10* mutants exhibit reduced 60S affinity

The hypothesis that *NMD3* suppressor alleles possess an inherently lower affinity for 60S subunits is based upon the observation that they are able to escape cytoplasmic entrapment on 60S subunits in the presence of defective Lsg1p or Rpl10p, allowing for a larger population of subunits to enter the translational pool (Figures 4.2 and 4.3). Also in agreement with this hypothesis is the recognition that several loss-of-function mutations in Nmd3p that disrupt 60S interaction fall within the "suppressor domains" (Table 4.2 and Figure 4.1A). Thus, in order to directly test this possibility, we incorporated the use of an assay that coupled *in vitro* reconstitution of the Nmd3p/60S complex with non-denaturing gel electrophoresis to assess the relative levels of Nmd3p capable of co-migrating with intact 60S subunits.

Wild-type and mutant Nmd3 proteins were expressed as chimeric fusions to GST for bulk purification in yeast, while free 60S ribosomal subunits were purified from the cellular pool of mature ribosomes as described in Chapter 2. Following standardization of input concentrations, the purified Nmd3 proteins were incubated with free 60S subunits under conditions that had previously been shown to allow for efficient complex formation *in vitro* ((Ho et al., 2000a) and Chapter 2). These reaction mixtures were then loaded onto a 2.5% polyacrylamide/0.5% agarose composite gel for resolution of the free 60S species or bound complex from unbound Nmd3p. The position of 60S subunits on the gel was assigned on the basis of western blotting against the core ribosomal protein, Rpl12p (not shown), and by ethidium bromide staining of ribosomal RNA, while the position of Nmd3p was demarcated by western blotting against the GST moiety.

While 60S and Nmd3p resolved as two distinct species prior to complex formation (Figure 4.4 lanes 1 and 2), wild-type Nmd3p co-migrated at the position of 60S after the binding reaction (Figure 4.4 lanes 3-5). In stark contrast to wild-type Nmd3p,

the strong suppressor mutant, Nmd3(I112T,I362T)p, remained in the unbound state throughout the concentration range examined (Figure 4.4 lanes 7-9), migrating as a diffuse band at the position of the unbound control (compare lanes 6 and 9). The Nmd3(L291F)p mutant, a moderate suppressor of both *lsg1* and *rpl10* mutants, exhibited an intermediate affinity for 60S subunits, requiring almost a 3-fold higher concentration of protein to achieve levels of binding comparable to the wild-type Nmd3 protein (Figure 4.4 lanes 12-14; and compare lane 14 against lane 4). As mentioned earlier in this chapter, the Nmd3(V340D)p mutant was identified as a strict loss-of-function mutant that exhibited a dramatic deficiency for 60S binding. Therefore, it served as a negative control in this assay and behaved in the expected manner, showing no detectable 60S binding under these conditions (Figure 4.4 lanes 16-18).

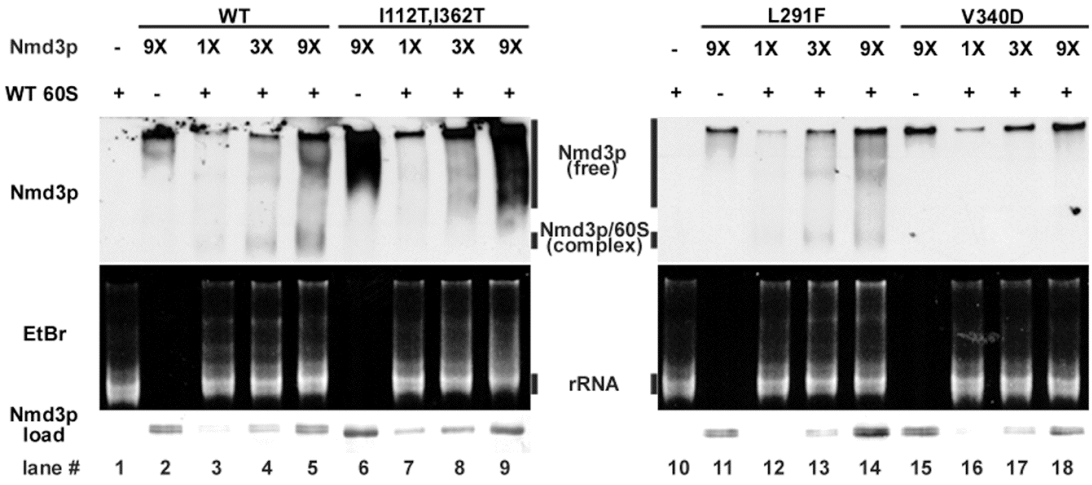

Figure 4.4 Nmd3 suppressor proteins have reduced affinity for 60S subunits.

Three-fold increasing amounts (1X ~ 30 ng) of affinity-purified wild-type GST-Nmd3p, GST-Nmd3(I112T, I362T)p, GST-Nmd3[L291F]p, or GST-Nmd3(V340D)p mutant proteins were incubated alone or with purified 60S subunits and resolved on 2.5% acrylamide/0.5% agarose composite gels as described in Chapter 2. The position of Nmd3p and 60S subunits was determined by western blotting using anti-GST and by ethidium bromide staining of rRNA, respectively. The positions at which unbound Nmd3p, Nmd3p/60S complex, and free 60S subunits (rRNA) migrate are demarcated for visual reference. Data contributed by John Hedges.

Thus, the suppressor mutants, in general, appear to maintain a lower affinity for 60S subunits than does wild-type Nmd3p. The degree of suppression seems to correlate inversely with the relative affinity of the suppressors for 60S subunits; as a moderate suppressor, Nmd3(L291F), showed intermediate 60S affinity, while the strong, Nmd3(I112T,I362T)p mutant was unable to form complex under the concentration range assayed. The apparent weakened 60S affinity could directly account for the ability of the suppressors alleles to avoid cytoplasmic entrapment in the absence of appropriate Rpl10p

or Lsg1p function. In this respect, Nmd3 suppressor proteins may release prematurely from nascent subunits in the cytoplasm in a manner that is now uncoupled from the concerted activities of Rpl10p and Lsg1p during 60S maturation. In turn, release of Nmd3p from nascent subunits may further stimulate subunit joining by either eliminating a direct physical barrier to joining or allowing for a dependent downstream event to transpire.

While the Nmd3p suppressor alleles exhibited significantly lower affinity for 60S subunits *in vitro*, they are still capable of supporting growth when they are expressed as the only copy of Nmd3p in cells (Figure 4.2B and data not shown). Therefore, the suppressor mutants must retain sufficient interaction with nascent subunits *in vivo* to sustain binding during translocation through nuclear pore complexes as discussed in Chapter 1. To gauge whether or not the mutant proteins interacted with 60S subunits *in vivo*, I introduced epitope-tagged versions of wild-type Nmd3p and the mutant alleles into a wild-type yeast strain to monitor the relative levels of 60S subunits co-immunopurified by the Nmd3 proteins. In this experiment, wild-type Nmd3p tagged with the oligomeric c-myc epitope served as a positive control for strong 60S binding, while the c-myc-tagged Nmd3(V340D)p mutant acted as a negative control for 60S binding, (Table 4.2 and Johnson, unpublished). Western blotting against the core ribosomal protein, Rpl8p, was utilized to assess the relative extent to which 60S subunits were able to be co-immunoprecipitated by the various Nmd3p alleles.

As shown in Figure 4.5, both the Nmd3(L291F)p and Nmd3(I112T,I362T)p mutants were capable of co-immunoprecipitating 60S subunits from cell extracts at levels similar to wild-type Nmd3p, albeit slightly lower for the Nmd3(I112T,I362T)p mutant (Figure 4.5). In contrast to the suppressor alleles, the Nmd3(V340D)p loss-of-function mutant exhibited a severely diminished interaction with 60S subunits, consistent with

previous observations. Therefore, despite their reduced affinity for 60S subunits *in vitro*, the suppressor alleles are still capable of sustained 60S interaction under quasi-*in vivo* conditions. The pronounced attenuation of 60S interaction for the V340D mutant both *in vitro* and *in vivo* correlates with its inability to either support growth on its own or suppress *rpl10* or *lsg1* mutants. Taken together, these observations suggest that weakened 60S affinity, but not loss of binding, factors into the mechanism by which Nmd3p suppressor alleles are able to functionally compensate for defects in Lsg1p or Rpl10p.

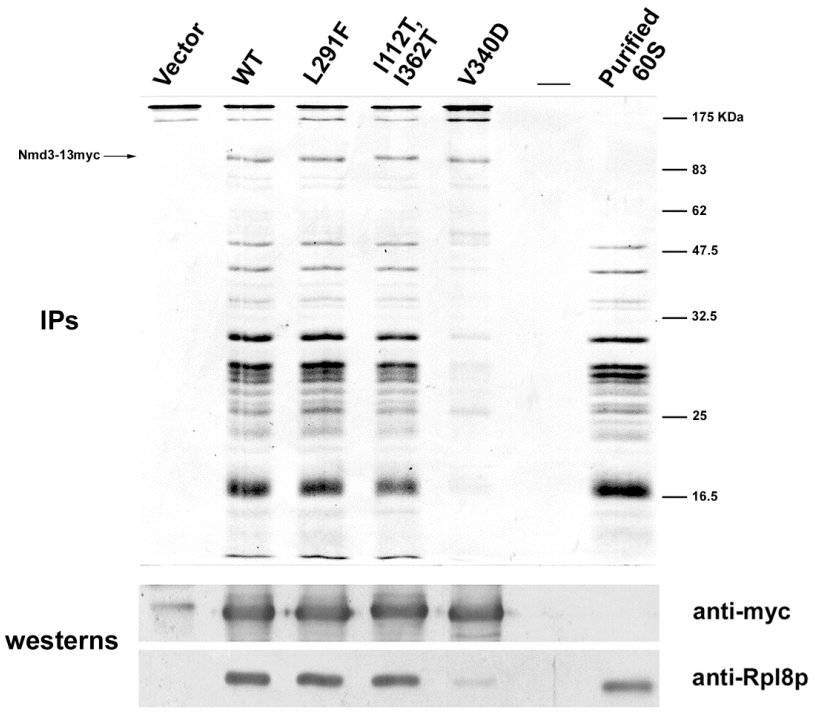

Figure 4.5 Nmd3p suppressor mutants retain the ability to bind 60S subunits *in vivo.*

α-myc immunoprecipitations were conducted in extracts prepared from strain W303 harboring either empty vector (pRS425), pAJ538 (*NMD3-myc*), pAJ1315 (*NMD3[I112T,I362T]-myc*), pAJ1070 (*NMD3[L291F]-myc*), or pAJ1299 (*nmd3[V340D]-myc*) as described in Chapter 2. Immunoprecipitated proteins and purified 60S subunits (for visual reference) were resolved on a 12% SDS-PAGE gel for staining with Coomassie Blue. Western blotting was also performed against the various Nmd3p alleles using α-myc or against the 60S core protein Rpl8p using anti-Rpl8p as described in Chapter 2.

To further test this model, I compared the sedimentation behavior for wild-type Nmd3p and the strong suppressor allele, Nmd3(I112T,I362T)p, in sucrose gradients. c-myc-tagged wild-type or mutant Nmd3p were constitutively expressed from low copy plasmids in a wild-type yeast strain. Extracts were prepared from these strains in the presence of cycloheximide and subjected to ultra-centrifugation through a 7-47% sucrose gradient. The gradients were then fractionated, and the positions of free ribosomal subunits and polysomes were monitored by UV-absorbance as detailed in Chapter 2. Western blotting against the c-myc epitope tag was then utilized to assess the sedimentation pattern for the Nmd3p alleles among gradient fractions. In the wild-type strain, native Nmd3p predominately co-migrated at the position of free 60S subunits (Figure 4.6A). In stark contrast to the wild-type allele, the vast majority of Nmd3(I112T,I362T)p sedimented at the top of the gradient, indicating a larger pool of free protein. The observed disparity between the sedimentation behavior for wild-type Nmd3p and the suppressor mutant is consistent with the I112T,I362T mutations weakening the Nmd3p/60S interaction.

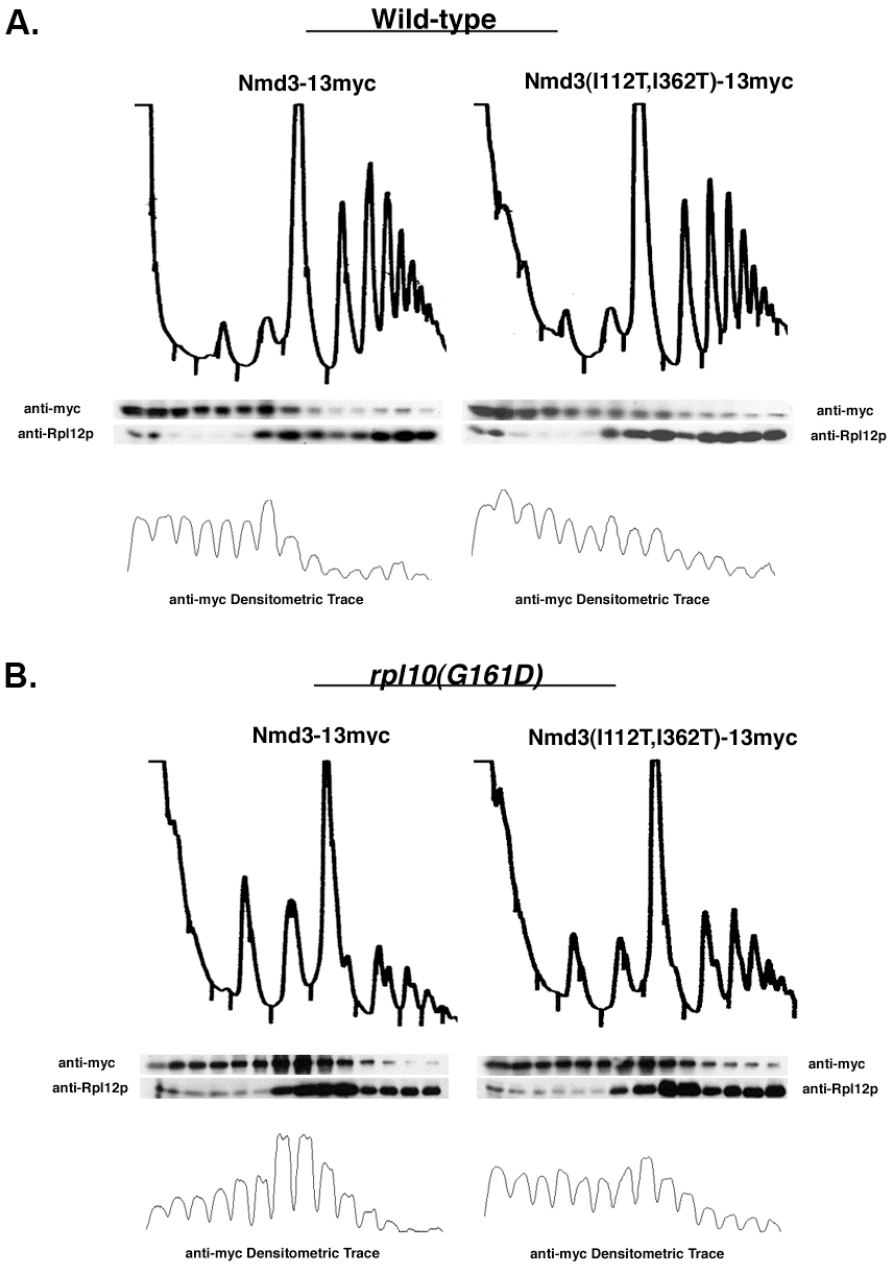

Figure 4.6 A strong Nmd3p suppressor mutant exhibits an attenuated 60S association in the presence of wild-type or mutant *RPL10*

Cultures of strains W303 or AJY1657 transformed with either pAJ538 (*NMD3-myc*) or pAJ1315 (*NMD3[I112T, I362T]-myc*) were grown constitutively at 30°C (W303) or shifted to 37°C for 3 h (AJY1657) before harvesting. Extracts were prepared in the presence of cycloheximide followed by analysis on sucrose gradients as described in in Chapter 2. Sucrose gradient fractions were analyzed by western blotting against the c-myc epitope (Nmd3p) or the core ribosomal protein, Rpl12p. Densitometric traces of anti-myc blots were conducted using NIH Image V.1.62.

It had previously been predicted that mutations in Nmd3p that suppress the *rpl10(G161D)* mutant restore Nmd3p's ability to interact with 60S subunits through a gain-of-function interaction with mutant Rpl10p ((Gadal et al., 2001b)). Therefore, I decided to examine the sedimentation pattern in sucrose gradients of an Nmd3p suppressor mutant in the *rpl10(G161D)* temperature sensitive strain background at non-permissive temperature. If the pre-existing model for the behavior of Nmd3p in this mutant *rpl10* background were correct, then wild-type Nmd3p would be predicted to show reduced binding to mutant 60S subunits, while suppressor mutations would be expected to restore this interaction. In this scheme, the strongest suppressor allele, Nmd3(I112T,I362T)p, should exhibit the strongest restoration of binding to subunits containing the Rpl10(G161D) mutant protein.

In sucrose gradients loaded with extracts prepared from the *rpl10(G161D)* strain cultured at restrictive temperature, wild-type Nmd3p co-sedimented at the position of free 60S subunits in a manner that reflected a tighter association than that observed for the same allele in a wild-type strain (compare the sedimentation pattern for Nmd3-13myc in *rpl10(G161D)* and wild-type strains, Figure 4.6A and B). In contrast, the Nmd3(I112T,I362T)p suppressor mutant exhibited a sedimentation pattern that more closely correlated with the pattern observed for native Nmd3p in a wild-type strain (compare the sedimentation pattern for Nmd3(I112T,I362T)-13myc in the *rpl10(G161D)* mutant with Nmd3-13myc in a wild-type background, Figure 4.6A and B). The enhanced proportion of wild-type Nmd3p that co-sedimented with free 60S subunits in the *rp10(G161D)* background is consistent with our observations that Nmd3p is trapped on

60S subunits in the cytoplasm in this strain at restrictive temperature (see section 4.2). Furthermore, the ability of suppressor mutations to redistribute Nmd3p away from mutant subunits in a pattern that more closely resembles wild-type conditions correlates well with the observed growth restoration and suppression of translational defects in the *rpl10(G161D)* strain. These results further support our model for a decreased 60S affinity conferred by the suppressor mutations and stand in opposition to the model offered up by others to account for the functional behavior of suppressor mutants in the context of the mutant *rpl10* allele. This discrepancy will be addressed further in subsequent sections and in the Discussion.

4.3.5 Nmd3p can associate with 60S subunits independently from Rpl10p

As described in section 4.2, it had been proposed that Rpl10p binds to nascent 60S ribosomal subunits in the nucleus, providing the binding site for Nmd3p on 60S prior to subunit export (Gadal et al., 2001b; Nissan et al., 2002). This model hinged largely upon the observations that mutations in *NMD3* can suppress an *rpl10* mutant and that 60S subunits accumulate in the nucleus upon disruption of Rpl10p function (Gadal et al., 2001b; Karl et al., 1999). Results presented in section 4.3.4 demonstrate that the suppressor mutations contribute to a loss of 60S affinity rather than strengthening Nmd3p's interaction with 60S in the presence of mutant Rpl10p. Furthermore, work from our lab has shown that the nuclear accumulation of 60S subunits observed in an *rpl10* mutant or upon transcriptional repression of *RPL10* results from a failure to release Nmd3p from subunits in the cytoplasm, thus preventing sustenance of the export pathway (Hedges et al., 2005). Like the results obtained in the context of *lsg1* mutants (see

Chapter 3, section 3.3.6), over-expression of Nmd3p restores subunit export in the absence of Rpl10p, indicating that Rpl10p is dispensable for the Nmd3p-mediated export event (Hedges et al., 2005). We were also able to show that perturbation of Crm1's (Xpo1p) export function with the drug leptomycin B (LMB), traps Nmd3p and 60S subunits, but not Rpl10p, in the nucleus, an unexpected result if Rpl10p serves as Nmd3p's binding site on 60S ((Ho et al., 2000b; West et al., 2005), and Hedges and Johnson, unpublished). Therefore, a prediction from our results is that Nmd3p binds upstream of Rpl10p loading and, thus, may associate with a population of subunits that are deficient for Rpl10p.

To test this prediction in a more directed fashion, I examined whether the pool of 60S subunits immunopurified by Nmd3p were sub-stoichiometric for Rpl10p. As a means of monitoring Rpl10p levels in Nmd3p-bound complexes, I expressed c-myc-tagged Nmd3p in a strain in which three tandem copies of the HA epitope had been integrated at the 3' end of genomic *RPL10*. After culturing these cells into mid-log phase, I prepared extracts for isolating the free pool of 60S subunits by sucrose gradient sedimentation (as described in Chapter 2). Following ultra-centrifugation, the gradients were fractionated, and Nmd3p was immunoprecipiated from the free 60S fraction. As immunoprecipitations were conducted against the Nmd3p population that co-sedimented at the position of free 60S, the stoichiometry between Nmd3p and core ribosomal proteins should be 1:1. Furthermore, if Rpl10p serves as the binding site for Nmd3p on 60S, it should also be stoichiometric to Nmd3p in these complexes. To assess this possibility, the relative amount of Rpl10-HA in subunits immunoprecipitated by Nmd3p

was monitored by western blotting and compared against the core ribosomal protein, Rpl12p.

While Nmd3p and Rpl12p did, indeed, appear to co-purify at comparable levels, Rpl10-HA was virtually absent within this population of subunits (Figure 4.7), demonstrating that Nmd3p is capable of binding to 60S subunits in the absence of stoichiometric levels of Rpl10p. For comparison, I assessed the levels of Rpl10-HA in the total pool of free 60S subunits, in intact 80S subunits, and in a polysomal fraction. In striking contrast to its abundance in joined subunits in the 80S peak and translating subunits in polysomes, Rpl10-HA levels in the free 60S pool were remarkably low in comparison to Rpl12p (Figure 4.7). The observation that Rpl10p is a major component of translating subunits yet is under-represented on free 60S suggests that Rpl10p loads late in the biogenesis pathway. Thus, in stark contrast to previous models for Nmd3p recruitment to 60S, these results demonstrate that Nmd3p can bind subunits independently of Rpl10p and are in closer agreement with a model in which Rpl10p loads after Nmd3p during 60S maturation, perhaps just prior to subunit incorporation into the translational pool.

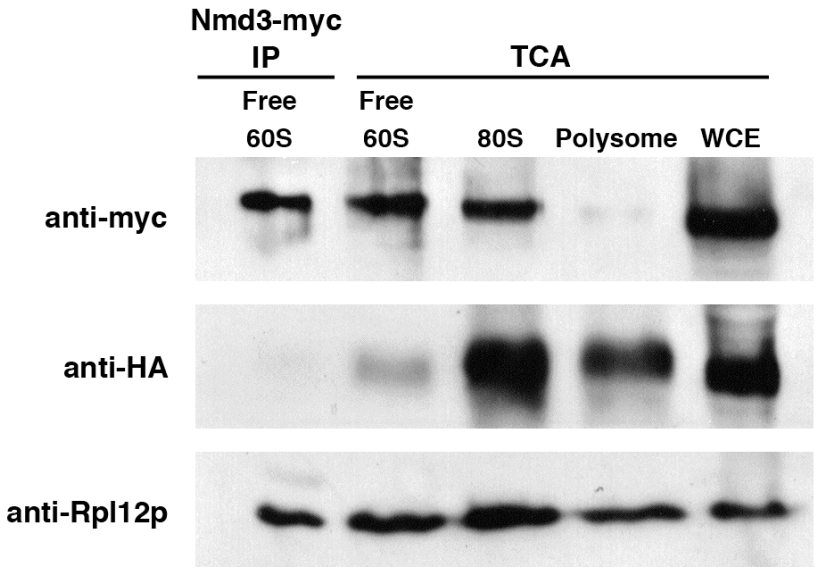

Figure 4.7 Nmd3p can bind to 60S subunits independently of Rpl10p.

Extracts were prepared from AJY1961 (*RPL10-3xHA*) containing pAJ538 (*NMD3-myc*) and resolved on a 7 to 47% sucrose gradient as described in Chapter 2. Immunoprecipitation of Nmd3-myc was performed using anti-myc from the free 60S gradient fraction. The ability of 60S subunits to co-immunoprecipitate with Nmd3p and the level of Rpl10-HA in these subunits were monitored by western blotting against the ribosomal protein Rpl12p and Rpl10-HA, respectively. The relative levels of Nmd3p-myc, Rpl10-HA, and Rpl12p in the free 60S, 80S, and polysomal fractions were analyzed by western blotting among proteins precipitated by trichloroacetic acid (TCA) from the appropriate fractions as described in Chapter 2.

4.3.6 Sqt1p becomes stably associated with 60S subunits in the presence of dominant negative Lsg1p mutants

The essential WD-repeat protein, Sqt1p, is a chaperone for free Rpl10p (Eisinger et al., 1997a; Hedges et al., 2005). While Sqt1p is restricted to the cytoplasm, it is required for the loading of Rpl10p into 60S subunits (Eisinger et al., 1997a). The striking phenotypic similarities between *rpl10* and *lsg1* mutants and the apparent late loading of Rpl10p into free 60S subunits (Figure 4.7) suggests that Rpl10p may load in the presence of Lsg1p during a late maturation event. In order to assess the possibility, I tested whether dominant negative mutations in Lsg1p could accumulate a loading intermediate for Rpl10p in the cytoplasm. Since Sqt1p is believed to be involved in Rpl10p's incorporation into 60S, yet typically exhibits only a transient interaction with subunits (Eisinger et al., 1997a; West et al., 2005), I examined whether the late 60S intermediates that accumulate upon expression of dominant negative Lsg1p alleles are enriched for Sqt1p. To this end, I immunoprecipitated 60S complexes with c-myc-tagged wild-type and dominant negative Lsg1p and monitored Sqt1p and Rpl12p (60S reporter) levels by western analysis against the endogenous proteins. As shown in Figure 4.8A, the amount of Sqt1p co-immunoprecipitated by dominant negative Lsg1p mutants (Lsg1[K349T]p and Lsg1[N173Y,L176S]p) was significantly higher relative to wild-type Lsg1p in the context of comparable 60S levels. This observation is consistent with Sqt1p loading Rpl10p in the presence of Lsg1p and that release of Sqt1p is dependent upon Lsg1p function.

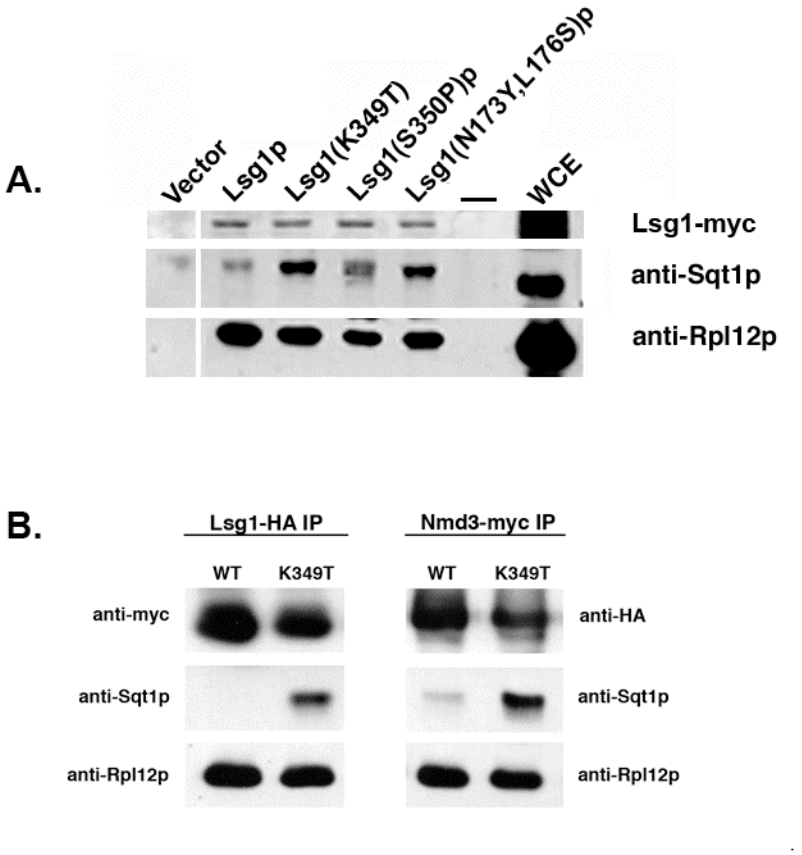

Figure 4.8 Dominant negative Lsg1p mutants trap Sqt1p on 60S subunits.

(A.) Overnight cultures of CH1305 containing either empty vector (pRS426), pAJ1107 (*GAL10*::*LSG1-myc*), pAJ1108 (*GAL10*::*LSG1[K349T]-myc*), pAJ1313 (*GAL10::LSG1[S350P]-myc*), or pAJ1105 (*GAL10::LSG1[N173Y,L176S]-myc*) were diluted to an OD_{600} of 0.15 in raffinose-containing medium. After culturing cells to mid-log phase, Lsg1p alleles were induced for 3.5 hrs by the addition of galactose. Extracts were prepared and immunoprecipitations were conducted using α-myc as described in Chapter 2. Immunoprecipitated samples (IP) and whole-cell extracts (WCE) were resolved on a 12% SDS-PAGE gel followed by coomassie staining (Lsg1-cmyc) or western blotting against Sqt1p (α-Sqt1p) or Rpl8p (α-Rpl8p) as a reporter for 60S. (B.) Overnight cultures of AJY272 (genomic *NMD3-myc*) and either pAJ1343 (*GAL10*::*LSG1-HA*) or pAJ1344 (*GAL10*::*LSG1[K349T]-HA*) were diluted to an OD_{600} of 0.15 in raffinose-containing medium. After culturing cells to mid-log phase, Lsg1p alleles were induced for 3.5 hrs by the addition of galactose. Extracts were prepared and immunoprecipitations were conducted with either anti-myc or anti-HA as in (A.).

Surprisingly, unlike Lsg1(K349T)p which also bears a point mutation in the Walker A motif of the GTPase core, the potent Lsg1(S350P)p mutant did not trap Sqt1p on 60S. (Figure 4.8A). The conserved lysine (K349) residue has been previously shown to play a critical role in GTP hydrolysis but not GTP binding in YjeQ, a bacterial protein in the same family of GTPases as Lsg1p (Daigle et al., 2002). The Lsg1(K349T)p allele, therefore, may be arrested in the GTP-bound state. As the Walker A motif (GX_4GKS/T: GYPNVGKS in Lsg1p) is necessary for coordinating both GTP-binding and hydrolysis (Saraste et al., 1990), mutating the conserved serine residue (S350) in this motif may arrest the protein in a different transition state of the GTPase-cycle (perhaps in a conformation that mimics the GDP-bound form) than that of the Lsg1(K349T)p allele. The variability of different Lsg1p mutants to trap Sqt1p on 60S may allow for the finer dissection of the timing and manner in which 60S maturation events transpire in the presence of Lsg1p and is reflective of the original driving motivation behind the isolation of dominant negative Lsg1p alleles. Our lab is currently in the process of characterizing the differences in the biochemistry and cellular dynamics for wild-type and mutant Lsg1p alleles to better understand the manner in which Lsg1p mediates its function during 60S biogenesis.

Dominant negative Lsg1p mutants also trap Nmd3p on cytoplasmic 60S subunits (see Chapter 3). To determine whether Sqt1p was enriched in the presence of Nmd3p by mutant Lsg1p, I repeated this experiment with galactose-inducible HA-tagged Lsg1p alleles in cells co-expressing c-myc-tagged Nmd3p from its genomic locus. Indeed, expression of the dominant negative Lsg1p mutants resulted in a marked increase in the quantities of Sqt1p immunoprecipitated by Nmd3p (Figure 4.8B). Taken together, these results are consistent with a model in which Sqt1p loads Rpl10p on Nmd3p-bound subunits in the presence of Lsg1p.

4.3.7 An Rpl10p truncation mutant that typically exhibits weak 60S incorporation can be trapped on the subunit in the presence of dominant negative Lsg1p

An Rpl10p C-terminal truncation mutant, Rpl10N187p, fails to be stably incorporated into 60S subunits. Work from our lab has shown that this truncated form of Rpl10p exhibits a supraphysiological affinity for its chaperone, Sqt1p (West et al., 2005). This aberrant interaction destabilizes endogenous Rpl10p by titrating out its chaperone, leading to a dominant defect in 60S biogenesis, phenocopying the effects observed upon repression of Rpl10p expression (Eisinger et al., 1997a; West et al., 2005). Therefore, the apparent failure of Rpl10N187p to be incorporated into subunits could reflect its inability to dissociate from Sqt1p or to sustain interaction with the subunit during accommodation.

In light of our observation that dominant negative Lsg1p mutants can trap Sqt1p on 60S subunits in the presence of Nmd3p, I tested whether these mutants could also stabilize Rpl10N187p's interaction with the subunit. To address this possibility, immunoprecipitations were carried-out against c-myc-tagged wild-type Lsg1p or the dominant Lsg1p mutant alleles in extracts prepared from cells in which Rpl10N187-GFP had been co-induced for expression. The extent to which the Rpl10p truncation mutant was able to be co-immunopurified in complexes bound by the various Lsg1p alleles was monitored by western analysis against the GFP moiety. Remarkably, Rpl10N187-GFP was efficiently co-immunoprecipitated in complexes bound by the dominant negative Lsg1(K349T)p and Lsg1(N173Y,L176S)p mutants (Figure 4.9). Although 60S levels were comparable in immunoprecipitations conducted against wild-type or mutant Lsg1ps, Rpl10N187-GFP did not co-purify to an appreciable extent in complexes bound by the wild-type Lsg1p allele (Figure 4.9).

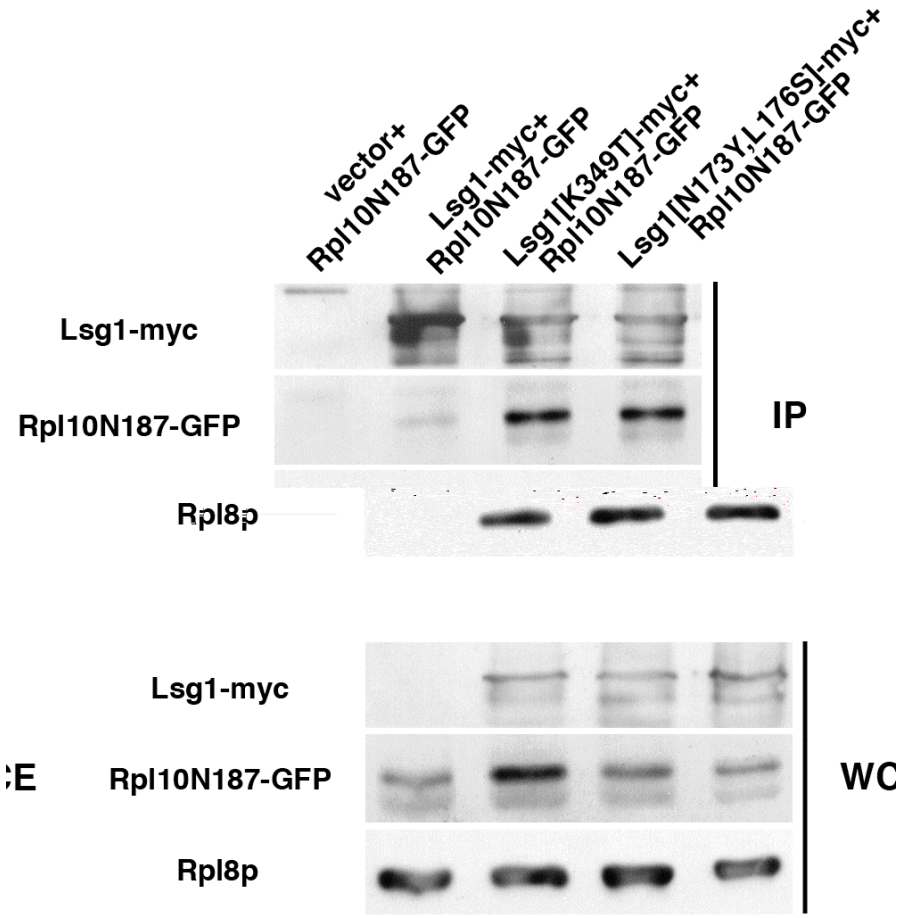

Figure 4.9 Rpl10N187p accumulates on 60S subunits containing dominant negative Lsg1p mutants.

Overnight cultures of CH1305 containing pAJ1100 (*GAL10*::*RPL10N187-GFP*) with either empty vector (pRS426), pAJ1107 (*GAL10*::*LSG1-myc*), pAJ1108 (*GAL10*::*LSG1[K349T]-myc*) or pAJ1105 (*GAL10*::*LSG1[N173Y,L176S]-myc*) were diluted to an OD_{600} of 0.15 in raffinose-containing medium. After culturing cells to mid-log phase, Lsg1p and Rpl10N187p were co-induced for 3.5 hrs by the addition of galactose. Extracts were prepared and immunoprecipitations were conducted using α-myc as described in Chapter 2. Immunoprecipitated samples (IP) and whole-cell extracts (WCE) were resolved on a 12% SDS-PAGE gel followed by western blotting against Lsg1-myc (α-myc), Rpl10N187-GFP (α-GFP), or Rpl8p (α-Rpl8p) as a reporter for 60S.

The entrapment of Rpl10N187p in complexes bound by dominant negative Lsg1p mutants demonstrates that this Rpl10p truncation fragment retains the ability to bind 60S. The absence of Rpl10N187p typically observed in wild-type 60S subunits most likely reflects its inability to be properly accommodated into its binding site. Under these circumstances, it would dissociate from the subunit presumably still bound to Sqt1p. This failure to accommodate Rpl10N187p into 60S may account for its persistent association with Sqt1p (West et al., 2005). The stabilization of a typically weak interaction with 60S subunits for Rpl10N187p (Figure 4.9) and Sqt1p (Figure 4.8) by dominant negative Lsg1p alleles is consistent with the accumulation of a transient intermediate in the 60S maturation pathway. These observations provide physical evidence that Lsg1p plays a role in loading Rpl10p into 60S subunits in the cytoplasm in the presence of Nmd3p. The culmination of this event likely includes the release of Sqt1p, Lsg1p, and Nmd3p from the subunit.

4.4 Discussion

Previous models for the nuclear export of nascent 60S ribosomal subunits attributed the recruitment of the export adapter, Nmd3p, to a direct protein-protein interaction with the ribosomal protein Rpl10p (Gadal et al., 2001b; Nissan et al., 2002). This scenario would require that Rpl10p load onto subunits in the nucleus and also predict that Nmd3p would be incapable of binding 60S in the absence of Rpl10p. A block in subunit export would then ensue. As outlined in section 4.2 of this chapter, several observations stand in opposition to this model, including the inability to trap Rpl10p in the nucleus upon disrupting Crm1-dependent export with the drug leptomycin B, a condition that readily blocks the export of Nmd3p-bound subunits ((West et al., 2005) and Hedges and Johnson, unpublished). Furthermore, in cells depleted for Rpl10p, Nmd3p becomes trapped on 60S subunits in the cytoplasm rather than existing in an

unbound state in the nucleus (Hedges et al., 2005; West et al., 2005). Cytoplasmic entrapment of Nmd3p is inconsistent with a model in which Rpl10p serves as the binding site for Nmd3p on 60S, but it would account for the block in 60S export typically associated with disruption of Rpl10p function. Remarkably, over-expression of Nmd3p is capable of restoring 60S export in these Rpl10p-depleted cells, suggesting that Rpl10p is, in fact, dispensable for the Nmd3p-mediated nuclear export event (Hedges et al., 2005; West et al., 2005). The cytoplasmic entrapment of Nmd3p upon disruption of Rpl10p and the ability of high-copy Nmd3p to restore 60S export under these conditions are reminiscent of the phenotypes associated with dominant negative Lsg1p mutants, as presented in Chapter 3. Thus, in light of the common effects on Nmd3p shuttling observed upon disruption of Lsg1p or Rpl10p function, I further examined a potential relationship between these two biogenesis factors in coordinating the release of Nmd3p from nascent subunits in the cytoplasm during a late 60S maturation event.

Work presented in this chapter has demonstrated that dominant mutations in Nmd3p that suppress *rpl10* temperature sensitive phenotypes also suppress *LSG1* dominant negative mutants. As shown in Figure 4.1A, these suppressor mutations predominantly mapped to two regions in Nmd3p. The N-terminal suppressor domain (suppressor domain I; approximately amino acids 100-115) includes several basic residues and may serve as an RNA binding surface, while the C-terminal suppressor domain (suppressor domain II; approximately amino acids 290-380) is inclusive of suppressor mutations (I279F, L291F, and A336P) that were previously identified in spontaneous suppressors of the *rpl10[G161D]* allele (Karl et al., 1999).

I have shown here that disruption of either Lsg1p or Rpl10p function can also be suppressed by loss-of-function (LOF) mutations in Nmd3p. The positional overlap between LOF mutants that are capable of suppressing *lsg1* and *rpl10* mutants and the

aforementioned suppressor domains suggests that suppression may be due to a partial loss of function for Nmd3p. In support for this prediction, several LOF mutants that map within the suppressor domains display attenuated 60S binding (Table 4.2). Additionally, mutations within these domains that severely perturb 60S interaction (i.e. V340D) are incapable of suppressing either *lsg1* or *rpl10* mutants, suggesting that weakened interaction but not loss of binding is important for suppression.

Consistent with this line of thinking, two suppressor proteins, Nmd3(L291F)p and Nmd3(I112T,I362T)p, exhibit lower affinity for purified 60S subunits than wild-type Nmd3p *in vitro* (Figure 4.4), suggesting that suppression is, indeed, correlated with a weakened 60S interaction. As a means of functionally addressing this possibility, I was able to demonstrate that the strong suppressor allele, Nmd3(I112T,I362T)p, is capable of avoiding cytoplasmic entrapment and restores Nmd3p shuttling and growth when expressed as the sole copy of Nmd3p in the context of the dominant negative Lsg1(K349T)p mutant. Furthermore, in contrast to expectations based upon the pre-existing model for the behavior of Nmd3p in the context of mutant Rpl10(G161D)p, I showed that wild-type Nmd3p accumulates on 60S subunits in sucrose gradients at restrictive temperature instead of existing as a free pool of unbound protein. This finding correlates with the observation that Nmd3p becomes trapped in the cytoplasm on 60S subunits rather than exhibiting a loss of 60S association when Rpl10p function is disrupted (Hedges et al., 2005; West et al., 2005). The Nmd3(I112T, I362T)p strong suppressor allele, on the other hand, dramatically enhanced the polysome profile in *rpl10(G161D)* mutants and exhibited a sedimentation pattern on sucrose gradients that mimics the pattern observed for native Nmd3p in a wild-type strain (Figure 4.6). As a whole, these findings are more consistent with a model in which suppressor mutants exhibit a weakened 60S interaction that decouples Nmd3p release from cytoplasmic

subunits from the activities of Lsg1p or Rpl10p. This behavior for the suppressor mutants would provide cells with a larger pool of free Nmd3p to sustain 60S subunit export upon disruption of Lsg1p or Rpl10p function and, perhaps, eliminate a direct physical or kinetic barrier to translation initiation.

Rpl10p is among the last ribosomal proteins to be loaded onto the 60S subunit during its maturation (Kruiswijk et al., 1978) and is essential for subunit joining during translation initiation (Dick et al., 1997; Eisinger et al., 1997b). Although it is believed to load onto subunits in the nucleus to provide the binding site for Nmd3p, I have presented evidence in this chapter that Nmd3p is capable of binding to 60S subunits that are substoichiometric for Rpl10p (Figure 4.7). In support of this observation, work from our lab has shown that over-expression of Nmd3p restores the 60S export defect that arises when Rpl10p is depleted from cells (Hedges et al., 2005; West et al., 2005), indicating that Rpl10p is not directly required for subunit export. As discussed earlier in this section, Rpl10p is not trapped in nuclei under conditions that block the export of Nmd3p-bound subunits, and it is important to note that loading of the human homologue of Rpl10p, QM, into nascent 60S subunits has been reported to be a cytoplasmic event (Nguyen et al., 1998).

The similar phenotypes observed upon disruption of Lsg1p or Rpl10p function suggest that these two factors may cooperate to induce a late 60S biogenesis event that results in the release of Nmd3p for subsequent cycles of 60S export. As demonstrated in Chapter 3, Lsg1p is confined to the cytoplasm, and in light of the modest levels of Rpl10p observed in free 60S subunits (Figure 4.7), it is reasonable to conclude that Rpl10p loading may, indeed, be a cytoplasmic event. In support of this idea, induction of the dominant negative Lsg1(K349T)p mutant traps both Sqt1p and an Rpl10p truncation mutant (Rpl10N187p) with low 60S affinity on subunits in the cytoplasm (Figures 4.8

and 4.9). Since Sqt1p forms a complex with free Rpl10p that appears to be necessary for its stability prior to its assembly into the subunit (Eisinger et al., 1997a; West et al., 2005), its entrapment by mutant Lsg1p is strong evidence that Rpl10p loading by Sqt1p takes place in the presence of cytoplasmic Lsg1p.

In our new model (Illustration 4.2), Nmd3p binds nascent subunits in the nucleus in the absence of Rpl10p for Crm1-mediated export. As subunits emerge from the nucleus, a complex of Rpl10p and its chaperone, Sqt1p, binds to 60S, perhaps contemporaneously with Lsg1p recruitment (presumably in a GTP-bound state). GTP hydrolysis on Lg1p may drive a late conformational change or structural rearrangement in 60S that culminates in the accommodation of Rpl10p in the subunit, while releasing Nmd3p and Sqt1p. Rpl10p accommodation coupled with the dissociation of Lsg1p, Nmd3p, and Sqt1p from subunits may be a prerequisite for translational activation. Therefore, mutations that disrupt Lsg1p function or Rpl10p accommodation would result in the accumulation of a late 60S biogenesis intermediate that is incapable of releasing Nmd3p (and perhaps Sqt1p) or progressing into the translational pool. Suppressor mutations in Nmd3p that weaken its interaction with 60S would allow for Nmd3p to dissociate prematurely from these trapped intermediates, sustaining 60S export and, perhaps, alleviating a physical obstruction to Rpl10p loading (see below).

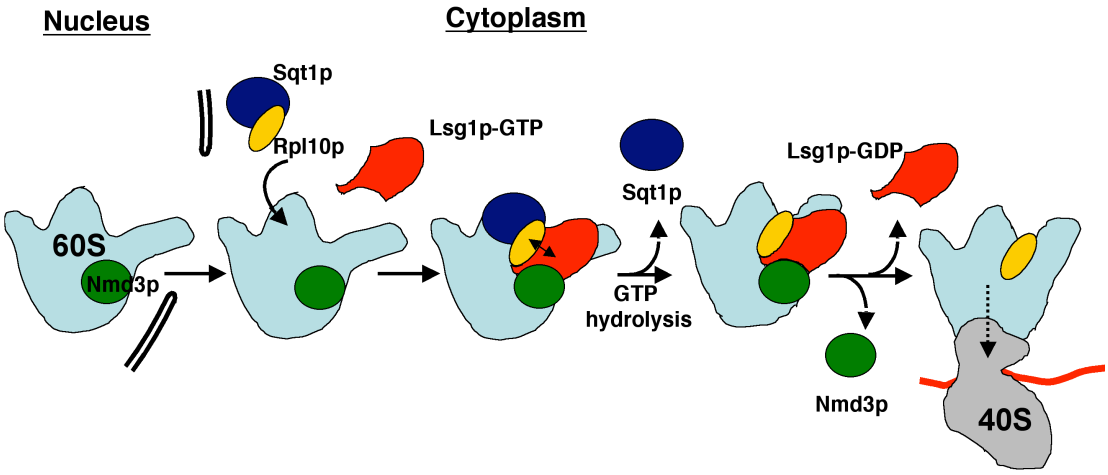

Illustration 4.2 Cartoon depicting our revised model for the Lsg1p-dependent release of Nmd3p and loading of Rpl10p into 60S subunits in the cytoplasm

Nmd3p binds nascent 60S subunits in the nucleus independently of Rpl10p. Following subunit export, Rpl10p in a complex with its chaperone, Sqt1p, binds to 60S, perhaps contemporaneously with Lsg1p recruitment. GTP hydrolysis on Lsg1p drives the accommodation of Rpl10p into the subunit, releasing Nmd3p and Sqt1p and allowing subunits to enter into the translational pool.

How might Rpl10p accommodation and release of Nmd3p be coordinated? Rpl10p is positioned on 60S ribosomal subunits in a cleft between the central protuberance and the GTPase stalk (Spahn et al., 2001; Yusupov et al., 2001) where it makes contacts with both the 25S and 5S rRNAs. Modeling the three-dimensional structure of the prokaryotic homologue of Rpl10p, L16, into the crystal structure of the large subunit has demonstrated that two unstructured regions in the unbound protein, an N-terminal tail (amino acids ~1-34 in *S. cerevisiae*) and a distended central loop (amino acids 102-112 in *S. cerevisiae*), become ordered upon insertion into the subunit (Nishimura et al., 2004). Remarkably, these two unstructured regions of L16 reorganize

to form a portion of the aa-tRNA binding surface in the A site (Nishimura et al., 2004) and make contact with IF2 (bacterial eIF5B) in cryo-EM reconstitutions of translation initiation complexes from *Escherichia coli* (Allen et al., 2005). Furthermore, the central loop has independently been reported to achieve a conformation in the bacterial large subunit that would allow for a direct interaction with the acceptor stem of tRNA (Bashan et al., 2003).

Due to the generally high degree of structural conservation between Rpl10p homologues, it is possible that these same unstructured regions play a critical role in forming the aa-tRNA binding site in yeast, and as a result, their proper insertion into the subunit may serve a structural proofreading function on nascent subunits. Consistent with this hypothesis, deletion of the central loop structure (amino acids 102-112) in the context of full-length yeast Rpl10p results in a strong dominant negative growth arrest coupled with the accumulation of a 60S species that fails to initiate and is enriched for Nmd3p, Lsg1p, and Sqt1p (Hofer, West, and Johnson, unpublished).

In euryarchaeota, Nmd3p is expressed as a chimeric fusion to an eIF5A-like domain. While the prokaryotic orthologue of eIF5A, EF-P, has been shown to stimulate peptidyl-transferase activity (Baxter et al., 1987; Ganoza et al., 1985), the role of eIF5A during translation is not well understood. Recent structural analysis of EF-P from the bacterium, *Thermus thermophilus*, demonstrated that the protein is composed of three *ß*-barrel domains that adopt an acidic L-shaped topology very reminiscent of the structure for tRNA (Hanawa-Suetsugu et al., 2004). Archaeal and eukaryotic eIF5As form structures that are super-imposable onto the structure for EF-P (Hanawa-Suetsugu et al., 2004). In contrast to EF-P, however, eIF5A is only comprised of two domains, approximately corresponding to the first two domains of EF-P (*β*-barrels I and II). Remarkably, in yeast, the region of Nmd3p coincident with the C-terminal suppressor

domain for *rpl10* and *lsg1* mutants shows weak sequence similarity to the N-terminal domain of eIF5A, perhaps harkening back to an evolutionary remnant of the aforementioned Archaeal chimeric fusion protein (Aravind and Koonin, 2000).

The persistence of this eIF5A-like domain in yeast Nmd3p and the observation that Archaeal Nmd3 exists as a fusion between these two proteins suggests that they may have related functions. Thus, it is possible that the C-terminal suppressor domain of Nmd3p acts in conjunction with Rpl10p to survey the region that is to become the A site in maturing subunits by cooperatively assessing the local structural topography of the rRNA. A positive structural assessment of the nascent tRNA acceptor site by these two proteins may result in a conformational change that signals back to Lsg1p to drive a late rearrangement in 60S that releases Nmd3p and stabilizes the insertion of Rpl10p into the subunit. In potential support of this type of cooperativity, the prokaryotic homologue of Rpl10p, L16, is required for the stimulation of peptidyl-transferase activity induced by EF-P (eIF5a orthologue) in ribosome reconstitution experiments (Ganoza et al., 1985) (Baxter et al., 1987).

Alternatively, Nmd3p and Rpl10p may compete for the same binding site on 60S, requiring Lsg1p activity to first release Nmd3p in order to fully accommodate Rpl10p into subunits. As a potential precedent for this type of maturation event on maturing 60S subunits, the ribosome biogenesis factor, Tif6p (see Chapter 1), appears to compete with EF-2 for a binding site on pre-60S particles (Graindorge et al., 2005b). The release of Tif6p by the cytoplasmic GTPase, Efl1p, is believed to expose this binding site for subsequent association of EF-2.

It has recently been demonstrated that, in yeast, newly-synthesized ribososmal subunits containing mutations in the peptidyl transferase center (PTC; 60S subunit) or the decoding site (DCS; 40S subunit) are rapidly degraded in the cytoplasm (Melissa J.

Moore, personal communication). This process, dubbed "nonfunctional rRNA decay" (NRD), may take advantage of a late structural assessment of these active sites prior to earmarking them for degradation. In light of Rpl10p's strategic position on 60S subunits and its requirement for subunit joining (Dick et al., 1997; Eisinger et al., 1997b), it is possible that a failure to accommodate Rpl10p may also trigger pre-60S particles for cytoplasmic degradation. In this sense, a nascent subunit that is structurally aberrant at the A site may fail to load Rpl10p and be rapidly shunted out of the translational pool. Work from our lab has also shown that nascent 60S subunits that are trapped in the nucleus in the absence of Nmd3p function are rapidly degraded (~ 4 minute half-life for 25S rRNA)(Ho and Johnson, 1999). Therefore, a failure to incorporate Rpl10p into subunits may directly influence 60S stability through NRD.

As Rpl10p is required for subunit joining (Dick et al., 1997; Eisinger et al., 1997b), the Lsg1p-mediated accommodation event may provide communication between ribosome biogenesis in the nucleus (through Nmd3p release) and translation initiation in the cytoplasm. Consistent with this line of thinking, Lsg1p, Nmd3p, and Rpl10p have all been previously shown to bind to recycling mature subunits in addition to nascent subunits (Ho et al., 2000a; Kallstrom et al., 2003; Zinker and Warner, 1976). Therefore, the loading of Rpl10p by Sqt1p coordinated with the Lsg1p-dependent release of Nmd3p could provide cells with a surveillance mechanism for assessing the levels of free 60s subunits in the cytoplasm available for subunit joining. In this system, the availability of free Nmd3p to recycle back to the nucleus may act to fine-tune the levels of newly-synthesized 60S subunits that are exported to the cytoplasm, perhaps optimizing the ratio of free 60S to 48S initiation complexes for translation initiation.

Chapter 5: A novel interaction of Nmd3p at the nuclear pore complex: insights into the export of 60S subunits

5.1 Introduction

It is now widely-accepted that Nmd3p provides the Crm1-dependent nuclear export signal for nascent 60S subunits in both yeast and metazoans. How Nmd3p is recruited to subunits and subsequently governs their translocation across the nuclear envelope, however, remain open questions. Earlier models proposed that the loading of Rpl10p onto nuclear subunits was a prerequisite for Nmd3p recruitment prior to 60S export. Results presented in Chapter 4, however, stand in opposition to this model, leaving the timing and manner in which Nmd3p is recruited to pre-60S particles in the nucleus unresolved. While our lab has devoted considerable effort towards defining the precise physical boundaries of Nmd3p's shuttling sequences, the manner in which they are regulated in the context of pre-60S particles is still unclear. Furthermore, the potential for specificity in the 60S export route through nuclear pore complexes has been implied from genetic analyses, yet has not been substantiated through physical interactions.

This chapter provides an initial characterization of a class of Nmd3p mutants that accumulate at nuclear pore complexes with the hope that analyzing this novel interaction will lead to a better understanding of the nature of the 60S export event. I will provide evidence that these mutant alleles arrest at an intermediate stage of Crm1-dependent translocation across the nuclear envelope. Immunopurification assays will then be incorporated to identify the components of the nuclear pore complex (NPC) involved in this interaction, providing insight into the spatio-temporal nature of the export arrest. Moreover, the high degree of overlap between NPC components identified in this screen

with those previously reported to influence 60S export provide physical evidence for specificity in the export route via Nmd3p/Crm1/NPC interactions. Lastly, the NPC-arrest for these Nmd3p mutants will be shown to correlate strongly with an abnormally stable Crm1/Nmd3p interaction *in vitro*, likely preventing efficient export complex disassembly *in vivo*. The discussion of this chapter will focus on the functional implications of these findings with emphasis on their relevance for 60S export and will address future work that will be necessary to achieve a more accurate depiction of the translocation event.

5.2 Background

The nucleocytoplasmic transport of proteins or protein complexes is mediated by karyopherins (Gorlich and Kutay, 1999), a conserved group of soluble transport factors dedicated to the unidirectional movement of cargo across the nuclear envelope. 14 karyopherins have been identified thus far in yeast (~20 in mammals) (Pemberton and Paschal, 2005), and they all share a common structural organization, including an amino-terminal Ran-binding loop, a central nucleoporin-binding domain, and a carboxy-terminal cargo-binding motif (Fried and Kutay, 2003). Karyopherins can be sub-categorized as either importins or exportins with respect to their functionality and differential capacity for binding cargo in the presence of RanGTP (Gsp1p in yeast) (Gorlich and Kutay, 1999). Importins bind to their cargo in the cytoplasm independent of Ran and translocate them into the nucleus where, upon binding RanGTP, they undergo a conformational change that results in cargo release. In contrast, exportins bind to their substrates in the nucleus in a cooperative fashion with RanGTP that enhances the exportin-cargo interaction. Upon translocation to the cytoplasm, Ran hydrolyzes GTP, resulting in a conformational change that disassembles the export complex.

To accommodate the efficient trafficking of both importins and exportins, the effector molecules that modulate Ran's nucleotide bound state are partitioned between

the nucleus and cytoplasm. The nucleotide exchange factor for Ran, RCC1 (Prp20p), is chromatin-bound in the nucleus (Ohtsubo et al., 1989), while Ran's GTPase activating factors, RanGAP1 (Rna1p) and RanBP1 (Yrb1p), are actively sequestered from the nucleus by Crm1 (Feng et al., 1999; Matunis et al., 1998; Richards et al., 1996) (Zolotukhin and Felber, 1997). Thus, there exists a concentration gradient of RanGTP and RanGDP across the nuclear envelope, as RCC1 allows for reloading of Ran with GTP in the nucleus and RanGAP1/RanBP1 strongly induce Ran's inherent GTPase activity in the cytoplasm (Gorlich and Kutay, 1999; Pemberton and Paschal, 2005).

As an exportin, Crm1 typically exhibits a weak affinity for its substrates and must bind cargo in a cooperative manner with RanGTP (Fornerod et al., 1997a). The collaborative nature of this interaction allows for the efficient release of cargo in the cytoplasm as Ran dissociates from the export complex following GTP hydrolysis. A recent structural analysis on human Crm1 has provided insight into the nature of ternary complex formation among exportins. Crm1 possesses a flexible Ran-binding loop that is typically held in a conformation that masks its cargo-binding site and hinders its stable association with Ran (Petosa et al., 2004). Upon interacting with either RanGTP or export cargo, this loop changes conformation to allow for the stable and synergistic assembly of the export (ternary) complex (Illustration 5.1). For importins, this binding loop is held in a cargo-accessible conformation in the unoccupied state, and upon binding RanGTP in the nucleus, it undergoes a conformational change that dislodges the bound cargo (Petosa et al., 2004). The common theme for assembly and disassembly of cargo complexes through conformational changes in the Ran-binding loop has allowed for the vast conservation and dynamic range of karyopherins in mediating nucleocytoplasmic transport (Pemberton and Paschal, 2005).

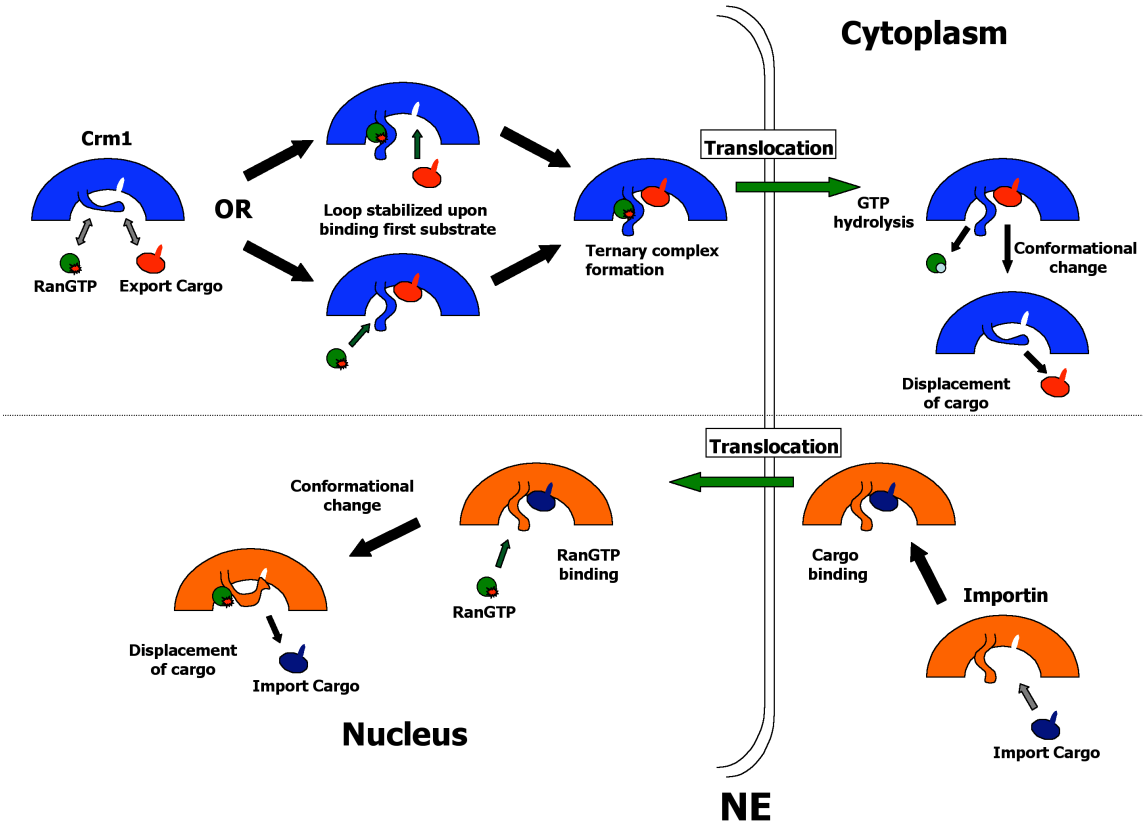

Illustration 5.1 Model depicting the behavior of the Ran-binding loop in exportins and importins

Exportins bind to their substrates in the nucleus in a cooperative fashion with RanGTP that stabilizes the position of the Ran-binding loop in a conformation that favors the exportin-cargo interaction. Upon translocation to the cytoplasm, Ran hydrolyzes GTP, resulting in a conformational change in the Ran-binding loop that disassembles the export complex. In contrast to exportins, the Ran-binding loop in importins is held in a cargo-accessible conformation in the absence of RanGTP. Importins bind to their cargo in the cytoplasm independent of Ran and translocate them into the nucleus where, upon binding RanGTP, the Ran-binding loop undergoes a conformational change that results in cargo release.

Among exportins, Crm1 boasts the most expansive collection of substrates, including cargoes as diverse as ribosomes and cell cycle regulators (Gorlich and Kutay, 1999). Crm1 binds cargo molecules that possess leucine-rich NESs (Fornerod and Ohno, 2002; la Cour et al., 2004). Upon formation of an export complex with RanGTP, Crm1 transports its cargo across the nuclear envelope through nuclear pore complexes (NPCs). NPCs are the massive (50-60 kDa in yeast), octagonally-symmetric assemblages of proteins that form the semi-permeable aqueous channels between the nucleus and cytoplasm (Suntharalingam and Wente, 2003). Through a fairly comprehensive range of experimental approaches, approximately 30 nuclear pore proteins, or nucleoporins (Nups), have been identified in yeast ((Suntharalingam and Wente, 2003) and references therein). Among these, many appear to be arranged in hierarchical sub-complexes that decorate either side of the nuclear envelope and differentially regulate the flux of molecules through the NPC. One such sub-complex composed of Nup82p, Nup159p, and Nsp1p (the "Nup82p complex") is located on the cytoplasmic side of the NPC and has been shown to play a critical role in the export of ribosomal subunits (Gleizes et al., 2001). Moreover, the mammalian homologue of Nup159p, Nup214, acts as a terminal binding site for Crm1 prior to export complex disassembly at the NPC (Kehlenbach et al., 1999). While the nucleoporin constituents of the Nup82p complex have also been implicated in the export of mRNPs, this function is physically separable from that of ribosome export (Gleizes et al., 2001).

As the export adapter for the 60S ribosomal subunit, Nmd3p must be imported into the nucleus from its site of synthesis in the cytoplasm in order to recruit Crm1 and RanGTP onto export-competent subunits for "quaternary complex" (Crm1/RanGTP/Nmd3p[NES]/60S) assembly. In yeast, Nmd3p is a 59.1 kDa protein that is 518 amino acids in length. Nmd3p's nucleocytoplasmic shuttling sequences are

located within its C-terminal 150 amino acids. Nuclear import of Nmd3p is governed by a basic cluster of amino acids within this region that comprise a nuclear localization signal (NLS: amino acids 399-419; Illustration 5.2) that is both necessary and sufficient for efficient access to the nucleus ((Gadal et al., 2001b; Ho et al., 2000b) and Hedges, West et al., manuscript in preparation). NLS-recognition and nuclear import of Nmd3p is thought to be mediated, at least in part, by the importin Kap123p (Sydorskyy et al., 2003). Nmd3p's leucine-rich nuclear export signal (NES: amino acids 496-505) is positioned just downstream of its NLS and exhibits marked similarity to the classical Crm1-dependent NES's of the protein kinase A inhibitor (PKI) and HIV-1 Rev proteins ((Kutay and Guttinger, 2005; Pemberton and Paschal, 2005) and Illustration 5.2). Nmd3p's NES is predicted to form an amphipathic helix with the hydrophobic residues critical for Crm1 interaction aligned on one surface, like that observed for the PKI NES (Illustration 5.2) (Hauer et al., 1999). Deletion or mutation of this NES results in the dramatic nuclear accumulation of both Nmd3p and its substrate, the nascent 60S ribosomal subunit ((Gadal et al., 2001b; Ho et al., 2000b) and Hedges, West et al., manuscript in preparation). Although a secondary NES (NES2: amino acids 445-456) has been proposed for yeast Nmd3p (Gadal et al., 2001b), it is unlikely that it is sufficient for export as point mutations that perturb the canonical NES (amino acids 496-505) result in lethality (Hedges, West et al., manuscript in preparation).

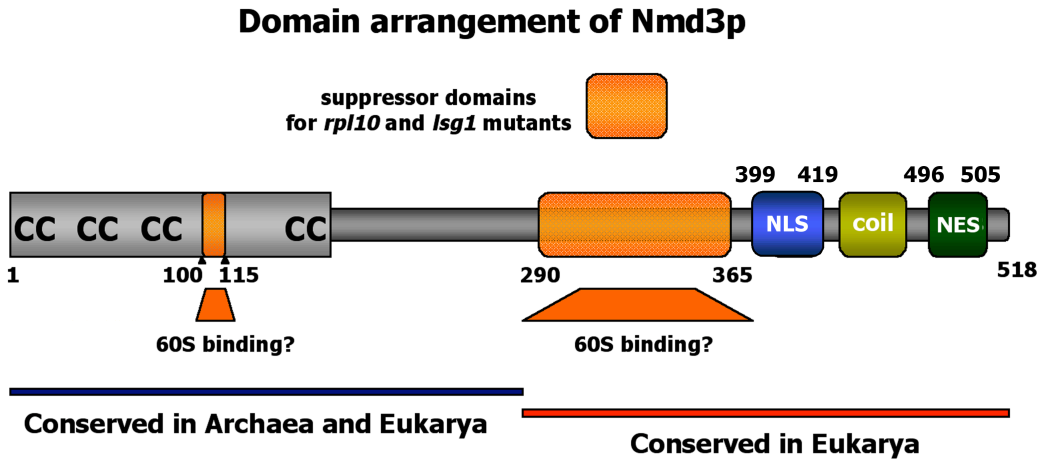

PROTEIN	NES Sequence
NES Consensus	$\Phi X_{2-3}\Phi x_{2-3}\Phi x\Phi$
PKI	LALKLAGLDI
HIV-1 Rev	L-PPLERLTL
Sc Nmd3	LLDELDEMTL
Sp Nmd3	LLDDVEAMHI
Dm Nmd3	LEEMLEDMTL
Hs Nmd3	LAEMLEDLHI

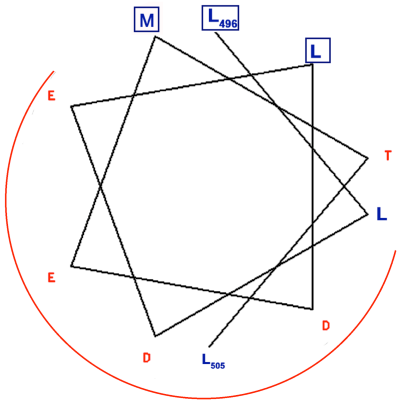

Nmd3p NES aa496-505

Illustration 5.2 Architecture of Nmd3p.

(A.) A large amino-terminal domain, conserved throughout Archaea and Eukarya, contains four Cys-X_2-Cys motifs (see section 5.4.1) and a region that is necessary for 60S binding. The two regions in eukaryotic Nmd3p in which point mutations suppress *LSG1* and *RPL10* mutants are also shown. The carboxy-terminal region of eukaryotic proteins contains the nuclear shuttling sequences. (B.) An alignment of the hydrophobic core of the NES from yeast Nmd3p (amino acids 496-505) is compared with NESs from other proteins. (C.) Amphipathic helical projection of Nmd3p's NES containing the three conserved residues (*boxed*) that form a hydrophobic surface critical for interaction with Crm1. The acidic face is indicated by a red semicircle.

Although Nmd3p's role in 60S export has been well-documented (Johnson et al., 2002), the *in vitro* assembly of the subunit-bound export complex has, thus far, proven elusive. Moreover, neither Ran nor Crm1 have been identified in proteomic analyses of late pre-60S particles ((Bassler et al., 2001; Fatica et al., 2002; Nissan et al., 2002; Saveanu et al., 2003) and Kallstrom and Johnson, unpublished). Intriguingly, the interaction between Nmd3p and 60S (Ho and Johnson, 1999; Thomas and Kutay, 2003) and between Crm1, RanGTP, and Nmd3p can be reconstituted separately *in vitro* ((Thomas and Kutay, 2003) and Kallstrom and Johnson, unpublished). The inability to assemble an export complex containing a 60S subunit suggests that the proper presentation of Nmd3p's NES may be masked upon binding 60S *in vitro* and, thus, may reflect the requirement for an additional factor(s) or specific 60S conformational state to facilitate export complex assembly *in vivo*.

5.3 Results

5.3.1 *nmd3* mutants disrupted for 60S binding accumulate at nuclear pore complexes

While screening for *nmd3* loss-of-function (LOF) mutants (as described in Chapter 4), we identified three mutants by fluorescence microscopy that exhibited an aberrant localization pattern when expressed as GFP-fusion proteins (Figure 5.1A). In contrast to wild-type Nmd3-GFP, which was distributed throughout the nucleus and cytoplasm, the Nmd3(I139T,L259S,L296P)-GFP, Nmd3(L263P,F318I)-GFP, and Nmd3(V340D)-GFP mutant proteins accumulated in a striking ring-like pattern within the cell interior (Figure 5.1A). This annular distribution was reminiscent of the localization pattern that is typically observed for nuclear envelope-associated factors.

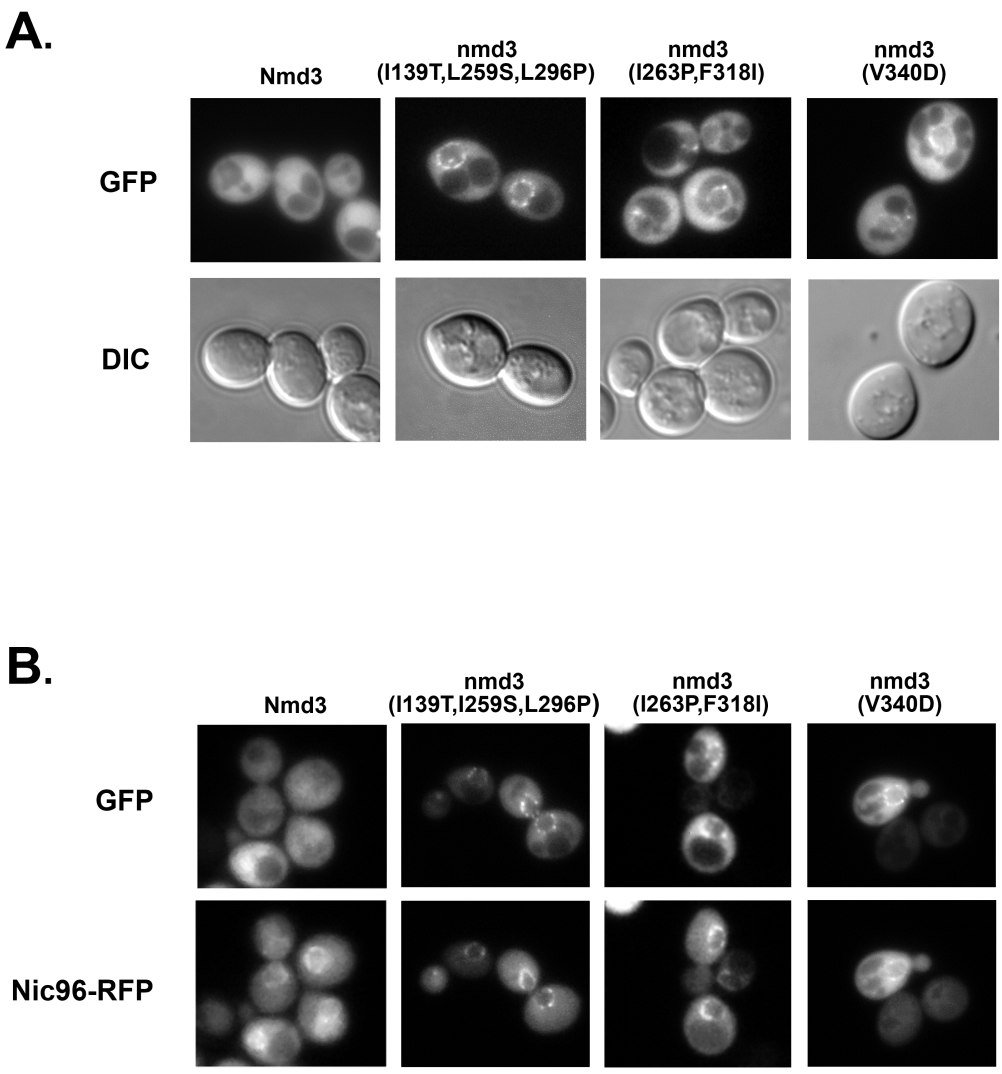

Figure 5.1 A class of Nmd3p loss-of-function mutants localize to the nuclear envelope.

(A.) Strain AJY1539 (*crm1[T539C]*) containing pAJ582 *(NMD3-GFP*), pAJ1406 (*nmd3[I139T,L259S,L296P]-GFP*), pAJ1407 (*nmd3[I263P,F318I]-GFP*), and pAJ1408 (*nmd3[V340D]-GFP*) was cultured overnight and diluted ten-fold into 2 ml of fresh glucose-containing medium. Cells were cultured at 30˚C to mid-log phase and visualized as described in Chapter 2. (B.) As in (A.) using strain AJY1849 (*NIC96-mRFP crm1[T539C]*).

In order to determine whether these *nmd3* LOF mutants were accumulating at the nuclear rim, I introduced the GFP-tagged mutant alleles into a strain, which expresses the nuclear envelope marker Nic96p as an mRFP-fusion protein from its genomic locus. In contrast to wild-type Nmd3-GFP, which was dispersed throughout the cell, the mutant Nmd3-GFP proteins co-localized with Nic96-mRFP along nuclear envelopes, with one mutant, Nmd3(I139T, L259S, L296P)-GFP, showing particularly strong envelope enrichment (Figure 5.1B). The nuclear envelope accumulation for this set of Nmd3p LOF mutants marks the first reported example of a factor involved in the 60S biogenesis pathway potentially trapped at the point of export/import at or within nuclear pore complexes.

The three "nuclear envelope-enrichment" ("NE") alleles possess point mutations within the regions of *NMD3* in which we have identified mutations that are capable of suppressing both *lsg1* and *rpl10* mutants (Figure 5.2A). In Chapter 4, I presented evidence that mutations within these two domains give rise to attenuated 60S affinity. *NMD3* alleles that possess mutations in either of these regions that severely disrupt 60S binding, however, are incapable of supporting growth or suppressing mutations in *lsg1* or *rpl10*. Intriguingly, the *nmd3(V340D)* identified among our "NE" mutants was initially characterized as a stringent LOF allele that was both incapable of binding 60S subunits or supporting growth when expressed as the only copy of Nmd3p in cells (see Chapter 4).

In order to examine whether the other "NE" mutants were defective for 60S binding, I performed immunoprecipitations (IPs) in extracts prepared from cells that had constitutively expressed oligomeric c-myc-tagged versions of the mutant alleles to assess the relative levels of co-immunoprecipitated 60S subunits. Western blotting against the core ribosomal protein, Rpl8p, among factors co-IP'd with the mutant Nmd3 proteins served as a reporter for relative 60S affinity. Although ectopic expression levels and IP

efficiencies were comparable, the "NE" mutants exhibited a dramatic deficit in 60S binding relative to wild-type Nmd3p (Figure 5.2). Indeed, the Rpl8p signal was virtually absent in IPs conducted against two of the mutants (compare Lane 2 with Lanes 3-4). Correlating the results obtained by western analysis with the observed nuclear envelope enrichment suggests that mutations in Nmd3p which disrupt 60S binding cause accumulation at NPCs that may represent a default state for Nmd3p in the absence of cargo binding (i.e. 60S subunits).

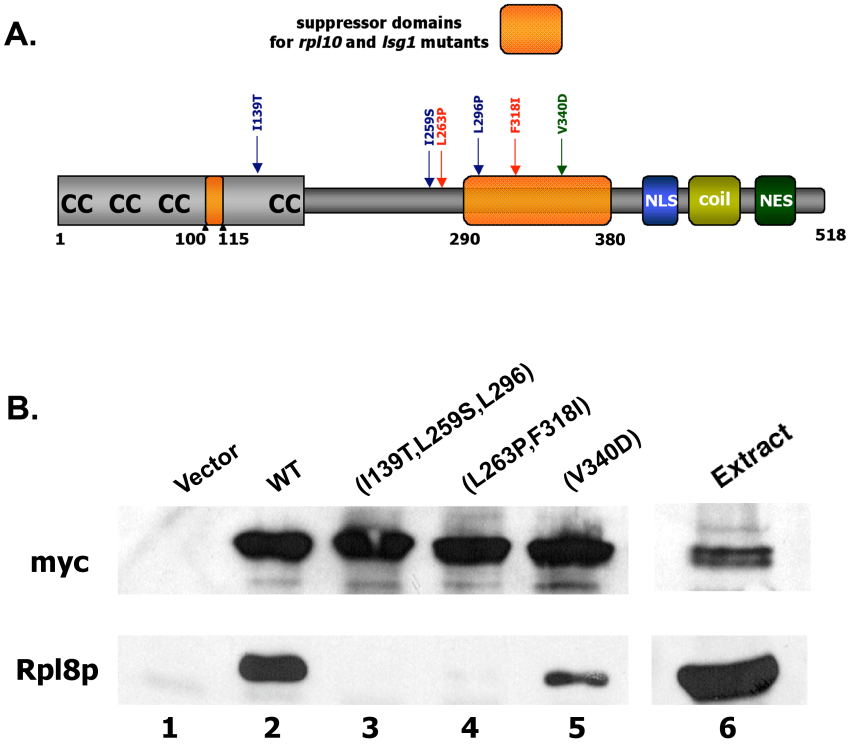

Figure 5.2 Nmd3p "NE" mutants are deficient for 60S binding.

(A.) Cartoon depicting positions of point mutations within the Nmd3p mutants that accumulate at the NE. Multiple substitutions within a single mutant are represented as a single color (i.e. red, green, or blue). (B.) α-cmyc immunoprecipitations were conducted in extracts prepared from strain AJY1539 (*crm1[T539C]*) harboring either empty vector (pRS415), pAJ538 (*NMD3-cmyc*), pAJ1298 (*nmd3[I139T,L259S,L296P]-cmyc*), pAJ1404 (*nmd3[L263P,F318I]-cmyc*), or pAJ1403 (*nmd3[V340D]-cmyc*) as described in Chapter 2. Immunoprecipitated proteins were resolved on an 8% SDS-PAGE gel followed by western blotting against the various Nmd3p alleles using α-cmyc or against the 60S core protein Rpl8p using anti-Rpl8p as described in Chapter 2.

5.3.2 Accumulation of Nmd3p "NE" mutants at the NPC is Crm1-dependent

This line of experimentation gained conceptual momentum when a similar localization pattern was observed for another Crm1-specific export cargo. In a screen designed to further characterize the specificity for Crm1 substrates using randomly-generated synthetic peptides, Engelsma *et al*. (2004) identified NES-like sequences of amino acids that exhibited a marked nuclear envelope accumulation in permeabilized HeLa cells. As the dissociation of export cargo from Crm1 and RanGTP at nuclear envelopes is typically very rapid, the presence of export complexes or cargos at NPCs is generally imperceptible by microscopy. These synthetic NESs were so potently strong, however, that they continued to interact with Crm1 following GTP hydrolysis on Ran and dissociation of the ternary export complex. The persistence of this interaction resulted in the entrapment of both Crm1 and the NES-like export cargo at NPCs. The authors designated these potent NES's as "supraphysiological" to denote their ability to associate with Crm1 in the absence of RanGTP and concluded that they represented a *bona fide* export complex-like intermediate at the nuclear pore.

To determine if our mutant Nmd3 proteins were behaving in a similar fashion, I performed co-immunoprecipitation experiments to test for enrichment of Crm1 with the mutant proteins. Immunoprecipitations were conducted against c-myc-tagged Nmd3p in extracts prepared from a strain co-expressing HA-tagged Crm1 from its genomic locus (*crm1[T539C]-3xHA*). Western blotting against the HA epitope revealed a significant and specific increase in Crm1 in the "NE" mutant IPs relative to the corresponding wild-type Nmd3p allele (~8-fold increase; Figure 5.3). The co-immunoprecipitation of Crm1 by one of its export cargoes is atypical, as the transient nature of the ternary complex most often prevents its detection. The persistent Crm1 interaction and nuclear envelope enrichment suggests that the mutant alleles are recruited to the nuclear pore in a Crm1-

dependent manner, consistent with the accumulation of an Nmd3p export complex-like intermediate at the nuclear rim.

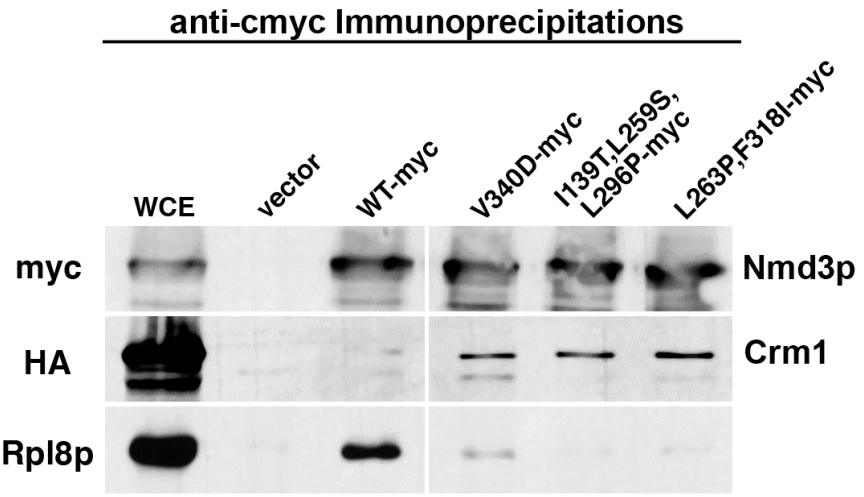

Figure 5.3 Crm1 is enriched in complexes bound by Nmd3p "NE" mutants.

α-cmyc immunoprecipitations were conducted in extracts prepared from strain AJY1539 (*crm1[T539C]-HA*) harboring either empty vector (pRS415), pAJ538 (*NMD3-cmyc*), pAJ1403 (*nmd3[V340D]-cmyc*), pAJ1298 (*nmd3[I139T,L259S,L296P]-cmyc*), or pAJ1404 (*nmd3[L263P,F318I]-cmyc*) as described in Chapter 2. Immunoprecipitated proteins were resolved on an 10% SDS-PAGE gel followed by western blotting against the various Nmd3p alleles using α-cmyc, Crm1 using anti-HA, or against the 60S core protein Rpl8p using anti-Rpl8p as described in Chapter 2.

As a means of more directly assessing the dependence for Crm1 on the NPC accumulation for the mutant Nmd3p alleles, I introduced point mutations into the canonical NESs of the mutants to attempt to disrupt Crm1 binding. We have previously shown by fluorescence microscopy that an Nmd3p mutant (Nmd3[AAA]p) possessing three point mutations within its NES (I493A, L497A, L500A; see Figure 5.5A below) exhibits a dramatic nuclear accumulation, mimicking the effects seen for wild-type Nmd3p in the presence of the Crm1-specific inhibitor leptomycin B (LMB) (Hedges et al., 2005; Ho et al., 2000b). Therefore, I sought to determine whether the GFP-tagged "NE" mutants possessing the AAA substitutions also exhibited a nucleoplasmic accumulation, indicating that NPC enrichment requires export complex formation.

Whereas mutant proteins possessing wild-type NES's localized to NPCs, those possessing the AAA mutations were dispersed throughout the nucleoplasm with no detectable nuclear envelope enrichment, in a manner analogous to that seen for wild-type Nmd3(AAA)-GFP (Figure 5.4). Consistent with this result, the mutant proteins possessing wild-type NESs were also efficiently displaced from the nuclear envelope upon incubating sensitized yeast cells with LMB (data not shown). Thus, Crm1 binding appears to be necessary for the recruitment and retention of the mutant Nmd3p alleles at the nuclear envelope. These results suggest that Crm1 interaction acts upstream of NPC accumulation.

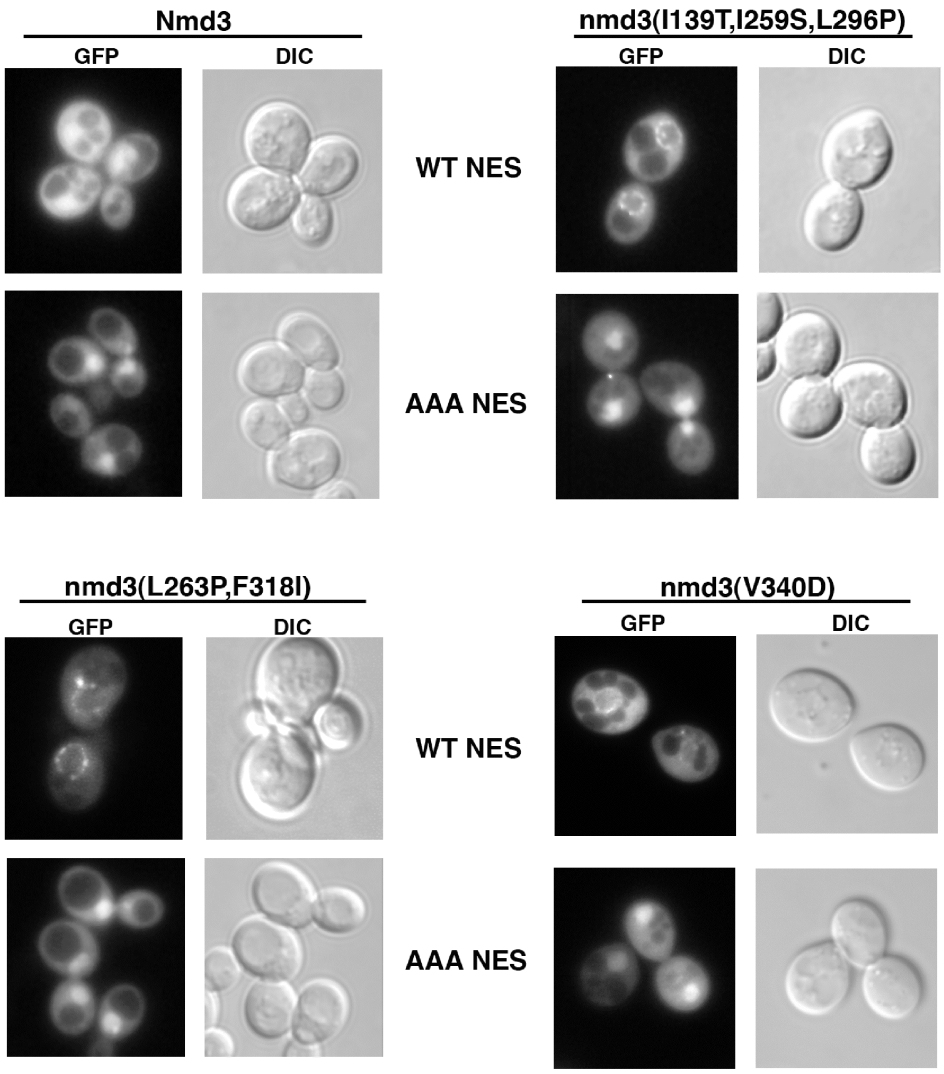

Figure 5.4 Point mutations that disrupt Crm1 binding redistribute Nmd3p "NE" mutants from the nuclear rim.

Strain AJY1539 (*crm1[T539C]*) containing pAJ582 *(NMD3-GFP*), pAJ754 (*nmd3[AAA]-GFP*), pAJ1407 (*nmd3[I263P,F318S]-GFP*), pAJ1413 (*nmd3[I263P,F318S][AAA]-GFP*), pAJ1406 (*nmd3[I139T,L259S,L296P]-GFP*), pAJ1412 (*nmd3[I139T,L259S,L296P][AAA]-GFP*), pAJ1408 (*nmd3[V340D]-GFP*), and pAJ1414 (*nmd3[V340D][AAA]-GFP*) was cultured overnight and diluted ten-fold into 2 ml of fresh glucose-containing medium. Cells were cultured at 30˚C to mid-log phase and visualized as described in Chapter 2.

As a means of demonstrating that the physical interaction between the "NE" mutant proteins and Crm1 was indeed disrupted by the mutated NES's, I constructed plasmids for expressing c-myc-tagged *nmd3AAA* alleles in the genomically-integrated *CRM1-HA* strain for co-immunoprecipitation analysis. I predicted that the mutants possessing the disrupted NES would show a marked attenuation in Crm1 binding relative to those maintaining the wild-type NES. Western blotting for Crm1-HA among proteins that co-immunopurified with the Nmd3p mutants revealed that the AAA mutations significantly reduced Crm1 binding relative to mutants with a wild-type NES (Figure 5.5, compare lanes 4, 6, and 8 with lanes 5, 7, and 9). This finding further supports the idea that NPC enrichment for the mutant Nmd3p alleles is dependent upon a classical, yet high-affinity, Crm1-cargo(NES) interaction.

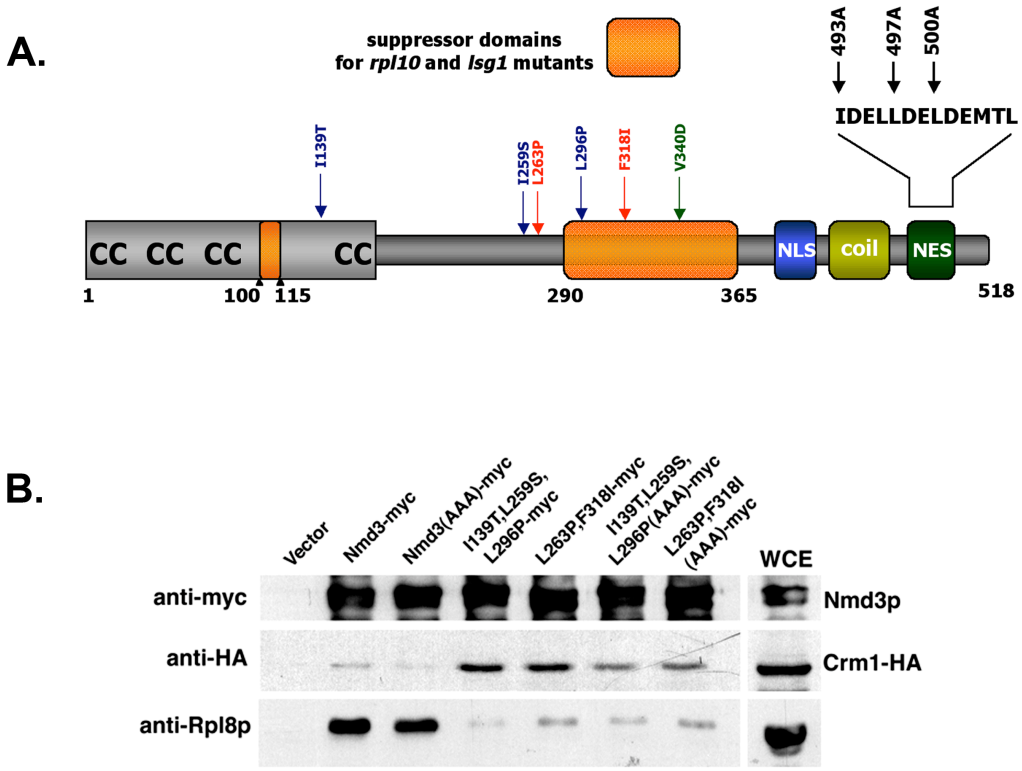

Figure 5.5 Mutations in the NES of Nmd3p "NE" mutants attenuate Crm1 enrichment.

(A.) Cartoon depicting positions of AAA mutations in the NESs of the Nmd3p "NE" mutants. (B.) α-cmyc immunoprecipitations were conducted in extracts prepared from strain AJY1539 (*crm1[T539C]-HA*) harboring either empty vector (pRS415), pAJ538 (*NMD3-cmyc*), pAJ752 (*nmd3[AAA]-cmyc*), pAJ1298 (*nmd3[I139T,L259S,L296P]-cmyc*), pAJ1515 (*nmd3[I139T,L259S,L296P][AAA]-cmyc*), pAJ1404 (*nmd3[L263P,F318I]-cmyc*), or pAJ1516 (*nmd3[L263P,F318I][AAA]-cmyc*) as described in Chapter 2. Immunoprecipitated proteins were resolved on a 10% SDS-PAGE gel followed by western blotting against the various Nmd3p alleles using anti-cmyc, against Crm1 using anti-HA or against the 60S core protein Rpl8p using anti-Rpl8p as described in Chapter 2.

It has been proposed that Nmd3p possesses a second NES (amino acids 445-456) upstream of its canonical primary NES (Gadal et al., 2001b). This putative secondary NES lies within a span of amino acids (446-460) that are predicted to form a coiled-coil (coil, see Figure 5.7A below). Although deletion of the coiled-coil region in the context of a wild-type Nmd3p allele results in a growth defect, it does not detectably inhibit Nmd3p or 60S export (Hedges, West, et al., manuscript in preparation). Intriguingly, this coiled-coil region is rendered essential in the context of an Nmd3(AA)p mutant, which contains two amino acid substitutions (L496A,L497A) in its primary NES that are typically tolerated even though they attenuate the rate of 60S export (Hedges, West, et al., manuscript in preparation). The strong 60S export arrest and resultant lethality conferred by an Nmd3ΔCC(AA)p double mutant suggest that the coiled-coil ("NES2") motif plays an auxiliary role in modulating inter- or intramolecular interactions during 60S export that become critical in the context of an inefficient primary NES.

To test whether the coiled-coil motif contributes to the aberrantly strong interaction observed between Crm1 and the Nmd3p "NE" mutants, I excised the coiled-coil region from the GFP-tagged Nmd3(I139T,L259S,L296P)p mutant and compared the localization of the resultant protein to the Nmd3(I139T,L259S,L296P)p allele possessing either wild-type or mutant (AA or AAA) NESs. While both the AA and AAA mutations redistributed the Nmd3(I139T,L259S,L296P)p mutant throughout the nucleoplasm, deletion of the coiled-coil motif did not disrupt its retention at the nuclear rim (Figure 5.6).

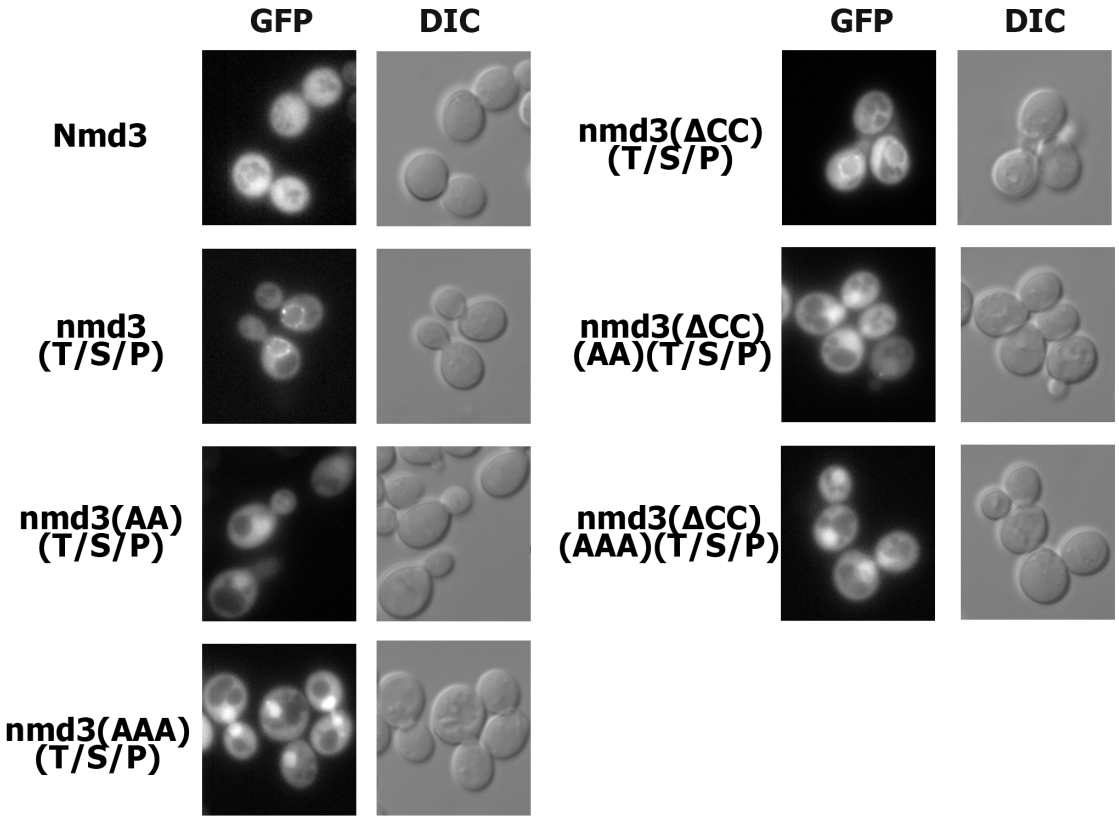

Figure 5.6 The coiled-coil motif ("NES2") is not required for the nuclear envelope localization of the Nmd3p "NE" mutants.

Strain AJY1539 (*crm1[T539C]*) containing pAJ582 *(NMD3-GFP*), pAJ1406 (*nmd3[I139T,L259S,L296P]-GFP*), pAJ1409 (*nmd3[I139T,L259S,L296P][AA]-GFP*), pAJ1412 (*nmd3[I139T,L259S,L296P][AAA]-GFP*), pAJ1531 (*nmd3[I139T,L259S,L296P][ΔCC]-GFP*), pAJ1534 (*nmd3[I139T,L259S,L296P][ΔCC][AA]-GFP*),), or pAJ1533 (*nmd3[I139T,L259S,L296P][ΔCC][AAA]-GFP* was cultured overnight and diluted ten-fold into 2 ml of fresh glucose-containing medium. Cells were cultured at 30˚C to mid-log phase and visualized as described in Chapter 2. The I139T/L259S/L296P amino acid substitutions are abbreviated as T/S/P. Coiled-coil deletion denoted as ΔCC.

These observations likely indicate that the coiled-coil is dispensable for the high-affinity Crm1 interaction. Alternatively, the coiled-coil may participate in preventing a "supraphysiological" interaction between Crm1 and Nmd3p in the context of the wild-type allele. As a result, its deletion may strengthen the Crm1/ Nmd3(I139T,L259S,L296P)p interaction. To address this possibility, I combined the coiled-coil deletion with either the AA or AAA mutations in the context of Nmd3(I139T,L259S,L296P)-GFP to monitor whether removal of the coiled-coil could counteract point mutations in the NES with respect to nuclear rim accumulation. As shown in Figure 5.6, uniting the coiled-coil deletion with either the AA or AAA Nmd3(I139T,L259S,L296P)p mutants did not alter the nucleoplasmic redistribution conferred by the NES point mutations. Moreover, western blotting against Crm1 among immunoprecipitations conducted with c-myc-tagged versions of these mutant proteins revealed a direct correlation between nuclear envelope accumulation and sustained interaction with Crm1 (Figure 5.7B). Taken together, these results suggest that the accumulation of the "NE" mutants at NPCs is directly attributable to an enhanced interaction with Crm1 through its canonical NES and that the coiled-coil ("NES2") motif does not play a major role in this aberrant association.

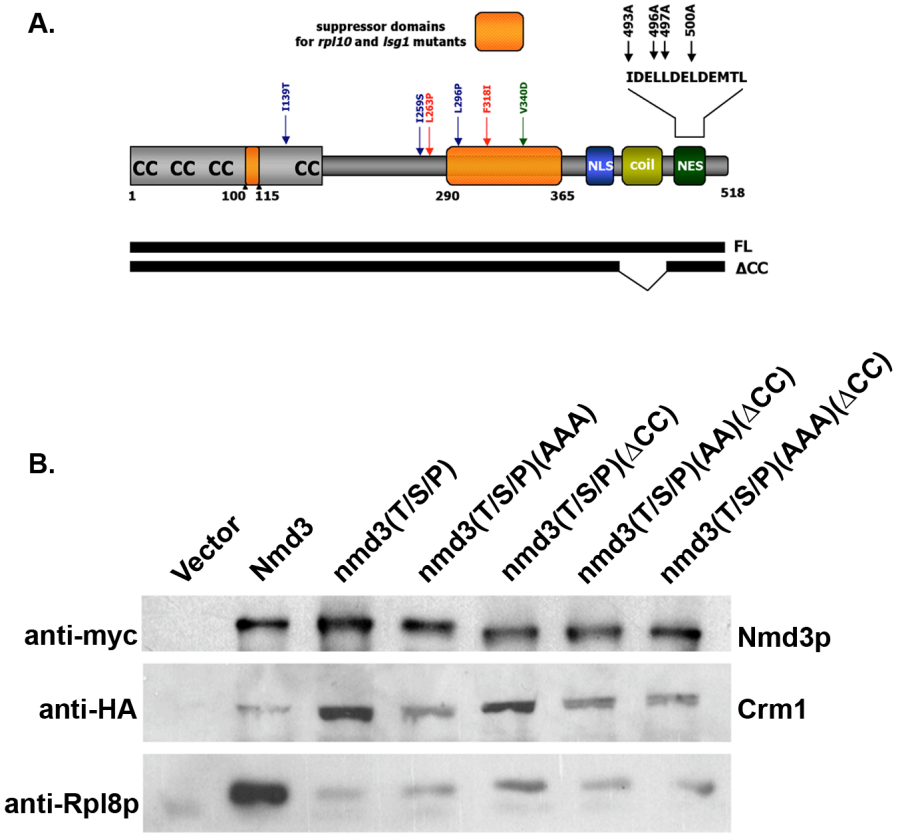

Figure 5.7 Deletion of the coiled-coil motif ("NES2") does not dramatically reduce Crm1 enrichment in complexes bound by Nmd3p "NE" mutants.

(A.) Cartoon depicting positions of AA and AAA mutations in the NESs of the Nmd3p "NE" mutants. A graphical representation of the coiled-coil deletion is also included for visual reference. (B.) α-cmyc immunoprecipitations were conducted in extracts prepared from strain AJY1539 (*crm1[T539C]-HA*) harboring either empty vector (pRS415), pAJ538 (*NMD3-cmyc*), pAJ1298 (*nmd3[I139T,L259S,L296P]-cmyc*), pAJ1515 (*nmd3[I139T,L259S,L296P][AAA]-cmyc*), pAJ1527 (*nmd3[I139T,L259S,L296P][ΔCC]-cmyc*), pAJ1528 (*nmd3[I139T,L259S,L296P][ΔCC][AA]-cmyc*), or pAJ1529 (*nmd3[I139T,L259S,L296P][ΔCC][AAA]-cmyc*) as described in Chapter 2. Immunoprecipitated proteins were resolved on a 10% SDS-PAGE gel followed by western blotting against the various Nmd3p alleles using anti-cmyc, against Crm1 using anti-HA or against the 60S core protein Rpl8p using anti-Rpl8p as described in Chapter 2. The I139T/L259S/L296P substitutions are abbreviated as T/S/P. ΔCC for coiled-coil deletion.

5.3.3 An Nmd3p "NE" mutant co-purifies with a subset of nucleoporins

Due to their marked enrichment at or within nuclear pore complexes, I anticipated that the Nmd3p "NE" mutants might be capable of co-purifying with a distinct subset of nucleoporins (Nups). It was my contention that the identification of nucleoporins bound by the mutant Nmd3 proteins might provide insight into the manner in which the wild-type allele interacts with NPCs during 60S export. To this end, I utilized a yeast GFP strain library (UCSF/Invitrogen) for assessing the relative enrichment of Nups or NPC-associated factors in complexes bound by the mutant Nmd3p alleles. This library is comprised of haploid yeast strains derived from a common progenitor in which a single gene has been C-terminally-tagged with GFP at its genomic locus by homologous recombination. From this strain collection, I selected a subset of GFP-tagged nuclear pore-associated factors for sampling based on their structural and functional distribution across NPCs, with particular emphasis on proteins that had previously been shown to inhibit 60S export when they were mutated ((Gleizes et al., 2001; Hurt et al., 1999; Stage-Zimmermann et al., 2000) and Table 5.1). For analysis of Nup120-GFP, which was absent from the library, I introduced *NUP120-GFP* on a *CEN* vector as the sole source of *NUP120* in a *nup120* deletion strain. Plasmids bearing oligomeric c-myc tagged versions of either wild-type *NMD3* or *nmd3(I139T,L259S,L296P)* were transformed into each of the GFP-tagged strains for affinity purification of Nmd3-bound complexes. Cell extracts from each strain were then immunoprecipitated with anti-cmyc, and the bound proteins were subjected to western blotting with an antibody that recognizes GFP.

Among the 22 nuclear pore-associated proteins that I examined in this assay, only five were enriched in complexes bound by Nmd3(I139T,L259S,L296P)-c-myc relative to the wild-type allele (Table 5.1). Among these, four (Nup82p, Nup159p, Nic96p, and

Nup85p) had previously been implicated in the nuclear export of pre-ribosomal particles ((Gleizes et al., 2001; Hurt et al., 1999; Moy and Silver, 1999; Stage-Zimmermann et al., 2000). In virtually all cases, the c-myc-tagged wild-type Nmd3p did not show any detectable co-purification of the nucleoporin under investigation, showing specificity for the interaction of the mutant export complex with the NPC (Figure 5.8). The high specificity of enrichment and the direct correspondence between nucleoporins that co-purified with the mutant Nmd3p allele with Nups known to participate in ribosome export are consistent with the entrapment of a physiologically-relevant Nmd3p export intermediate at the NPC.

NPC-Associated Factor	Localization	NPC subcomplex	Enrichment in Nmd3(T/S/P)p IP	Role in ribosome export
Nup49p	Symmetric	Nic96p	No	Yes
Nup53p	Symmetric	Nup53p	No	No
Nup57p	Symmetric	Nic96p	No	No
Nup59p	Symmetric	Nup53p	No	No
Nup60p	Nuclear	-	No	No
Nup82p	Cytoplasmic	Nup82p	Yes (++++)	Yes
Nup84p	Symmetric	Nup84p	No	No
Nup85p	Symmetric	Nup84p	Yes (++)	Yes
Nup100p	Cytoplasmic-biased	-	No	No
Nup116p	Cytoplasmic-biased	-	No	Yes
Nup120p	Symmetric	Nup84p	No	No
Nup133p	Symmetric	-	No	Yes (weak)
Nup145p	Symmetric	Nup84p	No	No
Nup157p	Symmetric	-	No	No
Nup159p	Cytoplasmic	Nup82p	Yes (++++)	Yes
Nup170p	Symmetric	Nup53p	No	No
Nic96p	Symmetric	Nic96p	Yes (+++)	Yes
Nsp1p	Symmetric	Nup82p,Nic96p	No	Yes
Gle1p	Cytoplasmic-biased	-	No	No
Seh1p	Symmetric	Nup84p	No	No
Sec13p	Symmetric	Nup84p	No	No
Pse1p	Symmetric	-	Yes (++)	No

Table 5.1 NPC-associated factors that are enriched in Nmd3(I139T,L259S,L296P)p-bound complexes.

NPC-associated factors that were specifically enriched in complexes co-immunopurified with Nmd3(I139T,L259S,L296P)-cmyc are highlighted in pink. The relative enrichment of NPC-associated factors in mutant IPs over complexes bound by wild-type Nmd3p are indicated parenthetically. Also listed are the subspatial distribution of these factors within the NPC, their designated subcomplexes (where appropriate), and whether they have been previously implicated in ribosome export.

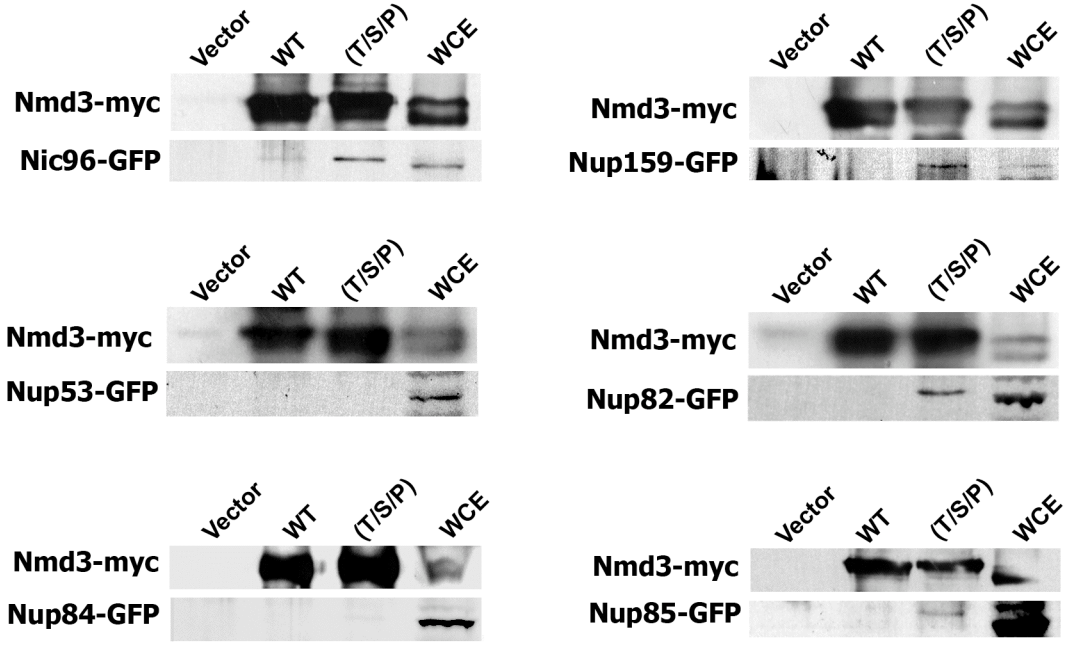

Figure 5.8 Representative westerns from NPC immunoprecipitation assays.

Extracts were prepared from strains AJY2155 (*NIC96-GFP*), AJY2154 (*NUP159-GFP*), AJY2163 (*NUP53-GFP*), AJY2161 (*NUP82-GFP*), AJY2164 (*NUP84-GFP*), and AJY2162 (*NUP85-GFP*) harboring either empty vector (pRS415), *NMD3-cmyc* (pAJ538), or *nmd3(I139T,L259S,L296P)-cmyc* (pAJ1298) as described in Chapter 2. Immunoprecipitations were carried-out against the cmyc-tagged Nmd3p alleles using anti-cmyc. Immunoprecipitated proteins were resolved on 8% SDS-PAGE gels and western analyses were conducted against cmyc-tagged Nmd3p using anti-cmyc or against the appropriate NPC-associated factor using anti-GFP. Whole cell extract (WCE).

The yeast NPC can be organized into distinct subcomplexes of nucleoporins based largely upon physical interaction networks derived from proteomic and biochemical analyses ((Suntharalingam and Wente, 2003) and references therein). Most prominent among these are the Nup82p complex (Nup82p, Nup159p, and Nsp1p), the Nup84p complex (Nup84p, Nup85p, Nup120p, Nup145p, Seh1p, and Sec13p), the Nic96p complex (Nic96p, Nup49p, Nup57p, and Nsp1p), and the Nup53p complex (Nup53p, Nup59p, and Nup170p) (Illustration 5.3). As shown in Figure 5.8, the Nmd3(I139T,L259S,L296P) mutant protein exhibited an enhanced interaction (~5-6-fold increase over wild-type) with components unique to the Nup82p complex (Nup82p and Nup159p, also see Table 5.1). In contrast, among the six nucleoporins of the Nup84p complex that I examined in the immunoprecipitation assay, only Nup85p was moderately enriched (~3-fold) in the Nmd3(I139T,L259S,L296P)p-bound complexes. Similarly, only Nic96p from the Nic96p complex purified to a greater extent with the mutant Nmd3p allele (~4-fold increase), while none of the constituents of the Nup53p complex were enriched relative to wild-type Nmd3p. These results suggest that the accumulation of Nmd3(I139T,L259S,L296P)p at the nuclear rim is likely confined to a finite set of nucleoporins that predominately reside within a distinct subcomplex (Nup82p) within the NPC.

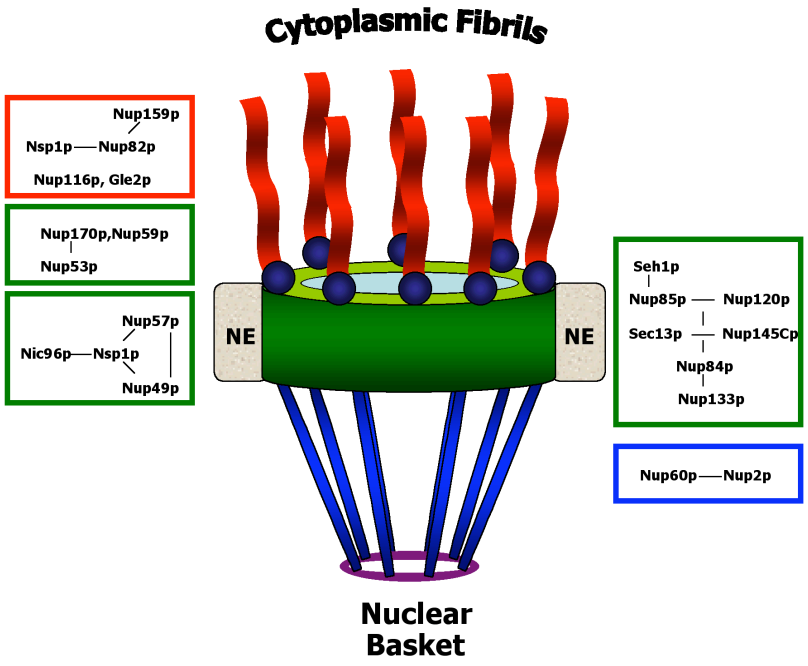

Illustration 5.3 Nucleoporin subcomplexes in yeast NPCs.

Nup-Nup subcomplexes defined by biochemical and molecular characterizations. Defined protein-protein interactions are designated by dashes. The relative distribution of subcomplexes across the nuclear envelope are indicated colorimetrically: red: cytoplasmic face only, blue: nucleoplasmic face only, green: symmetric, typically with two sets on each side of the NPC. Adapted from Suntharalingam and Wente (2003).

As depicted in Illustration 5.3, nucleoporins and nucleoporin subcomplexes occupy discrete positions within the NPC, contributing to unique protein compositions on the nuclear and cytoplasmic faces. The observation that Nmd3(I139T,L259S,L296P)p exhibits an enhanced association with nucleoporins that bind on the cytoplasmic side of the NPC (Nup82p,Nup159p), but not the nuclear face (Nup60p), suggests that cytoplasmic release from the NPC has become rate-limiting for this mutant (Table 5.1). In their recent publication, Engelsma *et al.* (2004) demonstrated that synthetic NES peptides with an aberrantly high affinity for Crm1 arrest at Nup358/RanBP2, a RanBP1 homologue that is bound to the cytoplasmic face of the NPC by Nup88 (Nup82p in yeast) and Nup214 (Nup159p in yeast) (Bernad et al., 2004). As yeast do not possess a homologue of Nup358, the sustained interaction between Nmd3(I139T,L259S,L296P)p and Nup82p/Nup159p in the immunoprecipitation assay is likely to be analogous to the behavior reported for the synthetic NESs in the vertebrate system. Intriguingly, Crm1 has also been shown to strongly interact with Nup214 (Nup159p) when bound to both cargo and RanGTP, leading to the idea that Nup214 may serve as a terminal binding site for Crm1-bound complexes following export (Askjaer et al., 1999; Fornerod et al., 1997b; Kehlenbach et al., 1999). By virtue of its apparent enrichment on the cytoplasmic face of the NPC and sustained interaction with Crm1 following export, it is possible that Nmd3(I139T,L259S,L296P)p holds Crm1 at the position of Nup82p/Nup159p in a conformation that mimics a pre-disassembly export complex intermediate. Moreover, as RanGTP is rapidly converted to RanGDP and released from export complexes in the cytoplasm by RanGAP and RanBP1, it is also likely that the Crm1/Nmd3(I139T,L259S,L296P)p interaction on the cytoplasmic face of the NPC is RanGTP-independent, thus implying a direct and stable interaction between Crm1 and Nmd3p "NE" mutants.

5.3.4 A mutant Nmd3p allele that accumulates at the nuclear envelope interacts directly and stably with Crm1 *in vitro*

In vivo, Crm1 binds to NESs cooperatively with RanGTP. As a result, the formation of stable Crm1-NES interactions in *in vitro* reconstitution assays typically requires the inclusion of RanGTP. My data suggest that Crm1 might stably interact with "NE" mutants even after dissociation of Ran from the export complex. To investigate whether Crm1 is capable of forming a stable interaction with an "NE" mutant, I performed an *in vitro* binding assay using recombinant Crm1, RanGTP, and GST-fusion proteins of wild-type or mutant Nmd3p. Both Crm1 and Ran were expressed and purified from *E. coli* as fusion proteins containing a hexameric histidine (His_6) affinity tag at their carboxy-termini. Following purification, Ran-His_6 was loaded with GTP according to standard protocols (as described in Chapter 2). While I had difficulty purifying sufficient quantities of the GST-tagged Nmd3p "NE" mutants from yeast, an N-terminal truncation allele (Nmd3Δ167p) that phenocopies the "NE" mutants (Figure 5.9) was amenable to purification. Therefore it was substituted for the original "NE" mutants in the reconstitution assays. Full-length wild-type Nmd3p and Nmd3ΔN167p were produced as GST-fusion proteins in yeast, while the classical NES from protein kinase A inhibitor (PKI) was fused to GST and purified from *E. coli*.

The GST-fusion proteins were then assayed for their dependence on RanGTP to form a stable complex with Crm1. To this end, recombinant GST-(PKI)NES, GST-Nmd3p or GST-Nmd3ΔN167p were incubated with Crm1 on ice for 30 minutes in the presence or absence of RanGTP. The GST-fusion proteins were recovered from the reactions by incubating the mixtures with glutathione-Sepharose beads for an additional one hour at 4˚C. Beads were washed three times and bound proteins were eluted in Laemmli buffer and resolved by SDS-PAGE for subsequent immunoblotting against Crm1, using antibodies against the His_6 tag.

As presented in Figure 5.9C, GST-(PKI)NES exhibited a weak interaction with Crm1 in the absence of RanGTP (lane 1). In the presence of RanGTP, however, the Crm1/GST-(PKI)NES interaction was greatly enhanced (approximately 20-fold, lane 2), consistent with the formation of a stable ternary complex. Similar to the results obtained for GST-(PKI)NES, wild-type GST-Nmd3p bound Crm1 in a RanGTP-dependent manner (compare lanes 3 and 4), reflecting their typically transient interaction *in vivo* in the absence of RanGTP. In contrast to (PKI)NES or wild-type Nmd3p, GST-Nmd3ΔN167p was capable of stably binding to Crm1 in the presence or absence of RanGTP (lanes 5 and 6). This finding supports the characterization of a "supraphysiological" interaction between Crm1 and Nmd3ΔN167p *in vivo*. The stability and RanGTP-independence of this interaction likely results in the observed enrichment of the Nmd3ΔN167p allele at the NPC, mimicking an export complex disassembly intermediate. It will be intriguing to see whether other "NE" mutants display a similar behavior with respect to Crm1 binding.

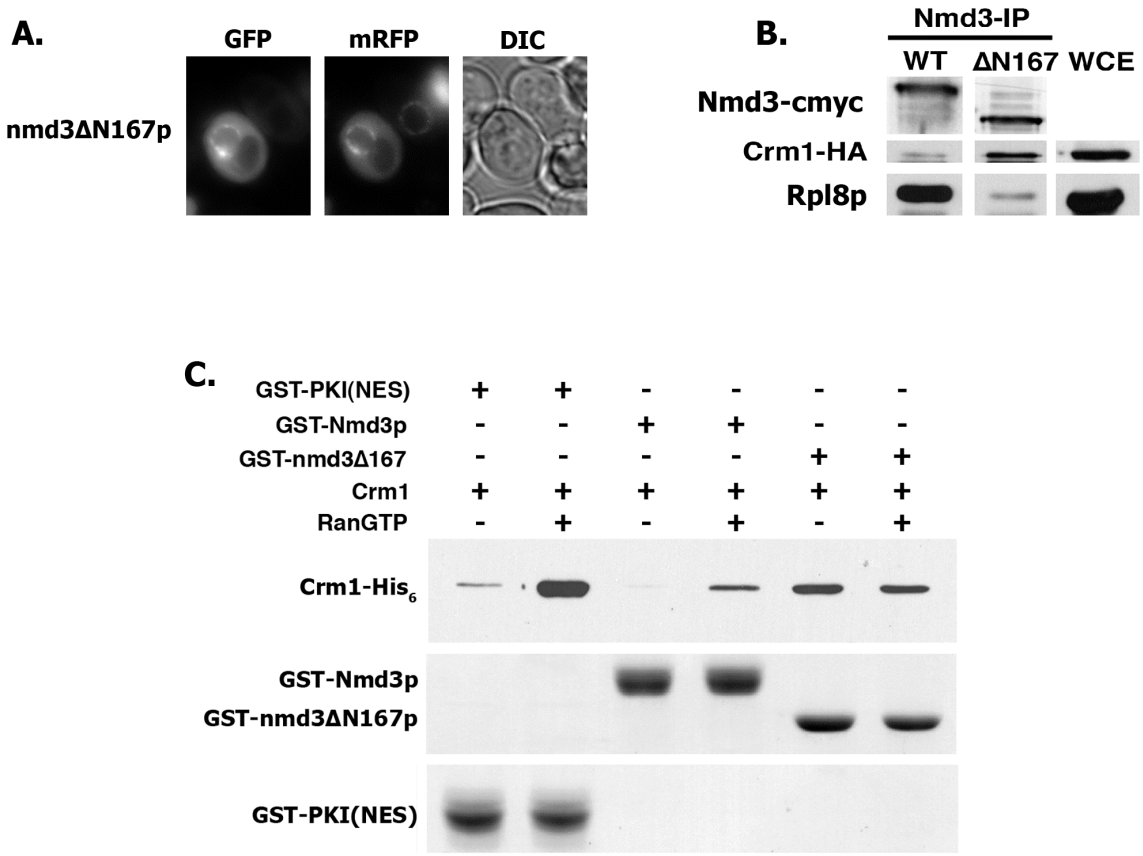

Figure 5.9 Export complex reconstitution assay

(A.) Dense overnight culture of strain AJY1848 (*NIC96-mRFP*) harboring pAJ1536 (*nmd3ΔN167-GFP*) was diluted ten-fold in fresh glucose-containing medium and culture at 30˚C to mid-log phase before visualizing cells as described in Chapter 2. (B.) Extracts were prepared from strain AJY1539 (*crm1[T539C]-HA*) harboring either pRS426 (empty vector), pAJ414 (*NMD3-cmyc*) or pAJ516 (*nmd3ΔN167-cmyc*) as described in Chapter 2. Immunoprecipitations were carried-out against the cmyc-tagged Nmd3p alleles using anti-cmyc. Immunoprecipitated proteins were resolved on a 10% SDS-PAGE gel and western analyses were conducted against cmyc-tagged Nmd3p using anti-cmyc against Crm1 using anti-HA, or against Rpl8p using anti-Rpl8p. Whole cell extract (WCE). (C.) Ran-GTP independent binding of Crm1 to GST-Nmd3ΔN167p. GST-tagged proteins (~75 pmol) were incubated with ~ 75 pmol Crm1-His_6 and with (+) or without (-) of ~125 pmol RanGTP as indicated and as described in Chapter 2. GST-tagged proteins were recovered on glutathione-Sepharose beads and bound proteins were visualized by Coomassie staining (GST fusion proteins) or by western blotting against Crm1 using anti-His_6.

5.4 Discussion

During the course of our *NMD3* loss-of-function screen, we unexpectedly identified a class of *NMD3* mutants that accumulate at the nuclear envelope (NE) and are deficient for 60S binding. Surprisingly, none of these mutants contain mutations within their conserved nucleocytoplasmic shuttling sequences. The NE enrichment exhibited by the mutant Nmd3p alleles did, however, represent a Crm1-Nmd3p export complex intermediate, as the aberrant localization pattern could be specifically disrupted by point mutations in Nmd3p's Crm1-dependent NES or by the Crm1 inhibitor, leptomycin B (LMB) (data not shown). Furthermore, Crm1 was greatly enriched in immunoprecipitations performed with the "NE" mutants, indicating a stable interaction between these two factors *in vivo*. Immunoprecipitation assays also revealed that a small subset of nucleoporins were specifically enriched in complexes bound by the "NE" mutant, Nmd3(I139T,L259S,L296P)p. These results demonstrated that the export complexes arrest on the cytoplasmic face of the NPC on constituents of the Nup82p subcomplex, suggesting that release from the NPC in the cytoplasm has become rate-limiting. A failure to release from cytoplasmic nucleoporins implies that, in the absence of a 60S subunit, Nmd3p and Crm1 might persist at the NPC even after dissociation of RanGDP, consistent with a "supraphysiological" (high-affinity) interaction between the "NE" Nmd3p mutants and Crm1. In support of this hypothesis, I was able to demonstrate that, in contrast to wild-type Nmd3p, an Nmd3p "NE" mutant (Nmd3ΔN167p) was able to stably and directly associate with Crm1 in the absence of RanGTP. Taken together, the data presented in this chapter are consistent with a model in which the potency of Nmd3p's NES corresponds with its capacity to interact with 60S subunits (see below).

5.4.1 *Nmd3p binds 60S subunits through a divalent interaction*

In yeast, Nmd3p is a 59.1 kDa protein that is 518 amino acids in length. Comparative sequence analyses predict that the amino-terminal ~30 kDa of Nmd3p (amino acids 1-280) constitutes a core domain that is conserved throughout Archaea and Eukaryotes but is conspicuously absent from Eubacteria (Illustration 5.4). This domain contains four Cys-X_2-Cys repeats that are predicted to bind Zn^2+ and likely participate in 60S binding via protein-protein interactions or electrostatic binding to ribosomal RNA (Mackay and Crossley, 1998; Teakle and Gilmartin, 1998). Indeed, point mutations in the second pair of putative Zn^2+ binding motifs (i.e. cysteine to serine substitutions) result in a dramatic reduction in 60S binding, coinciding with a loss of functional viability for the mutant proteins (Bussiere and Johnson, unpublished). Intriguingly, these latter two Cys-X_2-Cys motifs flank either side of the N-terminal *rpl10/lsg1* "suppressor domain," in which point mutations result in weakened 60S affinity (see Chapter 4 and Figure 5.2). Moreover, deletion analysis has confirmed the necessity of this region for 60S binding (Hedges, West, et al., manuscript in preparation). Therefore, it is likely that the N-terminal "suppressor domain" and the last two Zn^{2+} binding motifs cooperate to form the core 60S binding motif in both eukaryotic and archaeal Nmd3s (Illustration 5.4).

Data presented in Chapter 4 and Figure 5.2 indicate that yeast Nmd3p possesses a second C-terminal domain (amino acids 290-380) that is also important for 60S binding. Like the N-terminal 60S binding domain, point mutations in this region either weaken or abolish Nmd3p's stable association with 60S (Chapter 4 and Figure 5.2). This has led us to propose that Nmd3p exhibits a divalent interaction with the 60S subunit (Illustration 5.4). While the N-terminal binding domain (pI~11.5) may bind directly to ribosomal RNA, the predominately hydrophobic nature of the C-terminal interaction domain suggests that this region may facilitate protein-protein interactions on the 60S subunit.

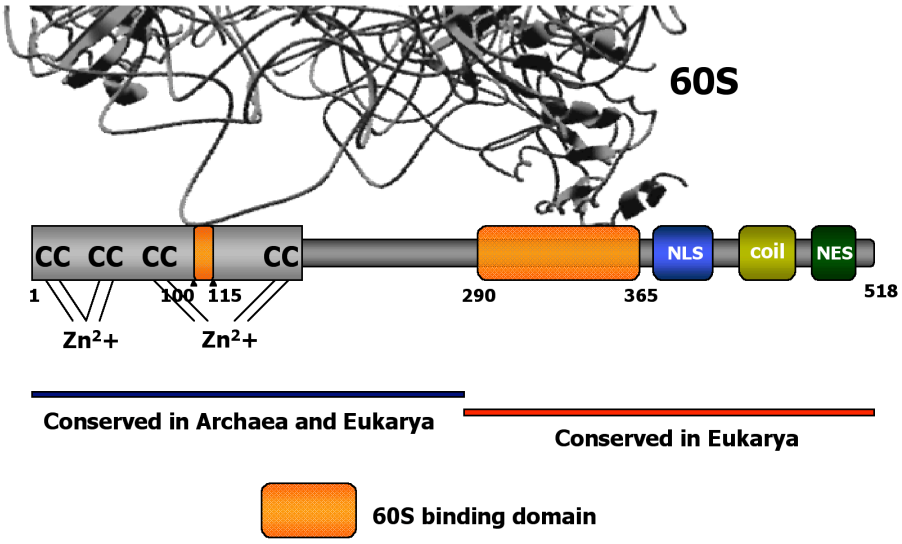

Illustration 5.4 Cartoon depicting Nmd3p's putative divalent interaction with the 60S subunit

A large amino-terminal domain that is conserved throughout Archaea and Eukarya contains four Cys-X_2-Cys motifs reminiscent of zinc fingers, the latter two of which are required for 60S binding. Orange squares represent the regions in Nmd3p that mutational analyses predict are necessary for 60S binding, leading to the interpretation that Nmd3p exhibits a divalent interaction with the 60S ribosomal subunit.

The carboxy-terminal ~150 amino acids of Nmd3p comprise a domain that is unique to eukaryotes and, not surprisingly, contains the nuclear shuttling sequences (Johnson et al., 2002). Our lab and others have shown that, in yeast Nmd3p, the nuclear localization signal (NLS) resides within a highly-basic cluster of amino acids between residues 399-419 (Illustration 5.4) (Gadal et al., 2001b; Ho et al., 2000b). While the importin Kap123p has been proposed to regulate Nmd3p's import (Sydorskyy et al.,

2003), it is unlikely to be the primary import factor in this pathway, as Δ*kap123* mutants are neither impaired for growth nor detectably mislocalize Nmd3p to the cytoplasm (West, Lo, and Johnson, unpublished). Nmd3p's classical Rev-like NES is located downstream of its NLS and functions to export 60S subunits in a Crm1-dependent manner (Gadal et al., 2001b; Ho et al., 2000b). Work presented here has shown that mutations in Nmd3p that disrupt 60S binding, yet do not alter the NES, result in an unusually strong interaction between Nmd3p and Crm1. This suggests that Nmd3p's association with 60S subunits helps to modulate its affinity for the export machinery (specifically Crm1). All three of the "NE" mutants identified in the loss-of-function screen possess mutations in the C-terminal 60S binding domain of Nmd3p (Illustration 5.4 and Figure 5.2A). As this region is absent from crenarchaeotic orthologues of Nmd3p, it is possible that eukaryotic Nmd3s have evolved a second 60S binding motif in order to regulate the proper presentation of their shuttling sequences in the context of the subunit.

5.4.2 *Regulation of Nmd3p's potent NES?*

While Crm1 (Xpo1p) recognizes a wide range of nuclear cargoes with variable NES compositions, it typically binds its substrates with a relatively low affinity (Askjaer et al., 1999; Paraskeva et al., 1999). In light of Crm1's central role in the export of most nuclear proteins and protein complexes, including the two ribosomal subunits, this discrepancy has been suggested to reflect the need for Crm1 to rapidly dissociate from its cargo in the cytoplasm following GTP hydrolysis on Ran to keep up with the export demands of the cell (Kutay and Guttinger, 2005). This proposal gained credibility in a recent report by Engelsma *et al.* (2004). These authors showed that, while Crm1 exhibits high-affinity for synthetically-derived NESs *in vitro*, the *in vivo* consequence of such an interaction is the entrapment of Crm1 and its cargo on the cytoplasmic face of the NPC

even after RanGDP was released from the export complex (Engelsma et al., 2004). These findings suggest that potent NESs have likely been bypassed evolutionarily in order to promote efficient export complex disassembly.

Although Crm1 exhibits a low affinity for the vast majority of its cargoes, two notable exceptions have been identified. One such high-affinity substrate is the snRNP import factor, snurportin 1. Snurportin 1 possesses a large, non-classical Crm1-binding surface that spans a region that is at least 159 amino acids in length (Paraskeva, 1999). In contrast to the "supraphysiological" interactions reported by Engelsma *et al*., however, it is believed that the atypically-large Crm1 binding site on snurportin contributes to the efficient disassembly of the export complex in the cytoplasm, perhaps through a large conformational change or by helping to recruit an additional factor(s) that aids in complex dissociation.

Surprisingly, the other reported case of a high-affinity Crm1/substrate interaction was that observed for human Nmd3 (Engelsma et al., 2004; Thomas and Kutay, 2003). This is remarkable in light of the fact that, like yeast Nmd3p, human Nmd3 possess a classical Rev/PKI-like NES ((Johnson et al., 2002) and Illustration 5.2). Tagging human Nmd3 at its amino-terminus with tandem copies of the z domain (IgG binding domain) from Protein A, converted it into a high-affinity Crm1 cargo with an interaction strength comparable to that reported for snurportin or the "supraphysiological" NES peptides (Engelsma et al., 2004; Paraskeva et al., 1999; Thomas and Kutay, 2003). The observation that a His_6-tagged hNmd3 (His_6-Nmd3) did not behave as a high-affinity Crm1 substrate, however, suggested to Thomas and Kutay (2003) that the zz tag might alter the structure of the recombinant protein in such a way as to enhance its Crm1 affinity. This hypothesis is consistent with the observation that the zz-tagged version of hNmd3 bound 60S subunits with lower affinity *in vitro* than did the His_6-tagged allele

(Thomas and Kutay, 2003). Furthermore, these findings imply that the canonical NES in human Nmd3 is not typically held in a conformation that supports a high-affinity Crm1 interaction. This may indicate that, like snurportin, Nmd3 possesses a larger Crm1 interaction surface that can be differentially exposed depending on Nmd3's conformational state.

Results presented in this chapter demonstrate that, like its human counterpart, yeast Nmd3p can be converted into a high-affinity Crm1 substrate in a manner that correlates with impaired 60S affinity. This correlation would suggest that the strong Crm1 interaction and NPC accumulation represent a default state for Nmd3p in the absence of its cargo (i.e. 60S). However, this hypothesis is not consistent with the observation that gross over-expression of wild-type Nmd3p fails to phenocopy the localization pattern of the Nmd3p "NE" mutants or Nmd3Δ167p (data not shown). Furthermore, in the absence of 60S, wild-type Nmd3p does not exhibit an aberrantly strong affinity for Crm1 *in vitro* like that observed for the Nmd3ΔN167p mutant (Figure 5.9B). As a result, it is unlikely that the unusual phenotypes exhibited by this class of *NMD3* mutants reflects the behavior of free Nmd3p in the cell. Like the interpretation proffered for the behavior of zz-hNmd3 (Thomas and Kutay, 2003), the enhanced Crm1 affinity exhibited by the "NE" mutants may reflect an improperly-regulated conformational state for Nmd3p that typically exists only transiently during 60S export.

The maturational state that signals "export competence" for nuclear 60S subunits may correspond with a conformational change in Nmd3p that presents an expanded Crm1 interaction surface to efficiently recruit the export complex to the subunit. The idea of an expanded Crm1 binding surface is supported by the observation that Nmd3(I139T,L259S,L296P)p and Nmd3ΔN167p that have been deleted for their classical NESs (i.e. truncation of the C-terminal 100 amino acids) still immunoprecipitate

greater amounts of Crm1 than wild-type Nmd3p with an intact NES (Appendix F and data not shown). Moreover, deletion analysis has revealed that Crm1 interaction is not abolished until the deletions include its C-terminal 60S interaction motif (Appendix F). This unexpected observation may indicate that the C-terminal 60S-binding domain possesses an overlapping Crm1 interaction surface that is typically inaccessible in the context of the wild-type protein. The modulated presentation of this interaction surface may ensure that Nmd3p only binds to Crm1 tightly when the C-terminal 60S binding motif adopts an appropriate conformation late in the 60S maturation pathway. However, as the nuclear envelope accumulation observed for the mutant Nmd3p alleles is dependent upon the canonical NES (Figure 5.4), this second putative interaction surface must only play a complementary role in this process.

It is possible that the strong Crm1-Nmd3p interaction observed for the "NE" mutants *in vivo* may also reflect a failure to recruit an additional factor(s) to properly regulate export complex assembly or disassembly. In higher eukaryotes, the Ran binding protein RanBP3 stabilizes export complexes to allow efficient export of Crm1-bound complexes (Englmeier et al., 2001. In yeast, the RanBP3 homologue, Yrb2p, has been shown to be necessary for the efficient export of the small ribosomal subunit {Moy, 2002 #335; Lindsay et al., 2001). The mRNP export factor, Mtr2p, has also been implicated in the late stages of ribosome export and exhibits genetic interaction with *NMD3* (Bassler et al., 2001; Ho et al., 2000b; Nissan et al., 2002). Although I monitored Nmd3(I139T,L259S,L296P)-GFP localization in the context of either high-copy Yrb2p or Mtr2p to assess whether NPC accumulation reflected a failure to recruit these factors to the mutant export complexes, neither Yrb2p nor Mtr2p over-expression altered Nmd3(I139T,L259S,L296P)-GFP's localization at the nuclear rim (data not shown).

These results do not rule out their involvement in this pathway, however, as they may require the 60S subunit to bridge the appropriate interaction.

Another factor that may participate in modulating the potency of Nmd3p's NES is the shuttling 60S biogenesis factor, Arx1p. Arx1p is recruited to nascent subunits late in the nuclear maturation pathway and is exported on Nmd3p-bound subunits into the cytoplasm (Hung and Johnson, 2005; Kallstrom et al., 2003; Nissan et al., 2002). *arx1*Δ mutants exhibit an impaired rate of Nmd3p and 60S export (Hung and Johnson, 2005). Furthermore, *arx1*Δ mutants are synthetic lethal with an *nmd3* mutant possessing a minor truncation of its NES (*nmd3*Δ*C14*), indicating that Arx1p may play an important role in optimizing 60S export (Hung and Johnson, unpublished). We are currently investigating whether Arx1p participates directly in this process.

5.4.3 *Nmd3p "NE" mutants arrest on the cytoplasmic face of the NPC and resemble export complex disassembly intermediates*

The finding that Nmd3(I139T,L259S,L296P)p co-purifies with a subset of nucleoporins previously implicated in 60S biogenesis bolsters its relevance for providing insight into how 60S subunits transit the NPC. While deletion analyses and conditional mutants have previously been utilized to delineate which Nups are important for 60S export (Gleizes et al., 2001; Hurt et al., 1999; Stage-Zimmermann et al., 2000), the results presented here provide physical evidence for their involvement in Nmd3p-mediated export. Furthermore, the demonstration that members of the Nup82p complex (Nup159p and Nup82p) were particularly enriched in Nmd3(I139T,L259S,L296P)p-bound complexes is consistent the entrapment of mutant export complexes on the cytoplasmic face of the NPC. These findings are in close agreement with the in situ hybridization analysis of ribosome export conducted by Gleizes et al. (2001), during which they showed that the Nup82p complex played a critical role in 60S export. As

Nup214 (Nup159p) serves as the site for Crm1-dependent export complex disassembly in higher eukaryotes (Kehlenbach et al., 1999), it is likely that the stable Crm1/mutant Nmd3p complexes fail to efficiently dissociate from the NPC following RanGDP release. We are currently collaborating with Dr. J. Michael McCaffery at Johns Hopkins University in Baltimore, Maryland to provide *in vivo* confirmation of this assessment via immuno-electron microscopy at the NPC.

5.4.4 *Model for Nmd3p/Crm1 export complex disassembly on the cytoplasmic face of the NPC*

The results presented in this chapter are consistent with the model depicted in Illustration 5.5. Under normal cellular conditions, Nmd3p binds nascent 60S subunits in the nucleus and, upon some late maturational cue, assembles into an export complex with Crm1 (Xpo1p) and RanGTP (Gsp1p)(Illustration 5.5A). This quaternary complex (60S/Nmd3p/Crm1/RanGTP) is translocated through the NPC and disassembles in the cytoplasm on components of the Nup82p complex following stimulation of RanGTP's intrinsic GTPase activity by RanGAP (Rna1p) and RanBP1 (Yrb1p). Crm1 and RanGDP recycle back to the nucleus independently, while Nmd3p remains bound to 60S until it is later recycled back to the nucleus by Lsg1p prior to translation initiation (see Chapters 3 and 4). Accessory factors may participate in both the assembly and disassembly of the export complex, modulating the potency of Nmd3p's NES.

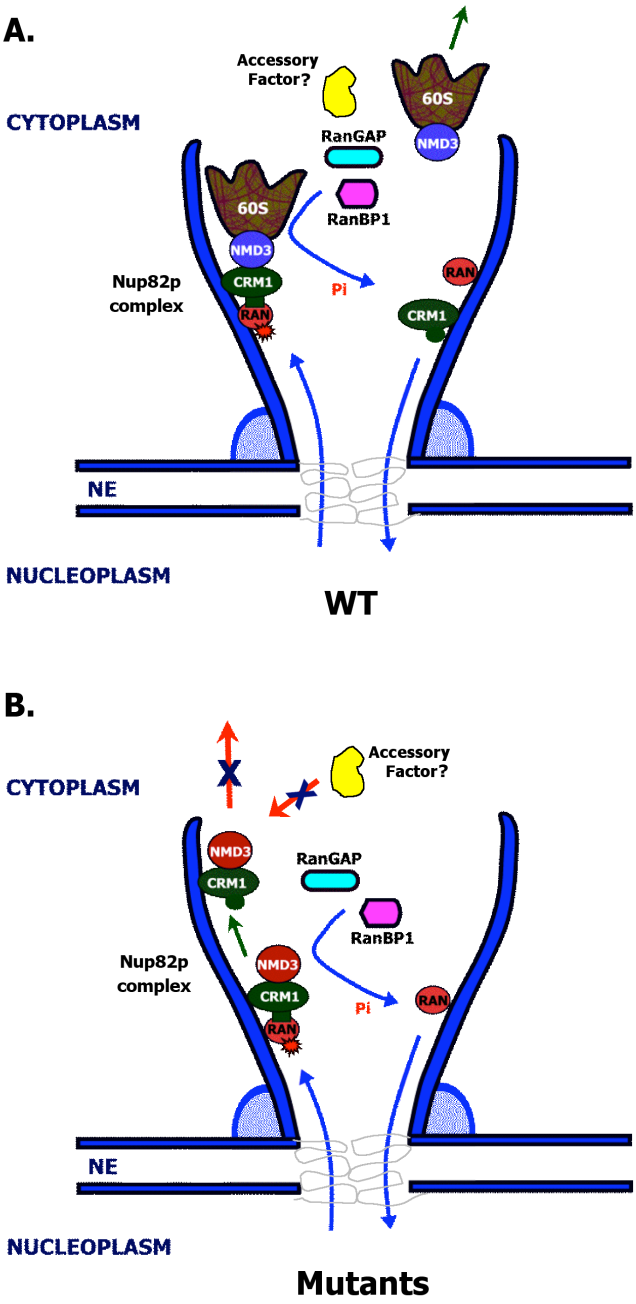

Illustration 5.5 Model explaining the proposed behavior of the Nmd3p "NE" mutants at the NPC

(A.) The interactions between Nmd3p, 60S, Crm1, RanGTP and effector molecules during 60S export are depicted under normal cellular conditions. (B.) The consequence of a stable Crm1-mutant Nmd3p interaction following translocation of the export complex. Both models are described in section 5.4.4.

The mutant Nmd3p alleles that arrest at the nuclear envelope are presumably held in a conformation that precludes 60S binding and promotes their assembly into a high-affinity ternary complex with Crm1 and RanGTP (Illustration 5.5B). Following translocation through the NPC, RanGTP is likely converted into RanGDP by its cytoplasmic effector molecules, allowing for its dissociation from the mutant export complex. The high-affinity interaction between Crm1 and the mutant Nmd3p alleles, however, holds Crm1 in a conformation that resembles a terminal export complex intermediate, precluding the efficient release of the two proteins from the cytoplasmic face of the NPC (i.e. from Nup82p complex). In the absence of 60S, additional factors that typically assist in the disassembly event may fail to be recruited to the mutant export complex, thus contributing to the inefficiency of NPC release.

5.4.5 *Conclusions and future aims*

In this chapter, I have presented an initial characterization of a unique class of *NMD3* mutants that exhibit a high-affinity for the export receptor Crm1(Xpo1p) both *in vivo* and *in vitro*. The propensity of these mutants to accumulate at the nuclear envelope in a Crm1-dependent manner provides *in vivo* support for the formation of a *bona fide* export intermediate in the Nmd3p shuttling pathway. Consistent with this proposal, these mutant Nmd3p alleles exhibit an enhanced interaction with a subset of nucleoporins that have previously been implicated in the nuclear export of Nmd3p's primary cargo, the 60S ribosomal subunit. Therefore, it is my contention that results presented here enhance our understanding of the manner in which Nmd3p may mediate the export of the large ribosomal subunit and reflect the potential cellular consequences of imprecise regulation of this critical cellular event.

As the mutations that enhance the stability of the Crm1/Nmd3p interaction also disrupt 60S binding, we can only obtain a partial understanding of how Nmd3p may

mediate the export of the large subunit through the NPC. To test the fidelity of these observations and to achieve a deeper understanding of this critical cellular event, it will be important to capture a similar Nmd3p-bound export complex at the NPC that retains its interaction with 60S. Mutating wild-type Nmd3p's NES to conform to the sequence observed for the supraphysiological peptides isolated by Engelsma *et al.* (2004) (LxxLFxxLSV) may provide us with the appropriate reagent to achieve this goal. Such a reagent may also prove useful in assessing pleiotropic effects on export by obstructing the nuclear channel with such a large cargo. Similarly, the entrapment of a 60S-bound export complex may be useful for assessing the structural accommodations within the NPC that are required for the 60S translocation event. Although Nmd3p's role as the 60S export adapter is conserved in both yeast and metazoans, the *in vitro* reconstitution of export complexes on 60S subunits has not yet been achieved ((Thomas and Kutay, 2003) and Kallstrom and Johnson, unpublished). This likely reflects the need for an additional accessory factor(s) or different 60S conformational state in these assays to modulate the presentation of Nmd3p's NES. Therefore, it will also be important to design a protocol for the large-scale purification of "export competent" nuclear pre-60S subunits to assess the protein composition of these complexes and to determine whether a particular Nmd3p-bound 60S maturation intermediate does, indeed, exhibit a particularly high affinity for Crm1.

Appendices

Appendix A Growth phenotypes for *LSG1* dominant negative mutants

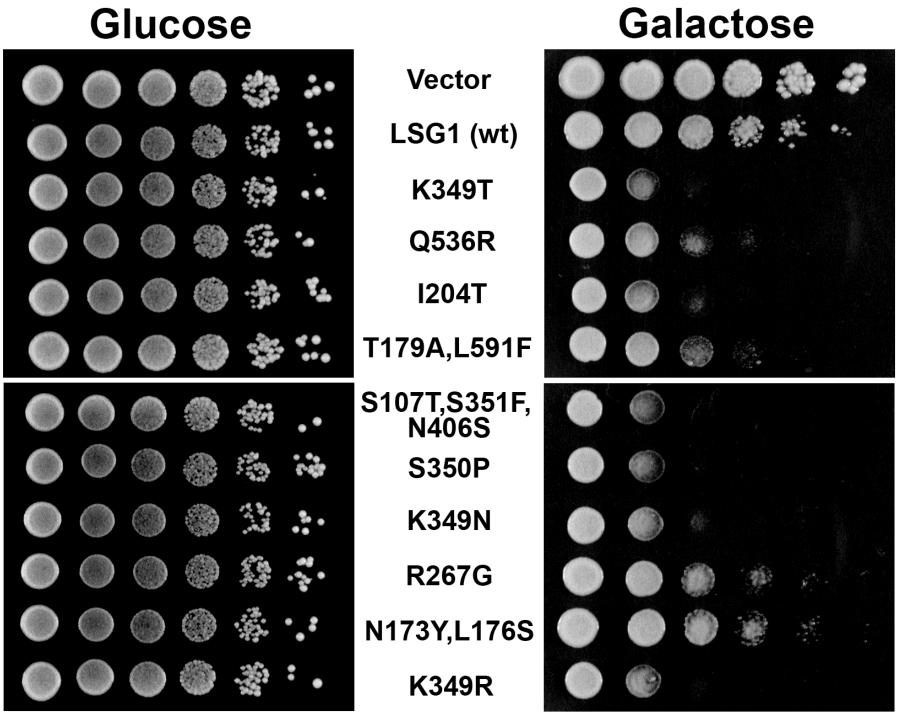

CH1305 (wild-type) transformants containing empty vector (pRS425), pAJ879 (*GAL10::LSG1*), or *LSG1* dominant negative mutants, *LSG1(K349T)* (pAJ1109), *LSG1(Q536R)* (pAJ1610), *LSG1(I204T)* (pAJ1132), *LSG1(T179A,L591F)* (pAJ1117), *LSG1(S107T,S351F,N406S)* (pAJ1119), *LSG1(S350P)* (pAJ1310), *LSG1(K349N)* (pAJ1613), *LSG1(R267G)* (pAJ1614), *LSG1(N173Y, L176S)* (pAJ1131), and *LSG1(K349R)* (pAJ1615), under control of the *GAL10* promoter were streaked onto drop-out plates containing either glucose (non-inducible) or galactose (inducible) as the sole carbon source. Plates were incubated at 30°C for 4 days.

Appendix B *LSG1* LOSS-OF-FUNCTION MUTANTS

Allele	Mutation(s)	Mutation(s) in G-motif	Relative 60S binding
wild-type	-	-	5+
L1-LOF 1-8	C388R	Y	1+
L1-LOF 1-9	S350P	Y	5+
L1-LOF 5-7	F519S	N	1+
L1-LOF 5-13	E182D,D447E	N	5+
L1-LOF 7-12	L83Q,S264P, C388R	Y	1+
L1-LOF 8-18	S114P,I439F	N	1+
L1-LOF 9-1	S351P,N354D, Y491H	Y	2+
L1-LOF 9-4	N177S,W188R, I439F	N	ND
L1-LOF 12-7	S350I	Y	5+
L1-LOF 13-3	G348C	Y	5+
L1-LOF 13-11	R52M,N105D, N184D	N	5+
L1-LOF 13-19	S365L	Y	3+
L1-LOF 15-3	E182D,D447E	N	ND
L1-LOF 19-5	S365L	Y	3+
L1-LOF 20-5	R183K,N184I, T242A	Y	3+

Appendix C Polysome profiles from cells expressing dominant negative Lsg1p mutants

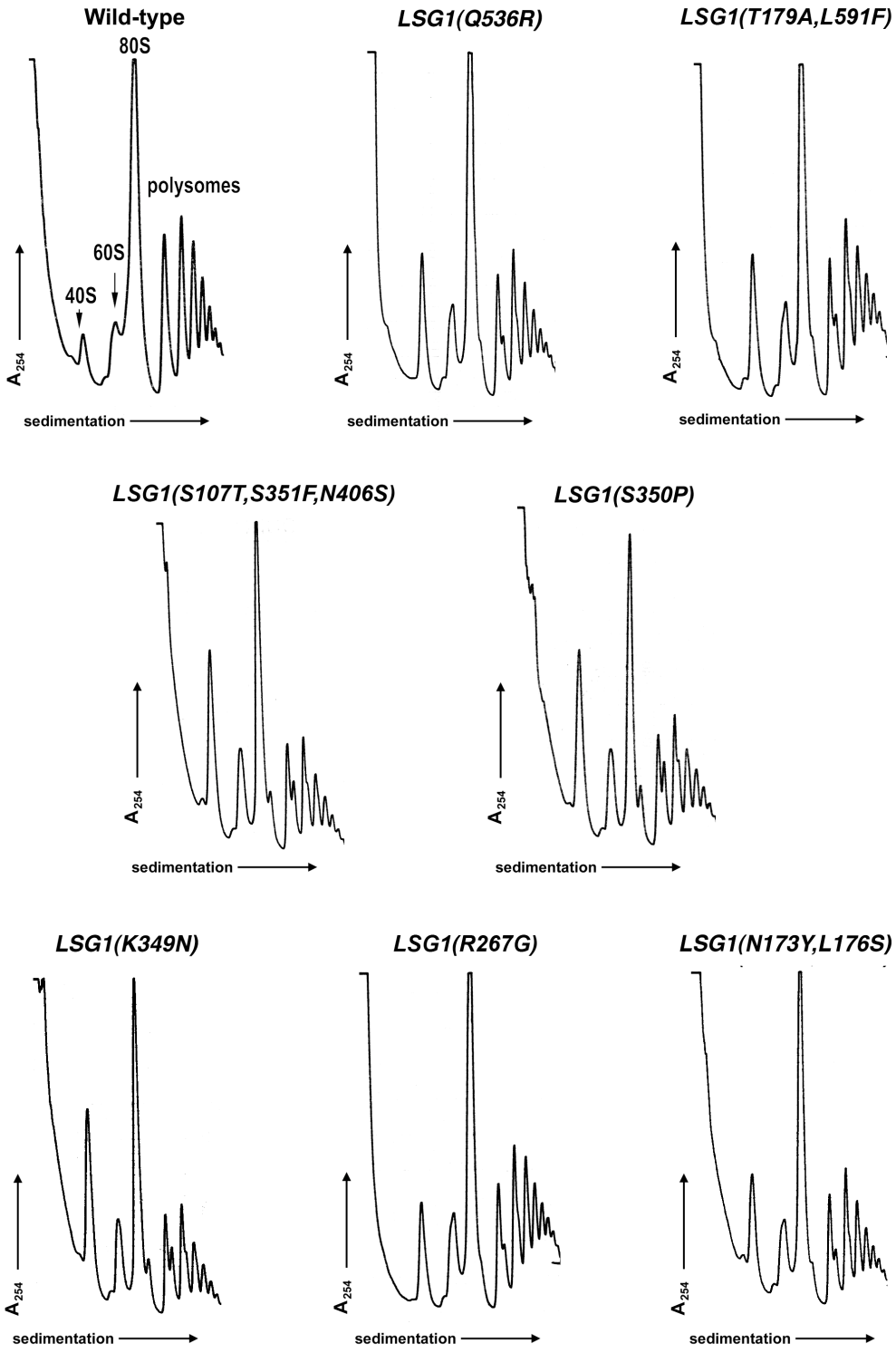

Appendix D Rpl25-eGFP localization upon expression of dominant negative Lsg1p mutants

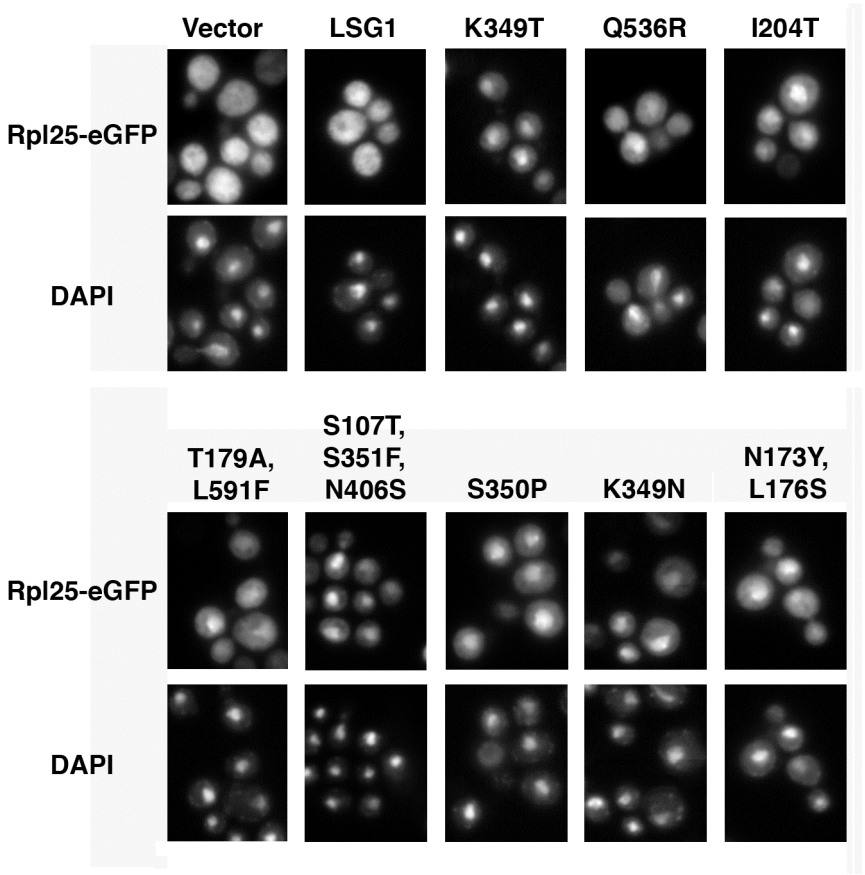

Rpl25-eGFP (pAJ908) was continuously expressed in strain CH1305 (wild-type) carrying either empty vector (pRS425), pAJ879 (*GAL10*::*LSG1*), or *LSG1* dominant negative mutants, *LSG1(K349T)* (pAJ1109), *LSG1(Q536R)* (pAJ1610), *LSG1(I204T)* (pAJ1132), *LSG1(T179A,L591F)* (pAJ1117), *LSG1(S107T,S351F,N406S)* (pAJ1119), *LSG1(S350P)* (pAJ1310), *LSG1(K349N)* (pAJ1613), *LSG1(R267G)* (pAJ1614), *LSG1(N173Y, L176S)* (pAJ1131), and *LSG1(K349R)* (pAJ1615). Overnight cultures were diluted to an OD_{600}~0.1 in fresh medium containing raffinose as a non-inducing carbon source. At OD_{600}~0.2, one half of each culture was induced by the addition of galactose (1% final concentration) for 3 h. Cells were fixed and DAPI stained as described in Chapter 2.

Appendix E Localization of chromosomally-expressed Nmd3-GFP upon expression of dominant negative Lsg1p mutants

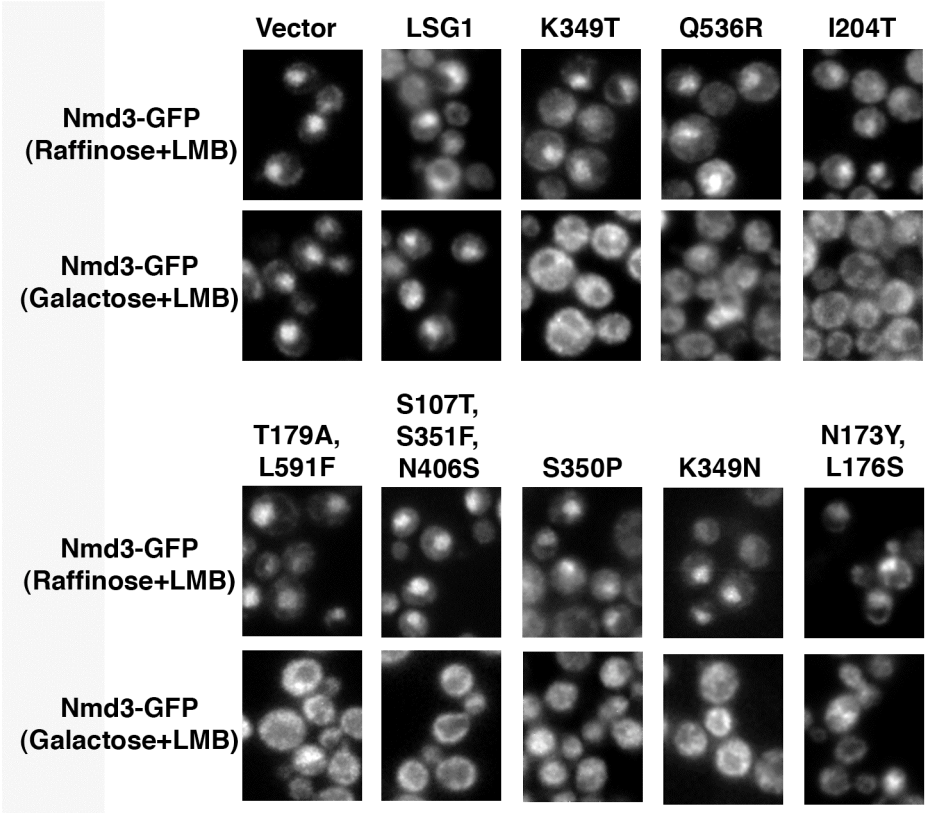

Nmd3-GFP was visualized in strain AJY1705 (*NMD3-GFP::KanMX6 crm1[T539C]*) carrying empty vector (pRS425), pAJ879 (*GAL10*::*LSG1*), or *LSG1* dominant negative mutants, *LSG1(K349T)* (pAJ1109), *LSG1(Q536R)* (pAJ1610), *LSG1(I204T)* (pAJ1132), *LSG1(T179A,L591F)* (pAJ1117), *LSG1(S107T,S351F,N406S)* (pAJ1119), *LSG1(S350P)* (pAJ1310), *LSG1(K349N)* (pAJ1613), *LSG1(R267G)* (pAJ1614), *LSG1(N173Y, L176S)* (pAJ1131), and *LSG1(K349R)* (pAJ1615), after culturing to mid-log phase followed by galactosed-induction of *LSG1* expression for 3 hours. Cells were treated with LMB, fixed, and stained with DAPI as described in Chapter 2.

Appendix F Deletion analysis of Nmd3p to identify additional Crm1 binding site(s)

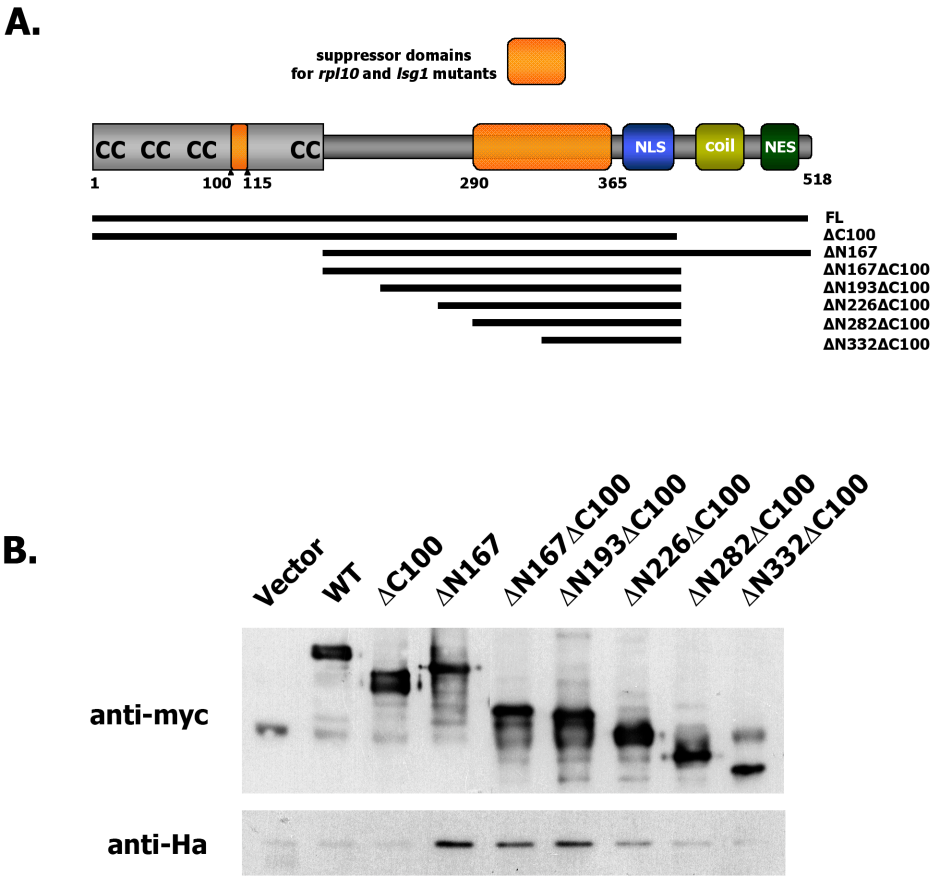

(A.) Cartoon representation of the Nmd3p truncation mutants used in (B.).
(B.) Extracts were prepared from strain AJY1539 (*crm1[T539C]-HA*) harboring either pRS416 (empty vector), pAJ414 (*NMD3-cmyc*), pAJ535 (*nmd3ΔC100-cmyc*), pAJ516 (*nmd3ΔN167-cmyc*), pAJ1548 (*nmd3ΔN167ΔC100-cmyc*), pAJ1549 (*nmd3ΔN193ΔC100-cmyc*), pAJ1550 (*nmd3ΔN226ΔC100-cmyc*), pAJ1601 (*nmd3ΔN282ΔC100-cmyc*), pAJ1602 (*nmd3ΔN332ΔC100-cmyc*) as described in Chapter 2. Immunoprecipitations were carried-out against the cmyc-tagged Nmd3p alleles using anti-cmyc. Immunoprecipitated proteins were resolved on a 10% SDS-PAGE gel and western analyses were conducted against cmyc-tagged Nmd3p using anti-cmyc or against Crm1 using anti-HA.

References

Allen, G.S., Zavialov, A., Gursky, R., Ehrenberg, M. and Frank, J. (2005) The cryo-EM structure of a translation initiation complex from Escherichia coli. *Cell*, **121**, 703-712.

Aravind, L. and Koonin, E.V. (2000) Eukaryote-specific domains in translation initiation factors: implications for translation regulation and evolution of the translation system. *Genome Res*, **10**, 1172-1184.

Askjaer, P., Bachi, A., Wilm, M., Bischoff, F.R., Weeks, D.L., Ogniewski, V., Ohno, M., Niehrs, C., Kjems, J., Mattaj, I.W. and Fornerod, M. (1999) RanGTP-regulated interactions of CRM1 with nucleoporins and a shuttling DEAD-box helicase. *Mol Cell Biol*, **19**, 6276-6285.

Bachellerie, J.P., Cavaille, J. and Huttenhofer, A. (2002) The expanding snoRNA world. *Biochimie*, **84**, 775-790.

Ban, N., Nissen, P., Hansen, J., Moore, P.B. and Steitz, T.A. (2000) The complete atomic structure of the large ribosomal subunit at 2.4 A resolution. *Science*, **289**, 905-920.

Bashan, A., Agmon, I., Zarivach, R., Schluenzen, F., Harms, J., Berisio, R., Bartels, H., Franceschi, F., Auerbach, T., Hansen, H.A., Kossoy, E., Kessler, M. and Yonath, A. (2003) Structural basis of the ribosomal machinery for peptide bond formation, translocation, and nascent chain progression. *Mol Cell*, **11**, 91-102.

Bassler, J., Grandi, P., Gadal, O., Lessmann, T., Petfalski, E., Tollervey, D., Lechner, J. and Hurt, E. (2001) Identification of a 60S preribosomal particle that is closely linked to nuclear export. *Mol Cell*, **8**, 517-529.

Basu, U., Si, K., Warner, J.R. and Maitra, U. (2001) The Saccharomyces cerevisiae TIF6 gene encoding translation initiation factor 6 is required for 60S ribosomal subunit biogenesis. *Mol Cell Biol*, **21**, 1453-1462.

Bataille, N., Helser, T. and Fried, H.M. (1990) Cytoplasmic transport of ribosomal subunits microinjected into the Xenopus laevis oocyte nucleus: a generalized, facilitated process. *J Cell Biol*, **111**, 1571-1582.

Baxter, R.M., Ganoza, M.C., Zahid, N. and Chung, D.G. (1987) Reconstruction of peptidyltransferase activity on 50S and 70S ribosomal particles by peptide fragments of protein L16. *Eur J Biochem*, **163**, 473-479.

Becam, A.M., Nasr, F., Racki, W.J., Zagulski, M. and Herbert, C.J. (2001) Ria1p (Ynl163c), a protein similar to elongation factors 2, is involved in the biogenesis of the 60S subunit of the ribosome in Saccharomyces cerevisiae. *Mol Genet Genomics*, **266**, 454-462.

Benne, R. and Hershey, J.W. (1978) The mechanism of action of protein synthesis initiation factors from rabbit reticulocytes. *J Biol Chem*, **253**, 3078-3087.

Bernad, R., van der Velde, H., Fornerod, M. and Pickersgill, H. (2004) Nup358/RanBP2 attaches to the nuclear pore complex via association with Nup88 and Nup214/CAN and plays a supporting role in CRM1-mediated nuclear protein export. *Mol Cell Biol*, **24**, 2373-2384.

Bertrand, E.a.F., M.J. (2004) The snoRNPs and Related Machines: Ancient Devices That Mediate Maturation of rRNA and Other RNAs. In Olson, M. (ed.), *The Nucleolus*. Kluwer Academic/Plenum Publishers, New York, New York.

Bischoff, F.R. and Gorlich, D. (1997) RanBP1 is crucial for the release of RanGTP from importin beta-related nuclear transport factors. *FEBS Lett*, **419**, 249-254.

Bourne, H.R. (1995) GTPases: a family of molecular switches and clocks. *Philos Trans R Soc Lond B Biol Sci*, **349**, 283-289.

Bourne, H.R., Sanders, D.A. and McCormick, F. (1991) The GTPase superfamily: conserved structure and molecular mechanism. *Nature*, **349**, 117-127.

Brune, C., Munchel, S.E., Fischer, N., Podtelejnikov, A.V. and Weis, K. (2005) Yeast poly(A)-binding protein Pab1 shuttles between the nucleus and the cytoplasm and functions in mRNA export. *Rna*, **11**, 517-531.

Burkhard, P., Stetefeld, J. and Strelkov, S.V. (2001) Coiled coils: a highly versatile protein folding motif. *Trends Cell Biol*, **11**, 82-88.

Caponigro, G. and Parker, R. (1995) Multiple functions for the poly(A)-binding protein in mRNA decapping and deadenylation in yeast. *Genes Dev*, **9**, 2421-2432.

Clissold, P.M. and Ponting, C.P. (2000) PIN domains in nonsense-mediated mRNA decay and RNAi. *Curr Biol*, **10**, R888-890.

Dahlberg, A.E. and Grabowski, P.J. (1990) Gel electrophoresis of ribonucleoproteins. In Rickwood, D. and Hames, B.D. (eds.), *Gel Electrophoresis of Nucleic Acids: A Practical Approach*. Oxford University Press, Oxford, pp. 275-289.

Daigle, D.M., Rossi, L., Berghuis, A.M., Aravind, L., Koonin, E.V. and Brown, E.D. (2002) YjeQ, an essential, conserved, uncharacterized protein from Escherichia coli, is an unusual GTPase with circularly permuted G-motifs and marked burst kinetics. *Biochemistry*, **41**, 11109-11117.

Damke, H., Binns, D.D., Ueda, H., Schmid, S.L. and Baba, T. (2001) Dynamin GTPase domain mutants block endocytic vesicle formation at morphologically distinct stages. *Mol Biol Cell*, **12**, 2578-2589.

de la Cruz, J., Kressler, D., and Linder, P. (ed.). (2004) *Ribosomal Subunit Assembly*. Kluwer Academic/Plenum Publishers, New York, New York.

Dick, F.A., Eisinger, D.P. and Trumpower, B.L. (1997) Exchangeability of Qsr1p, a large ribosomal subunit protein required for subunit joining, suggests a novel translational regulatory mechanism. *FEBS Lett*, **419**, 1-3.

Dohme, F. and Nierhaus, K.H. (1976) Total reconstitution and assembly of 50 S subunits from Escherichia coli Ribosomes in vitro. *J Mol Biol*, **107**, 585-599.

Doudna, J.A. and Rath, V.L. (2002) Structure and function of the eukaryotic ribosome: the next frontier. *Cell*, **109**, 153-156.

Dragon, F., Gallagher, J.E., Compagnone-Post, P.A., Mitchell, B.M., Porwancher, K.A., Wehner, K.A., Wormsley, S., Settlage, R.E., Shabanowitz, J., Osheim, Y., Beyer, A.L., Hunt, D.F. and Baserga, S.J. (2002) A large nucleolar U3 ribonucleoprotein required for 18S ribosomal RNA biogenesis. *Nature*, **417**, 967-970.

Dunbar, D.A., Dragon, F., Lee, S.J. and Baserga, S.J. (2000) A nucleolar protein related to ribosomal protein L7 is required for an early step in large ribosomal subunit biogenesis. *Proc Natl Acad Sci U S A*, **97**, 13027-13032.

Dundr, M. and Misteli, T. (2001) Functional architecture in the cell nucleus. *Biochem J*, **356**, 297-310.

Eisinger, D.P., Dick, F.A., Denke, E. and Trumpower, B.L. (1997a) SQT1, which encodes an essential WD domain protein of Saccharomyces cerevisiae, suppresses dominant-negative mutations of the ribosomal protein gene QSR1. *Mol Cell Biol*, **17**, 5146-5155.

Eisinger, D.P., Dick, F.A. and Trumpower, B.L. (1997b) Qsr1p, a 60S ribosomal subunit protein, is required for joining of 40S and 60S subunits. *Mol Cell Biol*, **17**, 5136-5145.

Engelsma, D., Bernad, R., Calafat, J. and Fornerod, M. (2004) Supraphysiological nuclear export signals bind CRM1 independently of RanGTP and arrest at Nup358. *Embo J*, **23**, 3643-3652.

Englmeier, L., Fornerod, M., Bischoff, F.R., Petosa, C., Mattaj, I.W. and Kutay, U. (2001) RanBP3 influences interactions between CRM1 and its nuclear protein export substrates. *EMBO Rep*, **2**, 926-932.

Englmeier, L., Olivo, J.C. and Mattaj, I.W. (1999) Receptor-mediated substrate translocation through the nuclear pore complex without nucleotide triphosphate hydrolysis. *Curr Biol*, **9**, 30-41.

Fatica, A., Cronshaw, A.D., Dlakic, M. and Tollervey, D. (2002) Ssf1p prevents premature processing of an early pre-60S ribosomal particle. *Mol Cell*, **9**, 341-351.

Fatica, A., Oeffinger, M., Dlakic, M. and Tollervey, D. (2003) Nob1p is required for cleavage of the 3' end of 18S rRNA. *Mol Cell Biol*, **23**, 1798-1807.

Feng, W., Benko, A.L., Lee, J.H., Stanford, D.R. and Hopper, A.K. (1999) Antagonistic effects of NES and NLS motifs determine S. cerevisiae Rna1p subcellular distribution. *J Cell Sci*, **112 (Pt 3)**, 339-347.

Floer, M., Blobel, G. and Rexach, M. (1997) Disassembly of RanGTP-karyopherin beta complex, an intermediate in nuclear protein import. *J Biol Chem*, **272**, 19538-19546.

Fornerod, M. and Ohno, M. (2002) Exportin-mediated nuclear export of proteins and ribonucleoproteins. *Results Probl Cell Differ*, **35**, 67-91.

Fornerod, M., Ohno, M., Yoshida, M. and Mattaj, I.W. (1997a) CRM1 is an export receptor for leucine-rich nuclear export signals. *Cell*, **90**, 1051-1060.

Fornerod, M., van Deursen, J., van Baal, S., Reynolds, A., Davis, D., Murti, K.G., Fransen, J. and Grosveld, G. (1997b) The human homologue of yeast CRM1 is in a dynamic subcomplex with CAN/Nup214 and a novel nuclear pore component Nup88. *Embo J*, **16**, 807-816.

Fried, H. and Kutay, U. (2003) Nucleocytoplasmic transport: taking an inventory. *Cell Mol Life Sci*, **60**, 1659-1688.

Fromont-Racine, M., Senger, B., Saveanu, C. and Fasiolo, F. (2003a) Ribosome assembly in eukaryotes. *Gene*, **313**, 17-42.
Fromont-Racine, M., Senger, B., Saveanu, C. and Fasiolo, F. (2003b) Ribosome assembly in eukaryotes. *Gene*, **313**, 17-42.
Fujimura, K., Tanaka, K. and Toh-e, A. (1993) A dominant interfering mutation in RAS1 of Saccharomyces cerevisiae. *Mol Gen Genet*, **241**, 280-286.
Gadal, O., Strauss, D., Braspenning, J., Hoepfner, D., Petfalski, E., Philippsen, P., Tollervey, D. and Hurt, E. (2001a) A nuclear AAA-type ATPase (Rix7p) is required for biogenesis and nuclear export of 60S ribosomal subunits. *Embo J*, **20**, 3695-3704.
Gadal, O., Strauss, D., Kessl, J., Trumpower, B., Tollervey, D. and Hurt, E. (2001b) Nuclear export of 60s ribosomal subunits depends on Xpo1p and requires a nuclear export sequence-containing factor, Nmd3p, that associates with the large subunit protein Rpl10p. *Mol Cell Biol*, **21**, 3405-3415.
Gadal, O., Strauss, D., Petfalski, E., Gleizes, P.E., Gas, N., Tollervey, D. and Hurt, E. (2002) Rlp7p is associated with 60S preribosomes, restricted to the granular component of the nucleolus, and required for pre-rRNA processing. *J Cell Biol*, **157**, 941-951.
Galani, K., Nissan, T.A., Petfalski, E., Tollervey, D. and Hurt, E. (2004) Rea1, a dynein-related nuclear AAA-ATPase, is involved in late rRNA processing and nuclear export of 60 S subunits. *J Biol Chem*, **279**, 55411-55418.
Ganoza, M.C., Zahid, N. and Baxter, R.M. (1985) Stimulation of peptidyltransferase reactions by a soluble protein. *Eur J Biochem*, **146**, 287-294.
Garbarino, J.E.a.G., I.R. (2002) BMC Genomics. **3**, 18-28.
Gavin, A.C., Bosche, M., Krause, R., Grandi, P., Marzioch, M., Bauer, A., Schultz, J., Rick, J.M., Michon, A.M., Cruciat, C.M., Remor, M., Hofert, C., Schelder, M., Brajenovic, M., Ruffner, H., Merino, A., Klein, K., Hudak, M., Dickson, D., Rudi, T., Gnau, V., Bauch, A., Bastuck, S., Huhse, B., Leutwein, C., Heurtier, M.A., Copley, R.R., Edelmann, A., Querfurth, E., Rybin, V., Drewes, G., Raida, M., Bouwmeester, T., Bork, P., Seraphin, B., Kuster, B., Neubauer, G. and Superti-Furga, G. (2002) Functional organization of the yeast proteome by systematic analysis of protein complexes. *Nature*, **415**, 141-147.
Gelperin, D., Horton, L., Beckman, J., Hensold, J. and Lemmon, S.K. (2001) Bms1p, a novel GTP-binding protein, and the related Tsr1p are required for distinct steps of 40S ribosome biogenesis in yeast. *Rna*, **7**, 1268-1283.
Gietz, D., St Jean, A., Woods, R.A. and Schiestl, R.H. (1992) Improved method for high efficiency transformation of intact yeast cells. *Nucleic Acids Res*, **20**, 1425.
Gleizes, P.E., Noaillac-Depeyre, J., Leger-Silvestre, I., Teulieres, F., Dauxois, J.Y., Pommet, D., Azum-Gelade, M.C. and Gas, N. (2001) Ultrastructural localization of rRNA shows defective nuclear export of preribosomes in mutants of the Nup82p complex. *J Cell Biol*, **155**, 923-936.
Gorlich, D. and Kutay, U. (1999) Transport between the cell nucleus and the cytoplasm. *Annu Rev Cell Dev Biol*, **15**, 607-660.

Graindorge, J.S., Rousselle, J.C., Senger, B., Lenormand, P., Namane, A., Lacroute, F. and Fasiolo, F. (2005a) Deletion of EFL1 results in heterogeneity of the 60 S GTPase-associated rRNA conformation. *J Mol Biol*, **352**, 355-369.

Graindorge, J.S., Rousselle, J.C., Senger, B., Lenormand, P., Namane, A., Lacroute, F. and Fasiolo, F. (2005b) Deletion of EFL1 Results in Heterogeneity of the 60S GTPase-associated rRNA Conformation. *J Mol Biol*, **352**, 355-369.

Grandi, P., Rybin, V., Bassler, J., Petfalski, E., Strauss, D., Marzioch, M., Schafer, T., Kuster, B., Tschochner, H., Tollervey, D., Gavin, A.C. and Hurt, E. (2002) 90S pre-ribosomes include the 35S pre-rRNA, the U3 snoRNP, and 40S subunit processing factors but predominantly lack 60S synthesis factors. *Mol Cell*, **10**, 105-115.

Hanawa-Suetsugu, K., Sekine, S., Sakai, H., Hori-Takemoto, C., Terada, T., Unzai, S., Tame, J.R., Kuramitsu, S., Shirouzu, M. and Yokoyama, S. (2004) Crystal structure of elongation factor P from Thermus thermophilus HB8. *Proc Natl Acad Sci U S A*, **101**, 9595-9600.

Harnpicharnchai, P., Jakovljevic, J., Horsey, E., Miles, T., Roman, J., Rout, M., Meagher, D., Imai, B., Guo, Y., Brame, C.J., Shabanowitz, J., Hunt, D.F. and Woolford, J.L., Jr. (2001) Composition and functional characterization of yeast 66S ribosome assembly intermediates. *Mol Cell*, **8**, 505-515.

Hauer, J.A., Barthe, P., Taylor, S.S., Parello, J. and Padilla, A. (1999) Two well-defined motifs in the cAMP-dependent protein kinase inhibitor (PKIalpha) correlate with inhibitory and nuclear export function. *Protein Sci*, **8**, 545-553.

Hector, R.E., Nykamp, K.R., Dheur, S., Anderson, J.T., Non, P.J., Urbinati, C.R., Wilson, S.M., Minvielle-Sebastia, L. and Swanson, M.S. (2002) Dual requirement for yeast hnRNP Nab2p in mRNA poly(A) tail length control and nuclear export. *Embo J*, **21**, 1800-1810.

Hedges, J., West, M. and Johnson, A.W. (2005) Release of the export adapter, Nmd3p, from the 60S ribosomal subunit requires Rpl10p and the cytoplasmic GTPase Lsg1p. *Embo J*, **24**, 567-579.

Ho, J.H. and Johnson, A.W. (1999) NMD3 encodes an essential cytoplasmic protein required for stable 60S ribosomal subunits in Saccharomyces cerevisiae. *Mol Cell Biol*, **19**, 2389-2399.

Ho, J.H., Kallstrom, G. and Johnson, A.W. (2000a) Nascent 60S ribosomal subunits enter the free pool bound by Nmd3p. *Rna*, **6**, 1625-1634.

Ho, J.H., Kallstrom, G. and Johnson, A.W. (2000b) Nmd3p is a Crm1p-dependent adapter protein for nuclear export of the large ribosomal subunit. *J Cell Biol*, **151**, 1057-1066.

Hovland, P., Flick, J., Johnston, M. and Sclafani, R.A. (1989) Galactose as a gratuitous inducer of GAL gene expression in yeasts growing on glucose. *Gene*, **83**, 57-64.

Huh, W.K., Falvo, J.V., Gerke, L.C., Carroll, A.S., Howson, R.W., Weissman, J.S. and O'Shea, E.K. (2003) Global analysis of protein localization in budding yeast. *Nature*, **425**, 686-691.

Hung, N.J. and Johnson, A.W. (2005) manuscript in preparation.

Hurt, E., Hannus, S., Schmelzl, B., Lau, D., Tollervey, D. and Simos, G. (1999) A novel in vivo assay reveals inhibition of ribosomal nuclear export in ran-cycle and nucleoporin mutants. *J Cell Biol*, **144**, 389-401.

Jacobson, A. and Peltz, S.W. (1996) Interrelationships of the pathways of mRNA decay and translation in eukaryotic cells. *Annu Rev Biochem*, **65**, 693-739.

Jensen, B.C., Wang, Q., Kifer, C.T. and Parsons, M. (2003) The NOG1 GTP-binding protein is required for biogenesis of the 60 S ribosomal subunit. *J Biol Chem*, **278**, 32204-32211.

Johnson, A.W., Lund, E. and Dahlberg, J. (2002) Nuclear export of ribosomal subunits. *Trends Biochem Sci*, **27**, 580-585.

Kahvejian, A., Svitkin, Y.V., Sukarieh, R., M'Boutchou, M.N. and Sonenberg, N. (2005) Mammalian poly(A)-binding protein is a eukaryotic translation initiation factor, which acts via multiple mechanisms. *Genes Dev*, **19**, 104-113.

Kaiser, C., Michaelis, S. and Mitchell, A. (1994) *Methods in yeast genetics*. Cold Spring Harbor Laboratory Press, Cold Spring Harbor, N.Y.

Kallstrom, G., Hedges, J. and Johnson, A. (2003) The putative GTPases Nog1p and Lsg1p are required for 60S ribosomal subunit biogenesis and are localized to the nucleus and cytoplasm, respectively. *Mol Cell Biol*, **23**, 4344-4355.

Kapp, L.D. and Lorsch, J.R. (2004) The molecular mechanics of eukaryotic translation. *Annu Rev Biochem*, **73**, 657-704.

Karl, T., Onder, K., Kodzius, R., Pichova, A., Wimmer, H., Th r, A., Hundsberger, H., Loffler, M., Klade, T., Beyer, A., Breitenbach, M. and Koller, L. (1999) GRC5 and NMD3 function in translational control of gene expression and interact genetically. *Curr Genet*, **34**, 419-429.

Kehlenbach, R.H., Dickmanns, A., Kehlenbach, A., Guan, T. and Gerace, L. (1999) A role for RanBP1 in the release of CRM1 from the nuclear pore complex in a terminal step of nuclear export. *J Cell Biol*, **145**, 645-657.

Kiss, T. (2001) Small nucleolar RNA-guided post-transcriptional modification of cellular RNAs. *Embo J*, **20**, 3617-3622.

Kranz, J.E. and Holm, C. (1990) Cloning by function: an alternative approach for identifying yeast homologs of genes from other organisms. *Proc Natl Acad Sci U S A*, **87**, 6629-6633.

Kressler, D., Linder, P. and de La Cruz, J. (1999) Protein trans-acting factors involved in ribosome biogenesis in Saccharomyces cerevisiae. *Mol Cell Biol*, **19**, 7897-7912.

Kruiswijk, T., Planta, R.J. and Krop, J.M. (1978) The course of the assembly of ribosomal subunits in yeast. *Biochim Biophys Acta*, **517**, 378-389.

Kutay, U. and Guttinger, S. (2005) Leucine-rich nuclear-export signals: born to be weak. *Trends Cell Biol*, **15**, 121-124.

la Cour, T., Kiemer, L., Molgaard, A., Gupta, R., Skriver, K. and Brunak, S. (2004) Analysis and prediction of leucine-rich nuclear export signals. *Protein Eng Des Sel*, **17**, 527-536.

Lafontaine, D., Delcour, J., Glasser, A.L., Desgres, J. and Vandenhaute, J. (1994) The DIM1 gene responsible for the conserved m6(2)Am6(2)A dimethylation in the 3'-terminal loop of 18 S rRNA is essential in yeast. *J Mol Biol*, **241**, 492-497.

Lafontaine, D., Vandenhaute, J. and Tollervey, D. (1995) The 18S rRNA dimethylase Dim1p is required for pre-ribosomal RNA processing in yeast. *Genes Dev*, **9**, 2470-2481.

Lalo, D., Mariotte, S. and Thuriaux, P. (1993) Two distinct yeast proteins are related to the mammalian ribosomal polypeptide L7. *Yeast*, **9**, 1085-1091.

Le, H., Tanguay, R.L., Balasta, M.L., Wei, C.C., Browning, K.S., Metz, A.M., Goss, D.J. and Gallie, D.R. (1997) Translation initiation factors eIF-iso4G and eIF-4B interact with the poly(A)-binding protein and increase its RNA binding activity. *J Biol Chem*, **272**, 16247-16255.

Lee, J.H., Pestova, T.V., Shin, B.S., Cao, C., Choi, S.K. and Dever, T.E. (2002) Initiation factor eIF5B catalyzes second GTP-dependent step in eukaryotic translation initiation. *Proc Natl Acad Sci U S A*, **99**, 16689-16694.

Leipe, D.D., Wolf, Y.I., Koonin, E.V. and Aravind, L. (2002) Classification and evolution of P-loop GTPases and related ATPases. *J Mol Biol*, **317**, 41-72.

Lewis, J.D. and Tollervey, D. (2000) Like attracts like: getting RNA processing together in the nucleus. *Science*, **288**, 1385-1389.

Lindsay, M.E., Holaska, J.M., Welch, K., Paschal, B.M. and Macara, I.G. (2001) Ran-binding protein 3 is a cofactor for Crm1-mediated nuclear protein export. *J Cell Biol*, **153**, 1391-1402.

Liu, H., Krizek, J. and Bretscher, A. (1992) Construction of a GAL1-regulated yeast cDNA expression library and its application to the identification of genes whose overexpression causes lethality in yeast. *Genetics*, **132**, 665-673.

Longtine, M.S., McKenzie, A., 3rd, Demarini, D.J., Shah, N.G., Wach, A., Brachat, A., Philippsen, P. and Pringle, J.R. (1998) Additional modules for versatile and economical PCR-based gene deletion and modification in Saccharomyces cerevisiae. *Yeast*, **14**, 953-961.

Lounsbury, K.M. and Macara, I.G. (1997) Ran-binding protein 1 (RanBP1) forms a ternary complex with Ran and karyopherin beta and reduces Ran GTPase-activating protein (RanGAP) inhibition by karyopherin beta. *J Biol Chem*, **272**, 551-555.

Mackay, J.P. and Crossley, M. (1998) Zinc fingers are sticking together. *Trends Biochem Sci*, **23**, 1-4.

Maden, B.E. (1998) Eukaryotic rRNA methylation: the calm before the Sno storm. *Trends Biochem Sci*, **23**, 447-450.

Makarova, K.S. and Grishin, N.V. (1999) The Zn-peptidase superfamily: functional convergence after evolutionary divergence. *J Mol Biol*, **292**, 11-17.

Maki, J.A., Schnobrich, D.J. and Culver, G.M. (2002) The DnaK chaperone system facilitates 30S ribosomal subunit assembly. *Mol Cell*, **10**, 129-138.

Mangiarotti, G. and Chiaberge, S. (1997) Reconstitution of functional eukaryotic ribosomes from Dictyostelium discoideum ribosomal proteins and RNA. *J Biol Chem*, **272**, 19682-19687.
Mangus, D.A., Evans, M.C. and Jacobson, A. (2003) Poly(A)-binding proteins: multifunctional scaffolds for the post-transcriptional control of gene expression. *Genome Biol*, **4**, 223.
Matunis, M.J., Wu, J. and Blobel, G. (1998) SUMO-1 modification and its role in targeting the Ran GTPase-activating protein, RanGAP1, to the nuclear pore complex. *J Cell Biol*, **140**, 499-509.
Maurer, P., Redd, M., Solsbacher, J., Bischoff, F.R., Greiner, M., Podtelejnikov, A.V., Mann, M., Stade, K., Weis, K. and Schlenstedt, G. (2001) The nuclear export receptor Xpo1p forms distinct complexes with NES transport substrates and the yeast Ran binding protein 1 (Yrb1p). *Mol Biol Cell*, **12**, 539-549.
Milkereit, P., Gadal, O., Podtelejnikov, A., Trumtel, S., Gas, N., Petfalski, E., Tollervey, D., Mann, M., Hurt, E. and Tschochner, H. (2001) Maturation and intranuclear transport of pre-ribosomes requires Noc proteins. *Cell*, **105**, 499-509.
Milkereit, P., Strauss, D., Bassler, J., Gadal, O., Kuhn, H., Schutz, S., Gas, N., Lechner, J., Hurt, E. and Tschochner, H. (2003) A Noc complex specifically involved in the formation and nuclear export of ribosomal 40 S subunits. *J Biol Chem*, **278**, 4072-4081.
Miller, O.L., Jr. and Beatty, B.R. (1969) Visualization of nucleolar genes. *Science*, **164**, 955-957.
Mougey, E.B., O'Reilly, M., Osheim, Y., Miller, O.L., Jr., Beyer, A. and Sollner-Webb, B. (1993) The terminal balls characteristic of eukaryotic rRNA transcription units in chromatin spreads are rRNA processing complexes. *Genes Dev*, **7**, 1609-1619.
Moy, T.I. and Silver, P.A. (1999) Nuclear export of the small ribosomal subunit requires the ran-GTPase cycle and certain nucleoporins. *Genes Dev*, **13**, 2118-2133.
Neville, M. and Rosbash, M. (1999) The NES-Crm1p export pathway is not a major mRNA export route in Saccharomyces cerevisiae. *Embo J*, **18**, 3746-3756.
Nguyen, Y.H., Mills, A.A. and Stanbridge, E.J. (1998) Assembly of the QM protein onto the 60S ribosomal subunit occurs in the cytoplasm. *J Cell Biochem*, **68**, 281-285.
Nishimura, M., Yoshida, T., Shirouzu, M., Terada, T., Kuramitsu, S., Yokoyama, S., Ohkubo, T. and Kobayashi, Y. (2004) Solution structure of ribosomal protein L16 from Thermus thermophilus HB8. *J Mol Biol*, **344**, 1369-1383.
Nissan, T.A., Bassler, J., Petfalski, E., Tollervey, D. and Hurt, E. (2002) 60S pre-ribosome formation viewed from assembly in the nucleolus until export to the cytoplasm. *Embo J*, **21**, 5539-5547.
Nissan, T.A., Galani, K., Maco, B., Tollervey, D., Aebi, U. and Hurt, E. (2004) A pre-ribosome with a tadpole-like structure functions in ATP-dependent maturation of 60S subunits. *Mol Cell*, **15**, 295-301.
Nomura, M. and Erdmann, V.A. (1970) Reconstitution of 50S ribosomal subunits from dissociated molecular components. *Nature*, **228**, 744-748.

Ofengand, J. (2002) Ribosomal RNA pseudouridines and pseudouridine synthases. *FEBS Lett*, **514**, 17-25.

Ofengand, J., Malhotra, A., Remme, J., Gutgsell, N.S., Del Campo, M., Jean-Charles, S., Peil, L. and Kaya, Y. (2001) Pseudouridines and pseudouridine synthases of the ribosome. *Cold Spring Harb Symp Quant Biol*, **66**, 147-159.

Ohtsubo, M., Okazaki, H. and Nishimoto, T. (1989) The RCC1 protein, a regulator for the onset of chromosome condensation locates in the nucleus and binds to DNA. *J Cell Biol*, **109**, 1389-1397.

Otero, L.J., Ashe, M.P. and Sachs, A.B. (1999) The yeast poly(A)-binding protein Pab1p stimulates in vitro poly(A)-dependent and cap-dependent translation by distinct mechanisms. *Embo J*, **18**, 3153-3163.

Pante, N. and Kann, M. (2002) Nuclear pore complex is able to transport macromolecules with diameters of about 39 nm. *Mol Biol Cell*, **13**, 425-434.

Paraskeva, E., Izaurralde, E., Bischoff, F.R., Huber, J., Kutay, U., Hartmann, E., Luhrmann, R. and Gorlich, D. (1999) CRM1-mediated recycling of snurportin 1 to the cytoplasm. *J Cell Biol*, **145**, 255-264.

Park, J.H., Jensen, B.C., Kifer, C.T. and Parsons, M. (2001) A novel nucleolar G-protein conserved in eukaryotes. *J Cell Sci*, **114**, 173-185.

Pemberton, L.F. and Paschal, B.M. (2005) Mechanisms of receptor-mediated nuclear import and nuclear export. *Traffic*, **6**, 187-198.

Pestova, T.V. and Kolupaeva, V.G. (2002) The roles of individual eukaryotic translation initiation factors in ribosomal scanning and initiation codon selection. *Genes Dev*, **16**, 2906-2922.

Pestova, T.V., Lomakin, I.B., Lee, J.H., Choi, S.K., Dever, T.E. and Hellen, C.U. (2000) The joining of ribosomal subunits in eukaryotes requires eIF5B. *Nature*, **403**, 332-335.

Petosa, C., Schoehn, G., Askjaer, P., Bauer, U., Moulin, M., Steuerwald, U., Soler-Lopez, M., Baudin, F., Mattaj, I.W. and Muller, C.W. (2004) Architecture of CRM1/Exportin1 suggests how cooperativity is achieved during formation of a nuclear export complex. *Mol Cell*, **16**, 761-775.

Powers, S., O'Neill, K. and Wigler, M. (1989) Dominant yeast and mammalian RAS mutants that interfere with the CDC25-dependent activation of wild-type RAS in Saccharomyces cerevisiae. *Mol Cell Biol*, **9**, 390-395.

Raue, H.A. (ed.). (2004) *Pre-Ribosomal RNA Processing and Assembly in Saccharomyces cerevisiae: The Machine That Makes the Machine*. Kluwer Academic/Plenum Publishers, New York, New York.

Ribbeck, K. and Gorlich, D. (2002) The permeability barrier of nuclear pore complexes appears to operate via hydrophobic exclusion. *Embo J*, **21**, 2664-2671.

Ribbeck, K., Kutay, U., Paraskeva, E. and Gorlich, D. (1999) The translocation of transportin-cargo complexes through nuclear pores is independent of both Ran and energy. *Curr Biol*, **9**, 47-50.

Richards, S.A., Lounsbury, K.M., Carey, K.L. and Macara, I.G. (1996) A nuclear export signal is essential for the cytosolic localization of the Ran binding protein, RanBP1. *J Cell Biol*, **134**, 1157-1168.

Robinson, N.G., Guo, L., Imai, J., Toh, E.A., Matsui, Y. and Tamanoi, F. (1999) Rho3 of Saccharomyces cerevisiae, which regulates the actin cytoskeleton and exocytosis, is a GTPase which interacts with Myo2 and Exo70. *Mol Cell Biol*, **19**, 3580-3587.

Rodriguez, M.S., Dargemont, C. and Stutz, F. (2004) Nuclear export of RNA. *Biol Cell*, **96**, 639-655.

Rouquette, J., Choesmel, V. and Gleizes, P.E. (2005) Nuclear export and cytoplasmic processing of precursors to the 40S ribosomal subunits in mammalian cells. *Embo J*, **24**, 2862-2872.

Rout, M.P., Aitchison, J.D., Suprapto, A., Hjertaas, K., Zhao, Y. and Chait, B.T. (2000) The yeast nuclear pore complex: composition, architecture, and transport mechanism. *J Cell Biol*, **148**, 635-651.

Rout, M.P. and Blobel, G. (1993) Isolation of the yeast nuclear pore complex. *J Cell Biol*, **123**, 771-783.

Russell, D.W. and Spremulli, L.L. (1979) Purification and characterization of a ribosome dissociation factor (eukaryotic initiation factor 6) from wheat germ. *J Biol Chem*, **254**, 8796-8800.

Sachs, A.B. and Davis, R.W. (1989) The poly(A) binding protein is required for poly(A) shortening and 60S ribosomal subunit-dependent translation initiation. *Cell*, **58**, 857-867.

Sachs, A.B. and Varani, G. (2000) Eukaryotic translation initiation: there are (at least) two sides to every story. *Nat Struct Biol*, **7**, 356-361.

Saraste, M., Sibbald, P.R. and Wittinghofer, A. (1990) The P-loop--a common motif in ATP- and GTP-binding proteins. *Trends Biochem Sci*, **15**, 430-434.

Saveanu, C., Bienvenu, D., Namane, A., Gleizes, P.E., Gas, N., Jacquier, A. and Fromont-Racine, M. (2001) Nog2p, a putative GTPase associated with pre-60S subunits and required for late 60S maturation steps. *Embo J*, **20**, 6475-6484.

Saveanu, C., Namane, A., Gleizes, P.E., Lebreton, A., Rousselle, J.C., Noaillac-Depeyre, J., Gas, N., Jacquier, A. and Fromont-Racine, M. (2003) Sequential protein association with nascent 60S ribosomal particles. *Mol Cell Biol*, **23**, 4449-4460.

Schlatter, H., Langer, T., Rosmus, S., Onneken, M.L. and Fasold, H. (2002) A novel function for the 90 kDa heat-shock protein (Hsp90): facilitating nuclear export of 60 S ribosomal subunits. *Biochem J*, **362**, 675-684.

Schlenstedt, G., Saavedra, C., Loeb, J.D., Cole, C.N. and Silver, P.A. (1995a) The GTP-bound form of the yeast Ran/TC4 homologue blocks nuclear protein import and appearance of poly(A)+ RNA in the cytoplasm. *Proc Natl Acad Sci U S A*, **92**, 225-229.

Schlenstedt, G., Wong, D.H., Koepp, D.M. and Silver, P.A. (1995b) Mutants in a yeast Ran binding protein are defective in nuclear transport. *Embo J*, **14**, 5367-5378.

Schwoebel, E.D., Talcott, B., Cushman, I. and Moore, M.S. (1998) Ran-dependent signal-mediated nuclear import does not require GTP hydrolysis by Ran. *J Biol Chem*, **273**, 35170-35175.

Senger, B., Lafontaine, D.L., Graindorge, J.S., Gadal, O., Camasses, A., Sanni, A., Garnier, J.M., Breitenbach, M., Hurt, E. and Fasiolo, F. (2001) The nucle(ol)ar Tif6p and Efl1p are required for a late cytoplasmic step of ribosome synthesis. *Mol Cell*, **8**, 1363-1373.

Shin, B.S., Maag, D., Roll-Mecak, A., Arefin, M.S., Burley, S.K., Lorsch, J.R. and Dever, T.E. (2002) Uncoupling of initiation factor eIF5B/IF2 GTPase and translational activities by mutations that lower ribosome affinity. *Cell*, **111**, 1015-1025.

Si, K. and Maitra, U. (1999) The Saccharomyces cerevisiae homologue of mammalian translation initiation factor 6 does not function as a translation initiation factor. *Mol Cell Biol*, **19**, 1416-1426.

Silberstein, S., Schlenstedt, G., Silver, P.A. and Gilmore, R. (1998) A role for the DnaJ homologue Scj1p in protein folding in the yeast endoplasmic reticulum. *J Cell Biol*, **143**, 921-933.

Spahn, C.M., Beckmann, R., Eswar, N., Penczek, P.A., Sali, A., Blobel, G. and Frank, J. (2001) Structure of the 80S ribosome from Saccharomyces cerevisiae--tRNA-ribosome and subunit-subunit interactions. *Cell*, **107**, 373-386.

Spremulli, L.L., Walthall, B.J., Lax, S.R. and Ravel, J.M. (1979) Partial purification of the factors required for the initiation of protein synthesis in wheat germ. *J Biol Chem*, **254**, 143-148.

Stage-Zimmermann, T., Schmidt, U. and Silver, P.A. (2000) Factors affecting nuclear export of the 60S ribosomal subunit in vivo. *Mol Biol Cell*, **11**, 3777-3789.

Suntharalingam, M. and Wente, S.R. (2003) Peering through the pore: nuclear pore complex structure, assembly, and function. *Dev Cell*, **4**, 775-789.

Sydorskyy, Y., Dilworth, D.J., Yi, E.C., Goodlett, D.R., Wozniak, R.W. and Aitchison, J.D. (2003) Intersection of the Kap123p-mediated nuclear import and ribosome export pathways. *Mol Cell Biol*, **23**, 2042-2054.

Tarun, S.Z., Jr. and Sachs, A.B. (1995) A common function for mRNA 5' and 3' ends in translation initiation in yeast. *Genes Dev*, **9**, 2997-3007.

Tarun, S.Z., Jr., Wells, S.E., Deardorff, J.A. and Sachs, A.B. (1997) Translation initiation factor eIF4G mediates in vitro poly(A) tail-dependent translation. *Proc Natl Acad Sci U S A*, **94**, 9046-9051.

Teakle, G.R. and Gilmartin, P.M. (1998) Two forms of type IV zinc-finger motif and their kingdom-specific distribution between the flora, fauna and fungi. *Trends Biochem Sci*, **23**, 100-102.

Thomas, F. and Kutay, U. (2003) Biogenesis and nuclear export of ribosomal subunits in higher eukaryotes depend on the CRM1 export pathway. *J Cell Sci*, **116**, 2409-2419.

Tollervey, D. (1996) Trans-acting factors in ribosome synthesis. *Exp Cell Res*, **229**, 226-232.

Tollervey, D., Lehtonen, H., Jansen, R., Kern, H. and Hurt, E.C. (1993) Temperature-sensitive mutations demonstrate roles for yeast fibrillarin in pre-rRNA processing, pre-rRNA methylation, and ribosome assembly. *Cell*, **72**, 443-457.

Trapman, J., Planta, R.J. and Raue, H.A. (1976) Maturation of ribosomes in yeast. II. Position of the low molecular weight rRNA species in the maturation process. *Biochim Biophys Acta*, **442**, 275-284.

Trapman, J., Retel, J. and Planta, R.J. (1975) Ribosomal precursor particles from yeast. *Exp Cell Res*, **90**, 95-104.

Traub, P. and Nomura, M. (1968) Structure and function of E. coli ribosomes. V. Reconstitution of functionally active 30S ribosomal particles from RNA and proteins. *Proc Natl Acad Sci U S A*, **59**, 777-784.

Trotta, C.R., Lund, E., Kahan, L., Johnson, A.W. and Dahlberg, J.E. (2003) Coordinated nuclear export of 60S ribosomal subunits and NMD3 in vertebrates. *Embo J*, **22**, 2841-2851.

Tschochner, H. and Hurt, E. (2003) Pre-ribosomes on the road from the nucleolus to the cytoplasm. *Trends Cell Biol*, **13**, 255-263.

Udem, S.A. and Warner, J.R. (1972) Ribosomal RNA synthesis in Saccharomyces cerevisiae. *J Mol Biol*, **65**, 227-242.

Udem, S.A. and Warner, J.R. (1973) The cytoplasmic maturation of a ribosomal precursor ribonucleic acid in yeast. *J Biol Chem*, **248**, 1412-1416.

Unbehaun, A., Borukhov, S.I., Hellen, C.U. and Pestova, T.V. (2004) Release of initiation factors from 48S complexes during ribosomal subunit joining and the link between establishment of codon-anticodon base-pairing and hydrolysis of eIF2-bound GTP. *Genes Dev*, **18**, 3078-3093.

Vale, R.D. (2000) AAA proteins. Lords of the ring. *J Cell Biol*, **150**, F13-19.

Vanrobays, E., Gelugne, J.P., Gleizes, P.E. and Caizergues-Ferrer, M. (2003) Late cytoplasmic maturation of the small ribosomal subunit requires RIO proteins in Saccharomyces cerevisiae. *Mol Cell Biol*, **23**, 2083-2095.

Vanrobays, E., Gleizes, P.E., Bousquet-Antonelli, C., Noaillac-Depeyre, J., Caizergues-Ferrer, M. and Gelugne, J.P. (2001) Processing of 20S pre-rRNA to 18S ribosomal RNA in yeast requires Rrp10p, an essential non-ribosomal cytoplasmic protein. *Embo J*, **20**, 4204-4213.

Venema, J. and Tollervey, D. (1995) Processing of pre-ribosomal RNA in Saccharomyces cerevisiae. *Yeast*, **11**, 1629-1650.

Venema, J. and Tollervey, D. (1999) Ribosome synthesis in Saccharomyces cerevisiae. *Annu Rev Genet*, **33**, 261-311.

Warner, J.R. (1990) The nucleolus and ribosome formation. *Curr Opin Cell Biol*, **2**, 521-527.

Warner, J.R. (1999) The economics of ribosome biosynthesis in yeast. *Trends Biochem Sci*, **24**, 437-440.

Wegierski, T., Billy, E., Nasr, F. and Filipowicz, W. (2001) Bms1p, a G-domain-containing protein, associates with Rcl1p and is required for 18S rRNA biogenesis in yeast. *Rna*, **7**, 1254-1267.

Wei, C.C., Balasta, M.L., Ren, J. and Goss, D.J. (1998) Wheat germ poly(A) binding protein enhances the binding affinity of eukaryotic initiation factor 4F and (iso)4F for cap analogues. *Biochemistry*, **37**, 1910-1916.

Wells, S.E., Hillner, P.E., Vale, R.D. and Sachs, A.B. (1998) Circularization of mRNA by eukaryotic translation initiation factors. *Mol Cell*, **2**, 135-140.

West, M., Hedges, J.B., Chen, A. and Johnson, A.W. (2005) Defining the order in which Nmd3p and Rpl10p load onto nascent 60S ribosomal subunits. *Mol Cell Biol*, **25**, 3802-3813.

Winey, M., Yarar, D., Giddings, T.H., Jr. and Mastronarde, D.N. (1997) Nuclear pore complex number and distribution throughout the Saccharomyces cerevisiae cell cycle by three-dimensional reconstruction from electron micrographs of nuclear envelopes. *Mol Biol Cell*, **8**, 2119-2132.

Woolford, J. (2002) Chaperoning ribosome assembly. *Mol Cell*, **10**, 8-10.

Yoon, H. and Donahue, T.F. (1992) Control of translation initiation in Saccharomyces cerevisiae. *Mol Microbiol*, **6**, 1413-1419.

Yusupov, M.M., Yusupova, G.Z., Baucom, A., Lieberman, K., Earnest, T.N., Cate, J.H. and Noller, H.F. (2001) Crystal structure of the ribosome at 5.5 A resolution. *Science*, **292**, 883-896.

Zebarjadian, Y., King, T., Fournier, M.J., Clarke, L. and Carbon, J. (1999) Point mutations in yeast CBF5 can abolish in vivo pseudouridylation of rRNA. *Mol Cell Biol*, **19**, 7461-7472.

Zinker, S. and Warner, J.R. (1976) The ribosomal proteins of Saccharomyces cerevisiae. Phosphorylated and exchangeable proteins. *J Biol Chem*, **251**, 1799-1807.

Zolotukhin, A.S. and Felber, B.K. (1997) Mutations in the nuclear export signal of human ran-binding protein RanBP1 block the Rev-mediated posttranscriptional regulation of human immunodeficiency virus type 1. *J Biol Chem*, **272**, 11356-11360.

Zuk, D., Belk, J.P. and Jacobson, A. (1999) Temperature-sensitive mutations in the Saccharomyces cerevisiae MRT4, GRC5, SLA2 and THS1 genes result in defects in mRNA turnover. *Genetics*, **153**, 35-47.

Vita

Matthew Blaine West was born in Oklahoma City, Oklahoma on October 15, 1976, the son of Marilyn Elizabeth West and Rick Kenneth West. After graduating from Choctaw High School in 1995, he attended Oklahoma State University, Stillwater, where he received Bachelor of Science degrees in May 1999 and May 2000. After completing his undergraduate degree, he was employed in the laboratory of Sharon von Braumsen at Oklahoma State University. In August of 2000, he entered the Graduate School at the University of Texas, Austin.

Permanent address: P.O. Box 1450, Choctaw, Oklahoma 73020

This dissertation was typed by the author.